CHARACTERIZATION AND OPTIMIZATION OF OIL PALM EMPTY FRUIT BUNCH-GLASS FIBRE REINFORCED RECYCLED POLYPROPYLENE HYBRID COMPOSITES

MAKSON RIVAI

Thesis submitted in fulfilment of the requirements
for the award of the degree of
Master of Engineering in Chemical

Faculty of Chemical and Natural Resources Engineering
UNIVERSITI MALAYSIA PAHANG

MAY 2013

SUPERVISOR'S DECLARATION

I hereby declare that I have checked this thesis and in my opinion this thesis is adequate in terms of scope and quality for the award of the degree of Master of engineering in Chemical Engineering.

Signature : _____

Name of Supervisor : ASSOCIATE PROF DR. ARUN GUPTA

Position : LECTURER IN FACULTY OF CHEMICAL AND NATURAL RESOURCES ENGINEERING

Date :

Signature : _____

Name of Co-supervisor : ASSOCIATE PROF DR. MOHAMMAD DALOUR HOSSEN BEG

Position : LECTURER IN FACULTY OF CHEMICAL AND NATURAL RESOURCES ENGINEERING

Date :

STUDENT'S DECLARATION

I hereby declared that the work in this thesis is my own except for quotations and summaries which have been duly acknowledged. The thesis has not been accepted for any degree and is not concurrently submitted for award of other degree.

Signature	:	_____
Name	:	MAKSON RIVAI
ID Number	:	MKC 10005
Date	:	

In the name of Allah, The Most Gracious and The Most Merciful

Dedicated to:

All of My Teachers

ACKNOWLEDGEMENT

Praise be to ALLAH SWT who has given me the blessings so that I could finish my thesis.

I would like to take this precious moment to express my sincere and wholehearted appreciation to my supervisor, Dr. Arun Gupta for kindness advice support, encouragement and time with me.

Special thanks to my co-supervisor Dr Mohammad Dalour Hossen Beg for knowledge, ideas, providing some new equipment, assistance and encouragement in writing and publishing paper.

I would also like to thank to all UMP staff, who has given me support for using facilities in UMP Gambang laboratory, I would like to express my gratitude to my lab-mates in polymer field for assistance in sample preparation, testing, discussion, and support. Thanks to all my friends for their encouragement to complete the study.

Very special thanks for Mr Bejo Soekarno. Ki Hadi Sugito, KH Zainal Abidin, Mr Rustam Aji, Mr Usman Wijaya, Dian Utami Vitasari and Siti Banks, Thank you to my parent, brothers and sisters for inspiring me to complete this study.

Finally, I realize that this thesis is still far from being perfect. However, I hope that this will be of some contribution to the development of composites material.

ABSTRACT

The tremendous utilization of plastics over last decades has led to the environmental problems due to non degradability of plastics. This lead to the development of the composites using natural fibre and plastic. The present study deals with the utilization of empty fruit bunch of oil palm (EFB), glass fibre, as fibre, recycled polypropylene and coupling agent [maleic anhydride grafted polypropylene (MAPP) and fusabond] as composites material. EFB fibres were treated with alkali treatment with conventional, homemade, microwave and ultrasonic methods. Blending of composite material was carried out using twin-screw extruder followed by injection moulding to produce specimens. Characterization of hybrid composites was then carried out to examine the alkali treatments and composition interactions. Fresh and sea water hygrothermal ageing test was performed at 27°C, 60 and 80°C. Accelerated weathering tests was conducted up to 1200 hours while natural weathering test was implemented for more than one year under natural weathering conditions. Tensile testing, FTIR analysis, melt flow index (MFI) analysis, thermo gravimetric analyser (TGA) test, differential scanning calorimetric (DSC) test, water absorptions, and scanning electron microscopy (SEM) were performed to examine the changes of hybrid composites during treatments. Results show that Ultrasonic EFB treatment has the highest properties' stability and rapid treatment compared to modified microwave, homemade alkali treatment and conventional treatment. Homemade alkali treatment provided low-cost and less amount of NaOH is needed. Compounding process, coupling agent, temperature treatments, soaking time, NaOH % and fibre ratio have an important role to offer optimum of physical and mechanical properties and hybrid composite's stability. Natural weathering has small degradation and has similar effects with accelerated weathering test. Results of accelerated weathering and hygrothermal ageing test shown the capabilities on enhancing properties of composites in specific harsh natural environment or marine application. Optimization was done using Response Surface Methodology (RSM) with tensile strength, modulus, elongation at break, and melt flow indexes as the dependent variables (responses) while the parameter of alkali treatment, coupling agent, fibre ratio and compounding process as the independent variables.The experimental results indicate that the proposed mathematical models could adequately describe the performance indicators within the limits of the factors being investigated.

ABSTRAK

Penggunaan plastic sejak sedekad lalu telah menyebabkan masalah pencemaran berikutan lambakan plastic yang sukar dinyahlupus. Masalah ini telah membuka ruang yang lebih luas terhadap pembangunan teknologi komposit daripada fiber asli. Melalui kajian ini, gentian tandan kelapa sawit, gentian kaca dan plastic kitar semula serta agen penggabung [maleic anhydrate grafted polyroylene (MAPP) dan fusabon] digunakan sebagai bahan komposit. Gentian tandan kelapa sawit (EFB) dirawat menggunakan alkali melalui kaedah tradisional, buatan tangan, microwave dan ultrasonic. Campuran bahan komposit dijadikan spesimen melalui teknik pengacuan suntikan menggunakan skru tekanan berkembar. Pengkriteriaan bahan komposit ditentukan berdasarkan rawatan alkali dan interaksi antara komposisi. Ujian penuaan higroterma dilakukan menggunakan air tawar dan air masin pada suhu 27, 60 dan 80^{0}C. Ujian pecutan cuaca dijalankan sehingga 1200 jam manakala ujian cuaca semulajadi dilakukan selama setahun. Ujian regangan, FTIR, indeks aliran cair (MFI), ujian termo gravimetric (TGA), ujian pembezaan pengimbasan kalorimetric (DSC), ujian penyerapan air dan mikroskopi imbasan electron (SEM) dijalankan untuk menguji perubahan bahan komposit semasa rawatan. dan keputusan membuktikan bahawa gabungan rawatan ultrasonic dan alkali menunjukkan hasil yang bagus berbanding lain lain kaedah. Keputusan kajian menunjukkan rawatan menggunakan teknik ultrasonic lebih stabil daripada sudut karakter berbanding lain-lain kaedah. Bagaimanapun teknik buatan tangan hanya memerlukan kos yang rendah dan kurang penggunaan bahan kimia. Perawatan maksima bagi serat, nisbah serat dan agen gandingan telah meperbaiki sifat-sifat fizikal dan mekanikal komposit. Perawatan dan nisbah bahan serat memainkan peranan penting dalam memperbaiki sifat-sifat komposit. Penguraian dan serapan air meningkat dengan meningkatnya jumlah kandungan EFB. Semasa pecutan pencuacana dan penuaan higroterma, sifat penguraian adalah lebih cepat bagi komposit yang mengandungi gentian kaca dan agen gandingan yang rendah. Pencuacaan semulajadi memberikan kesan yang sama kecil dengan pecutan pencuacaan. Formulasi yang berbeza bagi EFB-gentian kaca matrik dan agen gandingan menunjukkan keupayaan dalam meningkatkan sifat-sifat komposit dari segi pengkhususan di persekitaran semulajadi ataupun aplikasi dalam kelengkapan alatan marin.Optimasi menggunakan kaedah tindakbalas permukaan menunjukkan model matematik yang disarankan memenuhi keupayaan untuk menerangkan prestasi di antara had faktor yang dijalankan.

TABLE OF CONTENT

LIST OF TABLES

LIST OF FIGURES

LIST OF SYMBOLS AND ABBREVIATIONS

3D	Three dimension
Absp	Absorption
Ac	Accelerated Ageing
ANOVA	Analysis of variance
ASTM	American Society for Testing and Materials
D	Diffusion coefficient (m2/s)
DF	Degree of freedom
DH	Heat of fusion (J/g)
DSC	Differential scanning calorimetry
DTA	Differential thermal analysis
DTG	Differential thermogravimetry
Ea	Activation energy (kJ/mol)
EFB	Empty fruit bunch
EGRPP	EFB-Glass fibre recycled polypropylene composite
FD	Factorial Design
FS	Failure strain (%)
FTIR	Fourier transform infrared
HA	Hygrothermal ageing
HDPE	High density polyethylene
IR	Infrared
L	Thickness of the sample (m)
l0	Length of virgin fibre (mm)
lN	Average fibre length (mm)
M∞	Moisture content at the equilibrium
MA	Maleic anhydride
MAPP	Maleic anhydride grafted polypropylene
Mc	Modulus of composite
Mf	Modulus of fibre
MFI	Melt Flow Index
Mm	Modulus of matrix

MPa	Mega Pascal
Mt	Moisture content at time t
N	Number of times the materials were compounded
NaOH	sodium hydroxide
PE	Polyethylene
PP	Polypropylene
RPHC	Recycled polypropylene hybrid composite
RPP	Recycled polypropylene
RSM	Response Surface methodology
Sc	Strength of composite (MPa)
SEM	Scanning electron microscopy
Sf	Strength of fibre (MPa)
Sm	Strength of matrix (MPa)
sN	Tensile strength of the composites compounding N times
Std	Standard
Std. Dev	standard deviation
Temp	Temperature
Tg	Glass transition temperature (^{o}C)
TGA	Thermogravimetric analysis
Tm	Melting temperature (^{o}C)
TS	Tensile strength (MPa)
US	United States
UV	Ultra-violet
VPP	Virgin polypropylene
w0	weight at 0
WPC	Wood plastic composites
wt	weight
WTR	Water
y	Fraction of materials not been decomposed
YM	Young's modulus (MPa)
β	Heating rate (^{o}C/min)

CHAPTER 1.

INTRODUCTION

1.1 BACKGROUND OF STUDY

The pressure on industry to reduce the existing petroleum-based raw plastic materials or glass fibre reinforced plastic composite with an environmentally friendly and sustainable material are the main reason for the evaluation of palm oil-glass fibre hybrid recycled polypropylene composite. Natural fibres present some increasing number of applications and advantages in recent years such as lower density, high toughness, acceptable specific strength, biodegradability, lower price and have the potential to reduce synthetic fibres in fibre-reinforced composite's applications(López-Manchado and Arroyo, 2000; Seki, 2009; Torres and Cubillas, 2005). However, the main disadvantage of natural fibres-plastic matrix composites is the mechanical property variation and the poor compatibility between hydrophobic polymer-matrix and the hydrophilic fibres (Arbelaiz, Fernández, et al., 2005; Beg and Pickering, 2008c). This leads to the formation of a weak interface, which results in poor mechanical properties, where the stress transfer at the interface between two different phases is determined by the degree of adhesion. Another disadvantage of natural fibre composites is high moisture absorption and UV degradation. Lignin and hemicelluloses are the components of natural fibre, which are mostly responsible for moisture absorption and UV degradation (Ahmad and Luyt, 2012; Wang, Sain, and Cooper, 2006).

The physical, chemical and mechanical properties of EFB fibre and some methods of the EFB alkali treatment process were the Major factors controlling the performance of hybrid composites. In this study, recycled polypropylene as the matrix, and

combination of natural fibre from empty fruit bunch oil palm and glass fibre is used as the reinforcement. Polypropylene was selected because of its high recycling rate and high melt flow index(Sobczak, Lang, and Haider, 2012). EFB fibre is a choice because it is plentiful available, lightweight, non-toxic, low-cost and has great strength (Jawaid, Abdul Khalil, and Abu Bakar, 2010; Kim, Park, Seo, and Kim, 2012). Special emphasis was given on the methods of modification of EFB-Glass Fibre ratio as it plays an important role on mechanical properties of composites. Both hydrothermal and UV degradation behaviour of composites were assessed by natural and accelerated weathering(Assarar, Scida, El Mahi, PoilÃ¢ne, and Ayad, 2010). As the stability composites in extreme condition are becoming important, degree of degradation has been an important issue.

1.2 PROBLEM STATEMENT

Natural fibres have the potential to reduce polypropylene in fibre-reinforced composite applications as environmentally friendly material. However, the natural fibres' intrinsic properties cause the variation in the mechanical properties of the composite. Due to high moisture uptake, Incompatibility between natural fibres and polymer matrices (Beg and Pickering, 2008a; Shinoj, Visvanathan, Panigrahi, and Kochubabu, 2009), Degradation and low heat-resistance of natural fibres and their composites. The need of development composite for outdoor and marine environment, Lack of cost-effective and environment-friendly fibre pre-treatment processes are the reason for this researc.

The purpose of this study was to investigate the physical, mechanical and chemical properties of the hybrid recycled polypropylene composites. Alkali treatments, coupling agent and fibre ratio comparison were also examined. Degradation and properties of composite's stability after hygrothermal ageing, natural and accelerated weathering were also compared. This research is also studied on treatment properties and fabrication's method of hybrid palm oil-glass fibres reinforced recycled polypropylene matrix.

Conventional alkali treatment can be used to improve natural fibre, however, the disadvantages of this process are the treatment cost, power needed and high chemical waste generated due to mercerification. Home made alkali treatment, Microwave and Ultrasonic alkali treatment were another alternative for alkali treatment. The production of hybrid composite necessitates a search for economically and ecologically feasible

alkali treatment technologies. In this studied each alkali treatment were compared, and the evectifeness of the lignin removal were investigated to examine better treatment.

The optimization of hybrid composites is an important area. Classical optimization studies use the one-factor-at-a-time approach, is time-consuming and expensive. In addition, possible interaction effects between variables cannot be evaluated and misleading conclusions may be drawn (W. C. Lee, Yusof, Hamid, and Baharin, 2006). The response surface methodology (RSM) can overcome these difficulties, since it allows accounting for possible interaction effects between variables(Sun, Liu, and Kennedy, 2010), this powerful tool can provide the optimal conditions that improve a process (Yusoff, Ramasamy, and Yusup, 2011)

1.3 RESEARCH OBJECTIVES

The specific objectives in this research are:

1) Production and characterization of recycled PP hybrid composite based on fibre treatment, fibre ratio and coupling agent.
2) Evaluate the effects of different fibre treatment, coupling agent and fibre ratio on the physical and mechanical properties of hybrid composites.
3) Evaluate the hygrothermal ageing, natural and accelerated weathering and its effect on mechanical, thermal, and interfacial properties of composites.
4) Determine the mathematical model for hybrid composites to predict the physical properties of EFB-G fibre hybrid composites.
5) Optimization of EFB-Glass fibre hybrid composites by using design expert.

1.4 SCOPE OF THIS STUDY

1) Compare and optimize the standard, homemade, microwave and ultrasonic EFB fibre alkali treatments.
2) Production of hybrid composites using EFB-Glass fibre with recycled PP composites.
3) Optimization of the fibre treatment, EFB-Glass fibre ratio and coupling agent in the composites.
4) Study the weathering effect on mechanical, thermal, and interfacial properties of composites.
5) Evaluate the hygrothermal ageing, water absorption and its effect on the mechanical, thermal, and interfacial properties of composites.
6) Morphological analysis through optical microscopy and Scanning Electron Microscopy.
7) Optimization of EFB-Glass fibre hybrid composites using Response Surface Methods.

1.5 SIGNIFICANCE OF STUDY

Palm oil glass fibre reinforced recycled polypropylene composites can be used as an alternative raw material led to the replacement of current used glass fibre composite and improvement in natural fibre composites to reduce the cost of raw material in industry, reduce environmental problems caused by alkali treatment. Increase and optimize the physical and mechanical performance of the composites and enhance the use of hybrid composites for the external uses and marine conditions.

1.6 ORGANIZATION OF THESIS

The organization of this thesis goes as follows;

Chapter 1. It introduces hybrid composites and asserts the purpose and main objective of the research.

Chapter 2. Briefly describe and reviewed the natural fibre, matrix, glass fibre, fibre reinforced plastic, composite testing and properties and degradation of hybrid composites.

Chapter 3. Present the material, methodology and equipments, composite's testing and characterization, hybrid composite's treatments and analysis, data analysis and optimizations.

Chapter 4. Standart and homemade alkali treatment, mechanical properties, anova and statistical analysis, validation of empirical model, characterization and optimization conventional and homemade composites were discussed in this chapter.

Chapter 5. Describe the Microwave and ultrasonic hybrid composites, response surface and variable interactions, optimization Microwave and ultrasonic hybrid composites.

Chapter 6. Discuss the Comparison of accelerated weathering, hygrothermal ageing properties, comparison of water absorption and melt flow index composites.

Chapter 7. In this chapter summary, the major features of this thesis and proposes some research points that can be investigated in future work.

CHAPTER 2.

LITERATURE REVIEW

This chapter describes the physical, chemical and mechanical properties of fibre, matrix, and coupling agent, some methods of alkali treatment and mechanism of degradation also describe. Major factors that controlling the performance of hybrid composites were briefly described. Special emphasis was given on the methods of alkali treatment and modification of the fibre-matrix interface by coupling agent. Both hygrothermal and UV degradation behaviour of hybrid composites were also assessed.

2.1 NATURAL FIBRE

Natural fibre are subdivided into fruit fibre, seed fibre, bast fibre, leaf fibre, grass fibre, straw fibre and wood fibre. Modern process made natural fibre as industrial material that low cost, high strength and stiffness environmental friendly and wide range in quality and availability(J. K. Lee andHan, 2000; Liu, Song, Anderson, Chang, and Hua, 2012).

2.1.1 Chemical composition of natural fibre

Natural fibre is composed of cellulose, hemicellulose, and lignin. Softwoods and hardwoods have fairly similar cellulose contents, but the lignin content of softwoods is higher. A large number of modification reactions for lignins to improve fibre properties

has been reported throughout the literature (Bourry and Favis, 1998; Pantani, Coccorullo, Speranza, and Titomanlio, 2007).

Cellulose: Cellulose is the essential component of natural fibre. The molecular structure of cellulose is responsible for its chemical and physical properties. In previous study conduct by (Rauwendaal, 2002) concluded that cellulose type strongly enfluen fibre mechanical properties because geometrical conditions and cell geometry specific for each cellulose type.

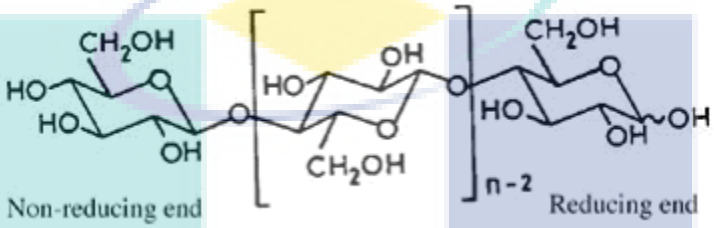

Figure 2.1: Structure of Cellulose.
Source :(Rauwendaal, 2002)

Hemi-cellulose: Hemi-cellulose is a form of cellulose that comprises of a group of polysaccharides (excluding pectin) that remains associated with the cellulose after lignin has been removed. The hemi-cellulose differs from cellulose in three important aspects. In the first place, they contain several different sugar units whereas cellulose contains only 1.4-β-D-glucopyranose units. Secondly, they exhibit a considerable degree of chain branching, whereas cellulose is a strictly linear polymer. Thirdly, the degree of polymerization of native cellulose is ten to one hundred times higher than that of hemi-cellulose. Unlike cellulose, the constituents of hemi-cellulose differ from plant to plant(Rauwendaal, 2002).

Lignin: Lignin is the reinforcing substance that makes tree cells wood ‘hard’ and 'woody' rather than soft, which are complex hydrocarbon polymer with both aliphatic and aromatic constituents. Softwood has 24–33% of Lignin content and 16–24% for hardwood (Bourry and Favis, 1998).

2.1.2 Physical and mechanical properties of natural fibre

Natural fibres are in general suitable to make reinforce plastics, due to their relative high strength and stiffness and low density (J. K. Lee and Han, 2000; Liu et al., 2012). The range of the mechanical and chemical characteristic values is one of the weaknesses for all natural fibre, the differences in fibre structure and properties due to the natural condition and overall environmental conditions during growth. Natural fibres can be processed in different ways to improve properties as reinforcing material as point out by many reseacher. (Beckermann and Pickering, 2009; Bergeret, Ferry, and Ienny, 2009; Colom, Carrasco, Pagès, and Cañavate, 2003; Demir, Atikler, Balköse, and TihmInlIoglu, 2006).

2.1.3 Oil palm empty fruit bunch fibre (EFB)

Oil palm fibre (OPF) extracted from the empty fruit bunches is proven as a good raw material for hybrid composites. The cellulose content of EFB is in the range of 43%–65% and lignin content is in the range of 13–25%. In the previous study conducted by (Sreekala, Kumaran, Joseph, and Thomas, 2001) The effect of hybridisation of the oil-palm fibres with glass fibres on the relaxation behaviour to explain the long-term behaviour of the composites. The suitability of EFB in various polymeric matrices such as, polypropylene, polyvinyl chloride, phenol formaldehyde, polyurethane, epoxy, polyester, etc. to form bio composites have reported (Shinoj, Visvanathan, Panigrahi, and Kochubabu 2009). Addition of EFB content in the composites became more hydrophilic and increase mechanical properties and Alkali treatments of the fibre surface improved the composite properties' fibre–matrix adhesion. High cellulose content and high toughness value of OPF make it suitable for composite applications. However, presence of the hydroxyl group makes the fibres hydrophilic, causing poor interfacial adhesion with hydrophobic polymer matrices during composite fabrication. This may lead to poor physical and mechanical properties of the composite (Shinoj et al. 2009).

Porous surface morphology in the palm oil fibre is useful for better mechanical interlocking with matrix resin in composite fabrication. However, the porous surface

structure also facilitates penetration of water into the fibre by capillary. Chemical treatments decrease hydrophilic property of the fibres and also significantly increase wet ability with polymer matrix. There are numbered of treatment methods on fibre to improve its properties and make it compatible with polymeric matrices (Asumani, Reid, and Paskaramoorthy, 2012;Colom et al., 2003; Kalam, Sahari, Khalid, and Wong, 2005).

2.1.4 Effect of fibre treatments.

Previous report present by Roy et al,(2012) explain that alkali fibre treatment by sodium hydroxide enhanced the tensile strength and elongation at break by 82% and 45%, respectively but decreased the hydrophilicity by 50.5% and the diameter of the fibres by 37%. Tensile test results by Roy et al (2012) and Shanmugam et al, (2013) showed that alkali-treated fiber composites increased in fracture strain twice to three times more than untreated fiber composites.Sodium hydroxide treatment of cellulose increases the amount of amorphous cellulose at the expense of crystalline cellulose. Hydrogen bonding network will be broken, and the hydroxyl groups of cellulose will become more active, and this fact improves the hydrophilicity of the fiber as well as its compatibility with the hydrophilic resin (Roy et al., 2012). The cellulose–sodium hydroxide reaction is thought to be as follows.

$$Cell\text{-}OH + NaOH \longrightarrow Cell\ O^{-}Na^{+} + H_2O + (surface\ impurities) \qquad (2.1)$$

Mercerization improves adhesion by removing surface impurities, thus exposing micro-fibrils, which then render the fibre topography with a rough texture. The rough and cleaned surface facilitates mechanical adhesion in addition to improved resin to penetration, wetting ability of the resin and fiber–matrix interaction at the composite's interface (Peng, Zhong, Ren, and Sun, 2010;Roy et al., 2012; Shanmugam and Thiruchitrambalam, 2013).

2.1.5 Hydrophilic and limitation fibre

Organic fibres have high moisture absorption that can result in swelling of the fibres and concern about the dimensional stability of the agro-fibre composites(Karlsson, Andersson, Berntsson, Chihani, and Gatenholm, 1998). The absorption of moisture by the fibre is minimized due to encapsulation by the polymer, introducing new surface properties and favoring dispersion in a polymeric matrix(Tabtiang and Venables, 2002). Peroxide treatment of fibre improved interfacial interactions reduced the hydrophilic fibre and eliminate the absorption of moisture (Hung, Chen, and Wu, 2012). The moisture absorption of the fibres can be dramatically reduced through the acetylating of some of the hydroxyl groups present on the fibre, but with the increase at the cost of the fibre. Good fibre-matrix bonding can also decrease the rate and amount of water absorbed by coupling agent in the composite (Lu, Askeland, and Drzal, 2008)

The porous structure of fibres leads to an initial capillary uptake which results in the large initial uptake in all cases. Treatment considerably reduces the overall water uptake at all temperatures, and the initial uptake due to the capillary action is also reduced(Karlsson et al., 1998). The decrease in uptake value for treated fibres will be attributed to the physical and chemical changes occurred to the fibres upon different treatments. Introduction of coupling agents and acetylation make the fibre hydrophobic and thus reducing moisture absorption and give a coating of the fibre surface, (Sreekala and Thomas, 2003).

While the advantages of natural fibres are particularly attractive to the composite industry, there are some limitations in their use, the low processing temperatures (due to deterioration of properties of the fibres when they are subjected to heat conditions), and weak surface adhesion(Colom et al., 2003). Natural fibres are hydrophilic materials while some thermoplastic as Polymers are hydrophobic leading to an incompatibility between them and the high moisture absorption that decreases adhesion forces between fibre and matrix and affects the dimensional stability of final products are some negative characteristics observed in lignocelluloses fibres composites.(Li, Mai, and Ye, 2000; Li and Pickering, 2008; Madsen, Thygesen, and Lilholt, 2009).

Water Absorption

Water absorption is a severe problem presented by agro-fibres. Cellulose, one of the main constituents of cell walls of plants, contains numerous hydroxyl groups that are

strongly hydrophilic (Dhakal, Zhang, and Richardson, 2007; Espert, Vilaplana, and Karlsson, 2004). Amorphous cellulose and hemicelluloses are considered to be major responsible for the high-water uptake of natural fibres, since they contain numerous easily accessible hydroxyl groups; whereas theoretically, composites with fibres containing higher lignin content should present lower values of water uptake, since lignin is a hydrophobic compound that acts against hydrothermal degradation in fibres(Beg and Pickering, 2008c). High-water contents could affect the dimensional stability of the final product, narrowing the field of application of EFB based composites(Pejic, Kostic, Skundric, and Praskalo, 2008). Some tests have been realized to obtain information about the long-term water absorption and the influence of water absorption of agro-fibres in polymeric blends; however, further understanding of different systems is still needed(Errajhi, Osborne, Richardson, and Dhakal, 2005).

Adhesion Ability

The incompatibility between agro-materials and polymers is usually confirmed by the weak interfacial bonding observed between the two surfaces. The filler-matrix interfacial phenomenon is responsible for the stress distribution and transfer between both components, determining the mechanical and physical behaviour of composites. It is well known that polar and non-polar surfaces can only promote poor adhesion between them, leading to low strength and stiffness blends (Hung et al., 2012).

Degradation

Agents such as water, ultraviolet radiation, thermal cycling and fungal attack can promote degradation of composites, thus, endorsing the degradation of composites that contain natural fillers. Khalil, Bhat, and Sartika (2010)had tested visual and mechanical characteristics of thermoplastic-natural fibre composites after exposure to some of these agents. Degradation dependence on the loading level of filler and matrix type was reported for the tested composites, oxidation was the most expressive sign of the degradation of the specimens(Harnnecker, dos Santos Rosa, and Lenz, 2011). In general, the main degradation happens in the fibre material, and the polymer matrix is the phase of the composites usually less affected. Temperature is the one that causes the highest

deterioration of the natural fibre properties due to degradation/modification of its chemical constituents(Khalil, Bhat, and Sartika, 2010). Physical and chemical changes are likely to occur when agro-fibres are submitted to elevated temperatures during either processing or labour, hence, compromising the performance of the composite. The rate of thermal decomposition of lingo cellulosic materials, for example, was reported to increase exponentially with an increase in temperature.(Mukhopadhyay and Srikanta, 2008; Zheng, Cao, Wang, and Chen, 2007).The degradation process at lower temperatures is associated with the degradation of hemi cellulose whereas higher temperature processes (280-300°C) would cause degradation of lignin. Furthermore, the rate of degradation was found to be dependent upon the preparation method. Such results indicate that some treatments are able to improve the thermal stability, enhancing their suitability for processing with a large number of thermoplastics that have their melting point somewhere between 160°C and 240°C(B. Singh, Gupta, and Verma, 2000).

2.2 MATRIX

2.2.1 Thermoplastics Matrix

Thermoplastics are made up of flexible linear chains, which allowed thermoplastics to undergo elastic deformation due to the stretching of covalent bond within the chain. In thermoplastics, most of the work reported so far, deals with polymers such as polypropylene (PP), polyethylene (PE), polystyrene (PS), polyamide and polyvinyl chloride (PVC). This is mainly because the processing temperature of thermoplastic is restricted to temperature below 200ºC to avoid thermal degradation of natural fibres. PP and PE have the lowest densities with a low level of moisture absorption.

The advantages of thermoplastic matrices were lower cost, Design flexibility ease of moulding flexible tough and Recycleable(Beier et al., 2008). PP has the best combination of strength and stiffness, therefore, Recycled PP was selected as a matrix for this study. The percentage of loading is limited by the process ability of the composite.

The weaknesses of the thermoplastic matrix were different chemical structure compared to natural fibres as they have a high non polar nature. The fibre orientation in the composites is random, and the property modification is not as high as is observed in the thermo set composites. Production is more complex and has a lower cross linked chain structure, which allows the chains to slide and rotate easily. This chain structure gives thermoplastic low strength, brittle and fewer stiffness properties (Huang and Young, 1996).

2.2.2 Polypropylene (PP)

Polypropylene (PP) is a thermoplastic polymer, can be made by the addition polymerisation process. PP has a melting point of about 165^{o}C, glass transition temperature (T_g) about -10^{o}C. The most commercial PP has an intermediate level of crystallinity, between 40-60%, Depending on their crystalline, density ranges from 0.85 g/cm^3 to 0.95 g/cm^3(Busico and Cipullo, 2001). Its Young's modulus is also intermediate. Although, it is less tougher than high-density polyethylene (HDPE) and less flexible than low density polyethylene (LDPE), it is much more brittle than HDPE (Busico and Cipullo, 2001). This allows PP to be used as a replacement for engineering plastics, such as acrylonitrile butadiene styrene (ABS). PP can be made translucent when uncoloured but not completely transparent as polystyrene or acrylic. Polypropylene has very good resistance to fatigue (Tjong, Xu, Li, and Mai, 2002).

2.2.3 Selection of thermoplastic

Several different EFB-glass fibres recycled polyprophylene composite's formulations were evaluated to determine if they had the ability to reduce glass fibre-reinforced material with better mechanical properties and lower cost. Recycled polypropylene with a very high melt flow index was used to aid in fibre matrix adhesion and to ensure proper wetting of the fibre (Sreekala et al., 2002; Yao et al., 2007). Composites were made with 40 % fibre content of empty fruit bunch and glass fibre provide better mechanical properties.(Reid, I'Ons, and Paskaramoorthy, 2004; Abdelmouleh, Boufi, Belgacem, and Dufresne, 2007).

2.3 FIBRE REINFORCED PLASTIC.

2.3.1 Glass fibre

Glass fibres are popular in many applications due to their high strength and low cost. Glass fibres are produced by extrusion of the molten mixture of silica ($Si0_2$) and other oxides through a bushing with small holes. This process produces glass fibres of amorphous microstructure and isotropic properties that tend to be high strength but low in stiffness. Glass fibre had density 2.55 g/cm^3, tensile strength 1454 MPa young's modulus 70 Gpa and diameter 16,1 µm.(Mohd Ishak, Ishiaku, and Karger-Kocsis, 2000; Plonka et al., 2004)

The bonding between glass fibre and thermosetting resin is normally enhanced by silane or MAPP treatment on the fibre surface. A general chemical formula of silane is X3Si-R, which is a multifunctional molecule that bonds both to the glass fibre surface and polymer matrix. There are three distinct structural regions in the interphase formed by MAPP layers. The outermost layer, furthest away from the glass fibre surface, is a physiosorbed layer consisting of weak oligomericsiloxanols possesses good resistance to hydrolysis. The inner most regions next to the glass surface are stable and resistant to extraction by hot water and may be regarded as a chemically reacted region where the interconnecting crosslinking is extensive, and a three-dimensional network of siloxane

exists. This region provides resistance of the interface bond in glass fibre composites to hydrothermal attack (Selmy, Elsesi, Azab, and Abd El-baky, 2012; Sreekala, George, Kumaran, and Thomas, 2002; Yao et al., 2007).

2.3.2 Coupling agent

Bonding at the fibre-matrix interface plays an important role in controlling composite properties. A strong interfacial bond is needed for efficient transfer of the applied load. In hybrid composites, MAPP and Fusabond P 613 coupling agents are used to improve physical, mechanical and chemical bonding between the fibres and the polymer matrix and to give greater durability and resistance to extreme conditions (Sreekala et al., 2002). Several mechanisms have been proposed to explain the coupling agent interfacial reinforcement. Coupling agents carry an organic functional group that can react with the matrix, and improve fibre-matrix bonding,(Abdelmouleh et al., 2007; Mohd Ishak, Ariffin, and Senawi, 2001; Sreekala et al., 2002; Xie, Hill, Xiao, Militz, and Mai, 2010).

2.3.3 Mechanism of Reinforcement

Reinforcement of a low modulus polymer with a high modulus, high-strength fibre uses the elasticity of the polymeric material under stress to transfer the load to the fibre. This gives a moderate strength high modulus composite. The aim of the combination is to produce a two-phase material in which the fibre is well dispersed and bonded by polymer matrix. The principal constituents influencing the strength and stiffness of composites are the reinforcing fibres, the matrix and the interface between the fibres and the matrix. (Jacob, Varughese, and Thomas, 2006; K. Joseph, Thomas, and Pavithran, 1995; S. Joseph, Sreekala, Oommen, Koshy, and Thomas, 2002).

Composite materials consist of two or more components, at least one of which is reinforcement and another matrix. The matrix acts as a binder, which keeps the reinforcement together and transfers the load to it. It also contributes toughness (the ability to absorb energy) to the composite which natural fibre or glass fibre alone would

not have(Fu, Wu, and Han, 2002). The reinforcement bears load and provides stiffness and strength to the composite. Based on the premise of "the whole is better than the sum of its parts," the material is created with properties that are better than those of the components that make it (Abdelmouleh et al., 2007; Saujanya and Radhakrishnan, 2001). EFB-Glass fibre reinforced recycled PP composites (EGRPP) are made of recycled polypropylene as a matrix and EFB fibres and glass fibre as reinforcement (Alsaeed, Yousif, and Ku, 2013; López-Manchado andArroyo, 2000). Due to their low cost, light weight and environmental benefits, these materials are expected to replacing traditional glass fibre composites and other human-made fibres in automotive industry, wood in furniture industry and some structural products in building or outdoor application.

2.3.4 Dispersion of Fibre in the Matrix

The surface adhesion between the fibre and the polymer plays an important role in the transmission of stress from the matrix to the fibre and thus contributes to the performance of the composite. Most polymers, especially thermoplastics, are non-polar (hydrophobic) substances that are not compatible with polar (hydrophilic) fibres; it prevents efficient fibre-matrix bonding. Therefore, the result is poor adhesion between polymer and fibre(Arbelaiz, Fernandez, et al., 2005). In order to improve the affinity and adhesion between fibres and thermoplastic matrices, chemical coupling agents have been employed.(Foulc, Bergeret, Ferry, Ienny, and Crespy, 2005; Gellert and Turley, 1999; George, Bhagawan, and Thomas, 1997).

Maleic anhydride (MA)-grafted polypropylene (MAPP) has been reported to function efficiently for lignocelluloses-PP systems. Earlier results suggest that the amount of MA grafted and the molecular weights are both important parameters that determine the efficiency of the additive. The Maleic anhydride present in the MAPP not only provides polar interactions, but can covalently link to the hydroxyl groups on the lingo cellulosic fibre (Yao et al., 2007). Grafting chemical series on to the fibre surface has also been reported to improve the interaction properties between the fibres and matrix. Although grafting can improve properties of the composites to a significant extent, this process increased the materials cost of the system. The use of dispersing agent and/or coupling agents is a cheaper route to improve properties and makes more practical

sense for high volume, low cost composites systems(Selmy et al., 2012; Sreekala et al., 2002; Yao et al., 2007)

2.3.5 Challenges of Glass fibre reinforced Recycled PP composites.

Glass fibre reinforced Recycled PP composites has advantages than bio composites include the lower of hydrophilic properties of natural fibres and higher compatibility with hydrophobic polymeric matrices, and relatively higher processing temperatures range to not degrade properties during manufacture(Arbelaiz, Fernandez, et al., 2005). Glass fibre reinforced Recycled PP composites are also more durable to biologic degradation, UV degradation, high bond strength and lower moisture absorption. Natural fibres are susceptible to degradation because organisms interact with carbohydrates in the natural fibres and break them down. Photochemical (UV) degradation takes place when some natural fibres are exposed to outside light. Natural composites must be surface treated to avoid these forms of degradation. Moisture absorption of the finished product is also a downside to bio composites.(Arbelaiz, Fernandez, et al., 2005; Ayrilmis, Jarusombuti, Fueangvivat, Bauchongkol, and White, 2011) .

Composites reinforced with short oil-palm empty fruit bunch fibres as a function of fibre loading, fibre treatment, effect of hybridisation of the oil-palm fibres with glass fibres, physical ageing and strain level has been studied by (Sreekala et al., 2001). Maximum stress relaxation was observed for 30 wt % fibre loading and Water ageing increased the rate of relaxation. (Sreekala et al., 2001) One possibility to improve mechanical performance is the reinforcement by two or more fibre types in a single matrix leading to hybrid composites with a great diversity of material properties. The advantage of using a hybrid composite is that one type of fibre could complement what is lacking in the other. Combining the higher mechanical performance of glass fibres and the environmental advantages of natural fibres improve performance and environmental advantages of composite material(Arbelaiz, Fernandez, et al., 2005).

2.3.6 Compounding

Compounding is a process of combining a number of different components into one. These different components combine to form a new material with properties of its own, which are not necessarily those of its constituents.A screw pushes thermoplastic granules or powder through a heated cylinder, changing the plastic from solid to liquid and mixing the plastics as it moves through the barrel, then through the die, which will give the plastic a constant cross section area. The plastic is melted in the barrel by the mechanical energy from the rotating screws, and the heat transferred from the high-temperature barrels(Padmanabhan, 2008).

There are two common types of extruders, single screw and double screw extruder. For single screw extruders, friction between the plastic and the rotating crew makes the resin rotate with the screw. The friction between the rotating resin and the barrel pushes the materials forward and generates heat. Single screw extruders are not positive displacement, so they are not effective mixing devices. A twin-screw extruder is a compounding device to uniformly blend plasticizers, fillers, etc. into the plastic melt. Twin screw extruders have been intermeshing screws, the relative motion of the flight of one screw inside the channel of another, pushes the material forward with very low friction(J. K. Lee andHan, 2000;Rauwendaal, 2002)

The twin-screw extruder is a versatile machine that can be used to form composite materials. The extrusion process melts and mixes powdered or granular polymers into a continuous melt. The melt stream is then sent to the die in this research recycled polypropylene was mixed with the coupling agent EFB and glass finer to make the new form of hybrid composites (Rauwendaal, 2002). The primary advantages of these extruders are their modularity that makes them very flexible and adaptable to specific process requirement, coupled with their excellent distributive and dispersive mixing. They also have wide residence time, temperature, screw speed and torque setting(Bourry and Favis, 1998).

2.3.7 Injection Molding

Injection molding is the most widely used composites' fabrication process. A large pressure and specific temperature must be used to inject the polymer into the hollow mould cavity. More melting composite must be packed into the mould during solidification to avoid shrinkage in the mould. Identical parts are produced through a cycle process involving the melting of pellet or powder resin followed by the injection of the polymer melt into the hollow mould cavity under higher temperature and pressure (Tabtiang and Venables, 2002). Injection molding can be used to form a wide variety of products, for both thermosets and plastics. Complexity is virtually unlimited. Sizes can vary, and excellent tolerance is also possible. Extrusion or compounding is used prior to injection molding when mixing of a thermoplastic, filler fibre and additive are required (Pantani et al., 2007; Tabtiang and Venables, 2002).

2.4 COMPOSITE PROPERTIES AND TESTING

2.4.1 Tensile Properties

In terms of practical application's yield strength, tensile strength, and elongation at break are the most important mechanical properties. These are commonly determined from stress-strain curves (Vasile and Pascu, 2005).Several Several different types of mechanical properties are used to characterize composites, but three important properties of load-bearing composites are usually tensile strength, stiffness, and toughness(Abdul Khalil, Hanida, Kang, and Nik Fuaad, 2007).

On the composite's samples, tensile testing is one of the most common forms of physical testing performed. Composite deformation can be very dependent on temperature and time. ASTM D 638 and ISO 517 is one of the most widely used in mechanical tests of composite plastics for determining mechanical properties such as tensile strength, yield strength, yield point, and elongation. The stress-strain curve from tension testing is also a convenient way to classify composite plastics (ASM-International, 2003).

2.4.2 Melt Flow Index

The melt index (MI) also known as the ‘‘melt flow index’’ (MFI) of a composite refers to the rate at which it extrudes from a capillary die under a standard set of conditions. The melt index of a composite's polypropylene depends on its molecular characteristics, primarily average molecular weight, molecular weight distribution, and branching characteristic's short chain versus long chain, concentration, and distribution (Peacock, 2000) One of the most common physical properties routinely reported on manufacturer resin data sheets is the melt index (MI) (for polyprophylene) or melt flow rate (MFR) (for all other thermoplastic resins, alloys, and composites)(ASM-International, 2003).ASTM D 3364-94 is similar to ASTM D 1238-98, but it uses a capillary die that is three times longer. ASTM D 1238-98 cites the average flow (g/10 min) of a thermoplastic material through a standardized orifice under standardized conditions (temperature and dead load).

2.4.3 Thermal Stability

Thermal stability of a material is stability against degradation upon exposure at elevated temperatures in an inert environment. Composites are often exposed at high temperatures during processing and for a wide range of applications, thermal stability is the most important properties of polymer (Bicerano, 1996). Thermal stability is characterized by degradation temperature and monitoring mass change in materials. Several reactions involve the mass changes, including dehydration, desorption, decomposition and oxidation (ASM-International, 2003). The TG technique is simple but effective for assessing thermal stability and chemical reactions in composites.

2.4.3.1 Accelerated Weathering Degradation

Accelerated weathering test combines factors that affect degradation in natural weathering, e.g. sunlight exposure, rain, humidity, condensation, heat or temperature, etc. During accelerated weathering measured variables can include exposure time, UV exposure as radiant energy over a specific wavelength range, and water exposure as the

number of cycles or time cycles (Al-Madfa (1998); Mohamed, and Kassem, 1998), (Beg and Pickering, 2008a). Laboratory accelerated weathering testing using environmental chambers and artificial light sources to approximately replicate outdoor conditions but with a greatly reduced test time under highly controlled conditions. Laboratory testing can quickly assess the relative stability of plastics but has the major disadvantage that the quicker the test the lower the correlation to real behavior on the field (K. Joseph et al., 1995).

Beg andPickering (2008a) have studied accelerated weathering of unbleached and bleached Kraft wood fiber reinforced polypropylene composites using QUV tester with UVA lamp (340 nm) at irradiance 0.68 W/m2. This study was conducted up to 1000 hours. (Al-Madfa et al., 1998) has also studied accelerated weathering of LDPE using QUV accelerated weathering tester at irradiance of 0.68 W/m2 and 340 nm (UVA lamp). The duration of test was up to 5000 hours. Islam, Pickering, and Foreman, (2009) have conducted a study on accelerated weathering of PLA using weathering device, which utilizes a UV lamp.

2.4.3.2 Natural Weathering Degradation

Weathering due to UV radiation can vary dramatically depending upon the location on the product on the world, and the intended application location should always be specified at the earliest stage. Temperature also plays a role in weathering since the degradation process is temperature dependent, it will occur more rapidly at higher temperatures. Tropical areas, therefore, suffer not only from increased UV exposure but also faster reaction rates because of the increased temperatures. Humidity is also important to be considered in natural degradation. Most weathering processes are considerably slower in hot dry climates than in hot wet climates(Hung et al., 2012)

Outdoor exposure can be performed on samples mounted on testing racks, oriented under standard conditions to expose the material to the full radiation spectrum besides the temperature and humidity of that location (Baljit Singh and Sharma, 2008). Ojeda et al., (2011) have studied natural weathering of PP, LLDPE, HDPE and LLDPE/HDPE blend. The samples was put on the platforms that were built with an angle of 30° to the ground, facing the equator, in Porto Alegre, RS (Brazil), 30°02'S; 51°12' W.

The results showed that PP and the HDPE/LLDPE with pro-oxidant additives blend are rapidly degrading materials, whereas HDPE and LLDPE degrade more slowly Ojeda et al., (2011).

2.5 DEGRADATION OF HYBRID COMPOSITES

2.5.1 Thermal Stability of the natural Fibre

The primary drawback of the use of agro-fibres is the lower processing temperature permissible due to the possibility of lignocelluloses degradation and/or the possibility of volatile emissions that could affect composite's properties. The processing temperatures are thus limited to about 200^{o}C, although it is possible to use higher temperatures for short periods of time. This limits the type of thermoplastics that can be used with agro-fibres to commodity thermoplastics such as polyethylene, polypropylene, polyvinyl chloride, and polystyrene(Hung et al., 2012).

2.5.2 Thermogravimetry Analysis

Thermogravimetry (TG) is a technique for measuring mass change of a sample with temperature. A sample to be measured is placed into a furnace and its mass change is monitored by a thermobalance (S. Nayak, 2009). The main application of TG is to analyze material decomposition and thermal stability through mass change of a function of temperature in scanning mode or as a function of time in the isothermal mode. TG curves are plotted as mass change expressed in percent versus temperature or time(Leng, 2008). Decomposition of a composite's sample is represented by two characteristic temperatures: Ti and Tf. Ti is the lowest temperature when the onset of mass change is detected, and Tf is the lowest temperature when the mass change is completed. The TG thermo balance structure includes a microbalance, furnace, temperature programmer and computer. The key component is the microbalance, which measures the mass change. A

typical microbalance is able to measure mass change of ±1µg with maximum mass of 100 mg (Leng, 2008).

2.5.3 Degradation by Moisture Absorption

Amorphous cellulose and hemicellulose are mostly responsible for the high-water uptake of natural fibres, since they contain numerous easily accessible hydroxyl groups, which give a high level of hydrophilic character to fibres. Due to this hydrophobicity, swelling by water uptake can lead to micro-cracking of the composite and degradation of mechanical properties (Mohd Ishak et al., 2000). Moisture penetration into composite materials occurs by three different mechanisms. The main process consists of diffusion of water molecules inside the micro-gaps between polymer chains. The other mechanisms are capillary transport into the gaps and flaws at the interfaces between fibres and polymer due to incomplete wettability and impregnation, and transport by micro-cracks in the matrix, formed during the compounding process (Akil, Cheng, Mohd Ishak, Abu Bakar, and Abd Rahman, 2009).

2.5.4 Degradation by Ultra-Violet (UV) Radiation

UV exposure can cause changes to the surface chemistry of the composite also known as photo degradation, which may lead to discoloration making the products aesthetically unappealing. Furthermore, prolonged UV exposure may ultimately lead to lose in mechanical integrity. The composites reinforced with fibres containing large amounts of lignin are more susceptible to natural weathering than those with negligible amounts of lignin. This is because lignin and hemicelluloses existing in the middle lamellae of wood fibres are more susceptible to chemical degradation than cellulose. Hemicelluloses are responsible for moisture sorption and biological degradation in wood

to a much greater extent than cellulose. Lignin is responsible for ultraviolet degradation,(Mascia and Zhang, 1995; Mohd Ishak et al., 2000).

2.5.5 Hygrothermal Ageing

Moisture penetration into composites caused by water molecule diffusion. Capillary and micro-crack transport by matrix can lead micro-cracking and degradation of mechanical properties,(Beg andPickering, 2008b;Akers and Studinka, 1989).

$$\% \text{ Uptake} = \left(\frac{wt-w0}{w0}\right) \text{ X } 100 \% \qquad \text{Equation 2-1}$$

Reduce moisture absorption in hybrid composites need an expensive surface barrier.(Akil et al., 2009;Alix, Lebrun, Morvan, and Marais, 2010), Optimization of interfacial adhesion between fibre's coupling agent and polypropylene matrix lead to better compatibility and adhesions and decrease moisture penetration and properties degradations(Assarar et al., 2010;B.C, 2006; Beg andPickering, 2008c;Cervenka, Young, and Kueseng, 2005;Wang et al., 2006;Pegoretti and Penati, 2004).

CHAPTER 3.

RESEARCH METHODOLOGY

This chapter has presented a detailed about the method was used for this study, also the implementation of methodology's procedure, there are seven sections to this chapter, namely overall research works, material, methodology and equipment, composite's testing and caracterisation, hybrid composite's treatments and analysis, data analysis and optimizations.

3.1 OVERALL RESEARCH WORKS

The study of characterization and optimization of oil palm empty fruit bunch-glass fibre reinforced recycled polypropylene hybrid composites comprised many experimental laboratory activities. The term of Hybrid means combination not only between EFB and glass fiber but also combination of two coupling agent (Fusabond and MAPP) to improve composite's properties. The main activities in this research were preparation of EFB treatment by conventional, homemade alkali treatment, microwave and ultrasonic assisted EFB alkali treatment, following by compounding. Compounding was carried out to mix of recycled polypropylene matrix, EFB, Glass fibre and coupling agent in various compositions. The compounds were then moulded by injection moulding machine to produce dumbbell specimens of samples. The properties of samples were observed. Treatment's namely thermal treatment, hygrothermal ageing, water absorption, accelerated weathering treatment, and natural weathering treatment, were applied to all samples of composites. The evaluations of samples were observed by comparing properties of samples before and after treatments and between each formulations.and

characterization to obtain their important properties, corelation and optimization of the each hybrid composites. The overall experimental works can be seen in Figure 3.1.

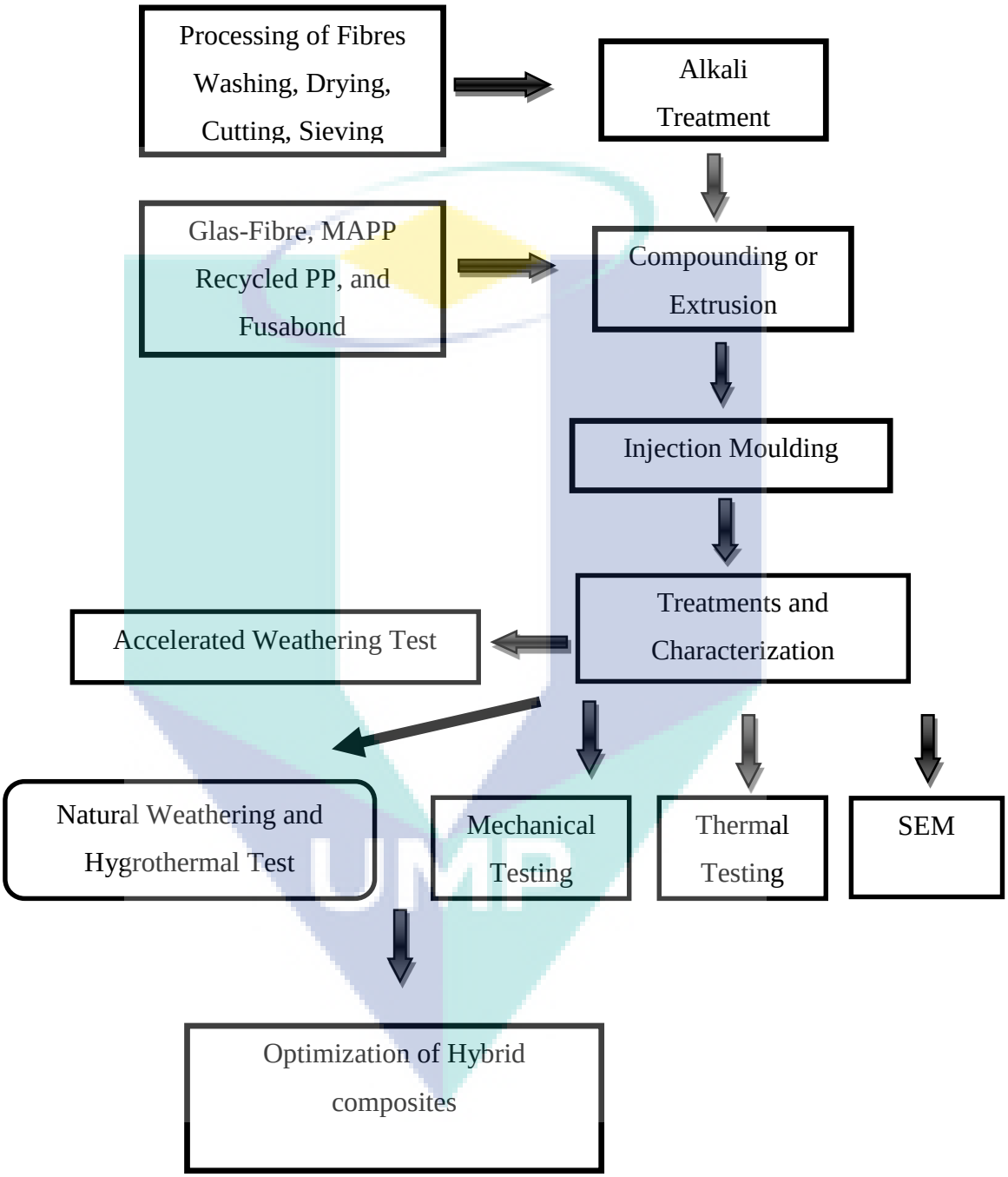

Figure 3.1: Research Methodology for fibre plastic composite

3.2 MATERIAL

Materials used in this study were recycled polypropylene from Alva Suplayer, Sdn Bhd Kuantan Pahang, The recycled polypropylene has a density of 0.951 kg/m^3 and melt flow index (MFI) 0.081 g/10 min at temperature of 190°C and a load of 2.16 kg. Oil palm fibre (OPF) extracted from the empty fruit bunches (fibre length ranged from 2-4 mm) was supplied by Lepar hilir palm oil, Kuantan Pahang Malaysia.Glass fibre (density of 2.56, fibre length ranged from 2-4 mm) was supplayed by Alva Suplayer. Fusabond P 613 coupling agent was made by DuPont, it has a density of 0.903, melt flow rate (190°C/1.0kg), melting point (DSC) 162°C (324°F) melt flow index 120 g/10 min, melting point (DSC) 162°C (324°F) maximum processing temperature 300°C (572°F). MAPP was made by Eastman polymer, polypropylene (Petronas Malaysia), sodium hydroxide, hydrogen peroxide and acetic acid were supplied by Merck.

3.3 METHODOLOGY AND EQUIPMENTS

3.3.1 Physical treatment

Preparation of EFB was carried out in two stages. The first stage is physical treatment where the empty fruit bunch was dried by sun for a minimum of four days, then the fibres were cut using crusher machine and was passed a sieve to obtain a uniform size of empty fruit bunch fibre. TST plastic crusher SC7514 series SCB 3140/14 Hp was used for this research to cut the dried EFB fibre at 2 to 3 mm fibre length.

3.3.2 Alkaline peroxide treatment of the empty fruit bunch (EFB)

Generally, preparation of EFB was carried out in two stages. Firstly, EFB fibres were soaked in hot distilled water at 70°C for 4-6 hours to remove impurities and large particles. Then, fibre was treated with alkaline peroxide by placing fibres in distilled water containing sodium hydroxide (NaOH) solution. These fibres were then soaked and maintained at certain temperature and times to active the OH group of the cellulose. The

fibre treatment method is commonly known as mercerization. After treatments, EFB fibres were taken out and washed with distilled water. Then, it was treated with 2% H_2O_2 solution at 45°C for couple hours, other the excess NaOH present in treated fibre residue was neutralized by using 10% (v/v) acetic acid (at room temperature) for 30min. The washings were repeated until all the cellulose residue is free from acid. Then, the treated fibre was dried in an oven at 80°C for 48 hours.(Beckermann and Pickering, 2008; Bledzki, Mamun, Jaszkiewicz, and Erdmann, 2009; Bledzki et al., 2009; Vilay, Mariatti, Mat Taib, and Todo, 2008; Van de Weyenberg et al., 2003; Sreekumar et al., 2009).

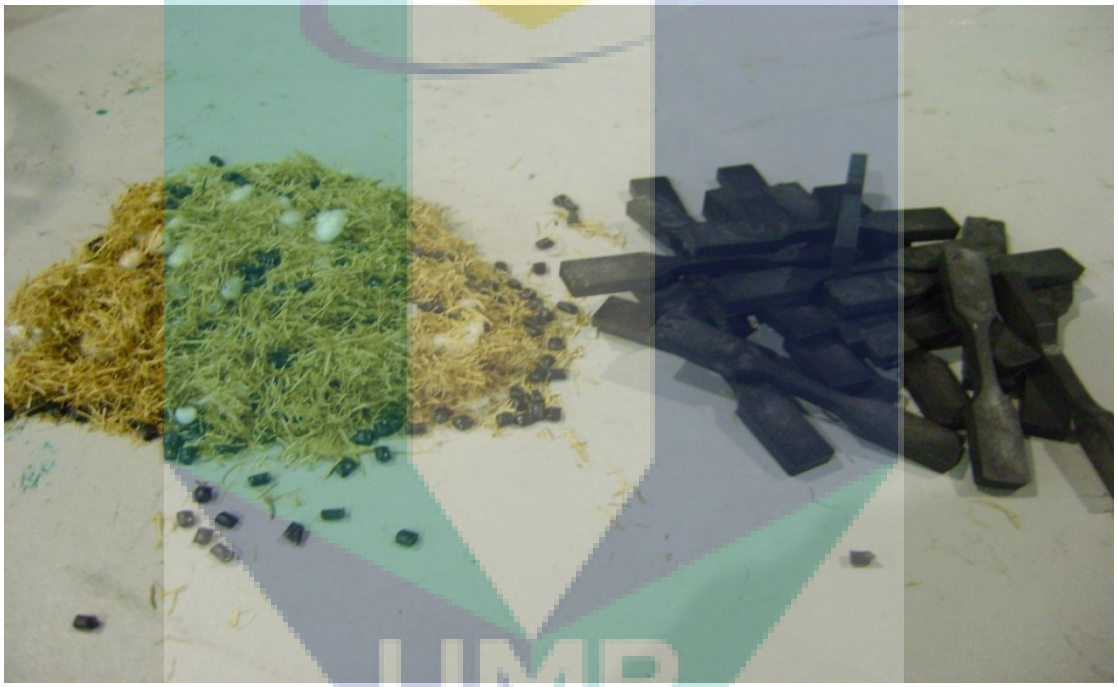

Figure 3.2: Composite raw material and final product

3.3.3 Conventional factor's levels and experimental layout

Conventional alkali treatment methods were used standard procedure and proper laboratory equipment. After the physical and pre-treatment of raw fibres was done, the empty fruit bunch fibre was sun-dried for a minimum four days, and then the fibres were cut using crusher machine and was passed through 500 µm sieve to obtain a uniform size. Untreated fibres were soaked with hot distilled water at 70°C in the water bath for 4-6 hours to remove impurities and large particles. Then, fibre was treated with alkaline

peroxide by placing about 25 g fibres in 500 ml Erlenmeyer flask of distilled water containing 15, 17.5 and 20% (w/w) of sodium hydroxide (NaOH) solution. These fibres were then soaked and maintained at 85°C about 3, 4 and 5 hours in the agitated water bath to activate the OH group of the cellulose.

After treatments, EFB fibres were taken out and washed with distilled water. Then, it was treated with 2% H2O2 solution in water bath at 45°C with a speed of 40 rpm for eight hours. The excess NaOH present in treated fibre residue was neutralized by using 10% (v/v) acetic acid (at room temperature) for 30 min. The washings were repeated until the cellulose residue is free from acid. Then, the treated fibre was dried in an oven at 80°C for 48 hours.

Figure 3.3: Water Bath/Conventional Alkali Treatment

Table 3.1: Conventional treatment factors levels.

Factors	Unit	Levels 1	Levels 2	Levels 3	Levels 4
A: Treatment Time	Hour	3	4	5	
B: NaOH	%	15	17.5	20	
C: Fibre Ratio	%	30	50	70	90

NaOH % was calculated based from dry EFB weight and fibre ratio explains the ratio between Dry weight of EFB and Glass fibre.

Table 3.2: Experimental layout of conventional alkali treatment

Conventional		Factor 1/A	Factor 2/B	Factor 3/C
Std	Run	Treatment Time	NaOH	Fibre Ratio
		Hour	%	%
1	19	5	20	50
2	11	3	17.5	90
3	17	5	17.5	30
4	18	5	20	30
5	5	3	20	70
6	1	4	15	70
7	9	4	20	90
8	7	5	15	90
9	10	3	20	90
10	22	4	17.5	70
11	23	4	20	50
12	15	4	15	90
13	4	5	15	70
14	13	3	17.5	70
15	14	5	17.5	90
16	24	5	20	70
17	16	4	15	30
18	6	3	15	50
19	2	3	15	30
20	20	4	17.5	50
21	12	5	15	50
22	3	3	17.5	50
23	21	4	20	30
24	8	3	17.5	30

3.3.4 Homemade factors levels and experimental layout

In order to reduce the chemical needed for the alkali treatment, reduce operational cost and for equipment's durability, homemade alkali treatment devices were built. It has used 750 watts electric heating source, mercury temperature controller and have 2500 grams of fibre capacity. The purpose of this method is to reduce alkali treatment cost but still maintain the fibre quality in this method Sun drying was used to reduce the operational costs.

Figure 3.4: Homemade Alkali Treatments

Table 3.3: Homemade treatment factors levels

Factors	Unit	Levels 1	Levels 2	Levels 3	Levels 4	Levels 5
A:Temperature	Celsius	60	67.5	75	87.5	90
B:treatment time	Hours	4	5	6	7	8
C:NaOH	%	10	12.5	15	17.5	20
D:Fusabond	%	0	2.5	5	7.5	10
E:MAPP	%	0	2.5	5	7.5	10
F:Fibre ratio	%	50	60	70	80	90

NaOH percentage was calculated based on dry EFB weight. Fusabond and MAPP percentage was calculated based on total weight of fibre. Fibre ratio explains the ratio between dry weight of EFB and Glass fibre.

Table 3.4: Experimental layout of homemade alkali treatment factorial design

Homemade STD	Run	Factor A Temp. Celsius	Factor B Treatmnt Hours	Factor C NaOH %	Factor D Fsabond %	Factor E MAPP %	Factor F Fibre Ratio %
1	5	60	4	10	0	0	50
2	2	60	5	12.5	2.5	2.5	60
3	14	60	6	15	5	5	70
4	12	60	7	17.5	7.5	7.5	80
5	11	60	8	20	10	10	90
6	16	67.5	4	12.5	5	7.5	90
7	4	67.5	5	15	7.5	10	50
8	21	67.5	6	17.5	10	0	60
9	19	67.5	7	20	0	2.5	70
10	10	67.5	8	10	2.5	5	80
11	1	75	4	15	10	2.5	80
12	24	75	5	17.5	0	5	90
13	20	75	6	20	2.5	7.5	50
14	3	75	7	10	5	10	60
15	17	75	8	12.5	7.5	0	70
16	25	82.5	4	17.5	2.5	10	70
17	22	82.5	5	20	5	0	80
18	15	82.5	6	10	7.5	2.5	90
19	23	82.5	7	12.5	10	5	50
20	6	82.5	8	15	0	7.5	60
21	8	90	4	20	7.5	5	60
22	9	90	5	10	10	7.5	70
23	18	90	6	12.5	0	10	80
24	13	90	7	15	2.5	0	90
25	7	90	8	17.5	5	2.5	50

3.3.5 Microwave factors levels and experimental layout

Regular microwave treatment only has power and time setting. It has a drawback in uncontrollable and low accuracy in the fibre treatment because uncontrollable temperature and mistake at the treatment setting time. To avoid this problem for this

research, special device was developed to manage treatment time and temperature during the alkali treatment.

Samsung TDS MW71E /800 W microwave was used in this experiment. Mercury thermostat and electronic timer connected with the magnetron power source of microwave to maintain the correct temperature during treatment times during the treatment. The overall process was similar with the conventional treatment instead a power source to the alkali treatment was from microwave energy.

Figure 3.5: Microwave Alkali Treatments

Table 3.5: Homemade factors levels

Factors	Unit	Levels 1	Levels 2	Levels 3	Levels 4
A:Temperature	Celsius	60	70	80	90
B:Treatent time	Minute	30	60	90	120
C:NaOH	%	10	13	15	18
D:Fusabond	%	2.5	5.0	7.5	10.0
E:Fibre ratio	%	50	60	70	80

Table 3.6: Experimental layout of microwave alkali treatment factorial design

MICR STD	Run	Factor A Temp Celsius	Factor B Time Minutes	Factor C Naoh %	Factor D Fusabond %	Factor E Fibre Ratio %
9	1	80.0	30.0	15.0	10.0	50.0
5	2	70.0	30.0	12.5	7.5	90.0
16	3	90.0	120.0	10.0	7.5	50.0
4	4	60.0	120.0	17.5	10.0	90.0
1	5	60.0	30.0	10.0	2.5	30.0
15	6	90.0	90.0	12.5	10.0	30.0
10	7	80.0	60.0	17.5	7.5	30.0
6	8	70.0	60.0	10.0	10.0	70.0
2	9	60.0	60.0	12.5	5.0	50.0
14	10	90.0	60.0	15.0	2.5	90.0
13	11	90.0	30.0	17.5	5.0	70.0
7	12	70.0	90.0	17.5	2.5	50.0
12	13	80.0	120.0	12.5	2.5	70.0
8	14	70.0	120.0	15.0	5.0	30.0
3	15	60.0	90.0	15.0	7.5	70.0
11	16	80.0	90.0	10.0	5.0	90.0

3.3.6 Ultrasonic factor's levels and experimental layout

Crest Ultrasonic 180DX83 001/230volt 6 amperes was used in the ultrasonic alkali treatment. Two of 1000 ml alkali treatment beaker contain EFB fibre in NaOH solution were soaking in each microwave treatment. The Ultrasonic wave was set in discontinuous mode at medium power to avoid overheating.

Figure 3.6: Ultrasonic Alkali Treatments

Table 3.7: Ultrasonic factors levels

Factors	Unit	Levels 1	Levels 2	Levels 3	Levels 4
A: Temperature	Celsius	60	70	80	90
B:Treatment time	Minute	30	60	90	120
C:NaOH	%	10	13	15	18
D:Extrusion time	Times	1	2	3	4
E:Fibre ratio	%	50	60	70	80

Table 3.8: Experimental layout ultrasonic alkali treatment factorial design

ULTR STD	Run	Factor A Temperature Celsius	Factor B Time Minutes	Factor C NaOH %	Factor D Extr.time Times	Factor E Fibre ratio %
1	5	60	30	10	1	30
2	9	60	60	12.5	2	50
3	15	60	90	15	3	70
4	4	60	120	17.5	4	90
5	2	70	30	12.5	3	90
6	8	70	60	10	4	70
7	12	70	90	17.5	1	50
8	14	70	120	15	2	30
9	1	80	30	15	4	50
10	7	80	60	17.5	3	30
11	16	80	90	10	2	90
12	13	80	120	12.5	1	70
13	11	90	30	17.5	2	70
14	10	90	60	15	1	90
15	6	90	90	12.5	4	30
16	3	90	120	10	3	50

3.3.7 Extrusion

In the present research work, twin –screw extruder was used. Composites were fabricated using Prism Eurolab 16 twin-screw extruder with maintaining five different temperature zones 140, 150, 160, 170 and 180^{o}C from feed zone to exit die and a screw speed setting of 80 rpm. Prior to extrusion, palm fibre, recycled plastic and coupling, agent was dried in an oven at 100^{o}C for a minimum of 48 hours. After the extrusion, the material was palletized into lengths of less than 5 mm by Standard Granulator Fixed Length Pelletiser 554-1330.

3.3.8 Processing methods

There are various methods for processing of randomly oriented fibre reinforced composites. These include the spray-up method, where polymer and resin are sprayed onto the mould simultaneously. Centrifugal casting, where polymer and fibre are placed

inside a cylinder mould which is rotated at very high speed. Vacuum bag and pressure bag processes, where fibre and polymer are placed on the mould, and a pressure or vacuum is applied. Hot and cold press, where fibre and polymer are placed in a mould, and pressure is applied with and without heat, Extrusion and injection moulding, where fibre and polymer are melted and mixed together then forced through a die to form a shape. This study will concentrate on extrusion and injection moulding processes.

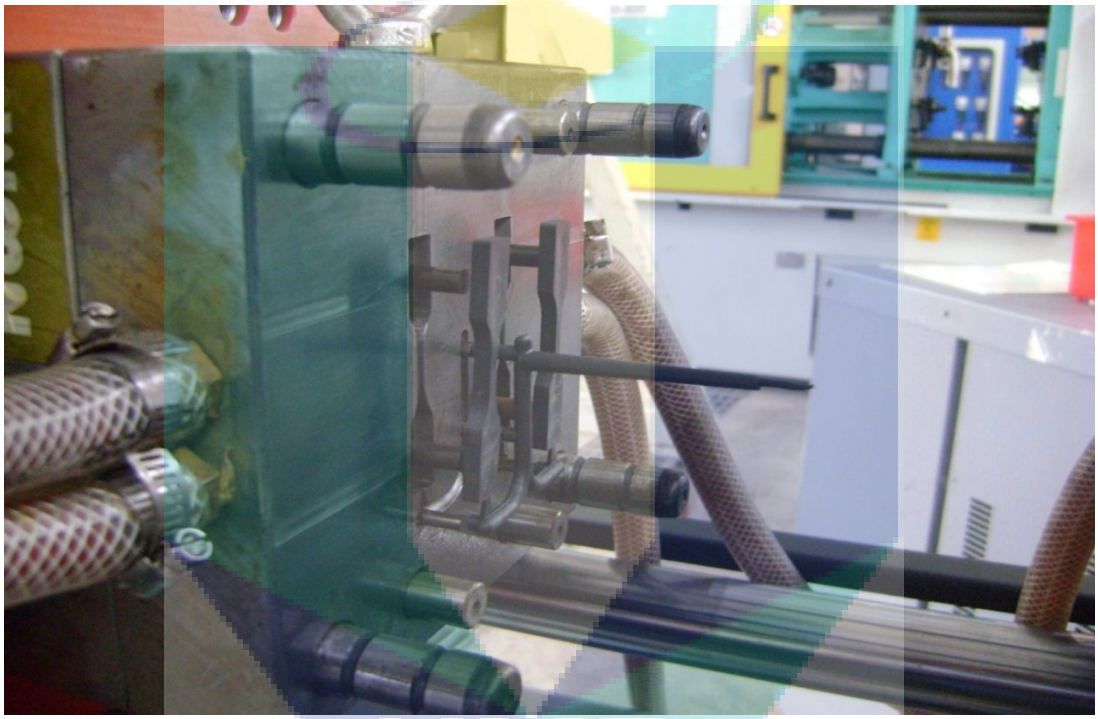

Figure 3.7: Injection moulding

3.3.9 Injection moulding

Nissei Injection moulding NS20 was used to manufacture composite at 100 rpm screw speed, temperature at 190 °C and 40% injection pressure. The screw speeds temperature and injection pressure were maintained at same setting for the production of all composites, After moulding, test specimens were conditioned at 23 ± 2°C, 50 % relative humidity for at least 40 h according to ASTM D618-99.(Barone, Schmidt, and Liebner, 2005).

3.3.10 Hot moulding press

Lotus Scientific LS 22025/25 Ton Hot moulding Press was used to manufacture the composites at 180˚C for 5 minutes. The mould has dimension 250 X250 mm and 5 mm thickness; top and bottom plate was covered by aluminium foil and 3 mm steel plates.

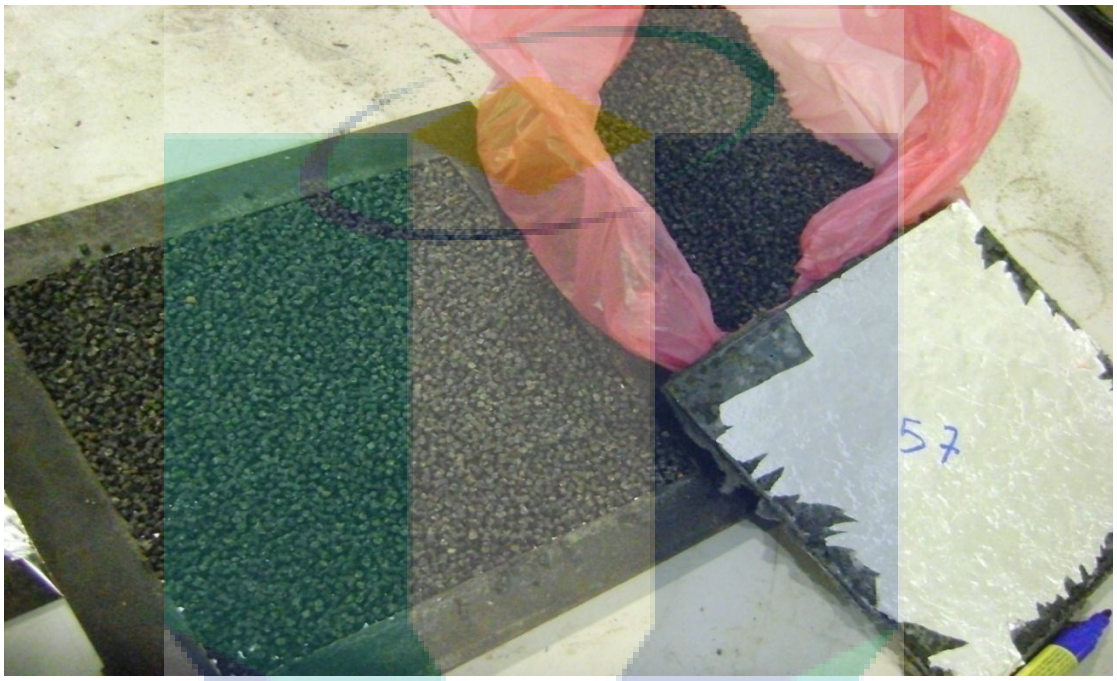

Figure 3.8 Hot press hybrid composites

3.4 COMPOSITE'S TESTING AND CHARACTERIZATION

3.4.1 Mechanical property analysis

The mechanical properties of composite were characterized using tensile tests(Kalam et al., 2005). The tensile tests were conducted according to ASTM D638-03: standard test method. Test specimens were placed into a conditioning chamber at 23^{o} C ± 3^{o} C and 50 % ± 5 % relative humidity for 40 h .The specimens were then tested using SHIMADZU (model AG-1) Universal Testing Machine with load cell of 5 KN, using crosshead speed of 5 mm/min and with a gauge length of 115 mm. Test was performed

until tensile failure occurred. Five specimens were tested for each batch with a gauge length of 50 mm.

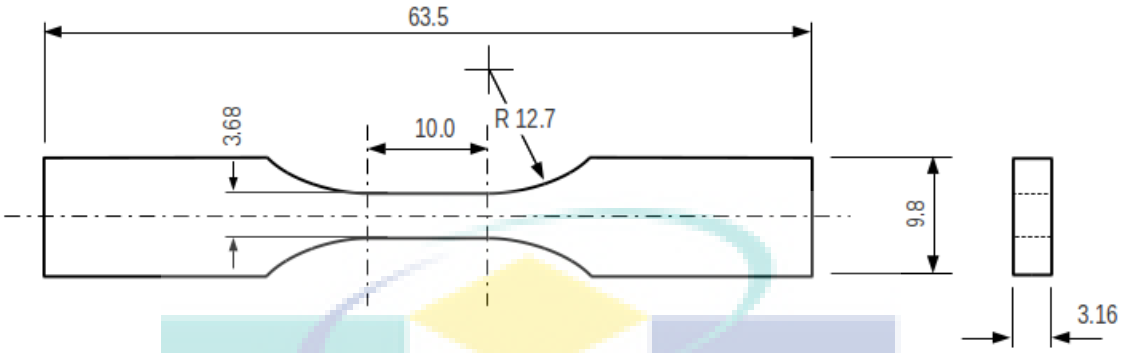

Figure 3.9: Dimension of a specimen

3.4.2 Thermal Properties

Differential scanning calorimetric (DSC) was carried out in a DSC model Q10 from TA instrument. For the DSC analysis, a film of each sample was prepared by heating around 1g of the sample at 180°C for 2 minutes and pressing it for 3 minutes under 3000 psi. The films were cooled down at an ambient temperatures. No temperature control or quenching was applied.

The thermal analysis testing procedure for each sample (About 4-5 mg weight) was as follows: First samples were heated from 40°C to 210°C (run I). After achieving this temperature, samples were then kept at 210°C for 5 minutes in order to reach thermal equilibrium and erase any trace of crystallinity or thermal history. Then, samples were cooled to 40°C using a scan rate of 10°C/min, after achieving 40°C; they were maintained at this temperature for 5 minutes. Finally, the samples go through another heating cycle from 40°C to 210°C (10°C/min rate) (run III). Thermal analysis of the additives and natural fibres were analysed in order to develop better understanding of the results.

3.4.3 Melt flow index testing

The melt flow index is obtained using a Dynisco D4004HV melt flow indexer following ASTM D1238: Standard test method for melt flow rates of thermoplastics by Extrusion Plastometer, using an applied load of 3.80 kg at 230^{o}C. Three independent tests were carried out on each sample.

3.4.4 Interfacial morphology analysis using SEM

Scanning electron microscope (SEM) (Model OXFORD) was used to an observed surface of composites before and after pre-treatment, cracking and swelling of the composites. Samples of air-dried composites fibres were fixed in a metal-base specimen holder using double-sided sticky carbon tape and then coated with gold using a vacuum sputter-coater to make them conductive prior to SEM observation.

3.4.5 Fourier transforms Infrared Spectrophotometer (FTIR)

Interfacial and etherification morphologies of composites were analysed by Fourier Transform Infrared Spectrophotometer (FTIR) (model: THERMO) using a standard KBr pellet technique. Each spectrum was recorded with 32 scans in frequency range from 4000cm^{-1} to 400cm^{-1} with resolution 4cm^{-1}.

3.4.6 Thermo gravimetric analysis (TGA)

TGA measurements were carried out using thermo gravimetric analyser (TA instruments, TGA Q500). Each specimens weighed about 10mg (±5mg) at scanning temperature range of 25ºC-600ºC and heating rate of 10ºC/min. TGA was conducted with the compounds placed in platinum crucible in nitrogen atmosphere at a flow rate of 40ml/min to avoid unwanted oxidation.

3.5 HYBRID COMPOSITE'S TREATMENTS AND ANALYSIS

3.5.1 Accelerated weathering test

Accelerated weathering tests of composites will be carried out using an accelerated weathering tester (Model QUV/ spray with solar eye irradiance control) following the ASTM G 154-00a: Standard practice for operating fluorescent light apparatus for UV exposure of non-metallic materials. A fluorescent bulb UVA with 0.68 W/m2 irradiance (at 340 nm) is used, with cycles consisting of UV irradiation for 8 hours followed by 15-minute spray of de-ionized water, then 3.45-hour condensations. The temperature maintained at 50ºC. The samples will be submitted to the aging process for durations of 200 hours, 400 hours, 600 hours, 800 hours 1000 and 1200 hours,(Beg and Pickering, 2008a)(Bergeret et al., 2009).

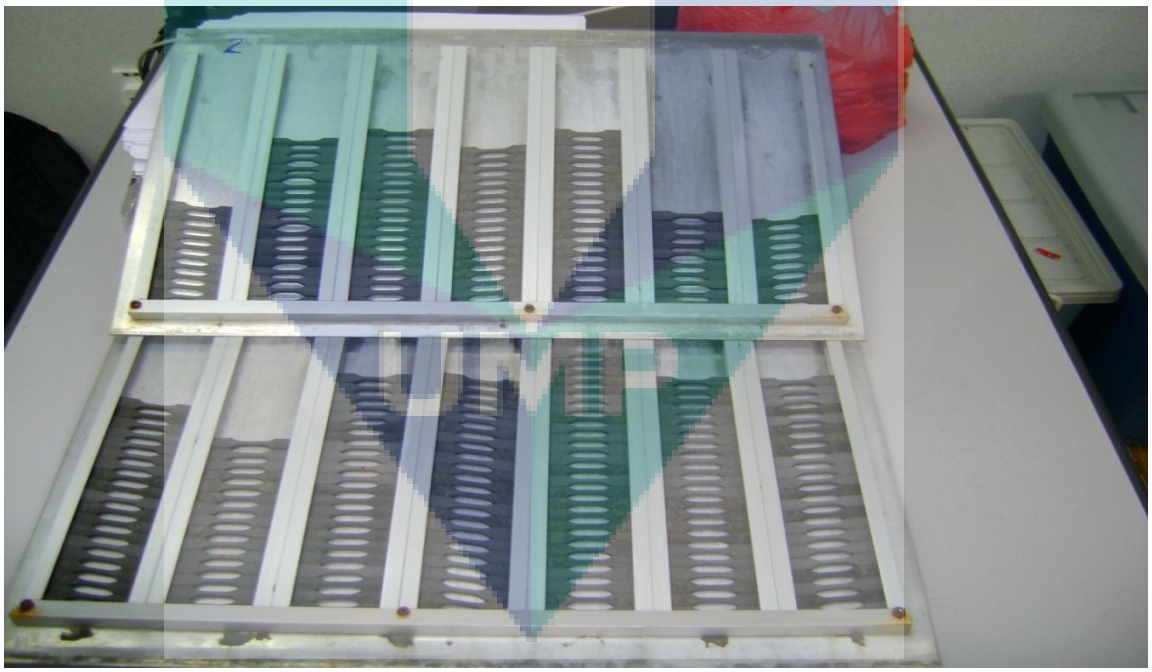

Figure 3.10: Sample preparation for accelerated weathering test.

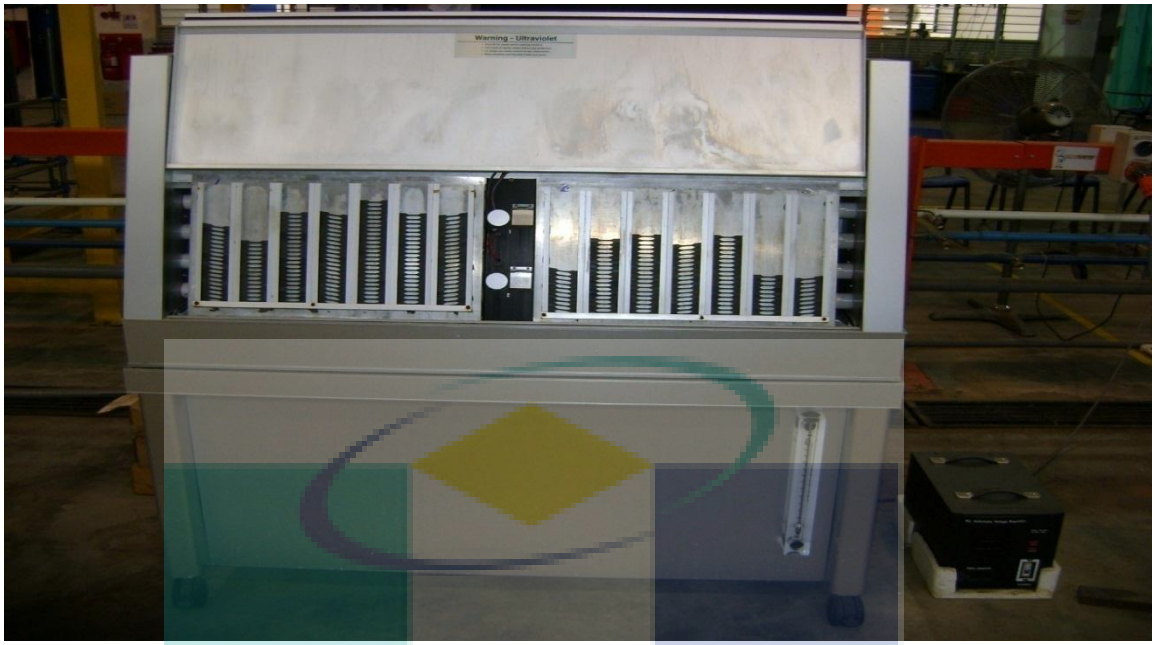

Figure 3.11: Accelerated weathering testing machine

3.5.2 Sunlight exposure treatment test

This treatment was done in UMP Gambang, Pahang, Malaysia for the period of November 2010- November 2011. Sunlight exposure treatment procedure: sample mounted on the glass roof rack. Since the location is at Northern part of equator, rack was facing southward face at an inclination of 45°.

Figure 3.12: Samples going through sunlight exposure treatment test

3.5.3 Natural weathering test treatment

This treatment was done in Gambang, Pahang, Malaysia from the period of November 2010-May 2011. Natural weathering testing procedure: sample mounted on the open rack. Since the location is at Northern part of equator, rack should be southward face at an inclination of 45°, (Stark andMatuana, 2006).

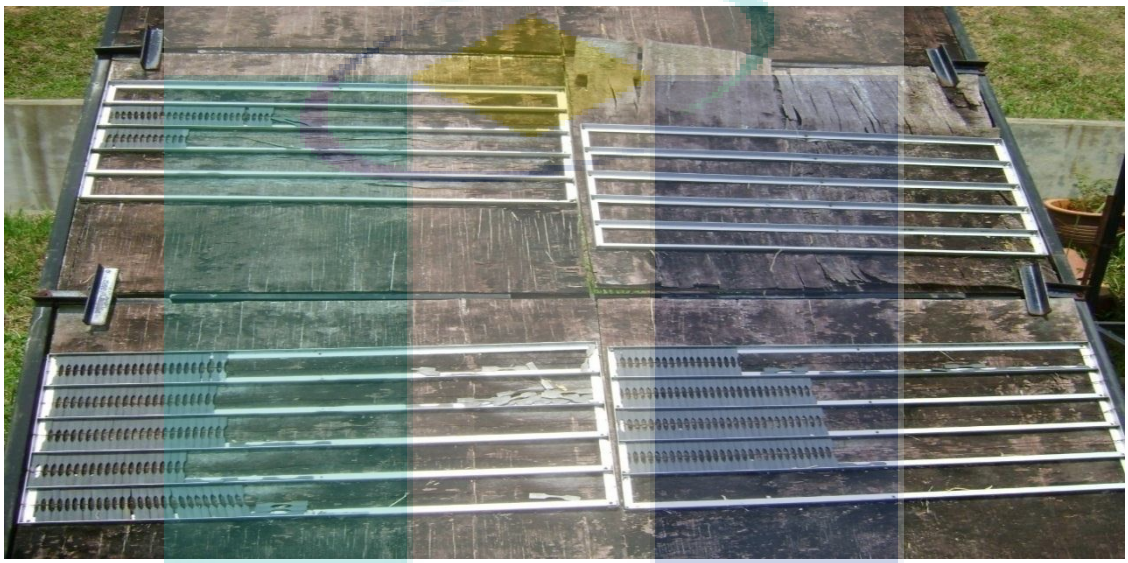

Figure 3.13: One year natural weathering

3.5.4 Hygrothermal Ageing testing

Fresh water and sea water homemade hygrothermal ageing was used for this research; mercury temperature controller was chosen to stabilize the temperature at 27, 60 and 80 °C for more than 2 months of hygrothermal testing without overheating. The fluctuation range of the temperature is only 1 to 2 % and evaporation compensation was done automatically by the level controller in the equipment. Teluk Cempedak beach sea water was used as hygrothermal ageing media at 1 week circulation time.

3.5.5 Water absorption

Due to the hygroscopic behaviour of agro based materials, the water absorption test was conducted. The water absorption test was carried out based on the ASTM D570-98 specifications. Ten specimens of each formulation were selected and dried in an air circulating oven for 1 hour at 108 ± 0.5°C. Following the drying stage, the specimens were allowed to cool down inside a chamber, weighted to a precision of 0.001g and then immersed in the hygrothermal ageing device. After 1 week of immersion in water, the amount of water absorbed by each specimen was measured. The samples were removed from water, patted dry and weighted again to a precision of 0.001g. The same measurement procedure was followed every week(Abdelmouleh et al., 2007). During the entire experiment period (60 consecutive days), the normal water and sea water temperature was maintained constant at 27, 60 and 80 ± 2ºC. The water was changed every week. After the experiment, images of the samples immersed in hygrothermal ageing were recorded with SEM. The amount of water absorbed by each composite was calculated by the following equation: (Arbelaiz, Fernández, et al., 2005),(Gellert andTurley, 1999).

$$\% \text{ Uptake} = \left(\frac{wt - w0}{w0}\right) \text{X } 100\ \% \qquad \text{Equation 3-1}$$

3.6 DATA ANALYSIS AND OPTIMIZATIONS

3.6.1 Statistical Calculation

Response surface methodology (RSM) is an effective and efficient statistical methode for optimizing complex processes or experiment setting because it is saving laborious and time compare to other approaches, in addition it allows more efficient and easier arrangement and interpretation of experiments compared with other methods (Yin, You, and Jiang, 2011).

The factorial design was conducted with each experiment. The range and levels of the processing parameters involved are tabulated in Table 3-1,3-.3-5,and 3-7, while the

factorial design matrices and experimental setting of each individual experiment are shown in Table 3-2,3-4,3-6 and 3-8.

The Quadratic model for predicting the optimal point Eq. (3-2). Where "y", is the response variable, b is the regression coefficient of the model, x is the coded levels of the independent variables. In general, the primary objective of RSM is to optimize the response (Y) based on the factors investigated. The Design Expert software 6.0.4 was used to develop the experimental plan and optimize the regression equations. The statistical significance of the second-order model equation was determined by performing Fisher's statistical test for analysis of variance (ANOVA). In particular, a good model must be significant based on the F-value and P-value. Moreover, the proportion of variance exhibited by the multiple coefficient of determination R^2 should be close to 1 as this would demonstrate a better correlation between the experimental and the predicted values.

$$Y = \beta 0 + \sum_{i=1}^{n} \beta iXi \quad + \sum_{i=1}^{n} \beta iiXi^2 + \sum_{i<j}^{n} \beta ijXiXj \qquad \text{Equation 3-2}$$

Where $Y\ is$ predicted response, $\beta 0$ is constant coefficient, βi is linear coefficient, βii is quadratic coefficient, βij is interaction coefficient, Xi and Xj are independent factors.

3.6.2 ANOVA Data analysis

The data analysis has been done by statistical analysis. Homogeneity (or lack of homogeneity) of the samples obtained were determined for each sampling method, where the parameters were measured at least in five testing replications. Statistical analysis was performed with analysis of variance (ANOVA) response surface methodology software. All data are expressed as the mean ± S.D. unless otherwise stated. The differences between means were analysed by one-way analysis of variance (ANOVA). The results for analysis of data in process range identification were shown in the table response.

3.6.3 Optimization of Hybrid Composites

Optimization of the manufacturing process of hybrid composite was done with the Response Surface Methodology (RSM). In the RSM, tensile strength, modulus elongation at break, and melt flow indexes were taken as the dependent variables (responses) whereas the parameters such as temperature, time, NaOH % of alkali treatment, Fusabond, MAPP and fibre ratio percentage is taken as the independent variables.

3.6.4 Validation

Adequacy of the developed empirical model needs to be verified or validated in order to confirm the prediction accuracy, which is generated by the regression equation in predicting the mechanical properties, such as tensile, modulus elongation, water absorptions and melt flow index within the range of level defined previously. The obtained actual values and its associated predicted values from the selected experiments were compared for further residual and percentage error analysis. The percentage error between an actual and predicted value of both responses over a selected range of operating levels are calculated based on Equation 3-2 and Equation 3-3.

$$\% \text{ Error} = \frac{residual}{actual} \text{ x } 100\% \qquad \textbf{Equation 3-3}$$

3.7 SUMMARY OF EXPERIMENTAL WORK

The whole research is divided into four major parts:

1) Alkali treatment of fibres using four different methods
2) Characterization of hybrid composite's properties,
3) Analysis of Variance (ANOVA), Validation and Statistical Analysis,
4) Optimization and confirmation run of the combine optimization conditions.

The result and discussion section of the thesis is divided into three sections:

Figure 3.14 show the operational framework of this research.

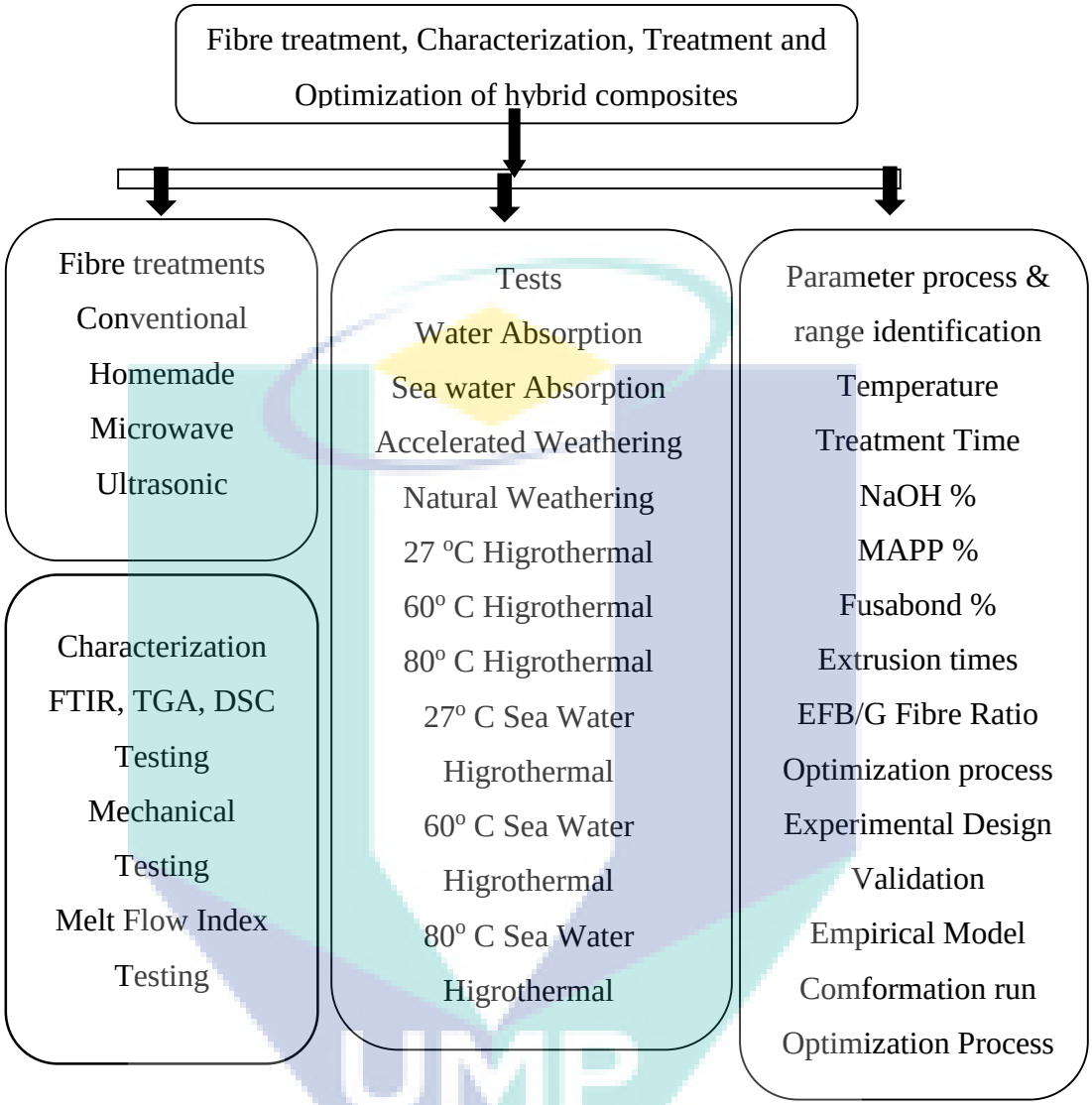

Figure 3.14 Operational Framework

CHAPTER 4.

CONVENTIONAL AND HOMEMADE HYBRID COMPOSITES

This chapter is divided into ten parts of results and discussion, it discuss standard and homemade alkali treatment, characterization of hybrid composite's properties, response surface of hybrid composites, Analysis of Variance, Statistical Analysis, Validation of Empirical Model Adequacy and Confirmation Run of the Optimization Conditions.

4.1 STANDARD ALKALI TREATMENT OF HYBRID COMPOSITES

In this researchs, experiments were carried out by standard alkali treatment in order to identify the each parameter interaction and the optimum operational condition that would result in a high properties of hybrid composites. The operational conditions involved were the Treatment time, NaOH percentage and fibre ratio. These findings at the end will provide important data on improving natural fibre treatments and composites fabrications.

4.1.1 DSC and TGA of the EFB-Glass fibre hybrid composites

Temperatures of crystallization, melting point and heat flow of crystallization of the EFB-Glass fibre hybrid composites have different value, as explained in Figure 4.1 and Table 4.1 there were no significant change in the crystallization temperature with respect to the alkali treatment time and temperature of the composites. However, all composites have shown higher crystallization temperatures, compared to recycled polypropylene. A small difference between sample containing 30 50, 70 and 90% of fibre

ratio was also observed in all conventional composites sample tested. Figure 4.1 shows DSC scanning curves of samples containing 30, 50, 70 and 90% ratio of fibre, prepared at 15% NaOH and 4 hour alkali treatment. No significant changes in the melting temperature of composites containing the same of fibre treatment were observed with changes in the fibre ratio. Moreover, the melting and crystallization curves were not significantly different (Agrawal, Saxena, Sharma, Thomas, and Sreekala, 2000).

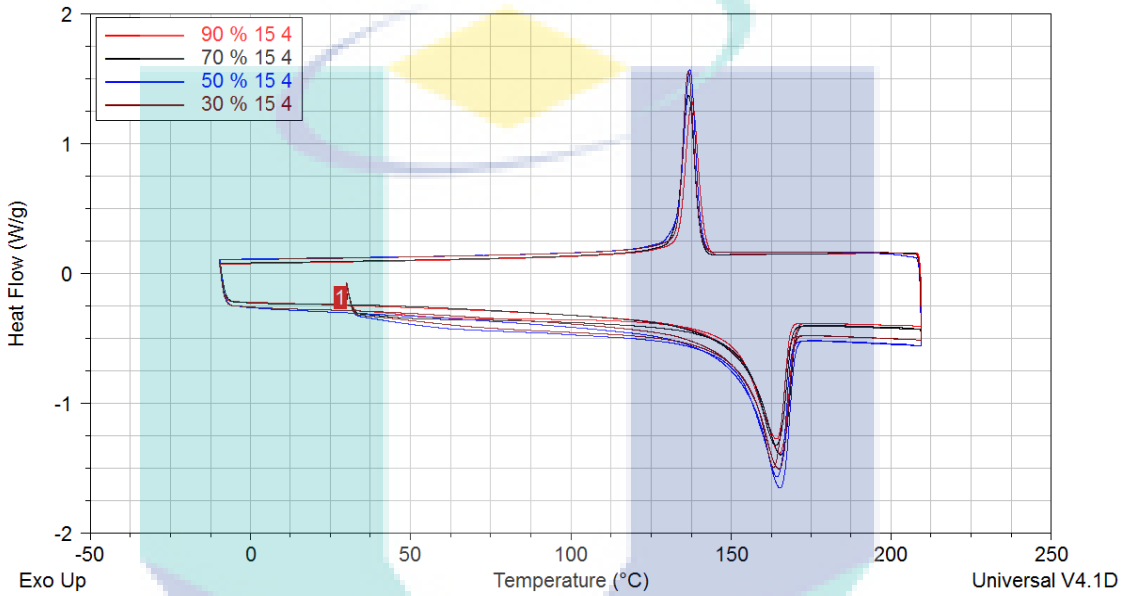

Figure 4.1: DSC graph of conventional hybrid composites

Table 4.1: Crystallization and melting heat flow temperature

Standard Std	Crystallization Heat Flow W/G	Crystallization Temp °C	Melting Heat Flow W/G	Melting Temp °C
30 % EFB	1.444	136.48	-1.39	162.92
50 % EFB	1.597	137.10	-1.59	164.17
70 % EFB	1.389	136.48	-1.35	163.85
90 % EFB	1.322	137.72	-1.27	164.17

TGA curve of recycled polypropylene matrix, and conventional hybrid composites as shown in the Figure 4.2. It show that the recycled polyprophylene and all the EFB hybrid composites merge with each other until the temperature reach 270° C.

The initial transition around 250 to 300ºC far all the composites's TGA curves show in the Figure 4.2 due to the start of EFB fibre degradations, high EFB content shifted curve slightly lower than small EFB content and The presence of the glass fibre has no effect. The decomposition temperature of the samples slightly different in the range of 300 to 450 as shown in the Figure 4.2 where the TGA traces shifted to lower temperatures with increasing EFB content and thermal stability of the high EFB content decrease significantly, this phenomena doe to degradation of EFB fibre in this temperature's range, similar finding was explaid by (Ota, Amico, and Satyanarayana, 2005). TGA transitions for composites remaining from 500 up to 650ºC also found shifted to noticable lower due to fibre ratio or Glass fibre residual content in the composites.

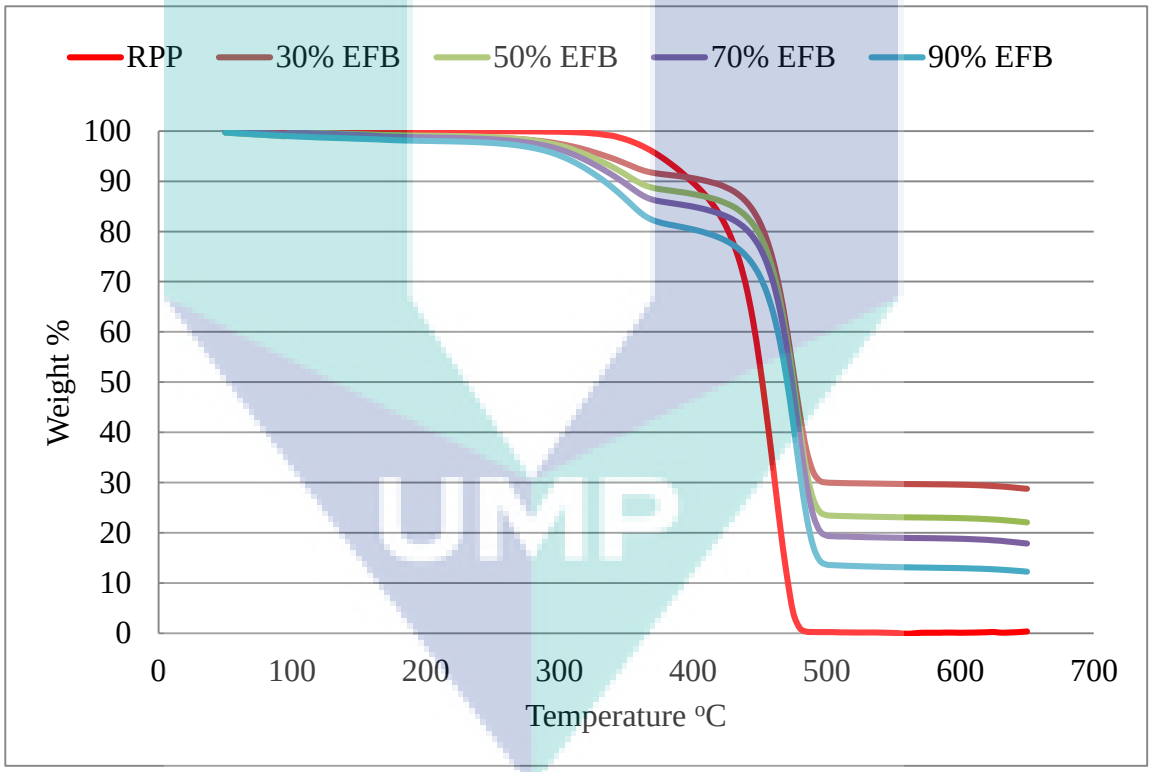

Figure 4.2: TGA graph of conventional hybrid composites

Accelerated weathering test causes TGA traces shifted to the lower temperature, it can be seen in the Figure 4.3 ,comparison of DSC 30 and 50 % EFB content before and after 1200 accelerated weathering. Accelerated weathering 1200 hour cause TGA trace slighly decrease compare withaut accelerated weathering. Figure 4.4 comparison of 70

and 90 % EFB content explain similar result that the decrease in thermal stability after accelerated weathering could be due to the reduction of recycled polypropylenes chain ,EFB fibre degradation and cracking in the fibre-matrix bounding surface.

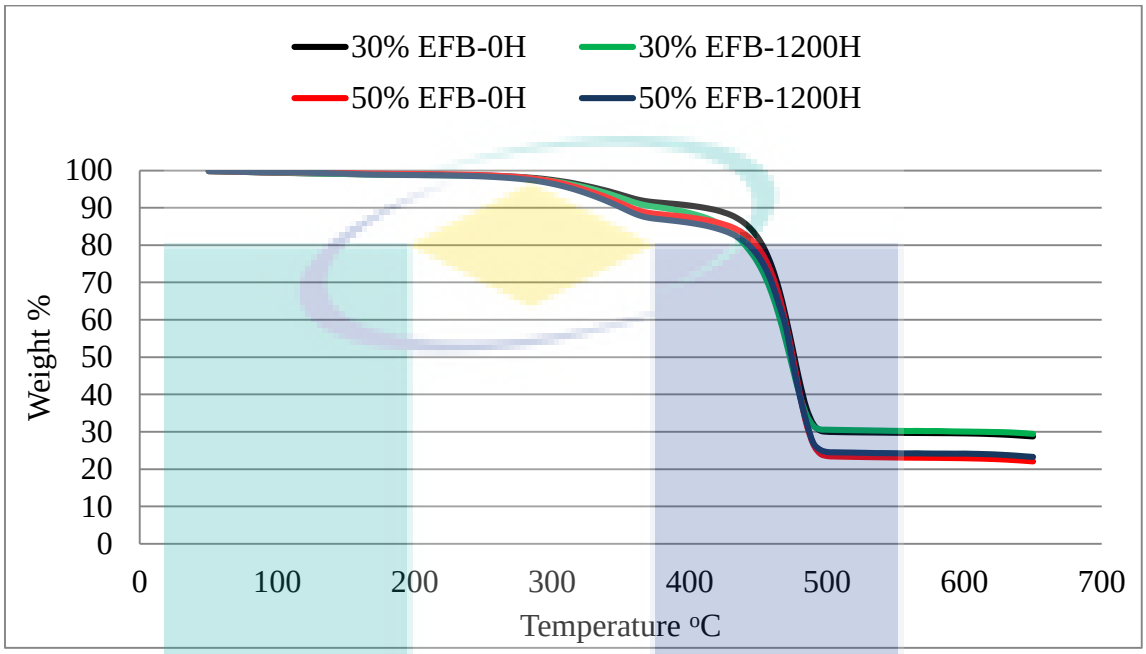

Figure 4.3: DSC graph of accelerated weathering hybrid composites

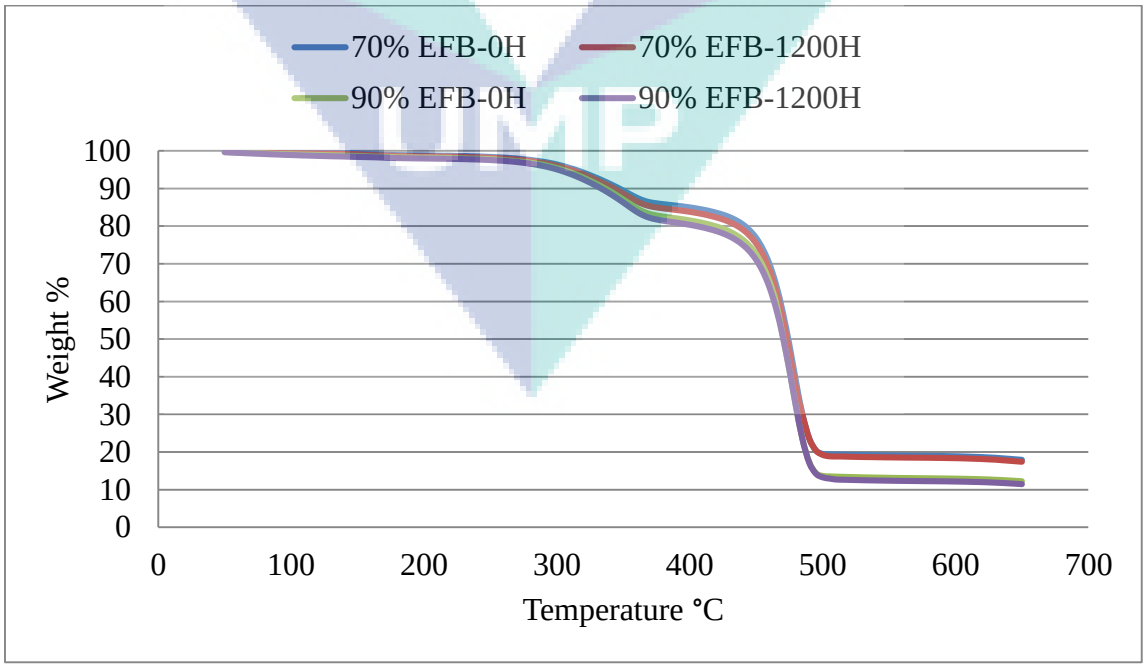

Figure 4.4: DSC graph of accelerated weathering hybrid composites

4.1.2 FTIR of Conventional alkali treatment

Alkali treatment process has a goal to decrease the lignin content, improve bonding properties and to obtain a greater degree of uniformity and stability of composites mechanical properties. There are four different ways of alkali treatment that has been used in this research, conventional, homemade alkali treatment, modified microwave and ultrasonic alkali treatments.

The FTIR spectrum of untreated EFB fibre as shown in Figure 4.5 contains eight major peaks at 3606.49, 3568.07, 3529.21, 3485.10, 3450.58, 3383.84, 3345.81, 3286.98, 3239.71, 3150.14, 2924.36, 1597.86, 1447.77, 1363,52, 1142.14, 1097.25 and 1032.35 cm^{-1}. The regions from 4000 to 1900 cm^{-1} for O-H and C-H stretching frequencies The absorbance peaks at around 1600 explain the lignin and hemicelluloses groups Whereas the overall FTIR spectrum of the treated EFB was also recorded at the lower peak's region in the same wave number: This finding indicates that it is significantly different between untreated and treated EFB fibre and the treated EFB have much lower lignin content.

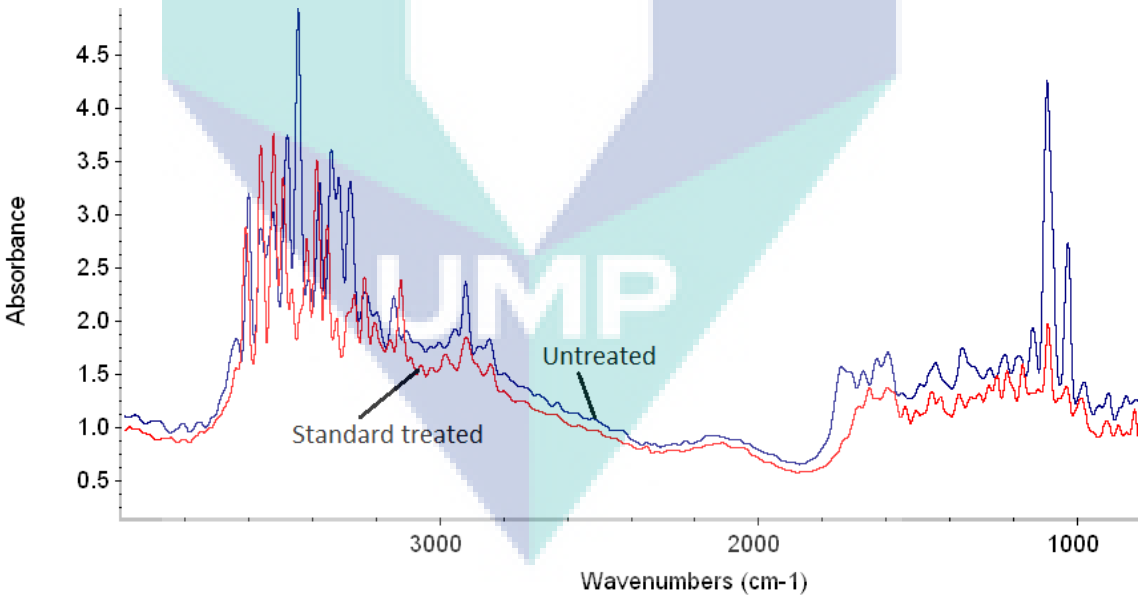

Figure 4.5: Infrared spectra of the untreated and conventional treated EFB fibre.

4.1.3 SEM of the EFB-Glass fibre hybrid composites

SEM testing has been used successfully to investigate the detailed fracture mechanism of several different composites. The morphology of the fracture EFB-glass fibre hybrid composites were analysed using scanning electron microscopy.Figure 4.6 showed that there are clean glass fibre surface and fibre pull-out that indicating poor wet ability and lack of adhesion. There is a damage in the matrix surface and surface between glass fibre and recycled PP matrix without fibre cracking, it indicates that bonding between glass fibre- recycled PP matrixes is very low and can be improved with matrix modification or fibre treatments. The interfacial strength plays a vital role in determining the mechanical behaviour of hybrid composites (Arbelaiz, Fernandez, et al., 2005).

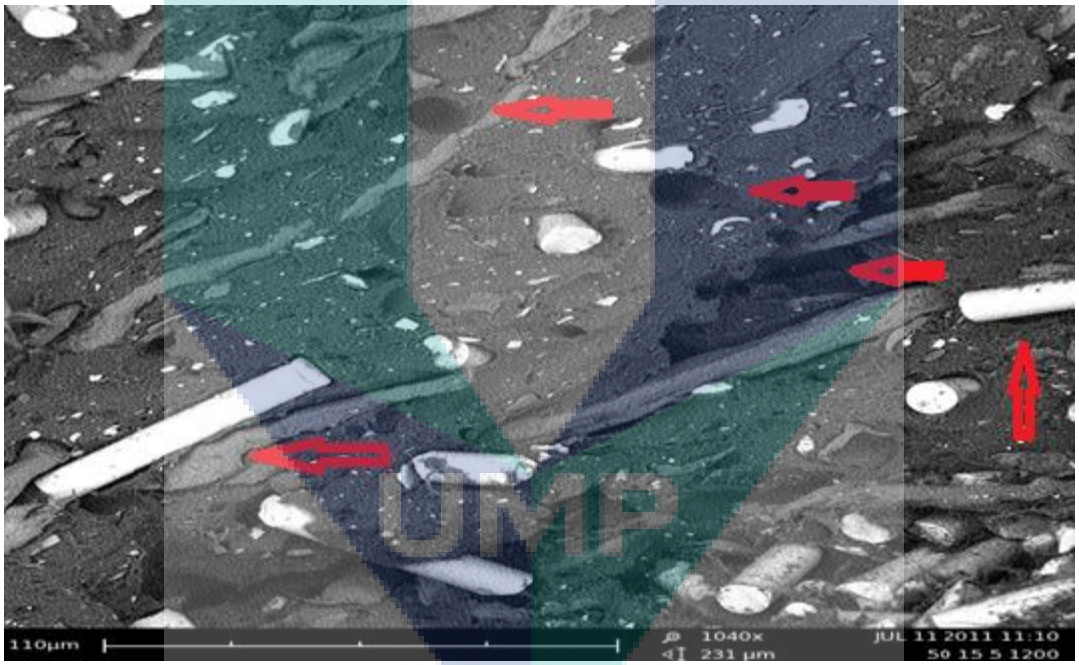

Figure 4.6: SEM of the conventional 50 % EFB hybrid composites

4.1.4 Water absorption of EFB-Glass fibre hybrid composites

Water sensitivity is an important selection criteria for many practical applications of hybrid composites. Water absorption in hybrid filled composites can be significant; the migration of water through the material can lead to a disturbance of the filler/polymer interface, thus changing the characteristics and physical performance of the composites.

In order to verify the fresh and sea water absorption behaviour of hybrid composites, immersion experiments were performed in the hygrothermal testing device for 60 days. Figure 4.7 and Figure 4.8 shows the water absorption properties in the fibre ratio of polypropylene composite with 30, 50, 70 and 90% of fibre's ratio, prepared at different temperatures and treatment times. The experiment recorded the absorption of the samples in the water and sea water at 27, 60 and 80ºC during 60 days.

For lignocelluloses thermoplastic composites water uptake is proportional to fibre loading as sorption of thermoplastic matrix such as polypropylene can be neglected (Selzer andFriedrich, 1997). From Figure 4.7 and Figure 4.8, it appears that with the increase of EFB fiber percentage, the percentage water absorption also increases it could because EFB more absorb water compare to glass fibre. Water absorbtion also increases with the climb in temperature in explain that hot water increase penetration that lead fibre-matrix surface bounding cracking, composite swelling and EFB absorbtion. The interesting finding that There is not much significant difference at water absorption values between normal water compare to sea water, salt content have not significant effect in composites absorbtion.

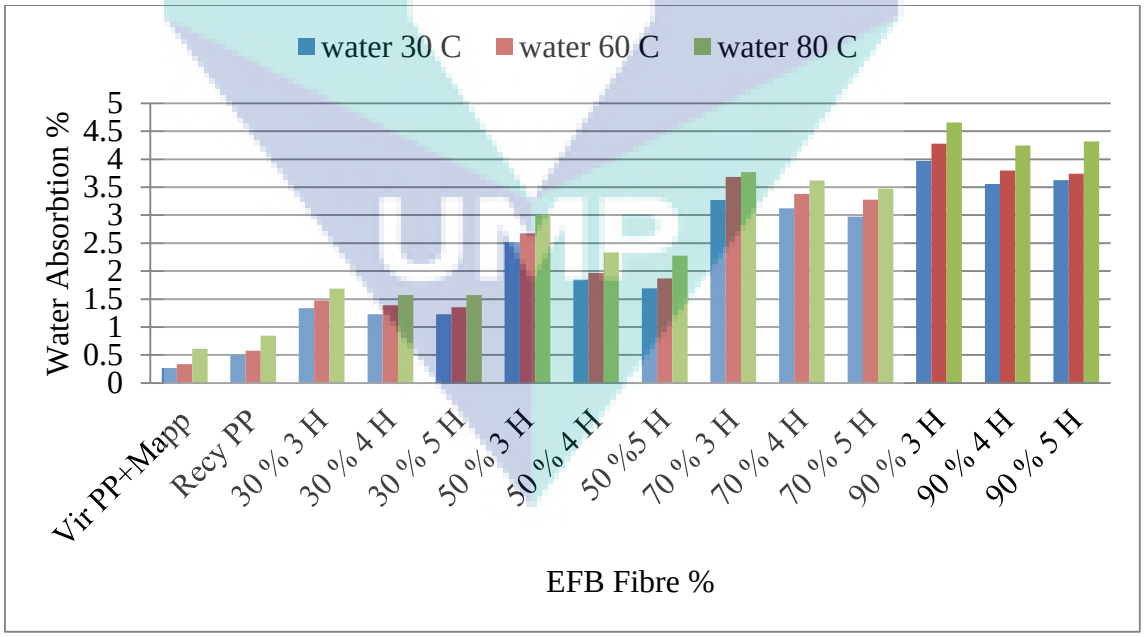

Figure 4.7: Water absorption hybrid composites

Alkali treatment hour as explained in the Figure 4.7 and Figure 4.8 give information that longger alkali treatment can reduce water and sea water absorbtion significantly 3 and 4 hour alkali treatment have higher water absorbtion compare to 5 hour alkali treatment, this phenomena explain that lignin removal EFB surface roughness and fibre-matrix surface bonding reduce water absorbtion.

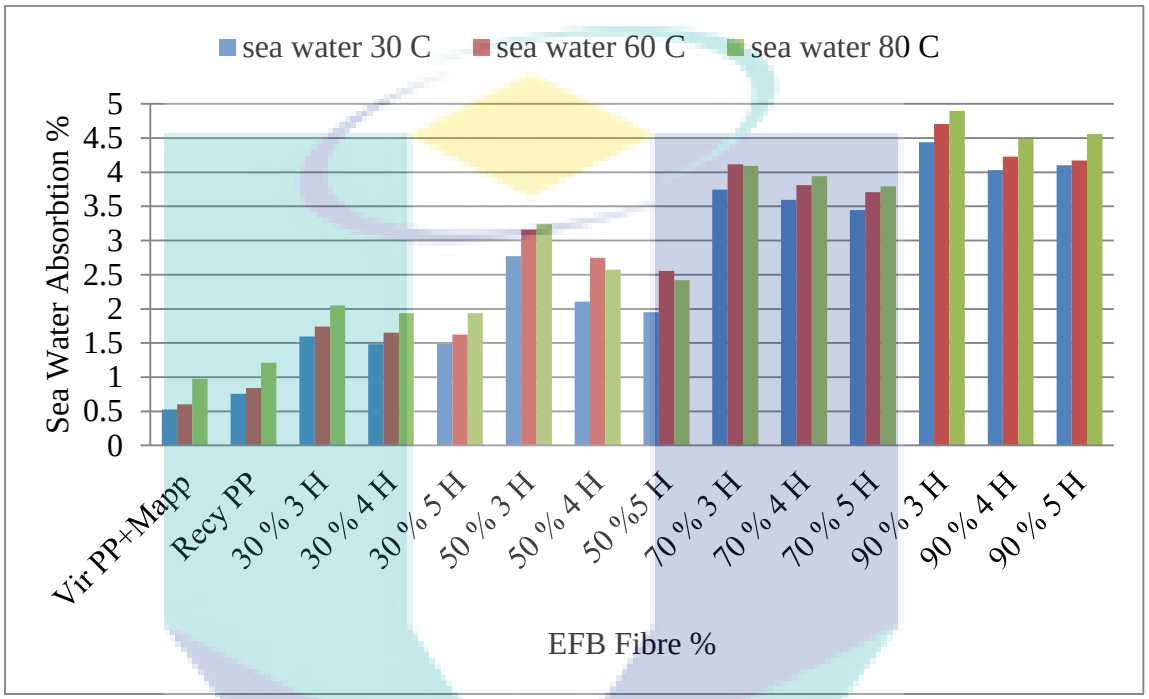

Figure 4.8: Sea Water absorption hybrid composites

4.1.5 Relationship between tensile properties and fibre ratio

The most crucial factor that affects the mechanical properties of fibre-reinforced recycled materials is the fibre volume fraction and fibre matrix interfacial adhesion. The quality of interfacial bonding is determined by several factors, such as polymer properties, coupling agent, the fibre aspect ratio, processing method and the treatment time: and nature of the fibre.

Figure 4.9, shows, the recycled polypropylene only has about 26-27 MPa strength as compared to virgin polypropylene at around 35-37 MPa and addition of MAPP decrease tensile strength and strain about 5%. Additional of fibre should improve the

tensile properties to around 40 to 45 MPa.When the fiber percentage is 40% and the recycled polypropylene is 60%, Composite's tensile strength are 26.5 to 35 MPa.

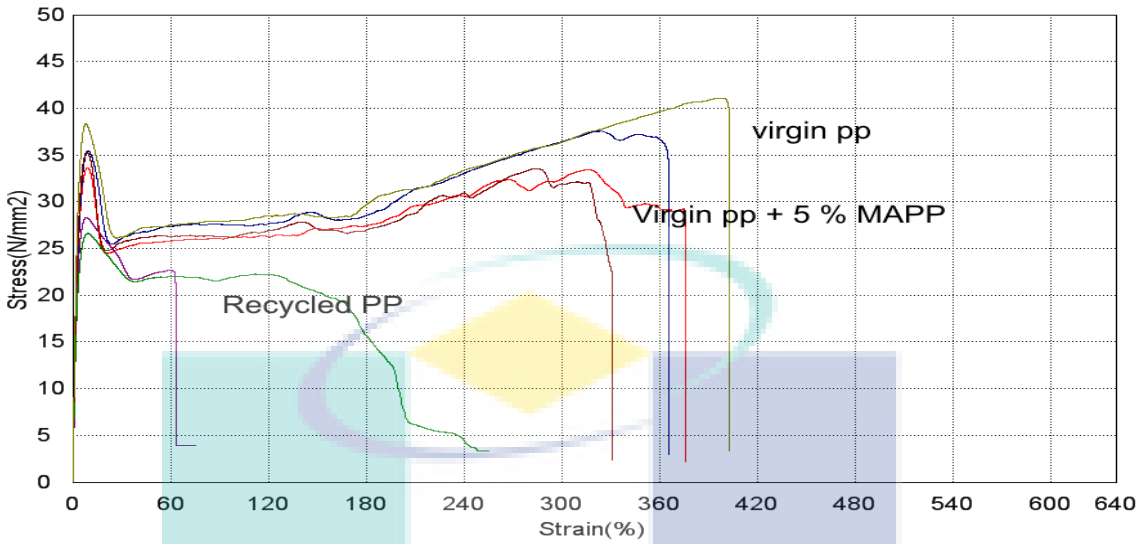

Figure 4.9: Tensile strengths of virgin PP, Virgin PP + MAPP and Recycled PP

From Figure 4.10, it can be seen that with the increase in the ratio of EFB/Glass fibre and alkali treatment in polymer recycled matrix composites. The tensile strength of 4 and 5 hour NaOH treatment recycled PP composites have slightly increased to about 30-35 MPa and this is due to better bonding between fibres and matrix. Surprisingly empty fruit bunch fibre gives better tensile improvement than glass fibre; Ratio EFB/Glass fibre at 30% only has 27 MPa compares to 70% EFB/Glass fibre at 35 MPa.

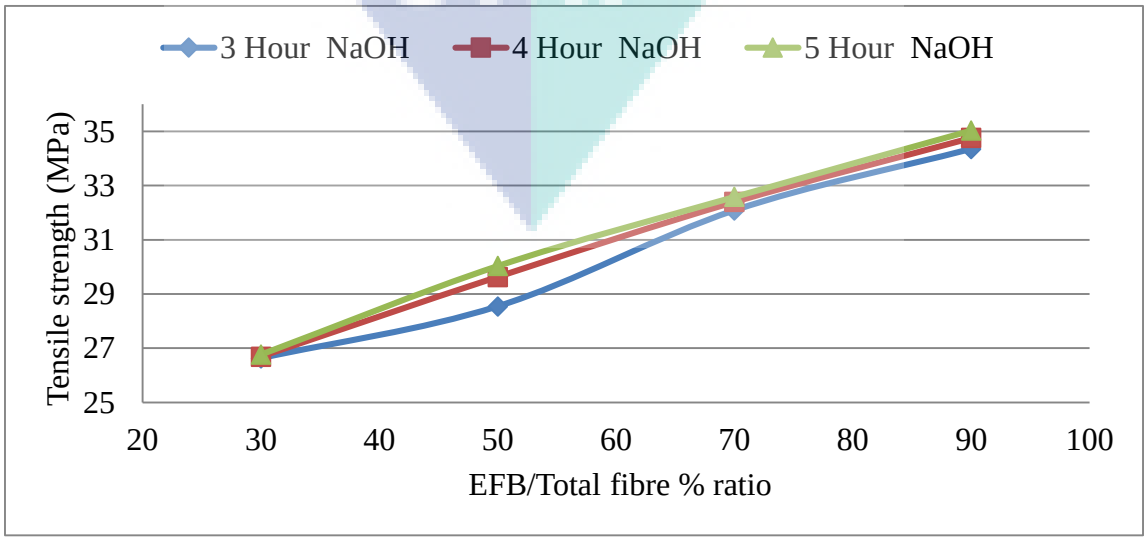

Figure 4.10: Tensile strengths of EFB-Glass Fibre Composites

$$\text{Tensile strength} = A_0X^2 + A_1X + A_2 \qquad \textbf{Equation 4-1}$$

Table 4.2: The Constanta values of Tensile strength

NaOH Treatment	A_0	A_1	A_2	R
3 Hour NaOH	-0.0005	0.1982	21.31	0.9995
4 Hour NaOH	-0.00004	0.1784	21.649	0.9999
5 Hour NaOH	0.00002	0.1071	23.071	0.9883

4.1.6 Dependence of Flexural modulus on fibre ratio

Figure 4.11 shows the flexural modulus of 3 hour, 4 hour and 5 hour alkaline peroxide treatment time. From the Figure, it can be seen that modulus of 4 hour and 5 hour treatment of alkaline composite is better than three hours. Treated composite with higher modulus are at 60% EFB/G-Fibre ratio compared to 50 and 70. Nevertheless, it decreases by increasing the ratio of EFB/Glass fibre to 90% ratio.This might be due to weak interfacial bonding between EFB fibre and matrix's.

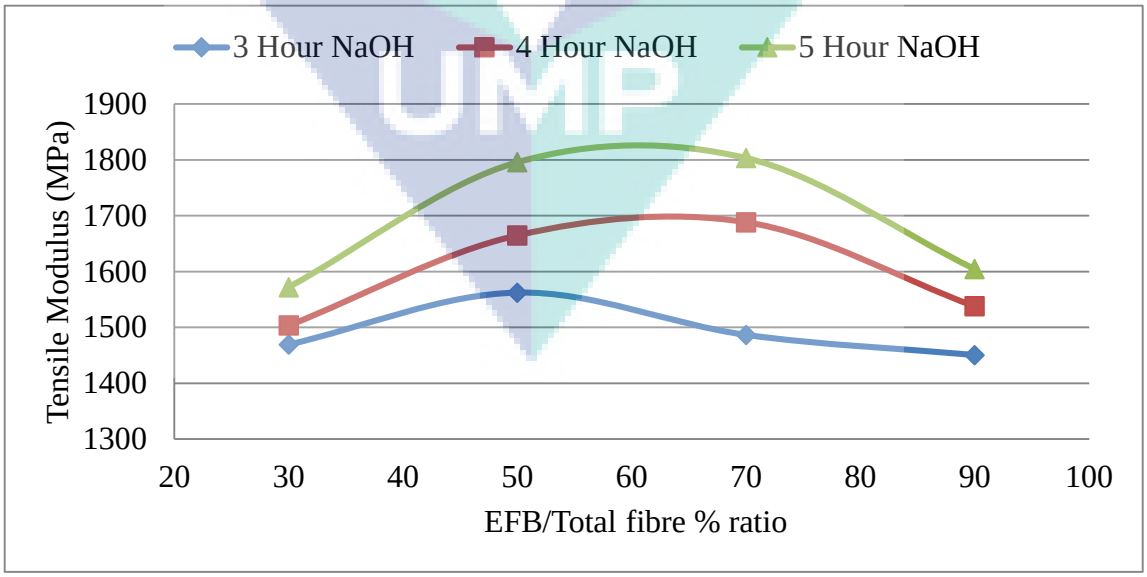

Figure 4.11: Flexural modulus of EFB-Glass Fibre Composites

$$\text{Flexural modulus} = A_0X^2 + A_0X^2 + A_1X + A_3 \qquad \textbf{Equation 4-2}$$

Table 4.3: The Constanta values of Flexural

NaOH Treatment	A_0	A_1	A_2	A_3	R
3 Hour NaOH	0.0043	-0.8634	52.429	555.82	1
4 Hour NaOH	-0.0008	-0.0584	16.448	1083	1
5 Hour NaOH	0.0002	-0.3014	34.301	808.54	1

4.1.7 Effect of fibre ratio on Elongation at break

Figure 4.12 shows the Elongation at break of 3 hour, 4 hour and 5hour alkaline peroxide pre-treatment composite. From the Figure, it can be seen that elongation of 3hour 4 hour and 5hour of treated alkaline composite is similar at 70 to 90 of fibre content. Hybrid composite with lower ratio EFB/Glass fibre has better elongation at break than the high ratio EFB/Glass fibre. It could be due to better glass fibre recycled matrix bonding interaction compare to EFB-matrix adhesion.

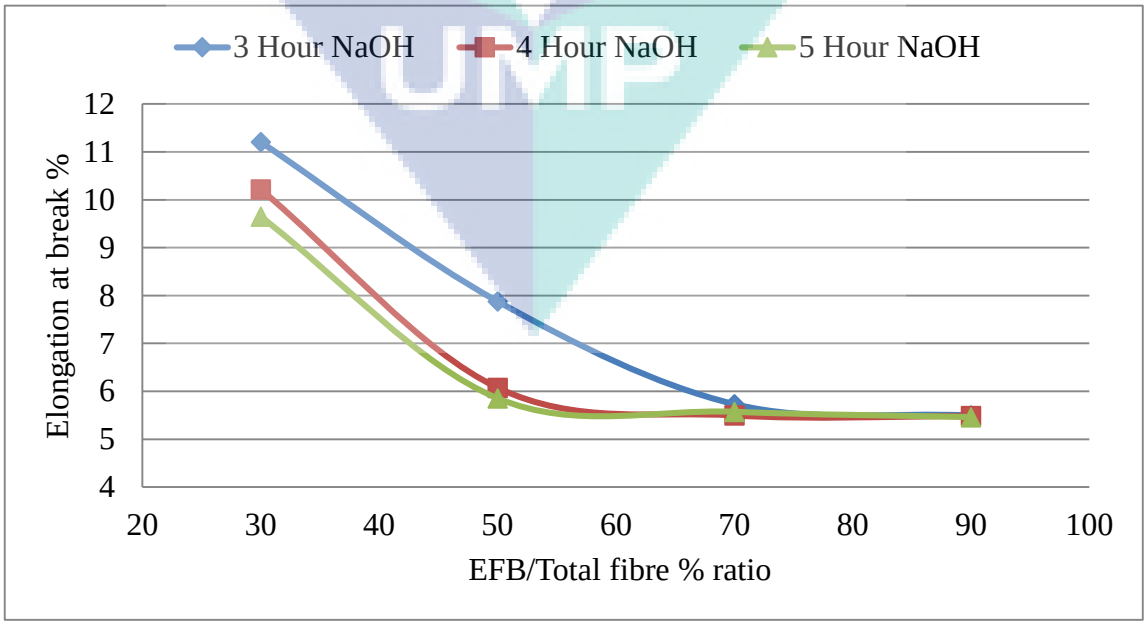

Figure 4.12: Elongation at Break of EFB-Glass Fibre Composites

$$\text{Elongation} = A_0X^2 + A_1X + A_2 \qquad \textbf{Equation 4-3}$$

Table 4.4: The Constanta values of Elongation

NaOH Treatment	A_0	A_1	A_2	R
3 Hour NaOH	0.0019	-0.3278	19.339	0.9987
4 Hour NaOH	0.0026	-0.3833	19.244	0.9712
5 Hour NaOH	0.0023	-0.3405	17.623	0.9542

4.1.8 Relation Melt Flow Index and fibre ratio

The influence of fibre ratio on the MFR under different NaOH treatment conditions is displayed in Figure 4.13. When the Naoh Treatment is constant, with increasing EFB content the MFR decrease as a quadratic function, given by:

$$\text{MFI} = A_0X^2 + A_1X + A_2 \qquad \textbf{Equation 4-4}$$

Where Ai (i=0, 1, 2) are constants.

Figure 4.13 and Table 4.5 shows the Melt Flow Index of 3, 4 and 5 alkaline peroxide pre-treatment composite. the values of R of the melts are very close to unity(1) or confidence interval more than 95 %, which suggests that the correlation between MFI and Fibre Ratio for the melts can be described using a quadratic equation.

From the Figure 4.13, it can be seen that Melt Flow Index of 4 and 5 of treated alkaline composite is better than three hours. Lower EFB content lead to significantly high melt flow index as seen in the picture. It could because EFB has low fluidity in composites melting conditions compare to glass fibre. In addition The dynamics of viscoelasticity of the composites melts were significantly effected by high EFB fibre content compared to Glass fibre, doe to bigger size of the fibre and partial misalignment of the EFB fibre and hindering the mobility of molecular chain in the composites melt

(Ota et al., 2005) Furthermore, it can be seen that MFI values not significantly effected by NaOH hour treatment.

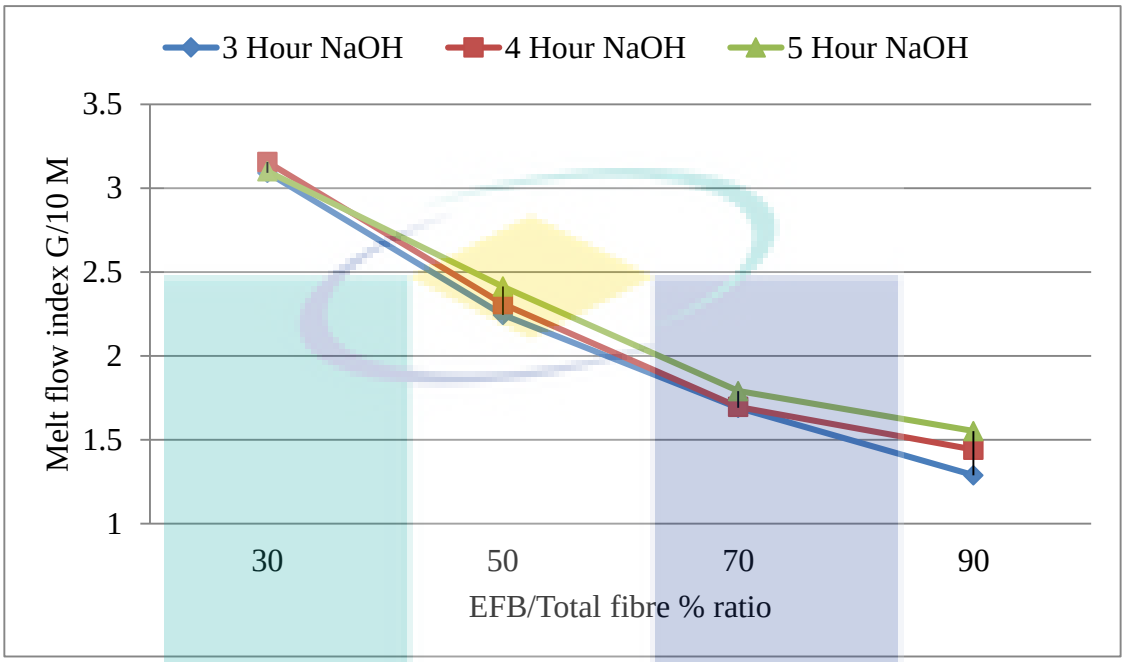

Figure 4.13: Melt Flow Index of EFB-Glass Fibre Composites

Table 4.5: The Constanta values of MFI

NaOH Treatment	A_0	A_1	A_2	R
3 Hour NaOH	0.1112	-1.1525	4.1262	0.9995
4 Hour NaOH	0.1481	-1.3162	4.3309	0.9995
5 Hour NaOH	0.112	-1.087	4.092	0.9965

4.2 MECHANICAL PROPERTIES

4.2.1 Tensile Strength of 1 year Gambang's Natural weathering

Tensile strength during natural accelerated weathering are presented in the

Figure 4.14 to Figure 4.16 . Tensile strength of 90 % EFB ratio is higher compare to lower EFB content doe to better load absorbtion and tensile properties of EFB fibre compare to polypropylene matrik. In natural weathering, the presence of UV ligh, thermal exposure and moisture penetration give simultaneous effects to the composite.

Figure 4.14 to Figure 4.16 show very small tensile degradation of hybrid composites in 1 year Gambang Pahang natural weathering, similar finding was provide by 1200 hours of accelerated weathering to predict around 4 to 5 years of hybrid composites outdoor applications.The highest tensile strength reduction was found for 90% EFB ratio composites. Tensile strength of 3, 4 and 5 hour NaOH treatment reduce around 2 to 3 MPa after 12 month Gambang's natural accelerated weathering. Low EFB content composite show high performance stability compare to high EFB content, it could be due low EFB lead less surface bonding cracking, moisture absorbtion and EFB degradation.

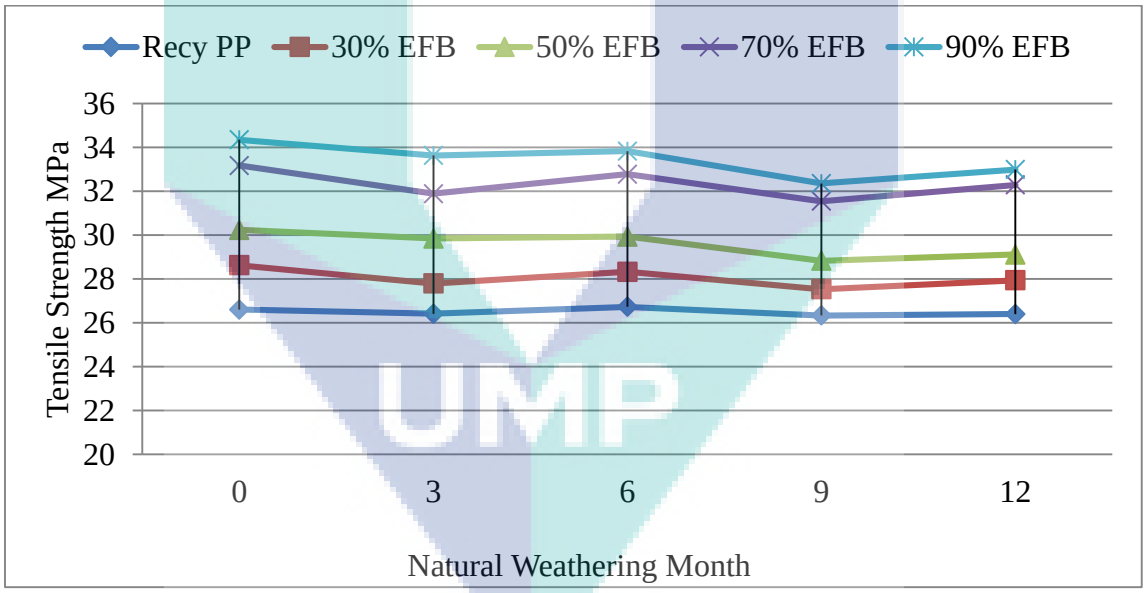

Figure 4.14: Natural weathering Tensile Strength of 3 hours 15 % NaOH

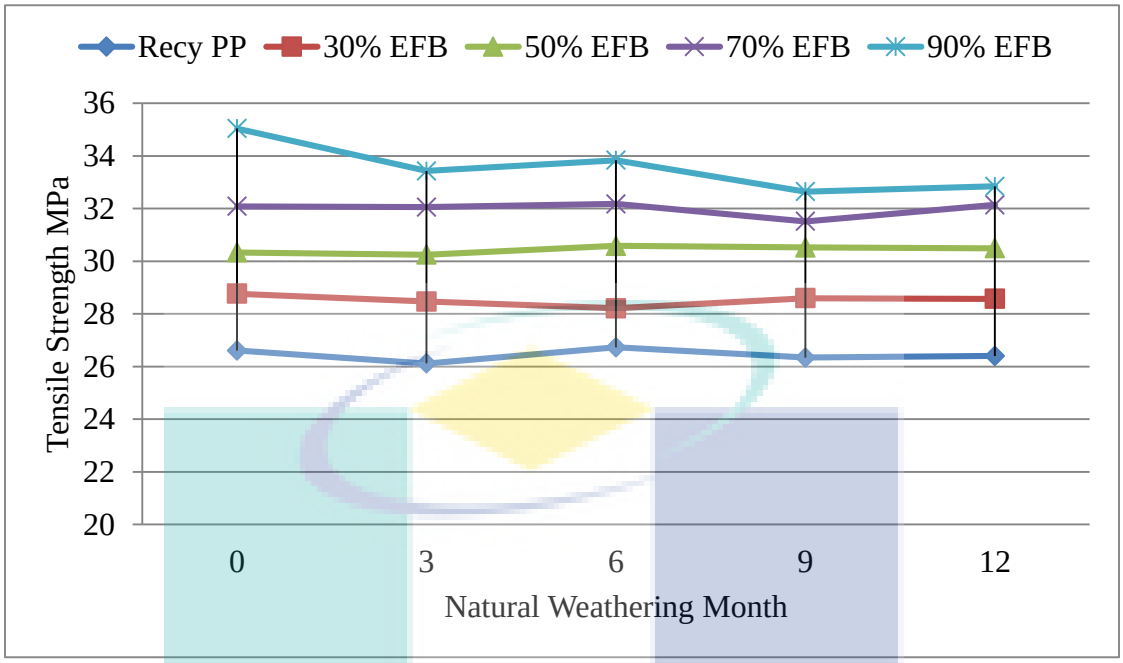

Figure 4.15: Natural weathering Tensile Strength of 4 hours 15 % NaOH

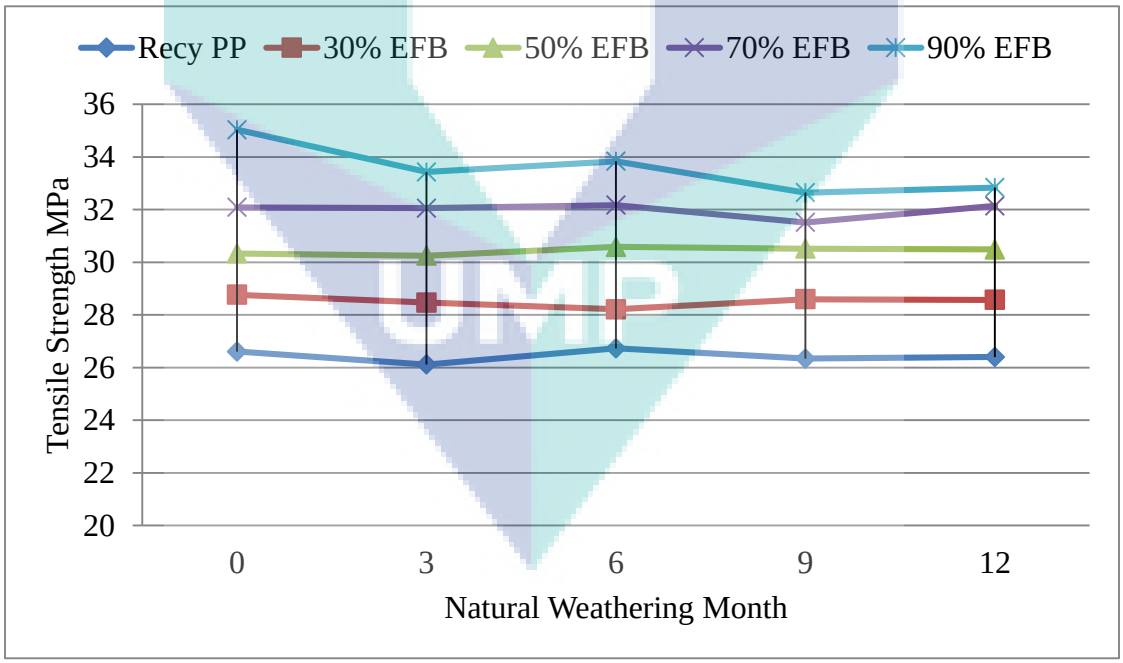

Figure 4.16: Natural weathering Tensile Strength of 5 hours 15 % NaOH

4.2.2 Tensile Strength of conventional treatment composites

The sample ware exposed in the accelerated weathering, the change in mechanical properties during weathering is presented in the Figure 4.17 to Figure 4.19. During weathering very little change in tensile and modulus was found in all conventional hybrid composites. Similar finding was found by (Beg and Pickering, 2008a). Small tensile and modulus reduction could be due to degradation of EFB and EFB matrix bonding, moisture absorption during spray process or by embrittlement of the recycled polypropylenes(Beg and Pickering, 2008a).

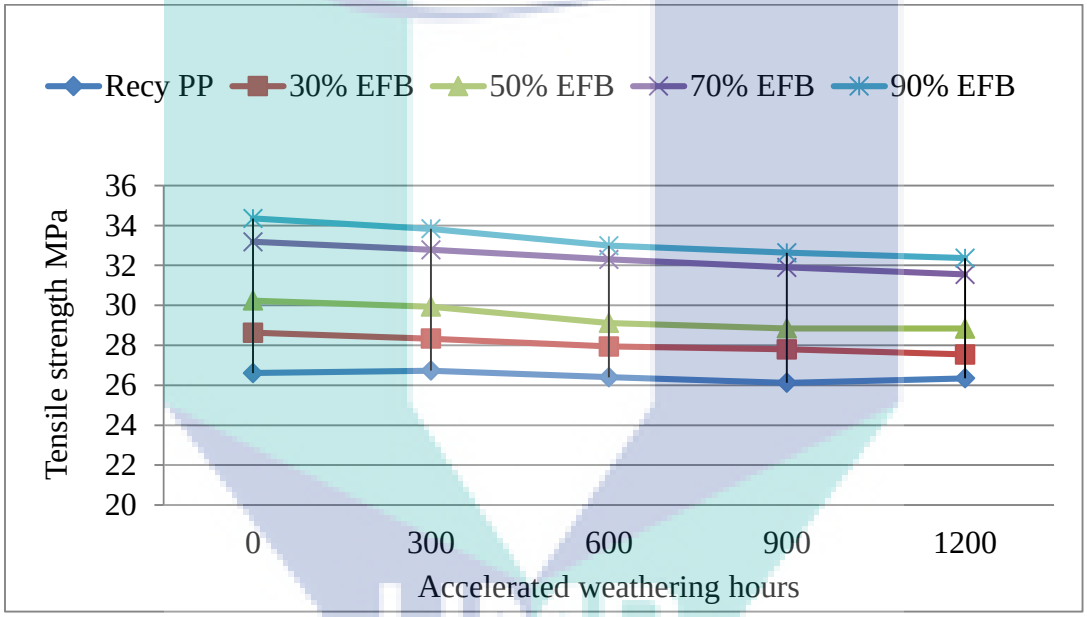

Figure 4.17: Tensile Strength of 15 % 3 hour NaOH Composites

The similar trend line and small reduction of tensile and modulus also occur in another different treatment time and NaOH % as explained earlier glass fibre polypropylenes interface bonding was as a dominant effect that cause decrease in accelerated weathering. Exposure to accelerated weathering degrade mechanical properties mainly due to swelling of fibre that cause micro-crack in the matrix,(Stark and Matuana, 2006).

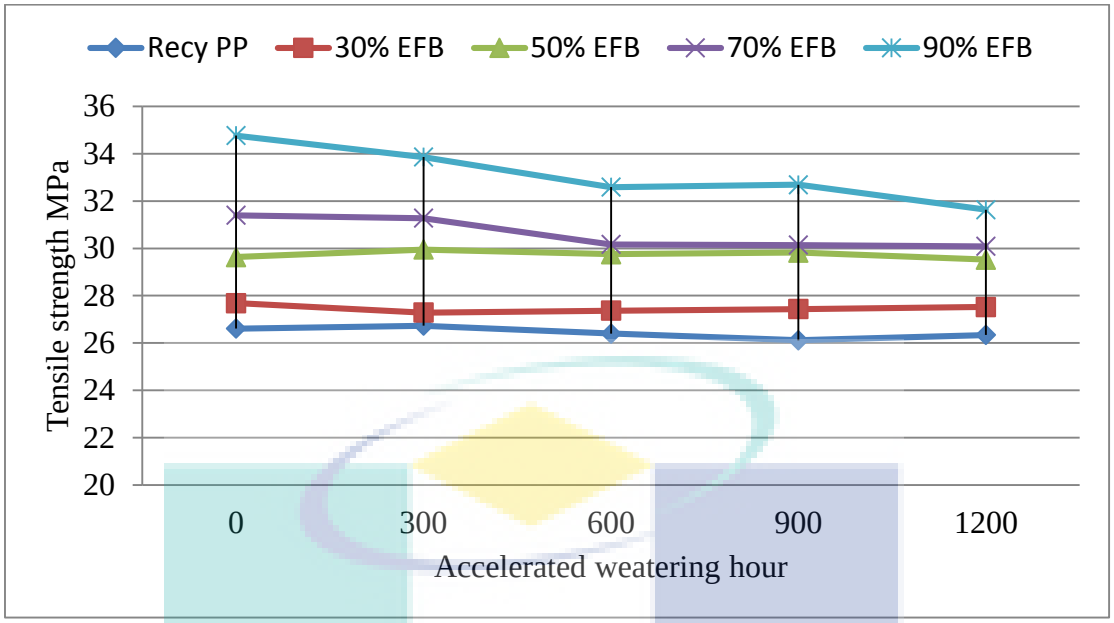

Figure 4.18: Tensile Strength of 15 % 4 hour NaOH Composites

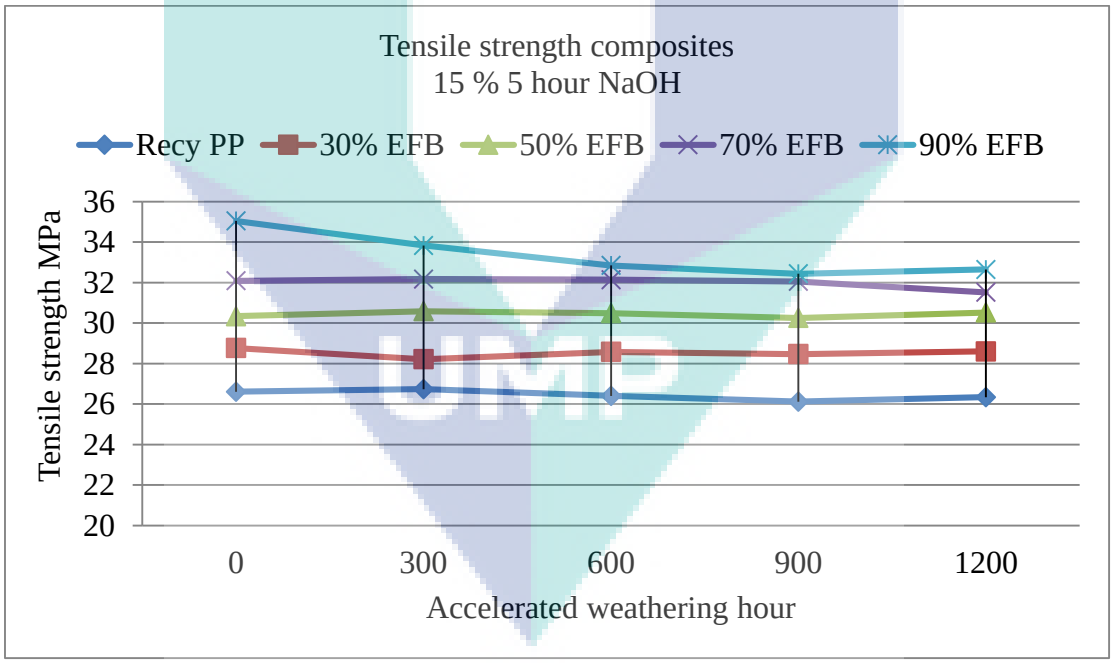

Figure 4.19: Tensile Strength of 15 % 5 hour NaOH Composites

4.3 ANOVA AND STATISTICAL ANALYSIS

4.3.1 Response Surface of Tensile Strength

4.3.1.1 ANOVA for Quadratic Model Tensile

The results obtained in the experiments are summarized in Table 4.6 . Table 4.6 shows the ANOVA table for Tensile Strength of hybrid composites after transformation as recommended by Box-Cox plot (State-Ease, Inc., 2000) using non transform (lambda = 1) (Figure B. 3). The experimental data had a correlation coefficient (R^2) of 0.9945. That means the calculated model was able to explain 99.45% of the results in the case of tensile strength. The results had indicated that the model used to fit the response variable was significant (p<0.0001) and adequate to represent the relationship between the response and the independent variables which denoted that the model was desirably fit.

Table 4.6: ANOVA for Quadratic Model Tensile

Source	Sum of Squares	DF	Mean Square	F Value	Prob > F
Model	167.84	9	18.65	282.28	< 0.0001
A	6.81E-04	1	6.81E-04	0.01	0.9206
B	0.16	1	0.16	2.47	0.1382
C	92.68	1	92.68	1402.81	< 0.0001
A2	19.63	1	19.63	297.18	< 0.0001
B2	39.09	1	39.09	591.69	< 0.0001
C2	0.077	1	0.077	1.16	0.2994
AB	2.25E-04	1	2.25E-04	3.41E-03	0.9543
AC	0.033	1	0.033	0.49	0.4943
BC	0.098	1	0.098	1.48	0.244
Residual	0.92	14	0.066		
Cor Total	168.76	23			

Std. Dev.	0.26	R-Squared	0.9945
Mean	32.11	Adj R-Squared	0.991
C.V.	0.8	Pred R-Squared	0.9859
PRESS	2.37	Adeq Precision	53.611

[a]Prob>F-value less than 0.05 is significant

The model is significant whereby C, A^2 and B^2 have the significant effects in this model term. C, A^2 and B^2 in this ANOVA table have the values of 'Prob>F' less than 0.05, which indicates the model is significant at a 95% confidence level. From the ANOVA table, it is shown that the C is the most significant effect, followed by B^2 and A^2. The difference between adjusted R^2 and predicted R^2 is lower than 0.2 whereby the result for this experiment is at 0.0086, and it is acceptable. Adequate precision also indicates an adequate signal, whereby the ratio obtains was 53.611, which are greater than 4. The normal probability plot of residuals, plot of predicted versus actual, and Box COX plots were performed, and these plots are shown in Appendix B.

Table 4.7: Conventional treatment factors levels

Factors	Unit	Levels 1	Levels 2	Levels 3	Levels 4
A: Treatment Time	Hour	3	4	5	
B: NaOH	%	15	17.5	20	
C: Fibre Ratio	%	30	50	70	90

4.3.1.2 Final equations for Quadratic Model Tensile

The Result in Table 4.6 explains that interactions between variables have significant effect on the tensile strength. Therefore, instead of studying single variable the interactions will be investigated which is significant and importance for a comprehensive optimization study.

The following equations were the final empirical models in terms of coded factors and actual factors for tensile strength respectively. These equations were generated by the Design Expert 6.0.4 software after the transformation had been carried out.

Final Equation in Terms of Coded Factors:

$$TENSILE = + 35.36 - 7.313E\text{-}003 * A + 0.11 * B + 2.90 * C - 1.95 * A^2 - 2.81 * B^2 - 0.13 * C^2 - 5.334E\text{-}003 * A * B + 0.067 * A * C - 0.12 * B * C$$

Equation 4-5

Final Equation in Terms of Actual Factors:

TENSILE = - 141.94278 +15.484 * Treatment Time Hour +15.89820 * NaOH % + 0.13664 * EFB/G Fibre Ratio % - 2.12801 * Treatment Time Hour^2 - 0.38923 * NaOH %^{2} - 9.81979E-004 * EFB/G Fibre Ratio %^{2} + 0.13475 * Treatment Time Hour * NaOH % + 0.017073 * Treatment Time Hour * EFB/G Fibre Ratio % + 7.91299E-004 * NaOH % * EFB/G Fibre Ratio %

Equation 4-6

In the model graph shown in Table 4.6, the significant effects that influence the tensile strength result were the fibre ratio (C), NaOH % (B^2) interaction with the treatment time (A^2). It could be seen that the maximum tensile strength corresponded in a positive correlation which indicated that interaction in synergistic effect.

4.3.1.3 Interactions between process variables

Figure 4.20 shows the response surface plots as functions of treatment time and NaOH % on the Tensile 0 H AW at 60% of fibre ratio. The typical plots like these are dome shaped. From the Figures, it is obvious that tensile strength increase from 3 to 4 treatment time and 15 to 17.5 NaOH %. The tensile decrease when treatment time increase from 4 to 5 and NaOH % increase from 17.5 to 20%. The appropriate maximum tensile strength was determine at a 4 hour treatment time and 17.5 NaOH %, led to the maximum tensile strength at 35.4 MPa.

The effect of varying treatment time and fibre ratio on the conventional hybrid composites at 17.5 NaOH % is provided in Figure 4.21 at high EFB-Glass fibre ratio significantly increase the tensile strength up to 90% fibre ratio and longer treatment time up to 4 hour also lead increase tensile strength and there after decrease further up to 5 hours.

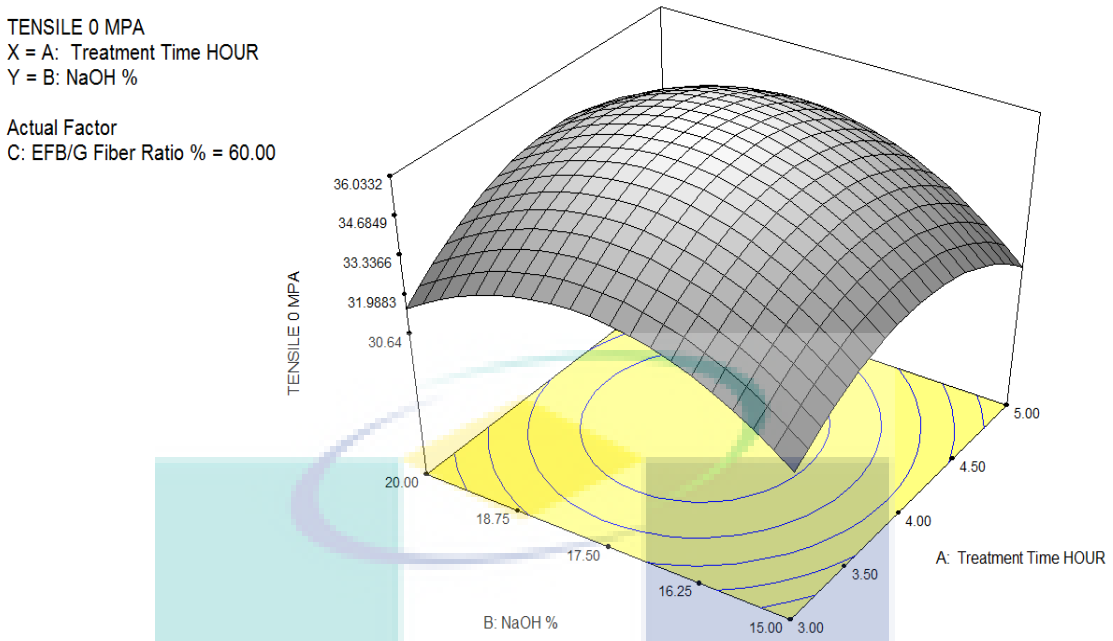

Figure 4.20: 3D graph of the – treatment time - NaOH % tensile strength

Correlation of tensile strength to NaOH % and Fibre ratio is also describe in Figure 4.22, NaOH concentration at 17.5 and higher fibre ratio led to raise the tensile strength up to 38 MPa. In particular, the tensile increased when the fibre ratio (C) was increased from 30 to 90% and as NaOH % (B) was increased from 15 to 17.5%. When the NaOH % (B) setting was increased from 17.5 to 20% and treatment time (A) was increased from 4 to 5 hour, the tensile strength had decreased too. While with the decrease of treatment time less than 4 hour and NaOH % under17.5%, there was a gradual decline in the response. It could be explained that, as the treatment time and NaOH % prolonged, the cellulose decomposition of the fibre might occur, resulting in a decrease in the tensile strength. Figure 4.20 to Figure 4.22 shows the 3D surface graph of tensile strength with respect to the treatment time (A) NaOH % (B) and the fibre ratio (C).

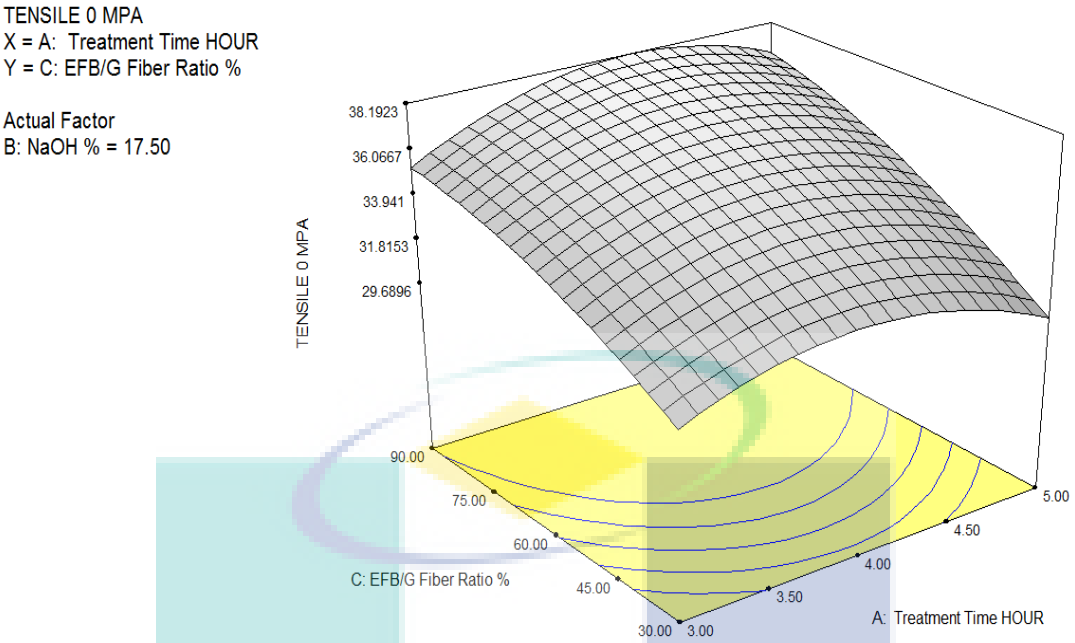

Figure 4.21: 3D graph of the fibre ratio – treatment time tensile strength

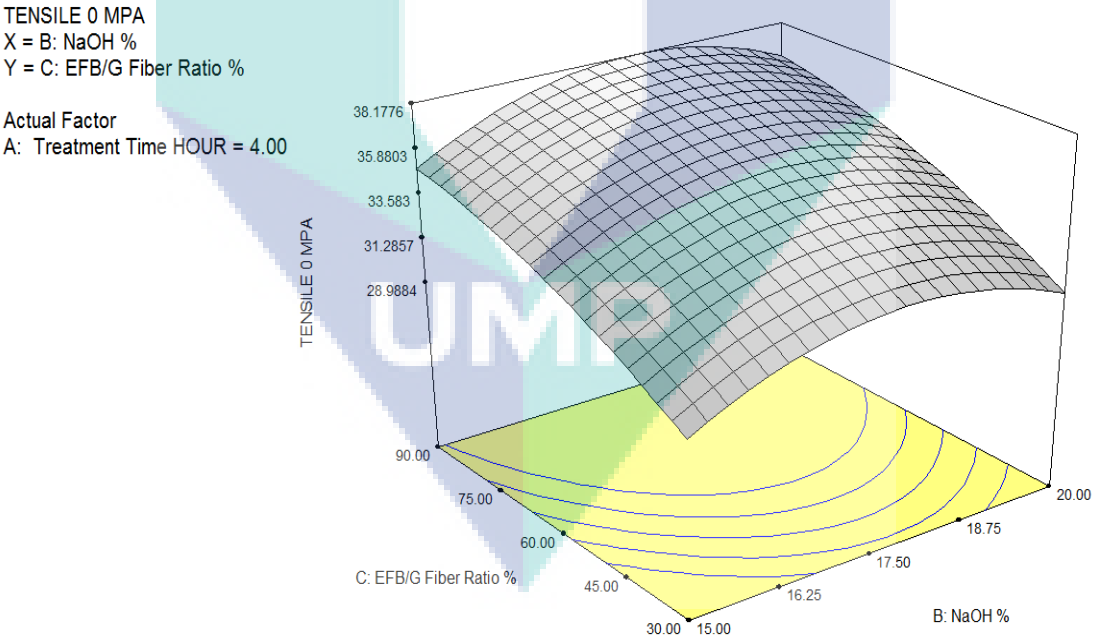

Figure 4.22: 3D graph of the fibre ratio - NaOH % tensile strength

4.3.2 Response Surface Analysis of modulus

4.3.2.1 ANOVA for Quadratic Model Modulus

Table 4.8 shows the ANOVA table for modulus of hybrid composites after transformation as recommended by Box-Cox plot (State-Ease, Inc., 2000) using non transform (lambda = 1)(Figure B. 6). The experimental data had a correlation coefficient (R^2) of 0.9682. That means the calculated model was able to explain 96.82% of the results in the case of modulus. The results had indicated that the model used to fit the response variable was significant (p<0.0001) and adequate to represent the relationship between the response and the independent variables, which denoted that the model was desirably fit.

Table 4.8: ANOVA for Quadratic Model Modulus

Source	Sum of Squares	DF	Mean Square	F Value	Prob > F
Model	2.59E+05	9	28805.9	28.49	< 0.0001
A	64751.47	1	64751.47	64.05	< 0.0001
B	1046.72	1	1046.72	1.04	0.3262
C	49443.47	1	49443.47	48.91	< 0.0001
A2	3610.69	1	3610.69	3.57	0.0797
B2	96113.69	1	96113.69	95.07	< 0.0001
C2	55344.01	1	55344.01	54.74	< 0.0001
AB	360.37	1	360.37	0.36	0.56
AC	2473.44	1	2473.44	2.45	0.1401
BC	984.2	1	984.2	0.97	0.3405
Residual	14153.21	14	1010.94		
Cor Total	2.73E+05	23			

Std. Dev.	31.8	R-Squared	0.9682
Mean	1669.53	Adj R-Squared	0.915
C.V.	1.9	Pred R-Squared	0.9613
PRESS	37924.14	Adeq Precision	20.468

[a]Prob>F-value less than 0.05 is significant

The model is significant whereby A, C, B^2 and C^2 have the significant effects in this model term. A, C, B^2 and C^2 in this ANOVA table have the values of 'Prob >F' less

than 0.05 which indicates the model is significant at a 95% confidence level. From the ANOVA table, it is shown that the B^2 is the most significant effect, followed by A, C^2 and C. The difference between adjusted R^2 and predicted R^2 is lower than 0.2 whereby the result for this experiment is at 0.0069, and it is acceptable. Adequate precision also indicates an adequate signal, whereby the ratio obtains was 20.468, which are greater than 4. The normal probability plot of residuals, plot of predicted versus actual, and Box COX plots were performed, and these plots are shown in Appendix B.

4.3.2.2 Final equations for Quadratic Model Modulus

In the model graph shown in Table 4.8, the significant effects that influence modulus result were the, NaOH % (B^2) interaction with the treatment time (A) and fibre ratio (C). It could be seen that the maximum modulus corresponded in a positive correlation which indicated that interaction in synergistic effect.

The following equations were the final empirical models in terms of coded factors and actual factors for tensile strength respectively. These equations were generated by the Design Expert 6.0.4 software after the transformation had been carried out.

Final Equation in Terms of Coded Factors:

$$\text{MODULUS} = +1840.16 + 71.32 * A + 9.01 * B + 66.89 * C - 26.42 * A^2 - 139.48 * B^2 - 108.05 * C^2 - 6.75 * A * B + 18.36 * A * C + 11.57 * B * C$$

Equation 4-7

Final Equation in Terms of Actual Factors:

$$\text{MODULUS} = -6211.66755 + 293.22144 * \text{Treatment Time Hour} + 786.24680 * \text{NaOH \%} + 11.48842 * \text{EFB/G Fibre Ratio \%} - 26.42233 * \text{Treatment Time Hour}^2 - 22.31701 * \text{NaOH \%}^2 - 0.12005 * \text{EFB/G Fibre Ratio \%}^2 - 2.70005 * \text{Treatment Time Hour} * \text{NaOH \%} + 0.61210 * \text{Treatment Time Hour} * \text{EFB/G Fibre Ratio \%} + 0.15423 * \text{NaOH \%} * \text{EFB/G Fibre Ratio \%}$$

Equation 4-8

4.3.2.3 Interactions between process variables

In particular, the modulus increased when the fibre ratio (C) was increased from 30 to 75% and as NaOH % (B) was increased from 15 to 17.5%. When the NaOH % (B) setting was increased from 17.5 to 20% and the fibre ratio (C) was increased from 75 to 90%, the modulus had decreased. While with the increase of treatment time from 4 to 5 hour and NaOH % around 17.5%, there was a gradual decline in the response. It could be explained that, as the treatment time and NaOH % prolonged, the better lignin decomposition of the fibre might occur, resulting in an increase in the tensile strength. Figure 4.23 shows the 3D surface graph of modulus with respect to the treatment time (A) NaOH % (B) and the fibre ratio (C).

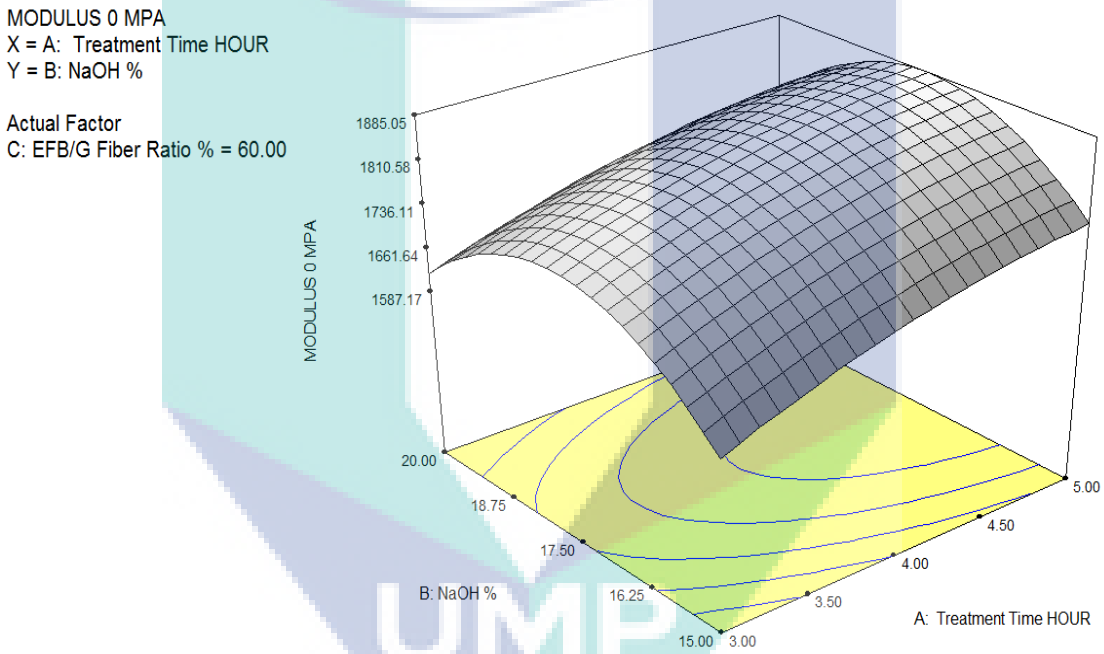

Figure 4.23: 3D graph of the NaOH % – treatment time modulus

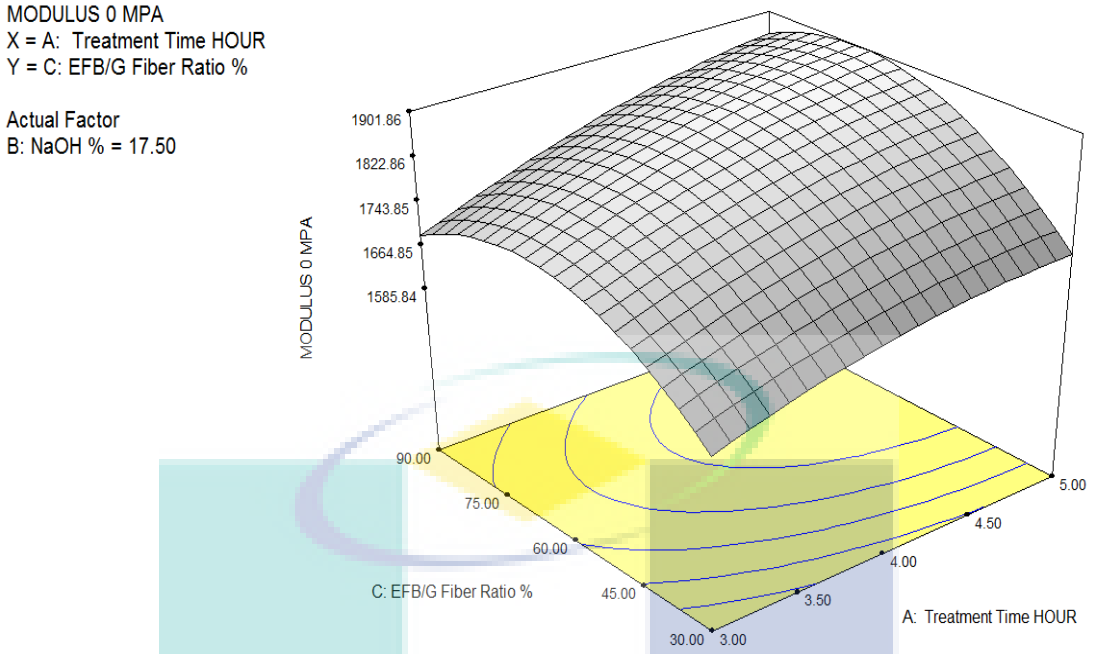

Figure 4.24: 3D graph of the fibre ratio – treatment time modulus

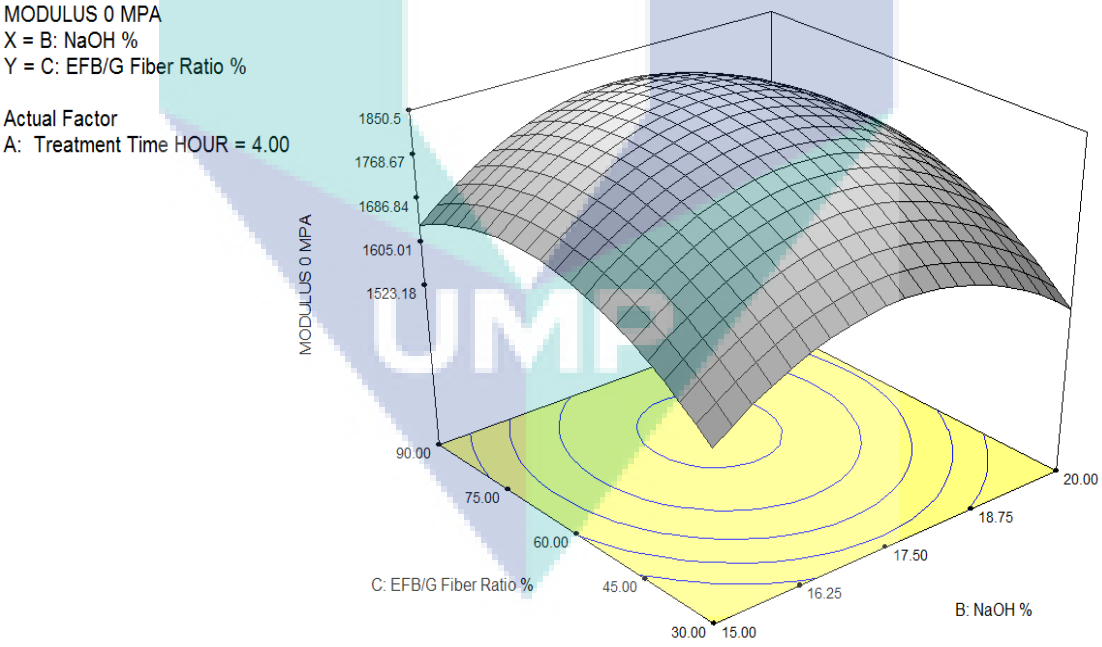

Figure 4.25: 3D graph of the fibre ratio – NaOH % modulus

4.3.3 Response Surface Analysis of elongation at break

4.3.3.1 ANOVA for Quadratic Model Elongation at Break

Table 4.9 shows the ANOVA table for elongation at break of hybrid composites after transformation as recommended by Box-Cox plot (State-Ease, Inc., 2000) using non transform (lambda = 1) (Figure B. 9). The experimental data had a correlation coefficient (R^2) of 0.9928. That means the calculated model was able to explain 99. 28% of the results in the case of modulus. The results had indicated that the model used to fit the response variable was significant (p<0.0001) and adequate to represent the relationship between the response and the independent variables, which denoted that the model was desirably fit.

Table 4.9: ANOVA for Quadratic Model Elongation at Break

Source	Sum of Squares	DF	Mean Square	F Value	Prob > F
Model	101.82	9	11.31	214.83	< 0.0001
A	7.81	1	7.81	148.24	< 0.0001
B	0.012	1	0.012	0.23	0.6392
C	71.9	1	71.9	1365.31	< 0.0001
A2	7.95E-03	1	7.95E-03	0.15	0.7035
B2	11.84	1	11.84	224.76	< 0.0001
C2	6.72E-04	1	6.72E-04	0.013	0.9117
AB	0.078	1	0.078	1.48	0.2443
AC	0.046	1	0.046	0.88	0.3649
BC	0.061	1	0.061	1.16	0.3003
Residual	0.74	14	0.053		
Cor Total	102.56	23			

Std. Dev.	0.23	R-Squared	0.9928
Mean	7.04	Adj R-Squared	0.9882
C.V.	3.26	Pred R-Squared	0.9745
PRESS	2.61	Adeq Precision	53.97

[a]Prob>F-value less than 0.05 is significant

The model is significant whereby A, C, and B^2 have the significant effects in this model term. A, C, and B^2 in this ANOVA table have the values of 'Prob >F' less than 0.05, which indicates the model is significant at a 95% confidence level. From the ANOVA table, it is shown that the C is the most significant effect, followed by B^2 and

A. The difference between adjusted R^2 and predicted R^2 is lower than 0.2 whereby the result for this experiment is at 0.0183, and it is acceptable. Adequate precision also indicates an adequate signal, whereby the ratio obtains was 53.97, which are greater than 4. The normal probability plot of residuals, plot of predicted versus actual, and Box COX plots were performed, and these plots are shown in Appendix B.

4.3.3.2 Final equations for Quadratic Model Elongation at Break

In the model graph shown in Table 4.9, the significant effects that influence elongation at the break results were the, NaOH % (B^2) interaction with the treatment time (A) and fibre ratio (C). It could be seen that the maximum elongation at break corresponded in a positive correlation which indicated that interaction in synergistic effect.

The following equations were the final empirical models in terms of coded factors and actual factors for tensile strength respectively. These equations were generated by the Design Expert 6.0.4 software after the transformation had been carried out.

Final Equation in Terms of Coded Factors:

ELONGATION % = + 8.04 + 0.78 * A + 0.031 * B - 2.55 * C + 0.039 * A^2 - 1.55 * B^2 + 0.012 * C^2 - 0.099 * A * B - 0.079 * A * C + 0.091 * B * C

Equation 4-9

Final Equation in Terms of Actual Factors:

ELONGATION % = - 67.51238 + 1.32244 * Treatment Time Hour + 8.76629 * NaOH % - 0.097268 * EFB/G Fibre Ratio % + 0.039201 * Treatment Time $Hour^2$ - 0.24766 * NaOH $\%^2$ + 1.32292E-005 * EFB/G Fibre Ratio $\%^2$ - 0.039673 * Treatment Time Hour * NaOH % - 2.64475E-003 * Treatment Time Hour * EFB/G Fibre Ratio % + 1.21344E-003 * NaOH % * EFB/G Fibre Ratio %

Equation 4-10

4.3.3.3 Interactions between process variables

In particular, the elongation at break decreased when the fibre ratio (C) was increased from 30 to 90% and as NaOH % (B) was increased from 15 to 17.5%. When the NaOH % (B) setting was increased from 17.5 to 20% the elongation at break had decreased. While with the increase of treatment time from 4 to 5 hour and NaOH % around 17.5%, there was a gradual decline in the response. It could be explained that, as the treatment time and NaOH % prolonged, the better lignin decomposition of the fibre might occur, resulting in an increase in the elongation at break. Figure 4.26 to Figure 4.28 shows the 3D surface graph of elongation at break with respect to the treatment time (A) NaOH % (B) and the fibre ratio (C).

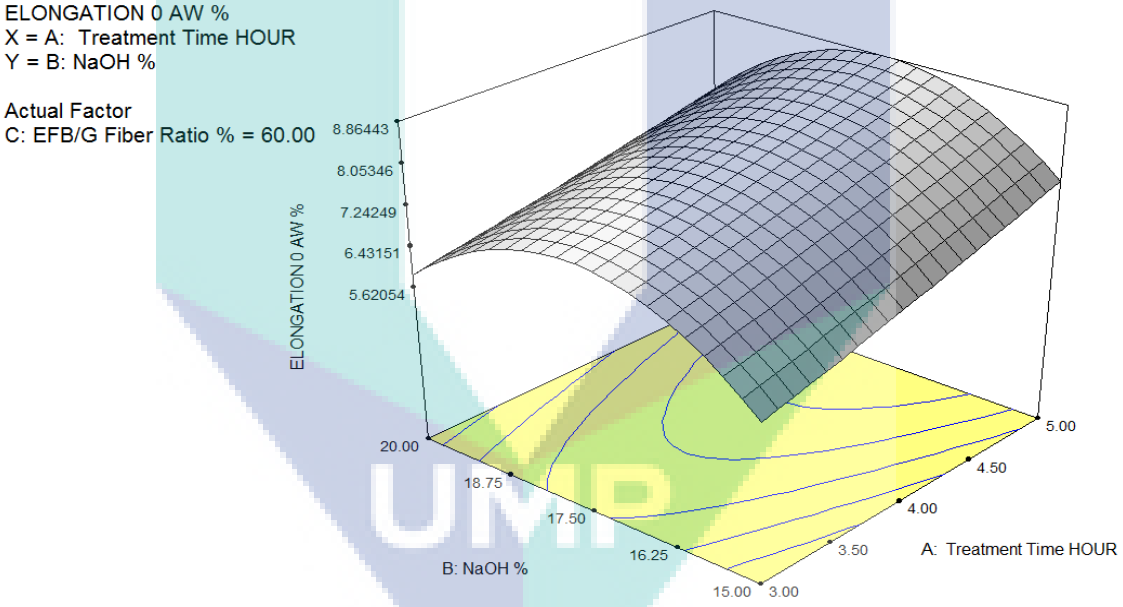

Figure 4.26: 3D graph of the Treatment time – NaOH % elongation

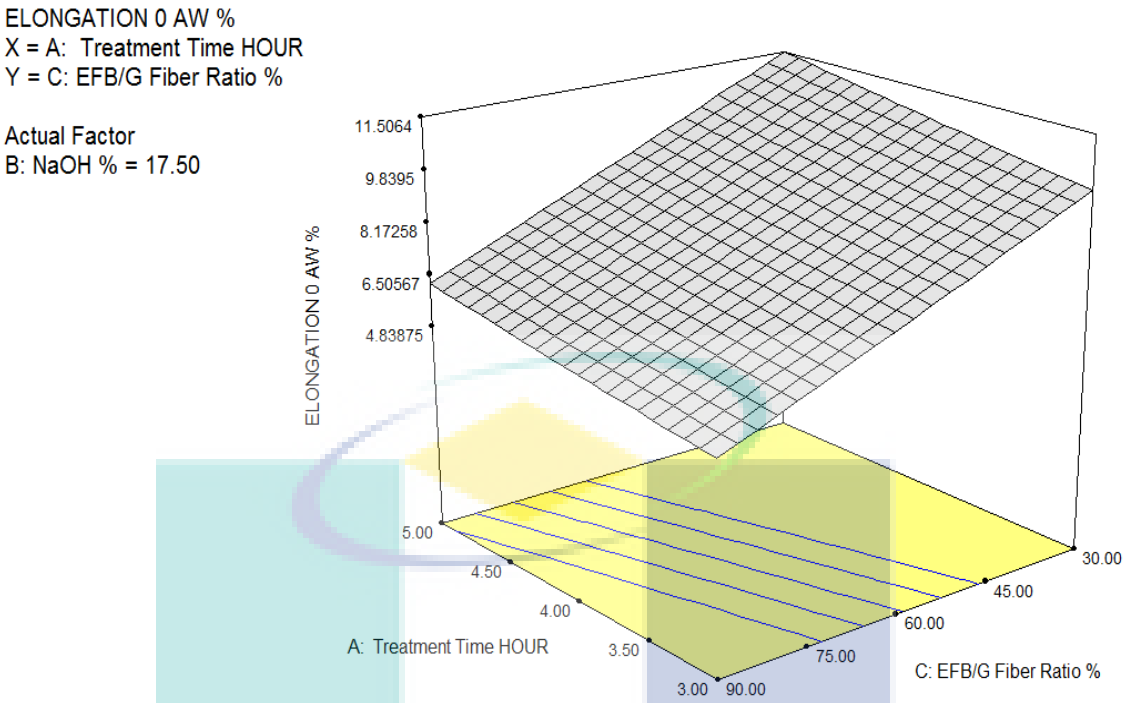

Figure 4.27: 3D graph of the Treatment time – fibre ratio elongation

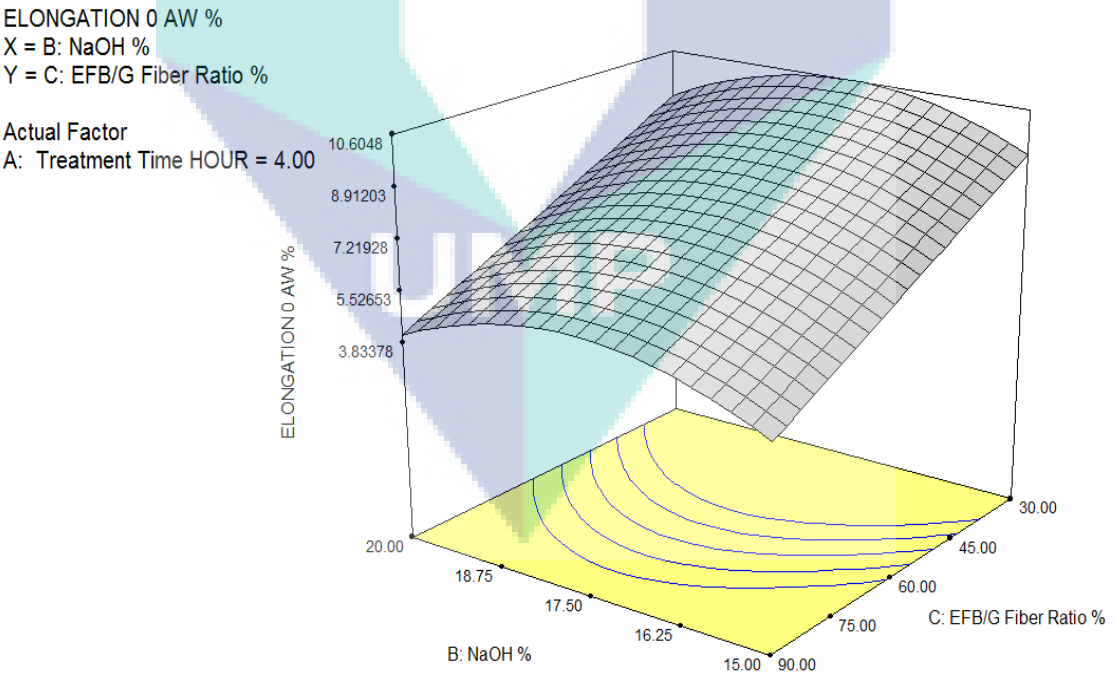

Figure 4.28: 3D graph of the fibre ratio – NaOH % elongation

4.4 VALIDATION OF EMPIRICAL MODEL ADEQUACY

Finding the solutions in optimizing the response (tensile strength, modulus and elongation at break) accuracy was generated by the Design Expert software. The setting for this optimum solution would maximize the goals. In order to verify the adequacy of the models that were developed (Equations 4-5, 4-7 and 4-9), 24 confirmation runs were performed. Using the point prediction tool of the software, the tensile strength, modulus and elongation at break of selected experiments were predicted from the confirmation runs when compared by calculating the residuals and percentage of error.

Table 4.10 shows an example of the output by using the point prediction tool based on the models that were developed by the software. The predicted and the actual values from confirmation runs were compared by calculating the residuals and percentage of error. These values are presented in Table 4.10,Table 4.11 and Table 4.12.

Based on confirmation trials it could be suggested that the empirical models for tensile strength (Table 4.10), modulus of elasticity (Table 4.11) and elongation at breaks (Table 4.12) that were developed were reasonably accurate and was acceptable. This was proven when all the actual values for the confirmation runs were within 95% prediction interval (PI). The percentage error between the actual and predicted value ranged from 0.01 to 2.11%, 0. 06 to 3. 17% and 0.09 to 4. 72% for tensile strength, modulus and elongation at break. Since the difference's percentage error between actual and predicted response were always less than 5%, thus provided its validity.

Table 4.10: Analysis of the confirmation experiments for Tensile Strength

	Tensile Diagnostics	Case Statistics		
Standard Order	**Actual Value**	**Predicted Value**	**Residual**	**% Error**
1	29.47	29.73	-0.26	-0.87
2	36.47	36.12	0.36	1.00
3	30.43	30.31	0.12	0.40
4	27.56	27.72	-0.16	-0.58
5	31.39	31.61	-0.22	-0.70
6	33.4	33.42	-0.018	-0.05
7	35.12	35.31	-0.19	-0.54
8	33.5	33.43	0.071	0.21
9	33.3	33.31	-0.00476	-0.01

10	36.17	36.31	-0.13	-0.36
11	32.39	31.71	0.67	2.11
12	35.22	35.31	-0.098	-0.28
13	31.49	31.49	-0.0039	-0.01
14	34.26	34.34	-0.085	-0.25
15	36.17	36.23	-0.063	-0.17
16	31.89	31.63	0.26	0.82
17	29.27	29.29	-0.018	-0.06
18	29.47	29.49	-0.014	-0.05
19	27.46	27.41	0.048	0.18
20	34.26	34.38	-0.12	-0.35
21	29.47	29.44	0.034	0.12
22	32.34	32.46	-0.11	-0.34
23	29.65	29.75	-0.094	-0.32
24	30.49	30.46	0.036	0.12

Table 4.11: Analysis of confirmation experiment for Modulus

	Modulus Diagnostics	**Case Statistics**		
Standard	**Actual Value**	**Predicted Value**	**Residual**	**% Error**
1	1683.85	1703.55	-19.7	-1.16
2	1683.85	1682.89	0.96	0.06
3	1727.08	1691.75	35.33	2.09
4	1527.39	1542.97	-15.58	-1.01
5	1640.62	1626.72	13.9	0.85
6	1750.46	1698.1	52.36	3.08
7	1679.01	1680.1	-1.09	-0.06
8	1683.85	1708.94	-25.09	-1.47
9	1554.16	1570.74	-16.58	-1.06
10	1835.16	1850.45	-15.29	-0.83
11	1699.01	1671.53	27.48	1.64
12	1619.01	1638.94	-19.93	-1.22
13	1770.31	1755.86	14.45	0.82
14	1770.31	1746.59	23.72	1.36
15	1893.54	1862.26	31.28	1.68
16	1770.31	1768.1	2.21	0.12
17	1532.55	1528.29	4.26	0.28
18	1574.16	1562.85	11.31	0.72
19	1427.7	1442.17	-14.47	-1.00
20	1748.69	1805.85	-57.16	-3.17
21	1683.85	1706.74	-22.89	-1.34
22	1683.85	1714.24	-30.39	-1.77
23	1532.55	1523.18	9.37	0.62
24	1597.39	1585.84	11.55	0.73

Table 4.12: Analysis of confirmation experiment for elongation at break

	Elongation Diagnostics	Case Statistics		
Standard Order	**Actual Value**	**Predicted Value**	**Residual**	**% Error**
1	8.09	8.1	-0.00767	-0.09
2	4.75	4.84	-0.093	-1.92
3	11.43	11.51	-0.076	-0.66
4	9.76	9.8	-0.04	-0.41
5	4.75	5.09	-0.34	4.72
6	5.58	5.58	-0.00236	-0.04
7	3.91	4.08	-0.37	-4.08
8	4.55	4.68	-0.13	-2.78
9	3.98	3.51	0.46	-4.84
10	7.22	7.19	0.03	0.42
11	7.65	7.35	0.31	4.22
12	3.96	3.83	0.12	3.13
13	6.42	6.48	-0.062	-0.96
14	6.36	6.48	-0.12	-1.85
15	6.42	6.25	0.17	2.72
16	6.42	6.4	0.014	0.22
17	8.96	9.12	-0.15	-1.64
18	6.42	6.48	-0.059	-0.91
19	8.35	8.19	0.15	1.83
20	8.98	8.89	0.091	1.02
21	8.43	8.29	0.13	1.57
22	8.14	8.12	0.019	0.23
23	8.97	9.14	-0.023	-0.26
24	9.76	9.78	-0.023	-0.24

4.5 OPTIMISATION CONVENTIONAL HYBRID COMPOSITES

Unite Optimization procedure had been conducted for Hybrid Composites and the prediction results of the empirical model were tabulated in Table 4.13. The treatment time (A), NaOH % (B) and the fibre ratio (C). were set to range within the levels defined in Table 4.7 including tensile strength, modulus , elongation at break water absorption and melt flow index were explained to each goal and importance value. Results had shown optimum treatment time (A) NaOH % (B) and fibre ratio for optimal tensile strength, modulus and fibre ratio were determined in the table 4-11with total desirability value of 0.972 to 0.975 was obtained on a scale of 0 to 1, where 0 represented a completely undesirable response and 1 represented the most desirable response. Under these proposed optimized conditions, the maximum value of the treatment times (A), NaOH % (B) and fibre ratio (C), predicted from the model were explained in the Table 4.14.

4.5.1 Combine Optimization of Run 1

Table 4.13: Conditions of the Combine Optimization Run 1

Name	Goal	Lower Limit	Upper Limit	Lower Weight	Upper Weight	impor tance
Treatment Time	is in range	3	5	1	1	3
NaOH %	is in range	15	19	1	1	3
EFB/G Fibre Ratio %	maximize	30	90	1	1	3
Tensile 0 AW MPa	maximize	27.459	36.472	1	1	5
Modulus 0 AW MPa	maximize	1427.7	1893.54	1	1	4
Elongation 0 AW %	is in range	5	8	1	1	3
Water ABSB 60^{O}C HA	is in range	2.11	5	1	1	3
Sea WTR ABSB 60^{O}C HA	is in range	1.942	5	1	1	3
Melt flow index G/10M	is in range	2.5	3.745	1	1	3

Table 4.14: Result of the Combine Optimization Conditions Run 1

Number	Treatment Time	NaOH %	EFB/G Fibre Ratio	Tensile 0 Aw	Modulus 0 Aw	Elongation 0 Aw %	Water Absb 60 Ha	Sea Wtr Absb 60 Ha	Melt Flow G/10m	Desirability
1	5	17.85	88.35	36.78	1868.22	6.36	4.98	4.88	2.50	0.975
2	5	17.83	88.15	36.76	1869.26	6.38	4.97	4.87	2.50	0.975
3	5	17.79	87.99	36.74	1870.14	6.40	4.97	4.86	2.50	0.975
4	5	17.9	88.66	36.81	1866.37	6.32	4.99	4.89	2.50	0.975
5	5	18.1	89.04	36.84	1861.46	6.24	5.00	4.90	2.51	0.973
6	5	17.59	86.2	36.57	1877.36	6.57	4.89	4.78	2.51	0.972

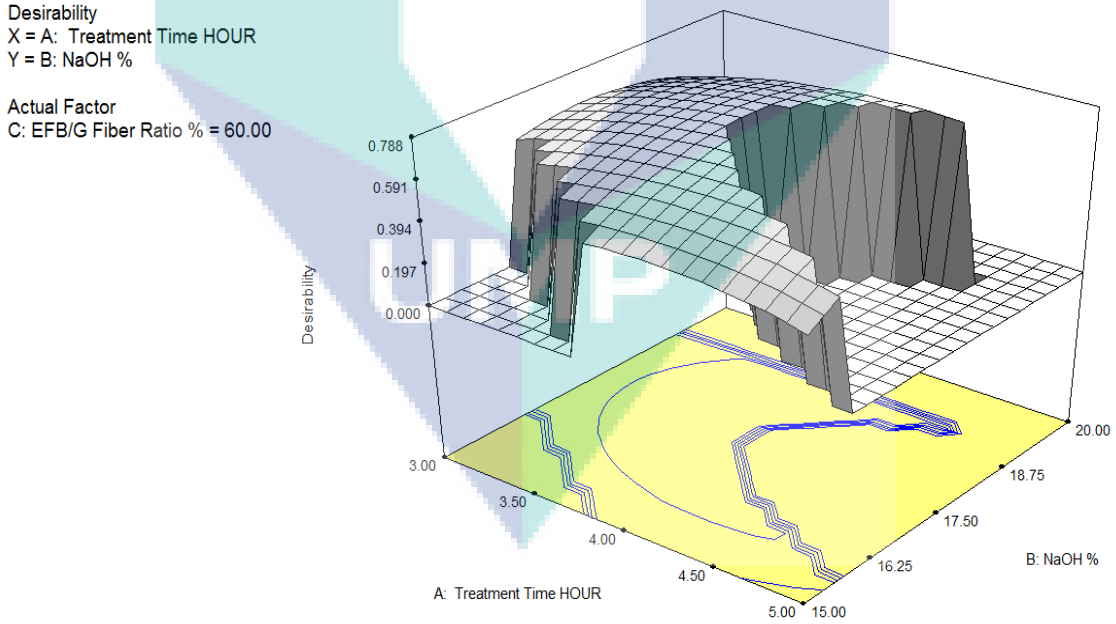

Figure 4.29: Result of the Combine Optimization Conditions Run 1 Graph

4.5.2 Combine Optimization of Run 2

Second Unite Optimization procedure had been conducted for Hybrid Composites and the prediction results of the empirical model were tabulated in Table 4.15. The treatment time (A) NaOH % (B) and the fibre ratio (C) were set to range within the levels defined in the Table 4.15 including tensile strength, modulus, and elongation at break after accelerated weathering and hygrothermal ageing were explained to each goal and importance value. Results had shown optimum treatment time (A) NaOH % (B) and fibre ratio for optimal tensile strength, modulus and fibre ratio were determined in the Table 4.15 with total desirability value of 0.82 was obtained on a scale of 0 to 1, where 0 represented a completely undesirable response and 1 represented the most desirable response. Under these proposed optimized conditions, the maximum values of the treatment time (A), NaOH % (B) and fibre ratio (C), predicted from the model were explained in the Table 4.16.

Table 4.15: Conditions of the Combine Optimization Run 2

Name	Goal	Lower Limit	Upper Limit	Lower Weight	Upper Weight	Importance
Treatment Time HOUR	is in range	3.2	4.7	1	1	3
NaOH %	is in range	16	19	1	1	3
Fibre Ratio %	is in range	40	80	1	1	3
Tensile 0 AW MPA	maximize	27.45	36.47	1	1	5
Modulus 0 AW MPA	maximize	1427.7	1893.5	1	1	4
Elongation 600 AW %	maximize	2.90	8.96	1	1	3
Tensile 1200 AW MPA	maximize	28	35.19	1	1	3
Tensile WTR 80^{O}C HA MPA	is in range	25	31.87	1	1	3
Tensile Sea WTR 60^{O}C HA	is in range	24	30	1	1	3
Tensile Sea WTR 80^{O}C HA	is in range	22	27.33	1	1	3
Water ABSB 80^{O}C HA %	is in range	2.178	5	1	1	3
Sea WTR ABSB 80^{O}C HA %	is in range	2.058	5	1	1	3
Melt flow index G/10M	is in range	2.5	3.745	1	1	3

Table 4.16: Result of the Combine Optimization Conditions Run 2

Number	Treatment Time	NaOH %	Fibre Ratio %	Tensile MPA	Modulus MPA	Elongation 600 AW	Tensile 1200 AW	Tensile WTR 80C HA	Tensile Sea WTR 60C	Tensile Sea WTR 80C	Water ABSB 80C HA	Sea Wtr ABSB 80C	Melt Flow G/10M	Desirability
1	4.49	17.54	65.75	35.4493	1879.2	6.22289	34.2121	30.9835	30	26.5715	4.68992	4.46797	2.77243	0.82

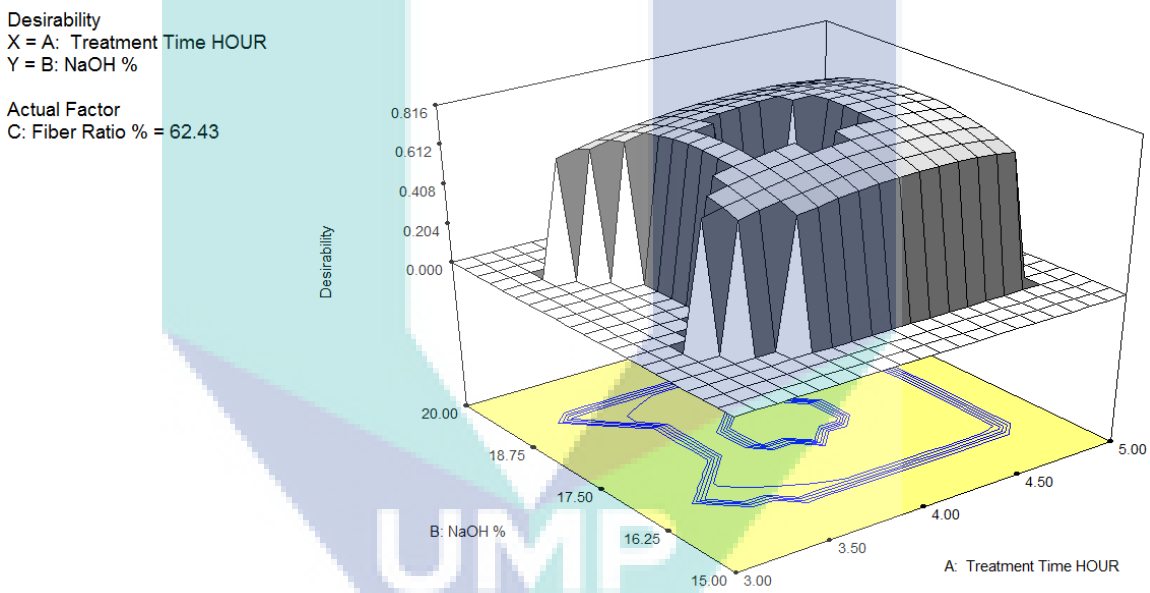

Figure 4.30: Result of the Combine Optimization Conditions Run 2 Graph

conventional treatment optimum condition as explain in Table 4.14 and setting condition in Table 4.13 were at 5 hour, 17,85 % NaOH, 88,35% Fibre Ratio and composites properties predicted is 36,78 MPa Tensile Strength 1868 MPa Modulus and 4,98 % water absorbtion. Second optimum condition as show in theTable 4.16 setting condition at Table 4.15 were were at 4,49 hour, 17,54 % NaOH, 65,75% Fibre Ratio and composites properties predicted is 35,45 MPa Tensile Strength 1879 MPa Modulus and 4,69 % sea water absorbtion.

4.6 HOMEMADE ALKALI TREATMENT OF HYBRID COMPOSITES

In this researchs, experiments were carried out by homemade alkali treatment in order to identify the each parameter's interaction and the optimum operational condition that would result in a high properties of hybrid composites. The operational conditions involved were the temperature, treatment time, NaOH percentage, Fusabond, MAPP percentage and fibre ratio. These findings at the end will give essential data on improving natural fibre treatments and hybrid composites fabrications.

4.6.1 DSC and TGA of the EFB-Glass fibre hybrid composites

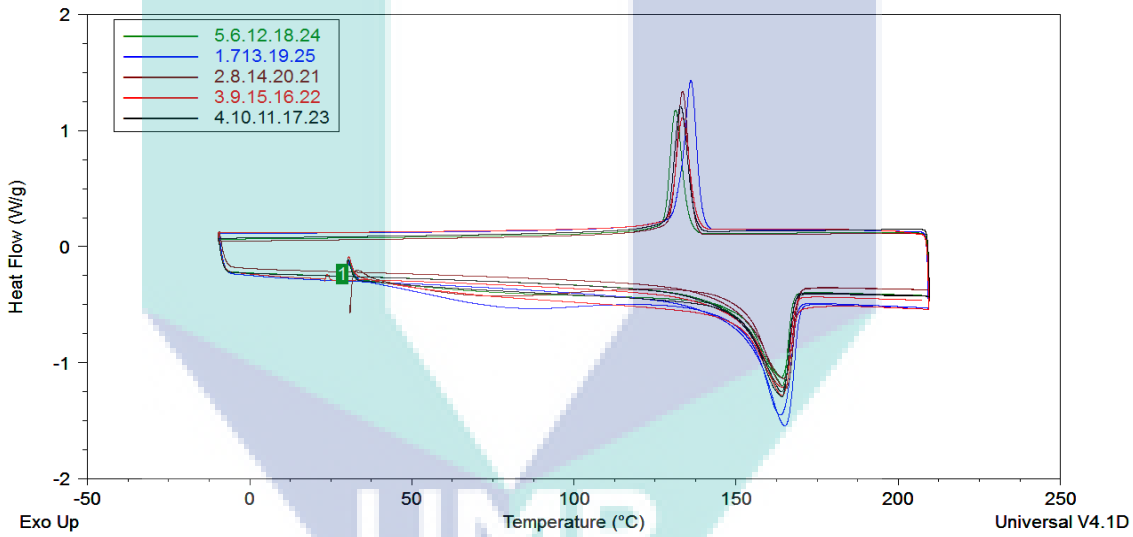

Figure 4.31: DSC graph of homemade hybrid composites

Table 4.17: Crystallization and melting heat flow-temperature

Homemade STD	Crystallization Heat flow W/G	Crystallization Temp C	Melting Heat flow W/G	Melting Temp C
1	1.332	137.86	-1.35	163.54
2	0.942	133.37	-0.73	165.79
3	1.244	135.68	-1.37	164.13
4	1.062	132.75	1.12	163.85
5	0.965	135.55	-1.18	164.23
6	0.925	134.55	-1.12	163.23
7	1.324	135.86	-1.63	163.54
8	0.962	133.37	-0.58	164.79

9	1.224	133.68	-1.54	165.17
10	1.072	133.75	1.81	163.85
11	1.092	132.75	1.61	163.85
12	0.935	135.55	-1.51	163.73
13	1.362	135.86	-1.43	163.54
14	0.982	134.37	-0.28	164.79
15	1.284	133.68	-1.34	164.97
16	1.244	134.68	-1.54	164.37
17	1.082	132.75	1.21	163.85
18	0.975	136.55	-1.21	163.23
19	1.343	135.86	-1.53	163.54
20	0.992	134.37	-0.75	164.29
21	0.952	133.37	-0.72	164.79
22	1.524	132.68	-1.38	164.87
23	1.702	132.75	1.31	163.25
24	0.965	135.55	-1.16	163.23
25	1.732	135.86	-1.37	163.54

Temperatures of crystallization, melting point and heat flow of crystallization of the EFB-Glass fibre hybrid composites have different value, as explained in Table 4.17 there was no significant change in the crystallization temperature with respect to the alkali treatment time temperature of the composites. However, all composites presented higher crystallization temperatures compared to recycled polypropylene. A small difference between sample containing of the fibre ratio was also observed in all composites sample tested.

Figure 4.32 shows DSC scanning curves of samples containing homemade of EFB fibre, prepared in 10 to 20 % NaOH and 4 to 8 hour fibre treatment. No significant changes in the melting temperature of composites containing the difference of fibre treatment and coupling agent were observed Moreover, with changes in the fibre ratio, the melting and crystallization curves were not significantly different.

TGA curve of recycled polypropylene matrix, and homemade hybrid composites are shown in Figure 4.32. All the composites TGA curves show the initial transition around 250 to 300ºC due to the start of EFB fibre degradations. The decomposition temperature of the samples slightly different in the range of 300 to 450 as shown in the Figure 4.32 where the TGA traces shifted to lower temperatures with increasing EFB content. TGA transitions for composites remaining from 500 up to 650ºC also found shifted to slightly lower doe the fibre ratio or glass fibre residual content of the composites.

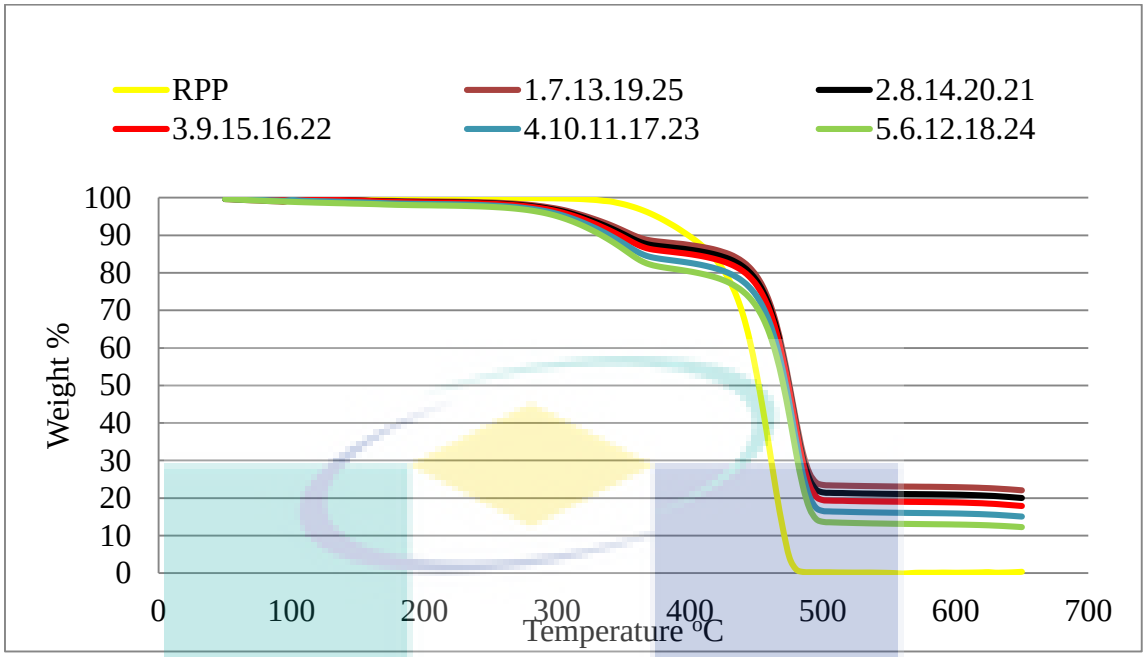

Figure 4.32: TGA graph of homemade hybrid composites

4.6.2 Water absorption of homemade hybrid composites

Water sensitivity is an important selection criterion for many practical applications of hybrid composites. Water absorption in hybrid filled composites can be significant; the migration of water through the material can lead to a disturbance of the filler/polymer interface, thus changing the characteristics and physical performance of the composites. In order to verify the fresh and sea water absorption behaviour of hybrid composites, immersion experiments were performed in the hygrothermal testing device for 60 days.Figure 4.33 to Figure 4.38 shows the water absorption properties in the fibre ratio of polypropylene composite with 50, 60, 70, 80 and 90% of the fibre's ratio, prepared temperatures at 60, 67.5, 75, 82.5 and 90ºC and 4 to 8 hours treatment times. The experiment recorded the absorption of the samples in the water and sea water hygrothermal ageing at 27, 60 and 80ºC during 60 days.

Figure 4.33 shows the response surface plots as functions of treatment time and temperature on the water absorption 27ºC Higrothermal ageing at 70% of the fibre ratio the typical plots like these is dome shaped. From the Figures, it is obvious that water absorption decrease from 60 to 90 treatment temperature and 4 to 8 hour of treatment

time. The water absorption decreased when the temperature increase from 60 to 90ºC. The appropriate minimum water absorption was determined at an 8 hour treatment time and 90ºC treatment temperature, led to the low-water absorption at 2.27%.

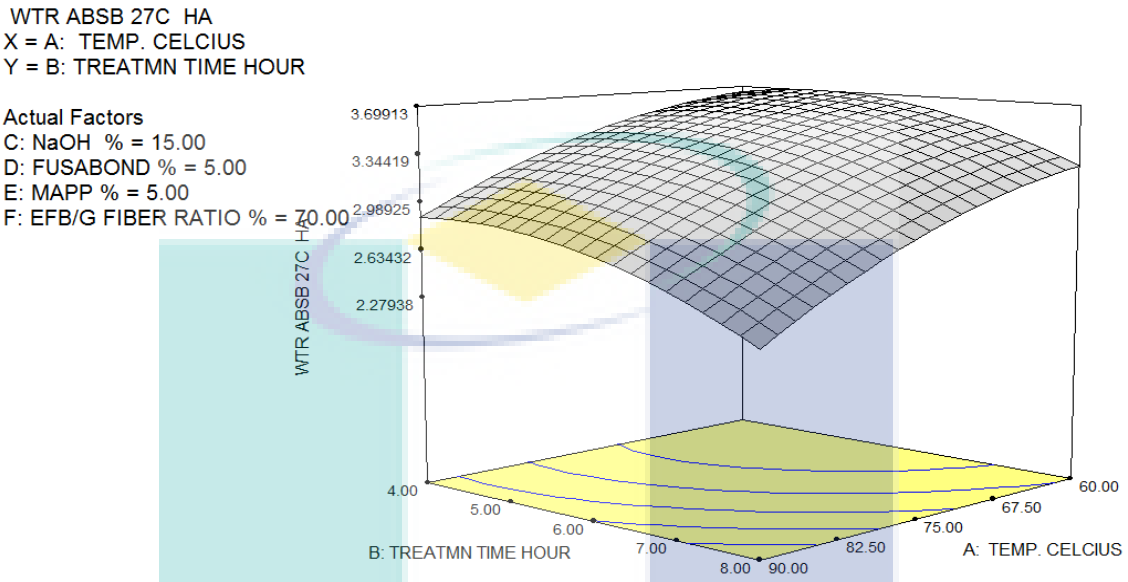

Figure 4.33: 3D Graph water absorption 27 ºC hybrid composites

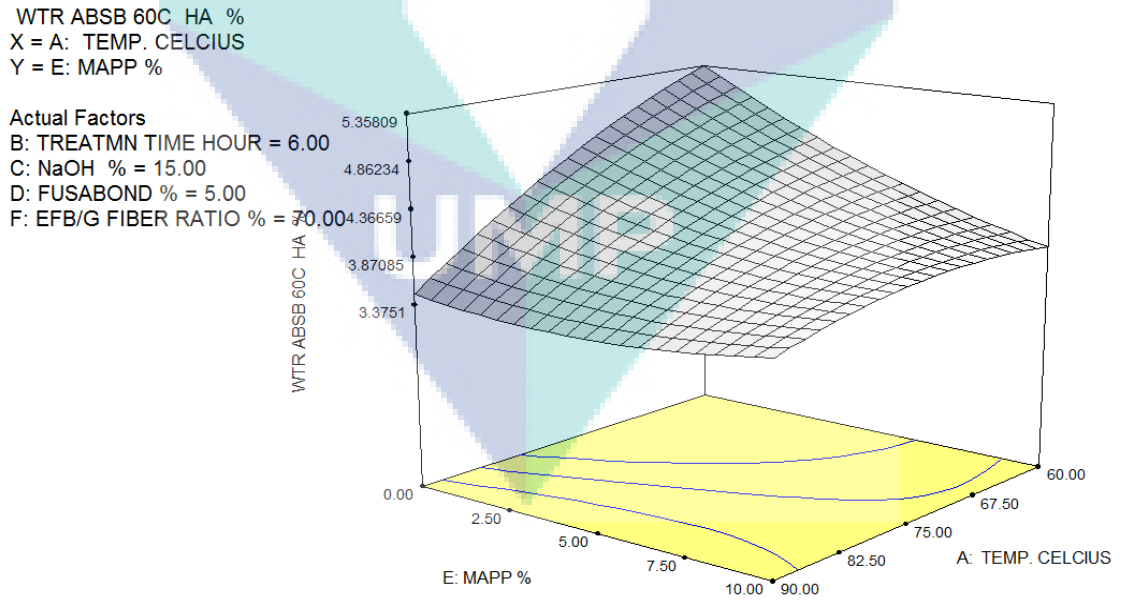

Figure 4.34: 3D Graph water absorption 60 ºC hybrid composites

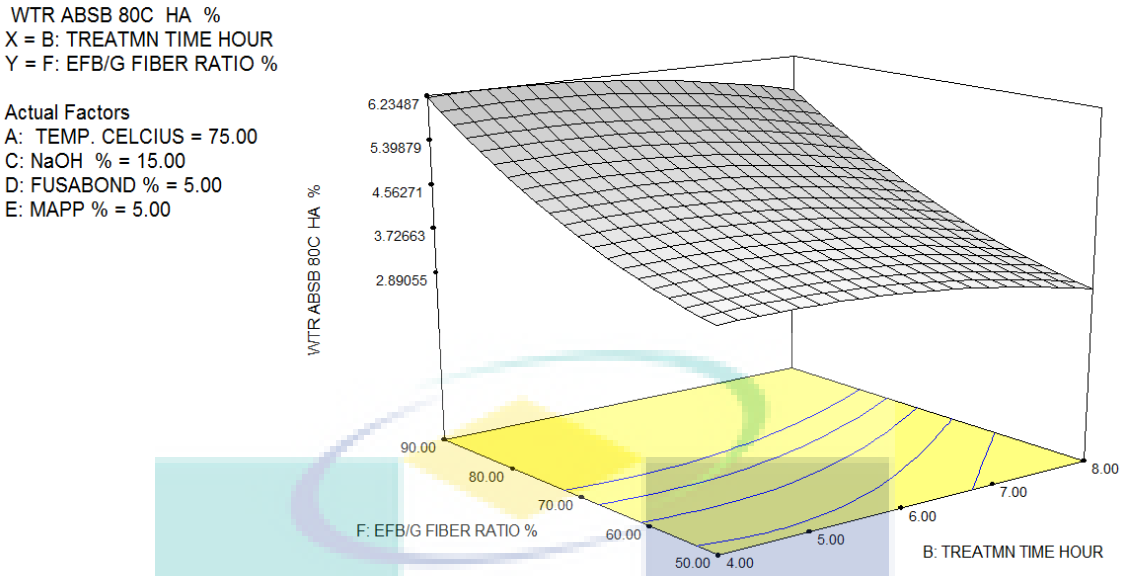

Figure 4.35: 3D Graph water absorption 80 ^{o}C hybrid composites

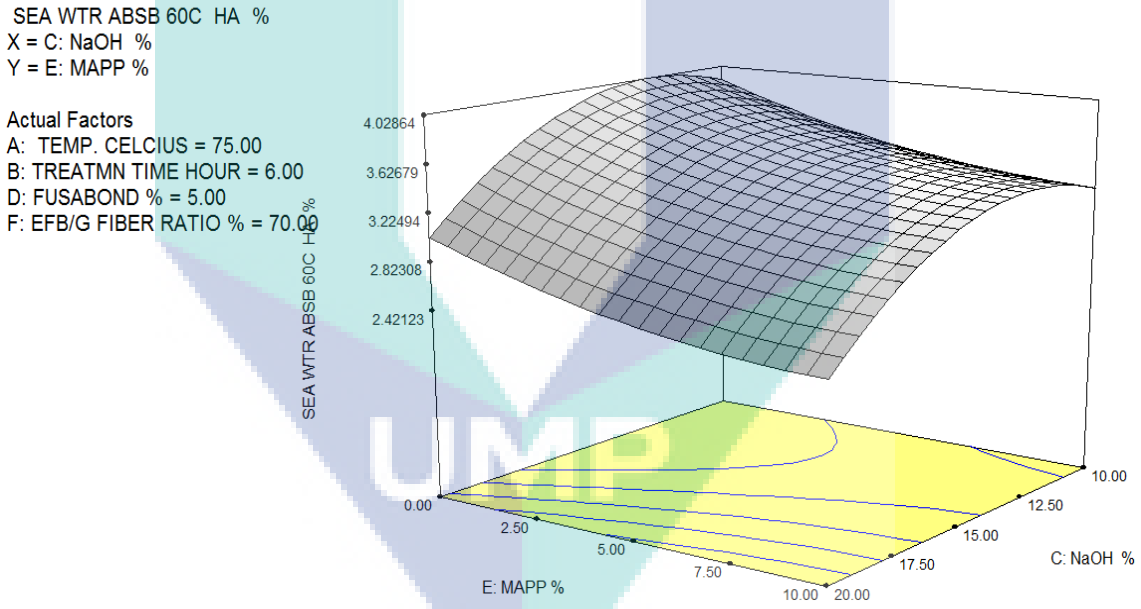

Figure 4.36: 3D Graph sea water absorption 60 ^{o}C hybrid composites

The effect of varying treatment time and fibre ratio on the Homemade hybrid composites at 15% NaOH 80^{o}C, Hygrothermal Ageing at 80^{o}C is provided in Figure 4.35 .at high EFB-Glass fibre ratio significantly increased the water absorption up to 90% fibre ratio and shorter treatment time up to 4 hours also lead increase water absorption. Correlation of sea water absorption to NaOH % and MAPP % is also described in Figure 4.36, temperature treatment at 75^{o}C, 6 hours and 70% fibre ratio. NaOH concentration up to 20% and higher MAPP % led to decrease the water absorption up to 2.4%.

Overall, the water absorption increased when the fibre ratio (F) was increased from 50 to 90% and as NaOH % (C), MAPP % (E), and temperature treatment (A) was decreased. When the NaOH % (C) setting was increased from 10 to 20% and treatment time (A) was increased from 4 to 8 hours, the water absorption had decreased. While with the decrease of treatment time less and NaOH %, there was a gradual decline in the sea water absorption response. It could be explained that, as the low treatment time and NaOH %, the less lignin decomposition of the fibre might occur, resulting in an increase in the water absorption. Figure 4.33 to Figure 4.38 shows the 3D surface graph of fresh water: and sea water absorption with respect to the treatment temperature (A), treatment time (B), NaOH % (C), Fusabond % (D), MAPP % (E) and the fibre ratio (F).

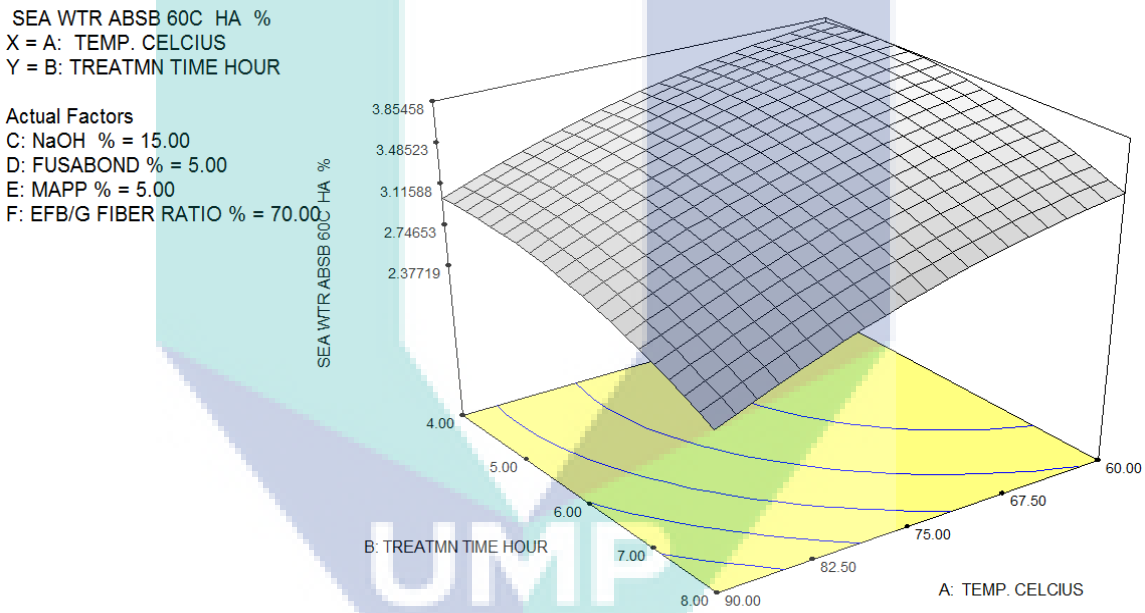

Figure 4.37: 3D Graph sea water absorption 60 ^{o}C hybrid composites

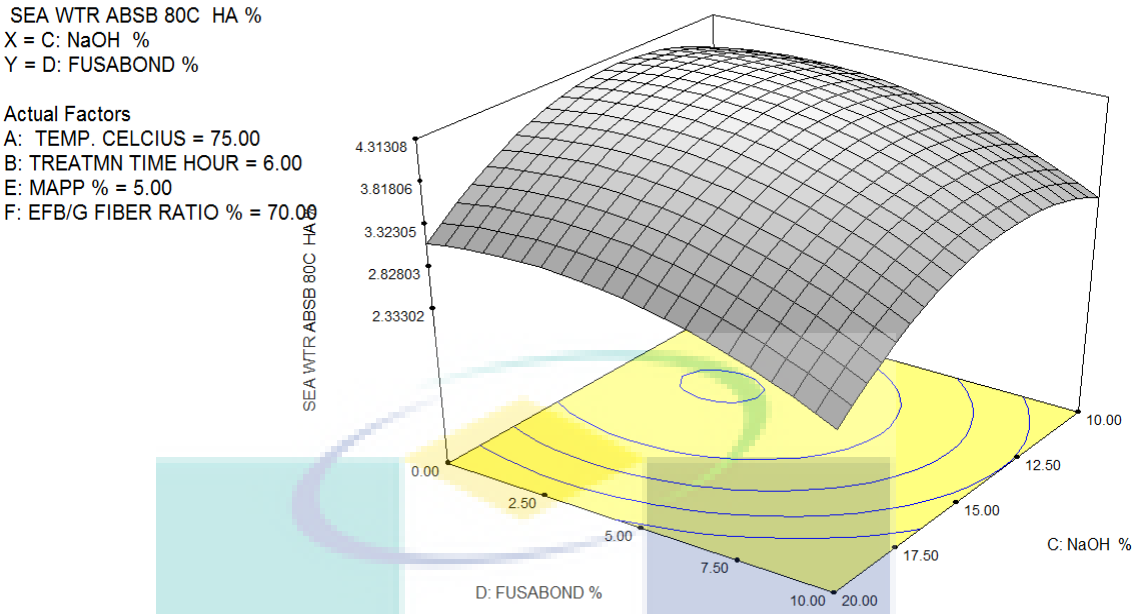

Figure 4.38: 3D Graph sea water absorption 80 ºC hybrid composites

4.6.3 Melt Flow Index

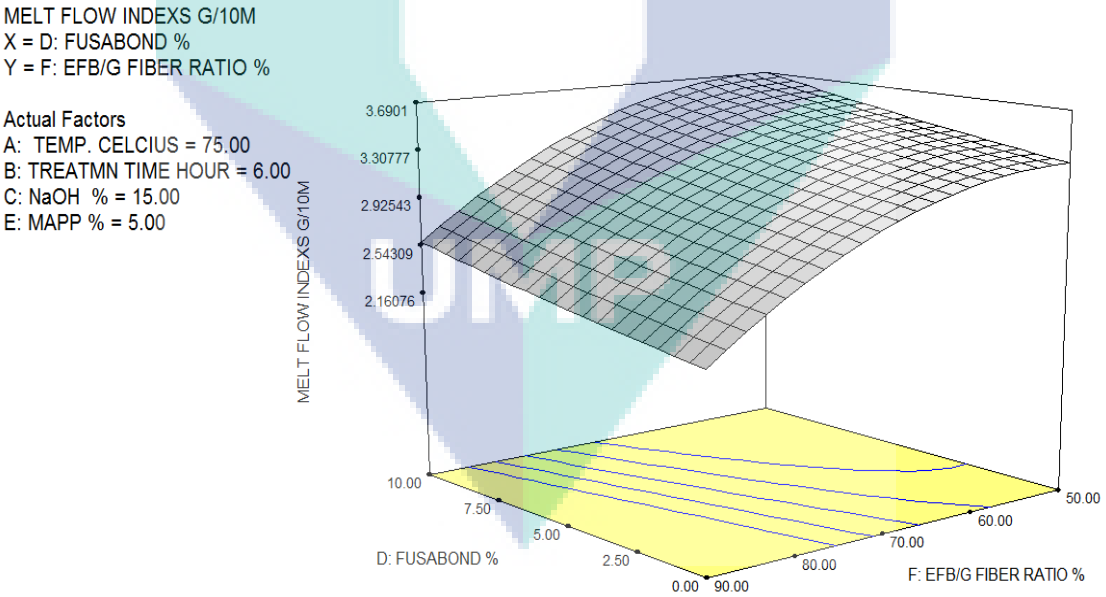

Figure 4.39: Melt Flow Index of EFB-Glass Fibre Composites

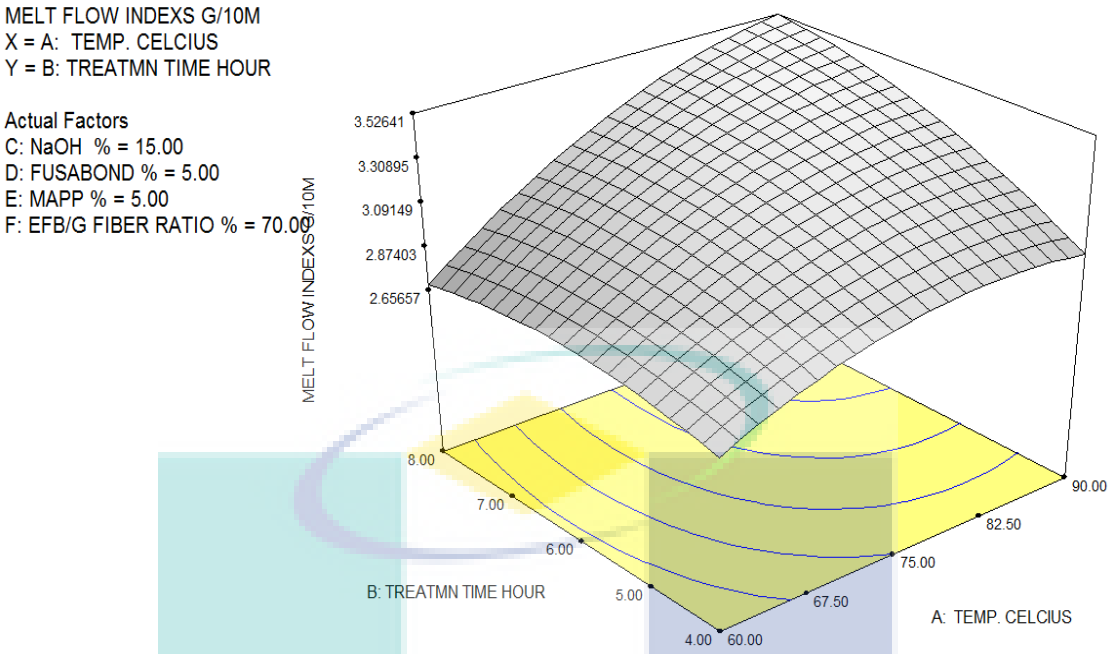

Figure 4.40: Melt Flow Index of EFB-Glass Fibre Composites

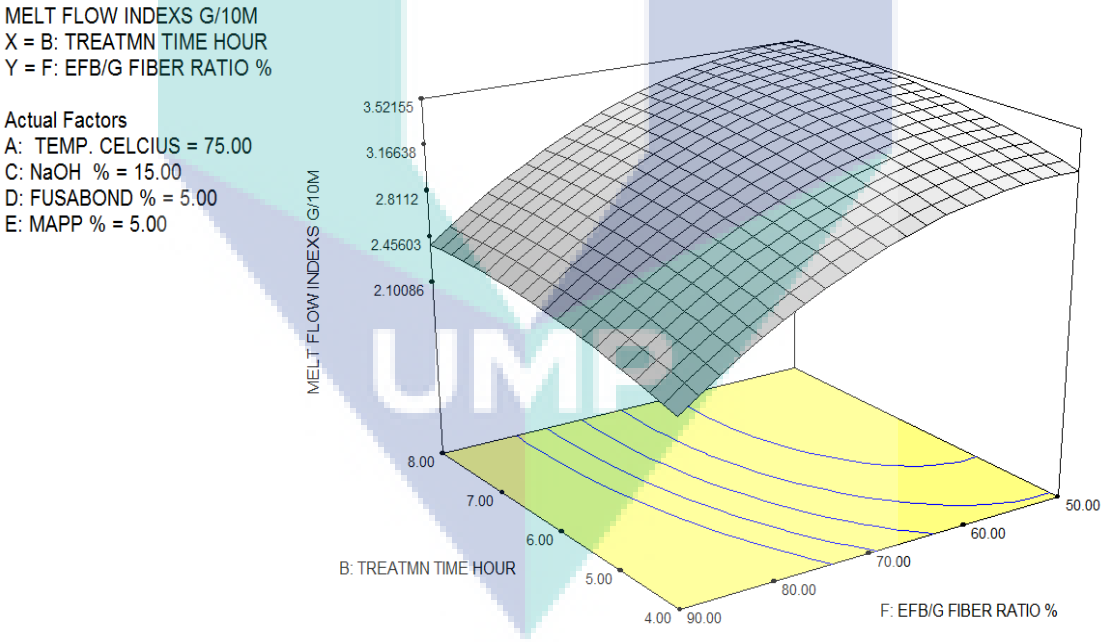

Figure 4.41: Melt Flow Index of EFB-Glass Fibre Composites

Figure 4.39 to Figure 4.41 shows the Melt Flow Index of homemade alkaline treatment composite. From the Figure, it can be seen that Melt Flow Index of 4 to 8 hours of treated homemade alkaline composite is similar. Treated composite with higher treatment time, NaOH, Fusabond and MAPP % was not noticeable changed to melt flow

index response. Ratio of EFB/Glass fibre from 50 to 90 had been significant melt flow response. The response was decreased by increased of Ratio EFB/Glass fibre from 3.52 to only 2.20 G/10 M. This might be due on low fluidity of EFB fibre in the composites' melting condition.

4.7 ANOVA AND STATISTICAL ANALYSIS

4.7.1 Response Surface Analysis of Tensile Strength

4.7.1.1 ANOVA for Quadratic Model Tensile

Table 4.19 shows the ANOVA table for Tensile Strength of hybrid composites after transformation as recommended by Box-Cox plot (State-Ease, Inc., 2000) using non transform (lambda = 1) (Figure C. 3). The experimental data had a correlation coefficient (R^2) of 0.9886. That means the calculated model was able to explain 98. 86% of the results in the case of tensile strength. The results had indicated that the model used to fit the response variable was significant (p<0.0001) and adequate to represent the relationship between the response and the independent variables which denoted that the model was desirably fit.

Table 4.18: Homemade treatment factors levels

Factors	Unit	Levels 1	Levels 2	Levels 3	Levels 4	Levels 5
A:Temperature	Celsius	60	67.5	75	87.5	90
B:treatment time	Hours	4	5	6	7	8
C:NaOH	%	10	12.5	15	17.5	20
D:Fusabond	%	0	2.5	5	7.5	10
E:MAPP	%	0	2.5	5	7.5	10
F:Fibre ratio	%	50	60	70	80	90

Table 4.19: ANOVA for Quadratic Model Tensile

Source	Sum of Squares	DF	Mean Square	F Value	Prob > F
Model	271.2	17	15.95	35.64	< 0.0001
A	8.29	1	8.29	18.52	0.0036
B	0.31	1	0.31	0.69	0.4328
C	0.68	1	0.68	1.52	0.2568
D	1.37	1	1.37	3.06	0.1235
E	0.55	1	0.55	1.22	0.3057
F	0.11	1	0.11	0.25	0.6328
A2	5.58	1	5.58	12.46	0.0096
B2	0.35	1	0.35	0.78	0.4054
C2	0.074	1	0.074	0.17	0.696
D2	0.3	1	0.3	0.67	0.4388
E2	2.04	1	2.04	4.57	0.0699
F2	0.97	1	0.97	2.16	0.185
AB	0.014	1	0.014	0.031	0.865
AC	0.7	1	0.7	1.57	0.25
AD	1.04	1	1.04	2.31	0.172
AE	1.32	1	1.32	2.96	0.1292
AF	0	0			
BC	0	0			
BD	0.77	1	0.77	1.73	0.23
BE	0	0			
BF	0	0			
CD	0	0			
CE	0	0			
CF	0	0			
DE	0	0			
DF	0	0			
EF	0	0			
Residual	3.13	7	0.45		
Cor Total	274.33	24			

Std. Dev.	0.67	R-Squared	0.9886
Mean	32.79	Adj R-Squared	0.9608
C.V.	2.04	Pred R-Squared	0.8051
PRESS	53.47	Adeq Precision	29.186

[a]Prob>F-value less than 0.05 is significant

The model is significant whereby A and A^2: had the significant effects in this model term. A and A^2 in this ANOVA table had the values of 'Prob>F' less than 0.05, which indicates the model is significant at a 95% confidence level. From the ANOVA

table, it is shown that the A is the most significant effect, followed by A^2. The difference between adjusted R^2 and predicted R^2 is lower than 0.2 whereby the result for this experiment is at 0.028, and it is acceptable. Adequate precision also indicates an adequate signal, whereby the ratio obtains was 29.186, which are greater than 4. The normal probability plot of residuals, plot of predicted versus actual, and Box COX plots were performed, and these plots are shown in Appendix C.

4.7.1.2 Final equations for Quadratic Model Tensile

The Result in Table 4.19 explains that interactions between variables have significant effect on the tensile strength. Therefore, instead of studying single variable the interactions will be investigated, which is significant and importance for a comprehensive optimization study.

The following equations were the final empirical models in terms of coded factors and actual factors for tensile strength respectively. These equations were generated by the Design Expert 6.0.4 software after the transformation had been carried out. The following equations were the final empirical models in terms of coded factors for tensile strength. These equations were generated by the Design Expert 6.0.4 software after the transformation had been carried out.

Final Equation in Terms of Coded Factors:

TENSILE = +36.51.+1.12 * A.-0.93 * B -1.15 * C +1.40 * D +0.95 * E +0.60 * F -1.25 * A^2 -0.66 * B^2 -0.39 * C^2 -0.61 * D^2 -2.67 * E^2 -1.84 * F^2 -0.16 * A * B -1.64 * A * C -2.73 * A * D -2.88 * A * E +0.93 * B * D

Equation 4-11

In the model graph shown in Table 4.19, the significant effects that influence the tensile strength result were treatment temperature. It could be seen that the maximum tensile strength corresponded in a positive correlation which indicated that interaction in synergistic effect.

4.7.1.3 Interactions between process variables

Figure 4.42 to Figure 4.47 shows the response surface plots as functions of treatment time and NaOH % on the Tensile 0 H AW at 60% of the fibre ratio the typical plot like this is dome shaped. From the Figures, it is obvious that tensile strength increase from 3 to 4 treatment time and 15 to 17.5 NaOH %.: The tensile decrease when the treatment time increase from 4 to 5 and NaOH % increase from 17.5 to 20%. The appropriate maximum tensile strength was determined at a 4 hour treatment time and 17.5 NaOH %, led to the maximum tensile strength at 35.4 MPa.

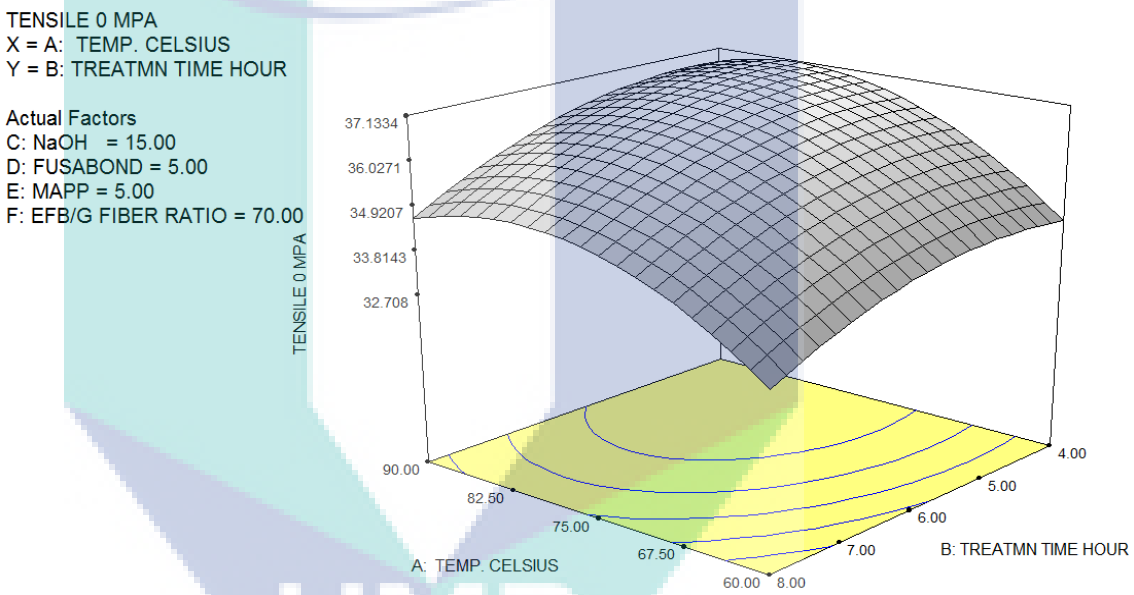

Figure 4.42: 3D graph of the temperature – treatment time tensile strength

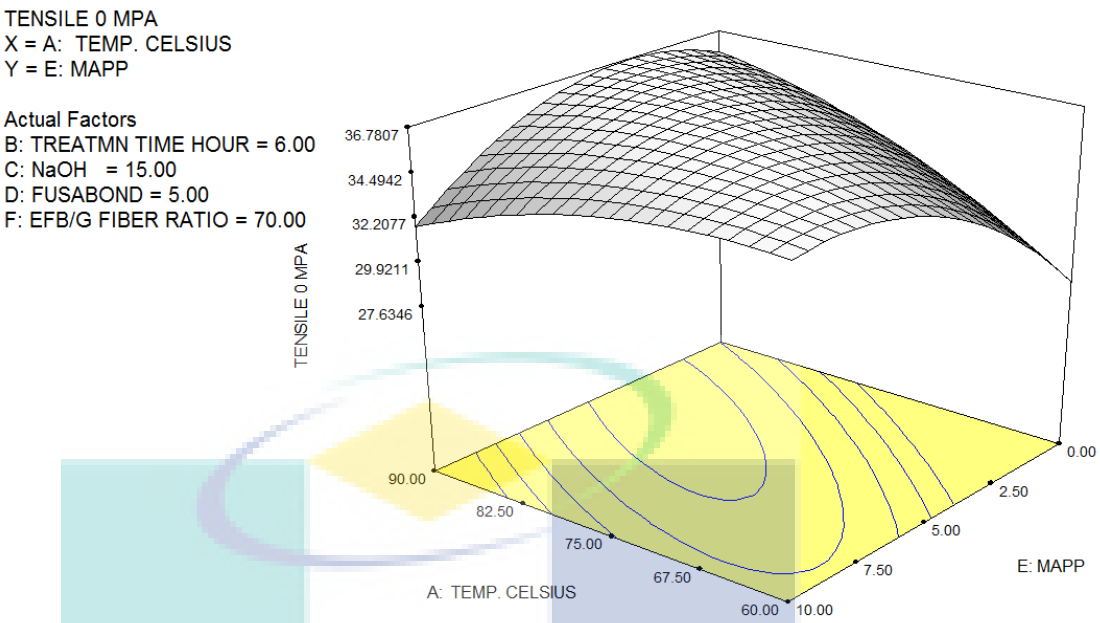

Figure 4.43: 3D graph of the temperature – MAPP % tensile strength

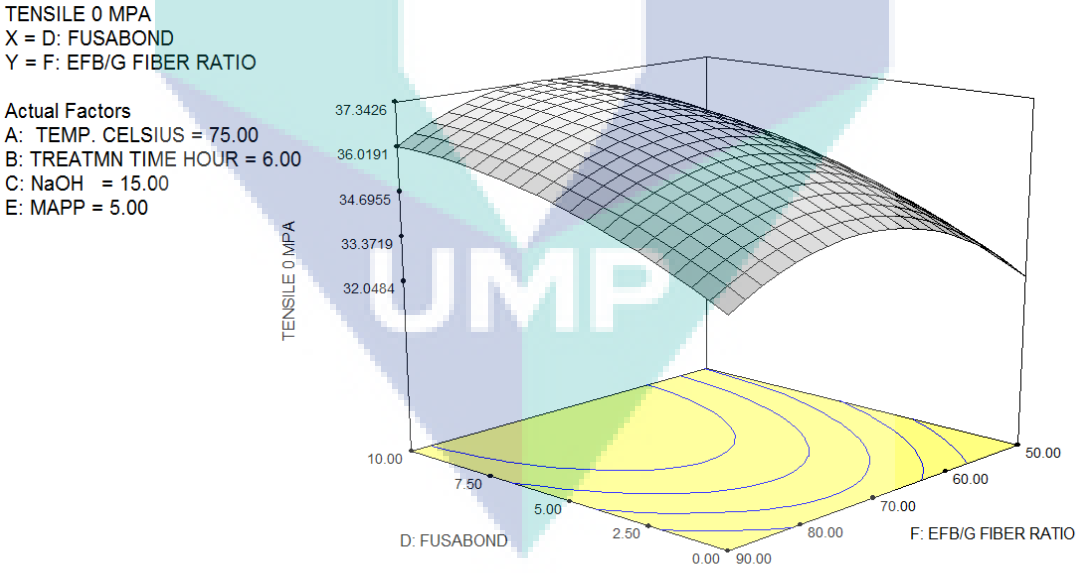

Figure 4.44: 3D graph of the fibre ratio - Fusabond % tensile strength

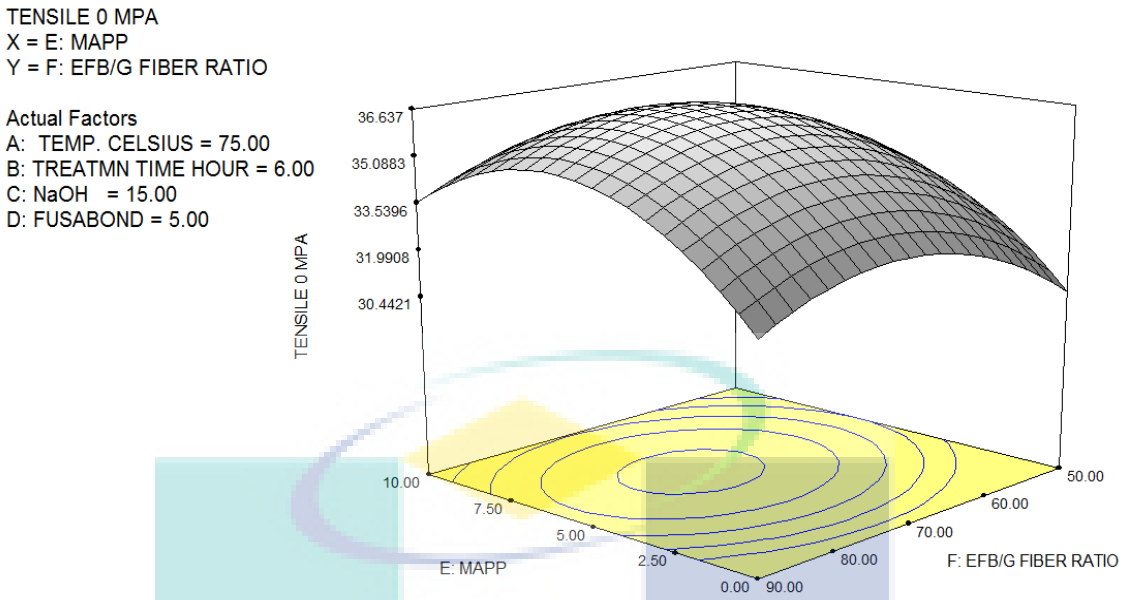

Figure 4.45: 3D graph of the MAPP % – fibre ratio % tensile strength

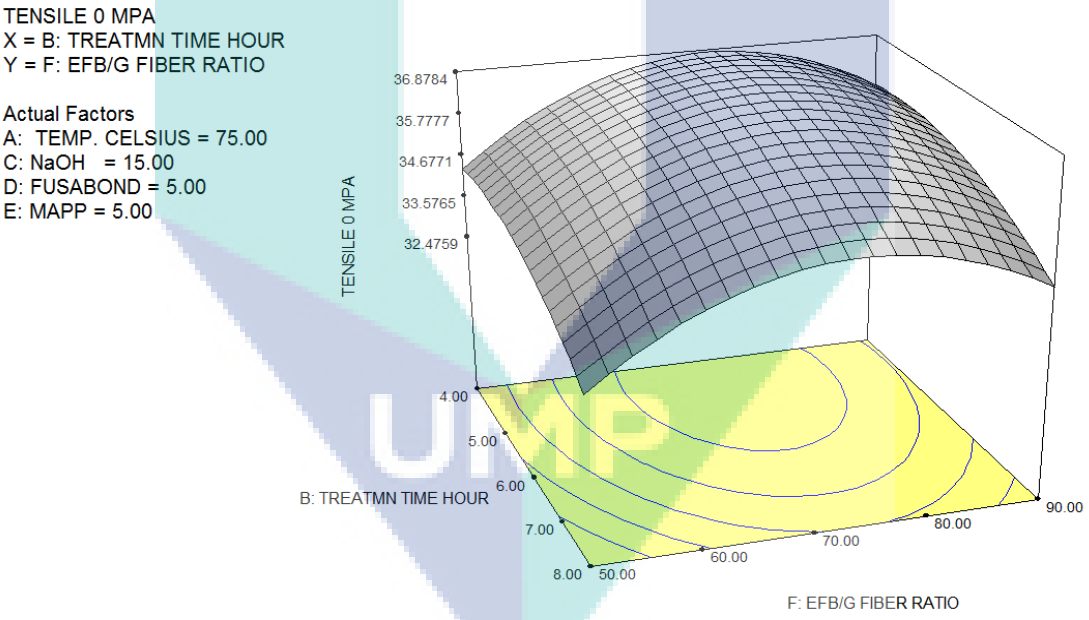

Figure 4.46: 3D graph of the fibre ratio – treatment time tensile strength

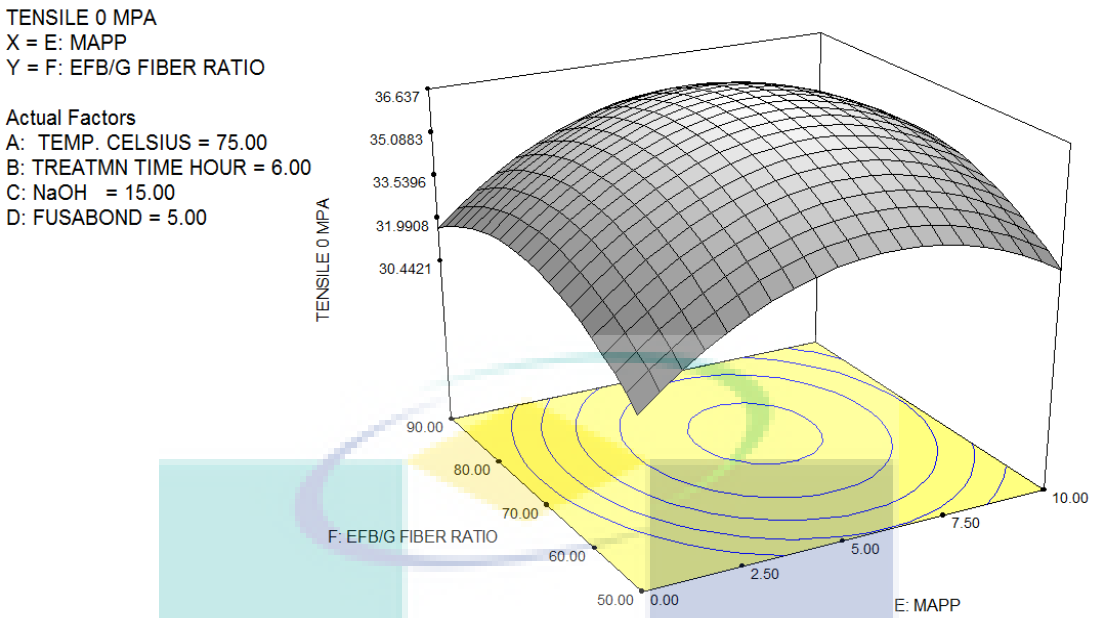

Figure 4.47: 3D graph of the MAPP – fibre ratio % tensile strength

4.7.2 Response Surface Analysis of modulus

4.7.2.1 ANOVA for Quadratic Model Modulus

Table 4.20 shows the ANOVA table for modulus of hybrid composites after transformation as recommended by Box-Cox plot (State-Ease, Inc., 2000) using non transform (lambda = 1) (Figure C. 6). The experimental data had a correlation coefficient (R^2) of 0.9585. That means the calculated model was able to explain 95. 85% of the results in the case of modulus. The results had indicated that the model used to fit the response variable was significant (p<0.0001) and adequate to represent the relationship between the response and the independent variables which denoted that the model was desirably fit.

The model is significant whereby A, C, B^2 and C^2 have the significant effects in this model term. A, C, B^2 and C^2 in this ANOVA table have the values of 'Prob >F' less than 0.05, which indicates the model is significant at a 95% confidence level. From the ANOVA table, it is shown that the B^2 is the most significant effect, followed by A, C^2 and C. The difference between adjusted R^2 and predicted R^2 is lower than 0.2 whereby the result for this experiment is at 0.0069, and it is acceptable. Adequate precision also

indicates an adequate signal, whereby the ratio obtains was 20,468, which are greater than 4. The normal probability plot of residuals, plot of predicted versus actual, plot of residual vs. predicted, and outlier T plots were performed, and these plots are shown in Appendix C.

Table 4.20: ANOVA for Quadratic Model Modulus

Source	Sum of Squares	DF	Mean Square	F Value	Prob > F
Model	1.89E+05	17	11089.55	9.5	0.0028
A	7748.11	1	7748.11	6.64	0.0367
B	286.72	1	286.72	0.25	0.6353
C	433.09	1	433.09	0.37	0.5617
D	0.15	1	0.15	1.30E-04	0.9912
E	12.52	1	12.52	0.011	0.9204
F	530.29	1	530.29	0.45	0.5219
A2	5214.46	1	5214.46	4.47	0.0724
B2	8.71	1	8.71	7.46E-03	0.9336
C2	454.98	1	454.98	0.39	0.5522
D2	5241.47	1	5241.47	4.49	0.0718
E2	2632.89	1	2632.89	2.26	0.1768
F2	6193.46	1	6193.46	5.31	0.0547
AB	154.35	1	154.35	0.13	0.7269
AC	1936.14	1	1936.14	1.66	0.2387
AD	488.72	1	488.72	0.42	0.5382
AE	919.52	1	919.52	0.79	0.4042
AF	0	0			
BC	0	0			
BD	721.3	1	721.3	0.62	0.4576
BE	0	0			
BF	0	0			
CD	0	0			
CE	0	0			
CF	0	0			
DE	0	0			
DF	0	0			
EF	0	0			
Residual	8170.26	7	1167.18		
Cor Total	1.97E+05	24			

Std. Dev.	34.16	R-Squared	0.9585
Mean	1761.05	Adj R-Squared	0.8576
C.V.	1.94	Pred R-Squared	0.3294
PRESS	1.32E+05	Adeq Precision	16.349

[a]Prob>F-value less than 0.05 is significant

The results obtained in the experiments are summarized in Table 4.20. In the model graph shown in Table 4.20, the significant effects that influence the modulus result were the, NaOH % (B^2) interaction with the treatment time (A) and fibre ratio (C).

4.7.2.2 Final equations for Quadratic Model Elongation at Break

The Result in Table 4.21 explains that interactions between variables have significant effect on the tensile strength. Therefore, instead of studying single variable the interactions will be investigated, which is significant and importance for a comprehensive optimization study.

The following equations were the final empirical models in terms of coded factors and actual factors for tensile strength respectively. These equations were generated by the Design Expert 6.0.4 software after the transformation had been carried out.

Final Equation in Terms of Coded Factors:

MODULUS = +1959.27 +34.09 * A -28.24 * B -28.90 * C +0.47 * D +4.56 * E-41.39 * F -38.21 * A^2 -3.30 * B^2 -30.86 * C^2 -81.06 * D^2 -95.91 * E^2 -147.10 * F^2 -16.63 * A * B-85.87 * A * C-59.19 * A * D-75.94 * A * E+28.42 * B * D

Equation 4-12

4.7.2.3 Interactions between process variables

It could be seen that the maximum modulus corresponded in a positive correlation which indicated that interaction in synergistic effect. In particular, the modulus increased when the fibre ratio (C) was increased from 30 to 75% and as NaOH % (B) was increased from 15 to 17.5%. When the NaOH % (B) setting was increased from 17.5 to 20 % and the fibre ratio (C) was increased from 75 to 90%, the modulus had decreased. While with the increase of treatment time from 4 to 5 hour and NaOH % around 17.5%, there was a gradual decline in the response. It could be explained that, as the treatment time and NaOH % prolonged, the better lignin decomposition of the fibre might occur, resulting in an increase in the tensile strength. Figure 4.48 and Figure 4.49

shows the 3D surface graph of modulus with respect to the treatment time (A) NaOH % (B) and the fibre ratio (C).

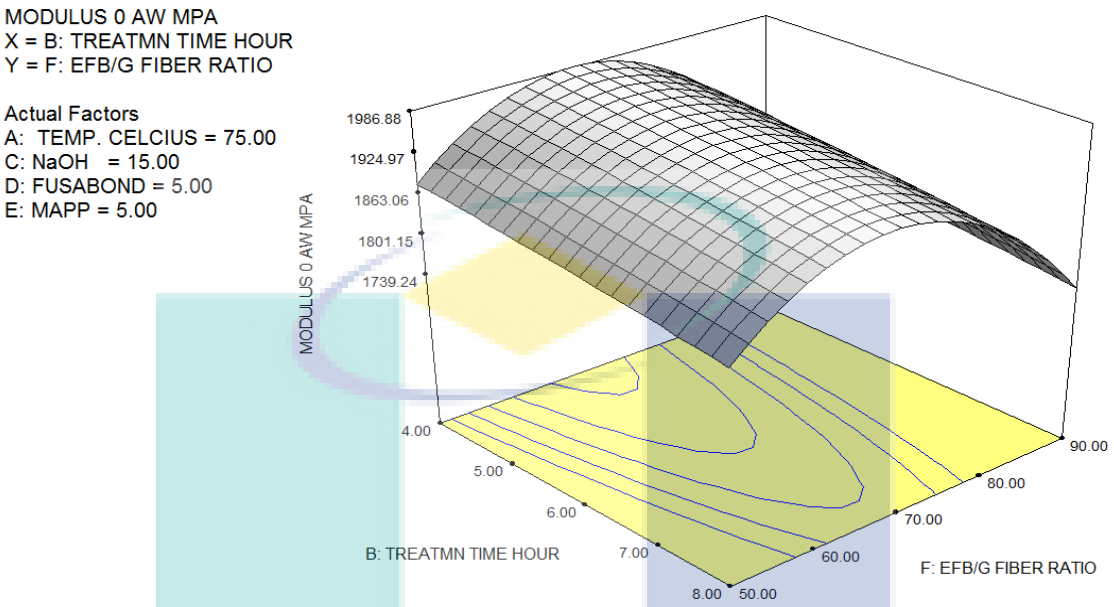

Figure 4.48: 3D graph of the fibre ratio % – treatment time modulus

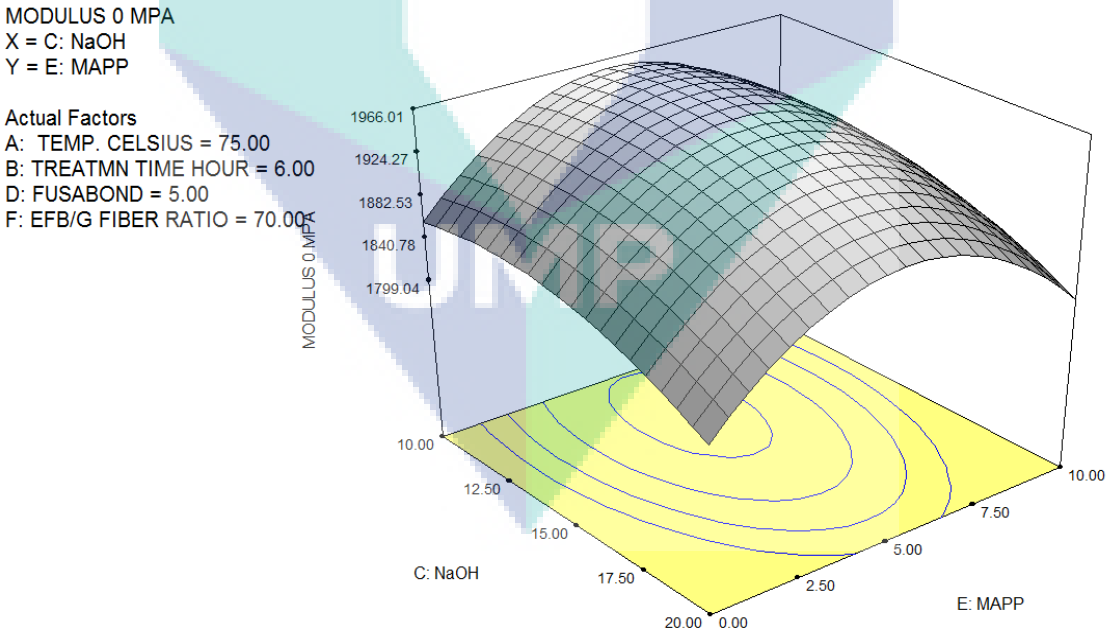

Figure 4.49: 3D graph of the NaOH % – MAPP % modulus

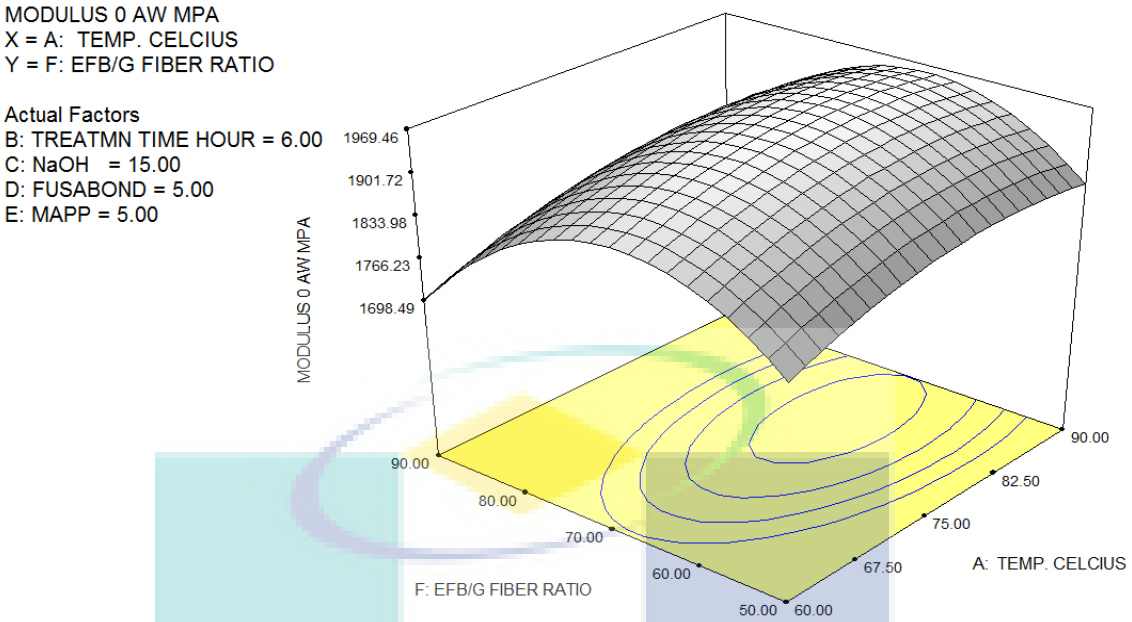

Figure 4.50: 3D graph of the fibre ratio % – treatment temperature modulus

4.7.3 Response Surface Analysis of elongation at break

4.7.3.1 ANOVA for Quadratic Model Elongation at Break

Table 4.21 shows the ANOVA table for elongation at break of hybrid composites after transformation as recommended by Box-Cox plot (State-Ease, Inc., 2000) using non transform (lambda = 1) (Figure C. 9). The experimental data had a correlation coefficient (R^2) of 0.999. That means the calculated model was able to explain 99. 9% of the results in the case of modulus. The results had indicated that the model used to fit the response variable was significant (p<0.0001) and adequate to represent the relationship between the response and the independent variables.

Table 4.21: ANOVA for Quadratic Model Elongation at Break

Source	Sum of Squares	DF	Mean Square	F Value	Prob > F
Model	1.81E+02	17	10.63	428.55	< 0.0001
A	0.22	1	0.22	8.92	0.0203
B	0.044	1	0.044	1.76	0.2268
C	0.18	1	0.18	7.43	0.0295
D	0.52	1	0.52	2.10E+01	0.0026
E	0.66	1	0.66	26.47	0.0013
F	3.59	1	3.59	144.57	< 0.0001
A2	0.015	1	0.015	0.59	0.4679
B2	0.031	1	0.031	1.24E+00	0.3026
C2	6.83E-03	1	6.83E-03	0.28	0.616
D2	1.53E-05	1	1.53E-05	6.16E-04	0.9809
E2	4.58E-04	1	4.58E-04	0.018	0.8957
F2	4.20E-08	1	4.20E-08	1.69E-06	0.999
AB	0.01	1	0.01	0.42	0.539
AC	6.78E-03	1	6.78E-03	0.27	0.6173
AD	4.72E-03	1	4.72E-03	0.19	0.6758
AE	4.07E-03	1	4.07E-03	0.16	0.6977
AF	0	0			
BC	0	0			
BD	0.015	1	0.015	0.59	0.4679
BE	0	0			
BF	0	0			
CD	0	0			
CE	0	0			
CF	0	0			
DE	0	0			
DF	0	0			
EF	0	0			
Residual	0.17	7	0.025		
Cor Total	1.81E+02	24			

Std. Dev.	0.16	R-Squared	0.999
Mean	8.81	Adj R-Squared	0.9967
C.V.	1.79	Pred R-Squared	0.9828
PRESS	3.12E+00	Adeq Precision	69.429

[a]Prob>F-value less than 0.05 is significant

The model is significant whereby A,C,D,E and F have the significant effects in this model term. A,C,D,E and F in this ANOVA table have the values of 'Prob >F' less than 0.05, which indicates the model is significant at a 95% confidence level. From the

ANOVA table, it is shown that the F is the most significant effect, followed by A C and D. The difference between adjusted R^2 and predicted R^2 is lower than 0.2 whereby the result for this experiment is at 0.0139, and it is acceptable. Adequate precision also indicates an adequate signal, whereby the ratio obtains was 69.429, which are greater than 4. The normal probability plot of residuals, plot of predicted versus actual, plot of residual vs. predicted, and outlier T plots were performed, and these plots are shown in Appendix C.

4.7.3.2 Final equations for Quadratic Model Elongation at Break

In the model graph shown in Table 4.21, the significant effects that influence elongation at the break results were the, fibre ratio(F), MAPP %, Temperature treatment(A), NaOH % and Fusabond % (F). It could be seen that the maximum elongation at break corresponded in a positive correlation which indicated that interaction in synergistic effect.

The following equations were the final empirical models in terms of coded factors for elongation at break. These equations were generated by the Design Expert 6.0.4 software after the transformation had been carried out.

Final Equation in Terms of Coded Factors:

$$\text{ELONGATION \%} = +8.98+0.18 * A +0.35 * B +0.60 * C +0.86 * D +1.04 * E-3.40 * F -0.064 * A^2 -0.20 * B^2 -0.12 * C^2 +4.377E-003 * D^2 +0.040 * E^2 -3.829E-004 * F^2 +0.14 * A * B +0.16 * A * C +0.18 * A * D +0.16 * A * E -0.13 * B * D$$

Equation 4-13

4.7.3.3 Interactions between process variables

Overall, the elongation at break increase when the temperature treatment, treatment time MAPP NaOH% and Fusabond were increased from level 1 to level 5. On the other hand, increase in the fibre ratio from level 1 to 5 decreased of elongation at break significantly.

It could be explained that, as the temperature treatment, treatment time MAPP NaOH% and Fusabond extended, the better lignin decomposition, of the fibre might occur and EFB- matrix bonding was increased, resulting in an increase in the elongation at break. Figure 4.52 to Figure 4.54 shows the 3D surface graph of elongation at break with respect to treatment temperature (A) treatment time (B) NaOH % (C) Fusabond (D) MAPP (E) and the fibre ratio (F).

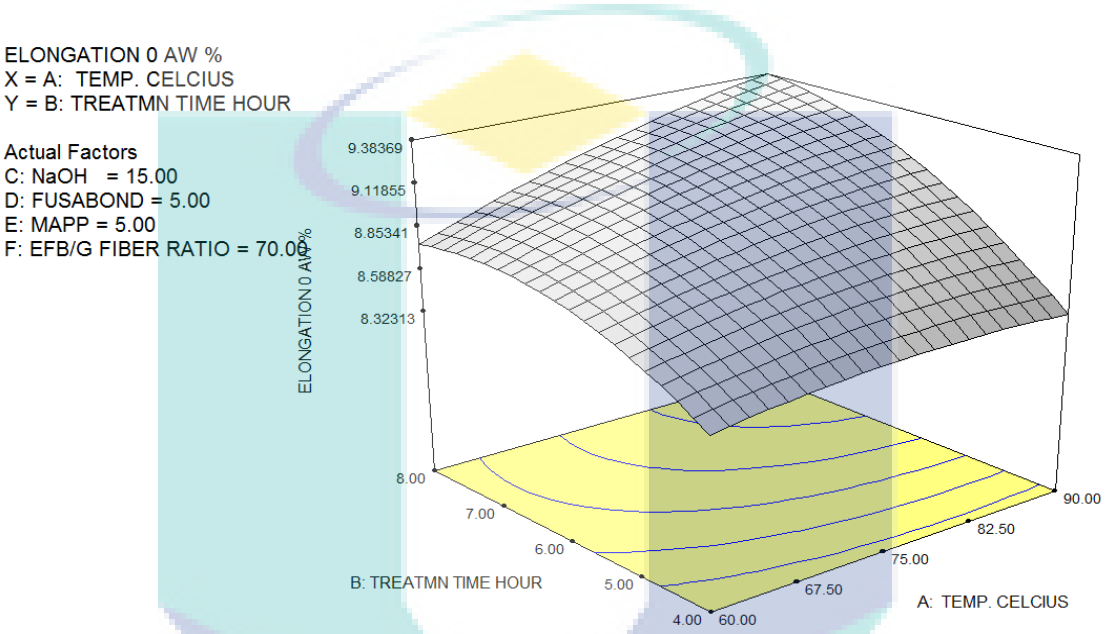

Figure 4.51: 3D graph of the Treatment time – temperature elongation

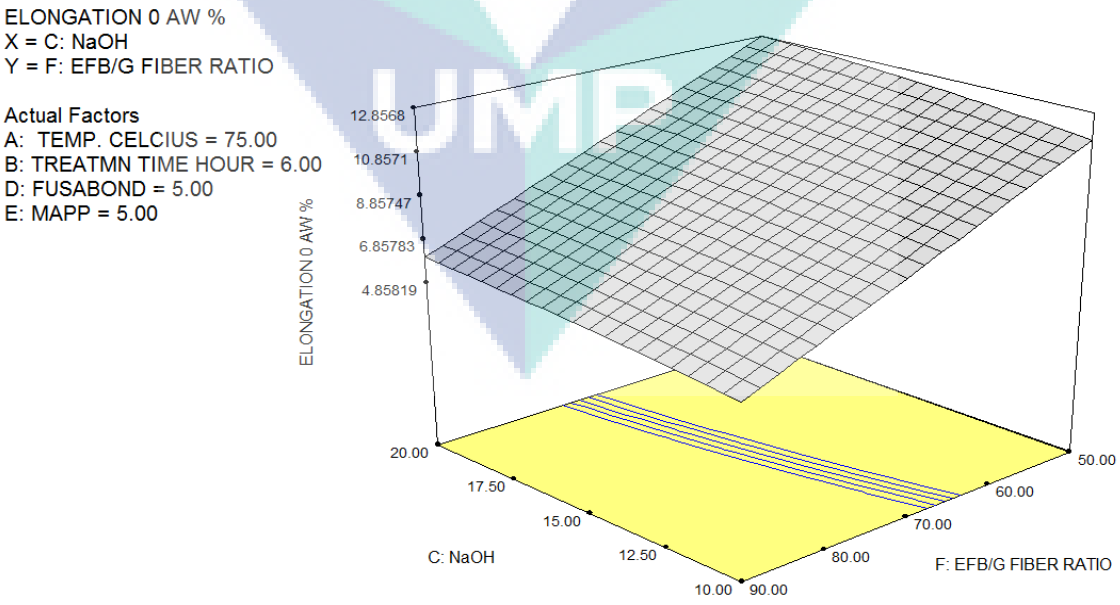

Figure 4.52: 3D graph of the Fibre ratio – NaOH % elongation

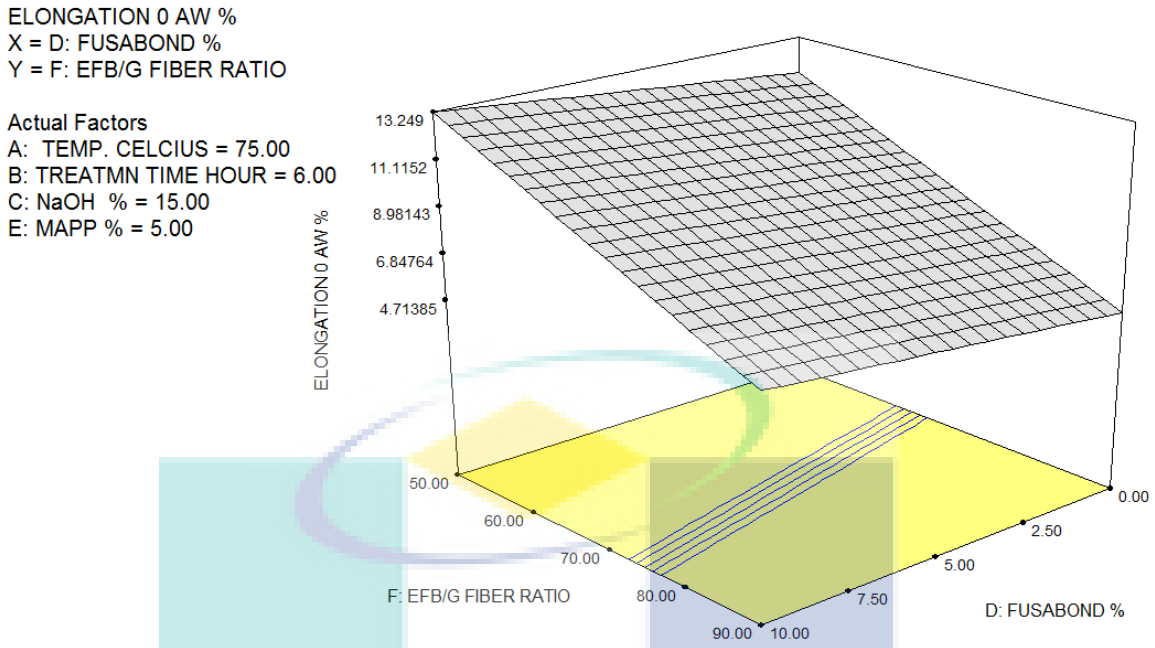

Figure 4.53: 3D graph of the Fibre ratio – Fusabond % elongation

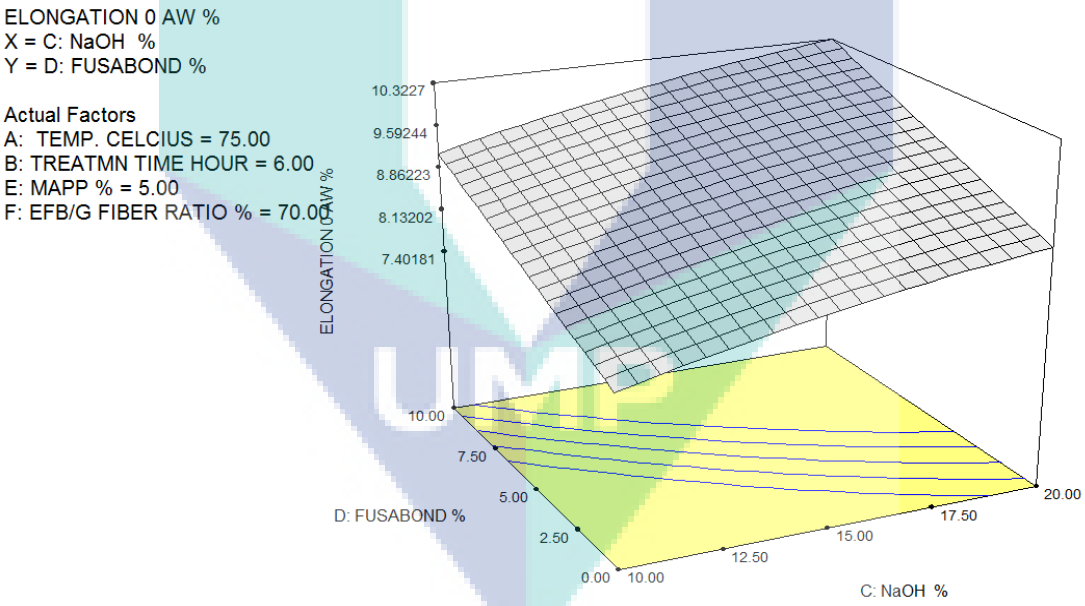

Figure 4.54: 3D graph of the Fusabond – NaOH % elongation

4.8 OPTIMISATION HOMEMADE HYBRID COMPOSITES

Unite Optimization procedure had been conducted for Hybrid Composites and the prediction results of the empirical model were tabulated in Table 4.22. Treatment temperature (A) treatment time (B) NaOH % (C) Fusabond (D) MAPP (E) and the fibre

ratio (F), were set to range within the levels defined in the Table 4.18 including tensile strength, modulus, elongation at break water absorption and melt flow index were explained to each goal and importance value. Results showed optimum treatment temperature (A) treatment time (B) NaOH % (C) Fusabond (D) MAPP (E) and the fibre ratio (F), for optimal tensile strength, modulus water absorption and melt flow index were determined in the Table 4.23 with total desirability value of 0.69 to 0.95 was obtained on a scale of 0 to 1, where 0 represented a completely undesirable response, and 1 represented the most desirable response. Under these proposed optimized conditions, the maximum value of the treatment temperature (A), treatment time (B), NaOH % (C), Fusabond (D), MAPP (E) and the fibre ratio (F), from the model were explained in the Table 4.23.

4.8.1 Combine Optimization of Run 1

Table 4.22: Conditions of the Combine Optimization Run 1

Name	Goal	Lower Limit	Upper Limit	Lower	Uppr Wight	Impr tance
Temp. Celsius	is in range	65	85	1	1	3
Treatmn Time Hour	is in range	4.3	7.7	1	1	3
NaOH %	is in range	10	19	1	1	3
Fusabond %	minimize	0	10	1	1	3
MAPP %	minimize	0	10	1	1	3
EFB/G fibre ratio %	maximize	50	90	1	1	3
Tensile 0 AW MPa	maximize	21.074	37.741	1	1	5
Modulus 0 AW MPa	maximize	1440	1912.5	1	1	4
Tensile WTR 80^{o}C HA	is in range	25	32.941	1	1	3
Tensile sea WTR 80^{o}C HA	is in range	20	28.25	1	1	3
WTR ABSB 80^{o}C HA	is in range	1.733	5	1	1	3
Sea WTR ABSB 80^{o}C HA	is in range	1.64	4	1	1	3
Melt flow indexs	is in range	2	3.935	1	1	3

Table 4.23: Result of the Combine Optimization Conditions Run 1

No	Temp C	Treatm n Time Hour	Naoh %	Fusab ond %	MAP P %	Efb/G Fibre Ratio %	Tensile 0 Aw MPa	Moduls 0 Aw MPa	Tensile Wtr 80c Ha	Tensile Sea Wtr 80c Ha	Wtr Absb 80c Ha	Sea Wtr Absb 80c	Melt Flow Indexs	Desir abilit y
1	85	4	11	0	0.17	81.15	37.26	1912	32.53	27.89	4.93	3.91	2.34	0.95
2	85	5	11	0	1.23	81.18	37.74	1919	32.94	28.25	4.90	4.00	2.48	0.94
3	85	4	13	0	0.07	79.97	36.63	1900	31.97	27.42	4.88	3.93	2.46	0.93
4	85	4	13	0	1.85	80.94	37.70	1927	32.91	28.22	4.83	3.91	2.54	0.93
5	85	4	15	0	2.06	80.43	37.23	1914	32.50	27.87	4.70	3.86	2.65	0.91
6	85	4	16	0	1.85	81.09	36.74	1891	32.07	27.50	4.70	3.89	2.66	0.90
7	85	4	18	0	2.98	78.08	36.25	1885	31.65	27.14	4.03	3.30	2.97	0.85
8	85	8	10	3	2.05	80.28	36.47	1915	31.84	27.30	4.31	3.75	2.73	0.84
9	85	6	14	1	4.07	68.41	37.23	1970	32.50	27.87	3.88	3.26	3.24	0.79
10	72	8	10	6	4.7	74.08	35.59	1891	31.06	26.64	4.32	3.97	2.82	0.69

Table 4.24: Result of the Combine Optimization Conditions Run 2

No	Temp C	Treatmn Time Hour	Naoh %	Fusabond %	MAPP %	Efb/G Fibre Ratio %	Tensile 0 Aw MPa	Moduls 0 Aw MPa	Tensile Wtr 80c Ha MPa	Tensile Sea Wtr 80c Ha MPa	Wtr Absb 80c Ha	Sea Wtr Absb 80c	Melt Flow Indexs	Desirability
1	85	4	10	2	0	78	37.70	1968	36.39	32.91	28.22	4.69	3.64	2.38
2	85	4	11	0	0	74	37.64	1963	36.33	32.85	28.17	4.32	3.19	2.57
3	85	4	10	3	0	66	37.72	2022	36.40	32.92	28.23	3.91	2.86	2.75
4	84	4	10	2	0	72	37.73	2002	36.42	32.94	28.24	4.30	3.25	2.60
5	85	4	10	0	0	62	37.62	1988	36.31	32.84	28.16	3.43	2.21	2.87
6	85	6	10	5	0	68	36.98	1983	35.69	32.28	27.68	4.05	3.32	2.89
7	85	5	10	4	0	63	36.82	1989	35.54	32.14	27.56	3.78	2.96	2.94
8	85	6	10	1	0	63	36.37	1949	35.11	31.75	27.23	3.61	2.72	3.00
9	85	5	10	7	0	60	35.85	1926	34.60	31.29	26.83	3.47	2.85	2.99
10	85	7	10	6	0	75	35.94	1913	34.68	31.37	26.90	3.91	3.40	2.92

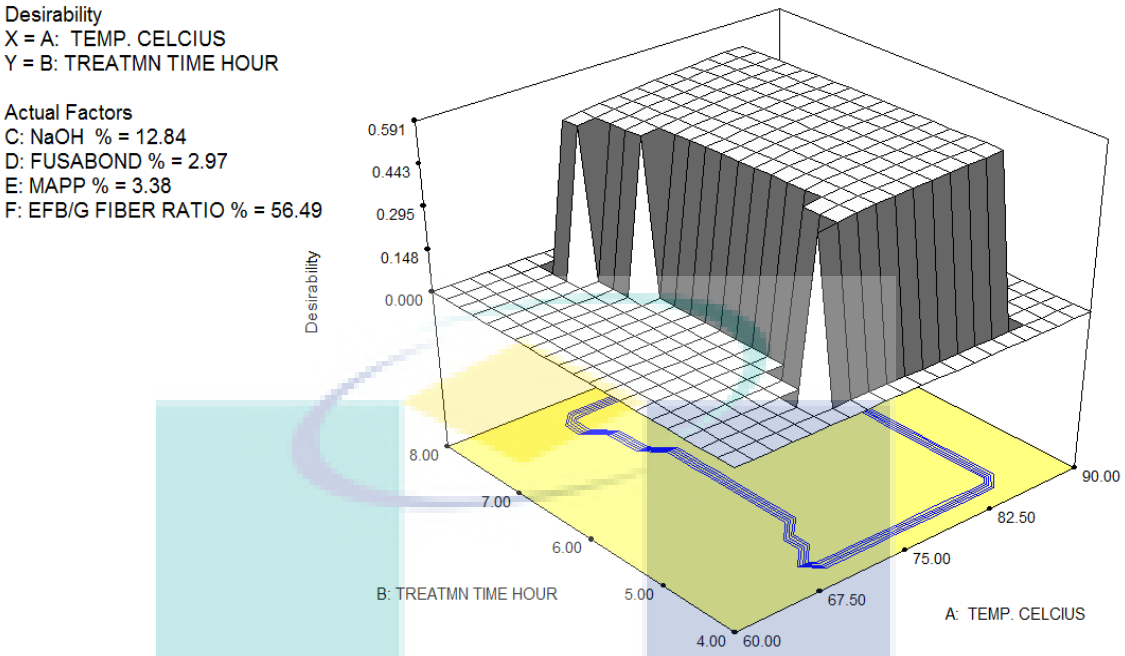

Figure 4.55: Result of the Combine Optimization Conditions Run 1 Graph

4.8.2 Combine Optimization of Run 2

Second Unite Optimization procedure had been conducted for Hybrid Composites and the prediction results of the empirical model were tabulated in Table 4.25. Treatment temperature (A), treatment time (B), NaOH % (C), Fusabond (D), MAPP (E) and the fibre ratio (F) were set to range within the levels defined in the Table 4.25 including tensile strength, modulus, elongation at break water absorption and melt flow index were explained to each goal and importance value. Results showed optimum treatment temperature (A), treatment time (B), NaOH % (C), Fusabond (D), MAPP (E) and the fibre ratio (F), for optimal tensile strength, modulus water absorption and melt flow index were determined in the Table 4.24 with total desirability value of 0.942 to 0.998 was obtained on a scale of 0 to 1, where 0 represented a completely undesirable response, and 1 represented the most desirable response. Under these proposed optimized conditions, the maximum value of The treatment temperature (A) treatment time (B), NaOH % (C), Fusabond (D), MAPP (E) and the fibre ratio (F) from the model were explained in the Table 4.24.

Table 4.25: Conditions of the Combine Optimization Run 2

Name	Goal	Lower Limit	Upper Limit	Lower Weight	Upper Weight	Importance
Temp. Celsius	is in range	65	85	1	1	3
Treatmn Time Hour	is in range	4.3	7.7	1	1	3
NaOH %	is in range	10	19	1	1	3
Fusabond %	is in range	0	10	1	1	3
MAPP %	minimize	0	10	1	1	3
EFB/G fibre ratio %	is in range	60	80	1	1	3
Tensile 0 AW MPA	maximize	21.074	37.741	1	1	5
Modulus 0 AW MPA	maximize	1440	1912.5	1	1	4
Tensile 1200 AW MPA	is in range	25	36.424	1	1	3
Tensile WTR 80^{o}C HA	is in range	25	32.941	1	1	3
Tensile sea WTR 80^{o}C	is in range	20	28.25	1	1	3
WTR ABSB 80^{o}C HA	is in range	1.733	5	1	1	3
Sea WTR ABSB 80^{o}C HA	is in range	1.64	4	1	1	3
Melt flow indexs	is in range	2	3.935	1	1	3

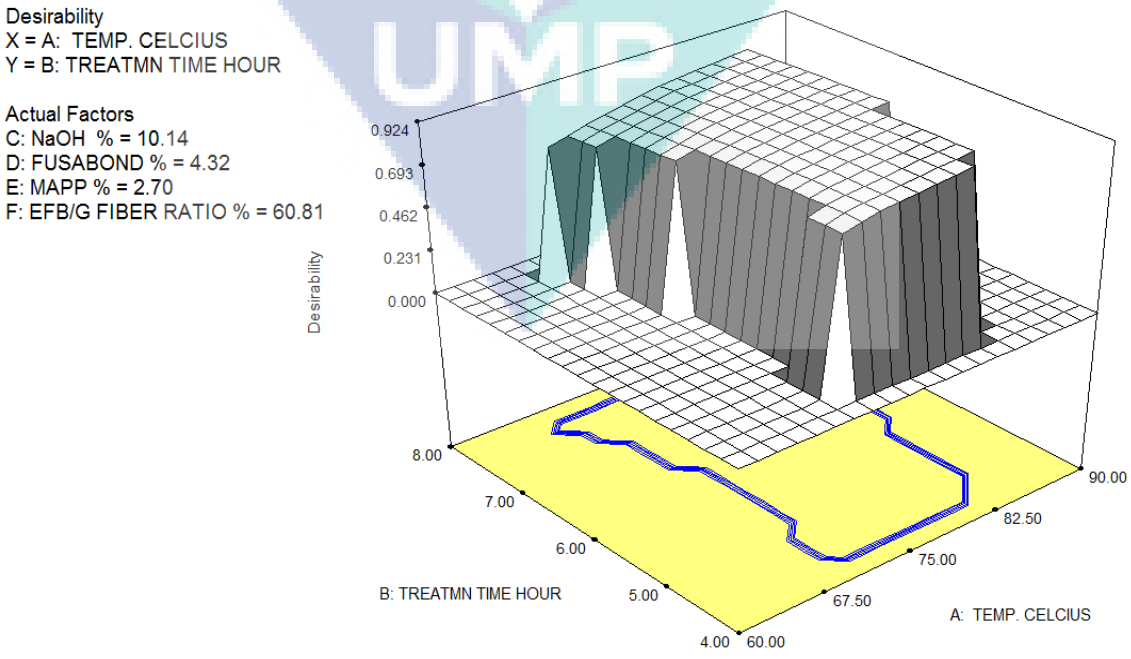

Figure 4.56: Result of the Combine Optimization Conditions Run 2 Graph

Homemade treatment optimum condition as explain in Table 4.23 and setting condition in Table 4.22 were at 85ºC 4 hour, 11 % NaOH, 0 % Fusabond, 0,17 % MAPP 81,15% Fibre Ratio and composites properties predicted is 37,26 MPa Tensile Strength 1912 MPa Modulus and 4,93 % water absorbtion. Second optimum condition as show in the Table 4.24 setting condition at Table 4.25 were were at 85ºC 4 hour, 10 % NaOH, 2 % Fusabond, 0,0 % MAPP 78,0% Fibre Ratio and composites properties predicted is 37,7 MPa Tensile Strength 1968 MPa Modulus and 4,69 % sea water absorbtion

4.9 CHARACTERIZATION OF HOMEMADE COMPOSITES

4.9.1 Alkali Treatment Technique

Homemade Alkali Treatment process was used in this research part to decrease the lignin content, improve fibre-matrix bonding properties and to obtain a greater degree of uniformity and stability of composites mechanical properties. Homemade Alkali Treatment was used low NaOH % to decrease chemical needed and longer fibre treatment to improve lignin removal, less energy density, fibre physical and chemical properties and the relative cost efficiency of Homemade Alkali Treatment should be improved.

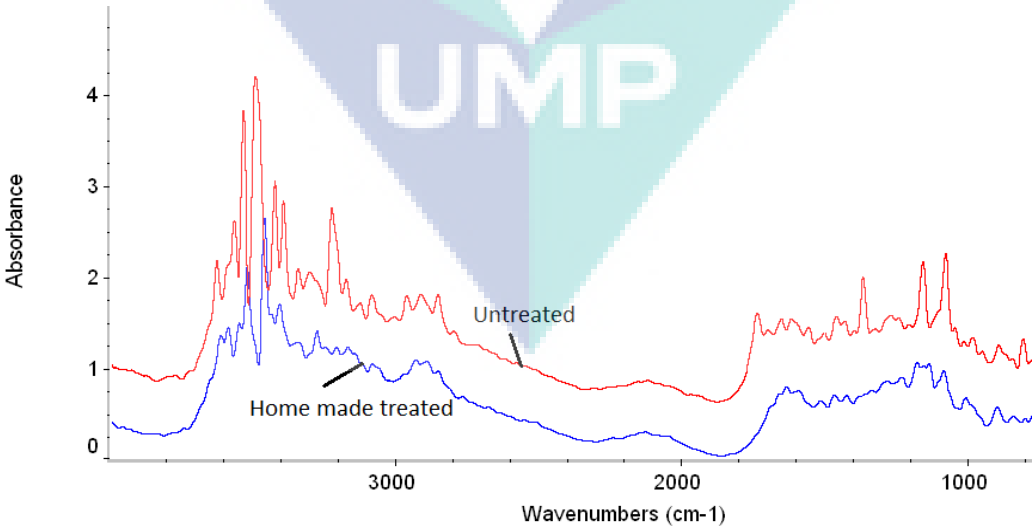

Figure 4.57: Infrared spectra of the Untreated and homemade treated EFB Fibre.

The FTIR spectrum of untreated EFB fibre (Figure 4.57) contains 17 major peaks at 3614.88, 3567.27, 3527.53, 3497.19, 3423.09, 3391.51, 3359.32, 3274.56, 3241.73,

3210.23, 3128.08, 2922.22, 1656.33, 1459.77, 1255.29, 1223.41, 1174.36, 1094.29, and 1032.35 cm^{-1}. The regions from 4000 to 1900 cm -1 for O-H and C-H stretching frequencies The absorbance peaks at around 1500 explain the lignin and hemicelluloses groups Whereas the 1595.03 to 1461.96 FTIR spectrum of the treated EFB was also recorded at the lower peak's region in the same wave number: This finding indicates that homemade treated EFB have much lower lignin content.

4.9.2 SEM of the homemade hybrid composites

SEM analysis was used to examine the surface interaction between fibre and matrix in homemade hybrid composites, and it was noticeable that there is better surface interaction between EFB fibre, and recycled polypropylene compare to standart alkali treatment but there are pulled out or damage in surface interaction between glass fibre and recycled PP matrix as seen in the Figure 4.58. It is indicated that bonding glass fibre recycled PP matrix should be improved again with better matrix modification or fibre treatment.

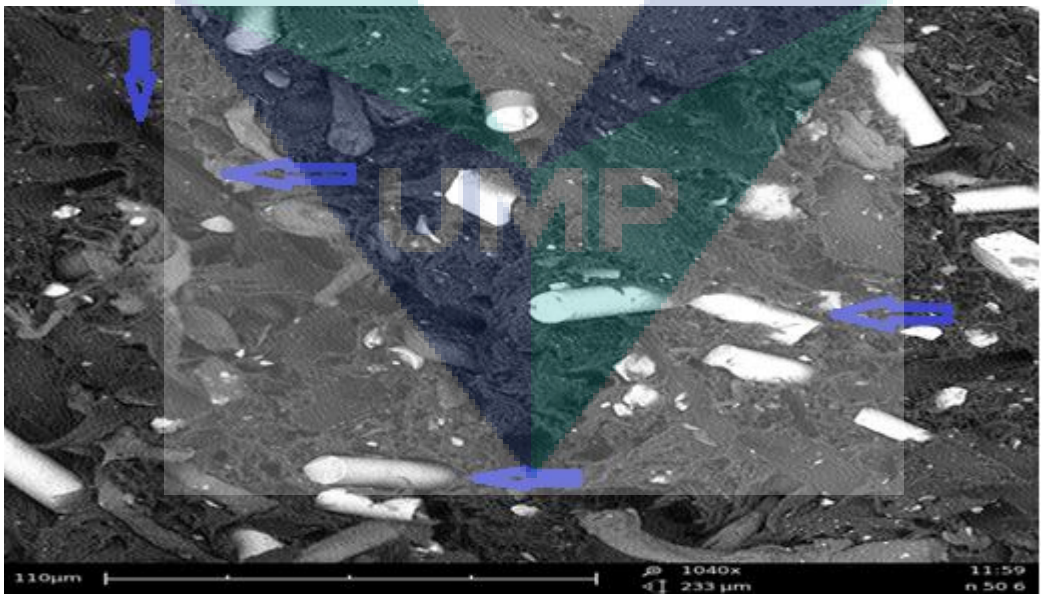

Figure 4.58: SEM of the homemade hybrid composites

.

CHAPTER 5.

MICROWAVE AND ULTRASONIC HYBRID COMPOSITES

This chapter was divided into eight parts of results and discussion, It explaint the microwave and ultrasonic alkali treatment, characterization of the hybrid composite's properties, response surface of hybrid composites. ANOVA-Statistical Analysis, Validation of Empirical Model Adequacy and Optimization Confirmation Run.

5.1 MICROWAVE HYBRID COMPOSITES

5.1.1 Alkali Treatment Technique of microwave Hybrid composites

Microwave modified Alkali Treatment process was used in this research part to decrease the lignin content, improve fibre-matrix bonding properties and to obtain a greater degree of uniformity and stability of composites mechanical properties. The microwave device was used temperature controller to maintain the treatment temperature decrease overheating, less energy density, better fibre physical and chemical properties, microwave Alkali Treatment should be improved lignin removal, shorter fibre treatment and the relative cost efficiency. The operational conditions involved were the temperature, treatment time, NaOH percentage, Fusabond percentage and fibre ratio in order to identify the each parameter’s interaction and the optimum operational condition that would result in a high properties of hybrid composites.

5.1.2 DSC and TGA of the microwave hybrid composites

Temperatures of crystallization, melting point and heat flow of crystallization of the EFB-Glass fibre hybrid composites have different value, as explained in Table 5.1, there was no significant change in the crystallization temperature with respect to the alkali treatment time temperature of the composites. However, all composites presented higher crystallization temperatures compared to recycled polypropylene. A small difference between sample containing of the fibre ratio was also observed in all composites sample tested.

Figure 5.1 shows DSC scanning curves of samples containing microwave of EFB fibre, prepared in 10 to 17.5% NaOH and 30 to 120 minutes fibre treatment. No significant changes in the melting temperature of composites containing the difference of fibre treatment and coupling agent were observed Moreover, with changes in the fibre ratio. The melting and crystallization curves were not significantly different.

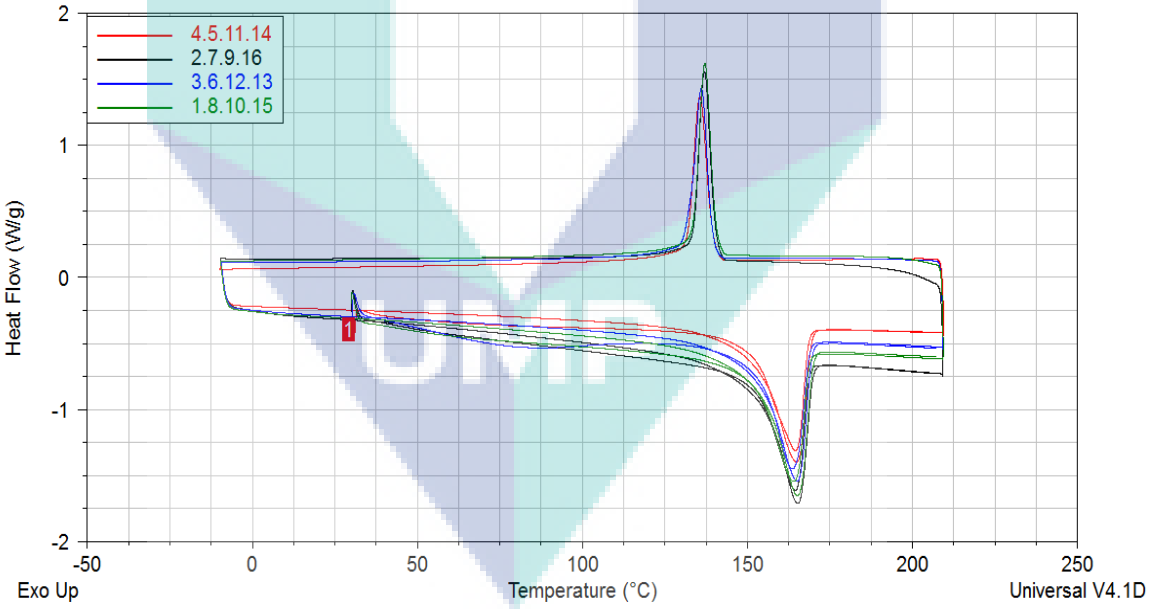

Figure 5.1: DSC graph of microwave hybrid composites

Table 5.1: Crystallization and melting heat flow-temperature

Micro wave STD	Crystallization Heat flow W/G	Crystallization Temp C	Melting Heat flow W/G	Melting Temp C
1	1.124	136.98	-1.15	164.26
2	1.167	136.88	-1.17	164.52
3	1.266	135.76	-1.32	163.49
4	1.039	135.46	-1.08	164.47
5	1.049	135.36	-1.03	164.43
6	1.216	135.74	-1.36	163.39
7	1.025	136.38	-1.12	164.62
8	1.057	136.28	-1.18	164.74
9	1.026	136.58	-1.12	164.18
10	1.072	136.79	-1.15	164.16
11	1.059	135.26	-1.09	164.85
12	1.236	135.66	-1.33	163.29
13	1.296	135.16	-1.38	163.59
14	1.079	135.76	-1.03	164.25
15	1.107	136.28	-1.19	164.42
16	1.028	136.79	-1.18	164.17

TGA curve of recycled polypropylene matrix, and microwave hybrid composites are shown in Figure 5.2. All the composites TGA curves show the initial transition around 250 to 300^{o}C due to the start of EFB fibre degradations. The decomposition temperature of the samples slightly different in the range of 300 to 450 as shown in the Figure 5.2 where the TGA traces shifted to lower temperatures with increasing EFB content.

TGA transitions for composites remaining from 500 up to 650^{o}C also found shifted to slightly lower doe the fibre ratio or glass fibre residual content of the composites.

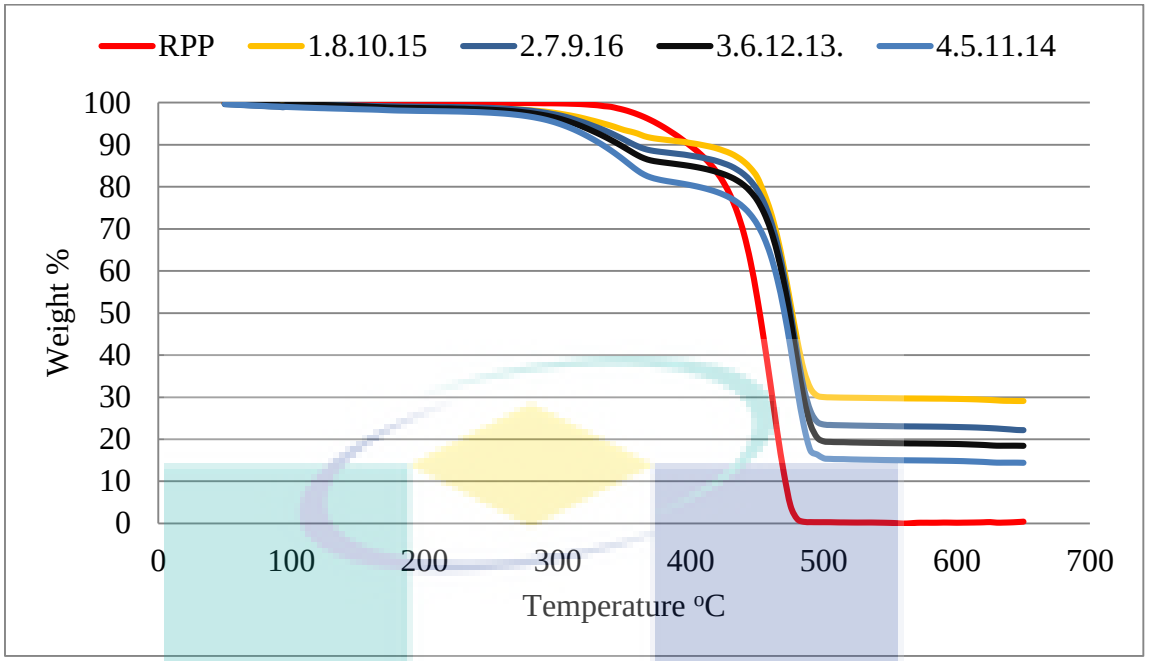

Figure 5.2: TGA graph of microwave hybrid composites

5.1.3 FTIR Microwave treatment spectrum

The FTIR spectrum of untreated EFB fibre (Figure 5.3) contains 17 major peaks at 3606.49, 3568.07, 3529.21, 3485.10, 3450.58, 3383.84, 3345.81, 3286.98, 3239.71, 3150.14, 2924.36, 1597.86, 1447.77, 1363.52, 1142.14, 1097.25 and 1032.35 cm^{-1}. The regions from 4000 to 1900 cm^{-1} for O-H and C-H stretching frequencies The absorbance peaks at around 1500 explain the lignin and hemicelluloses groups Whereas the 1600 to 1400 FTIR spectrum of the microwave treated EFB was also recorded at the lower peak's region in the same wave number; This finding indicates that microwave treated EFB have much lower lignin content compare to untreated.

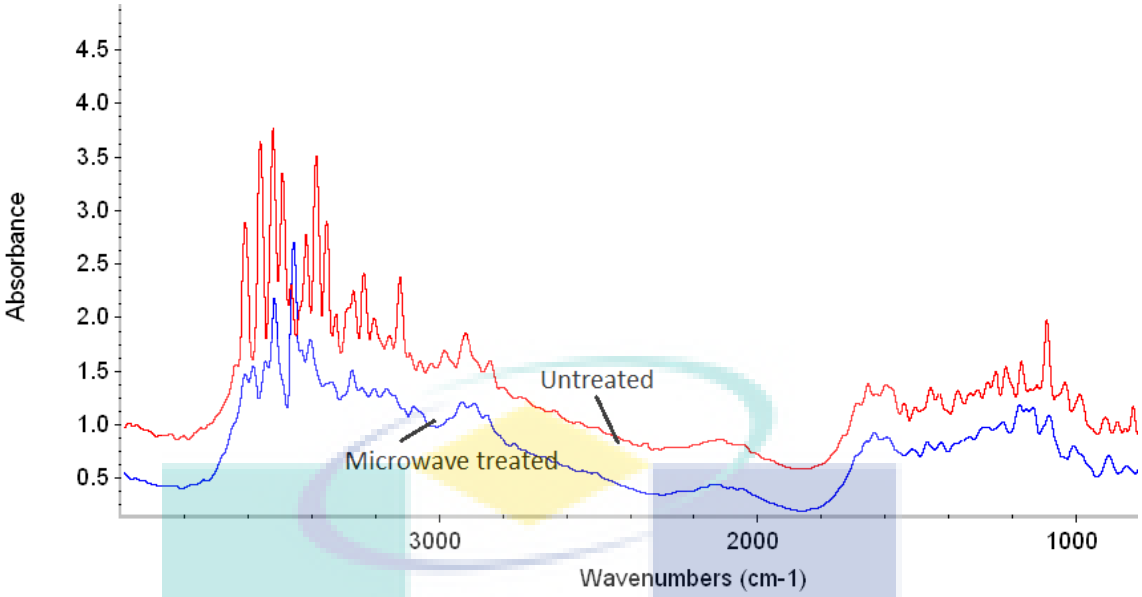

Figure 5.3: Infrared spectra of the Untreated and microwave treated EFB Fibre.

5.1.4 SEM of the microwave hybrid composites

The morphologies of the EFB-glass fibre hybrid composites were analysed using scanning electron microscopy to examine cracking behaviour of the composites under tensile load. The surface interaction between fibre and matrix in microwave hybrid composites noticeable increase compare to standart composites and there is less surface interaction between EFB fibre and recycled polypropylene cracking, pulled out or damage in surface interaction between glass fibre and recycled PP matrix as shown in Figure 5.4. It is indicated that bonding fibre recycled PP matrix in microwave treatment already improve and better matrix modification or fibre treatment compare to standart alkali treatment.

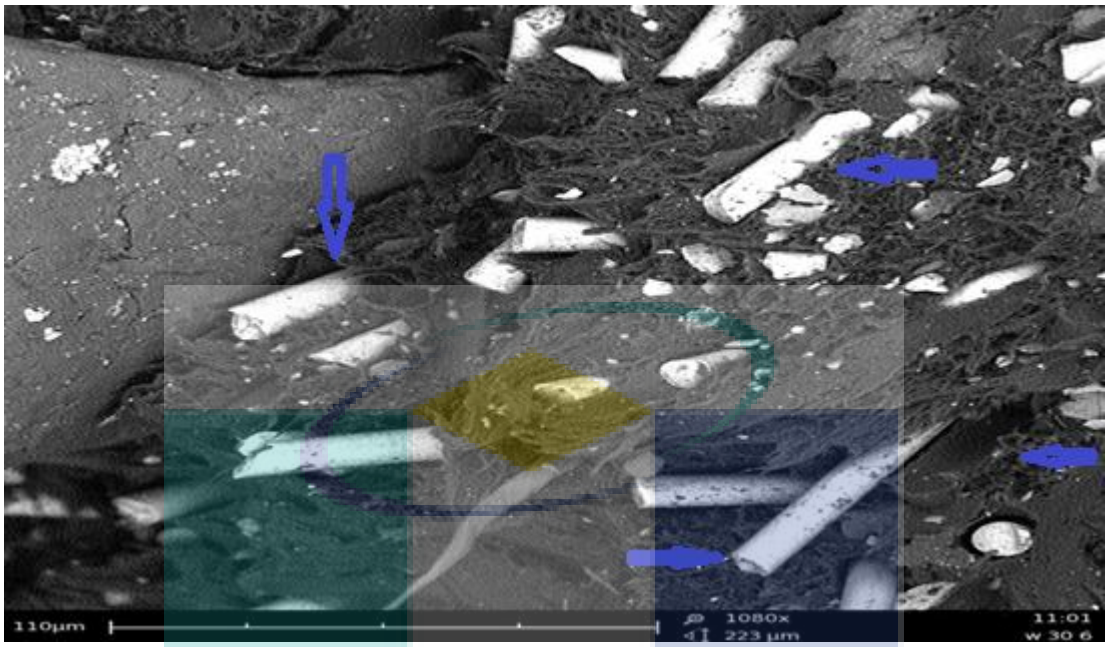

Figure 5.4: SEM of the microwave hybrid composites

5.1.5 Melt Flow Index

Figure 5.5 to Figure 5.7 shows the Melt Flow Index of microwave alkaline treatment composite. From the Figure, it can be seen that Melt Flow Index of 30 to 120 minutes of treated microwave composite is similar. Treated composite with higher treatment time, NaOH, and Fusabond % was not noticeable changed to melt flow index response. Ratio of EFB/Glass fibre from 30 to 90 had been significant changed melt flow response. The response was decreased by increased of Ratio EFB/Glass fibre from 3.34 to only 2.33 G/10 M. This might be due on low fluidity of EFB fibre in the composites' melting condition.

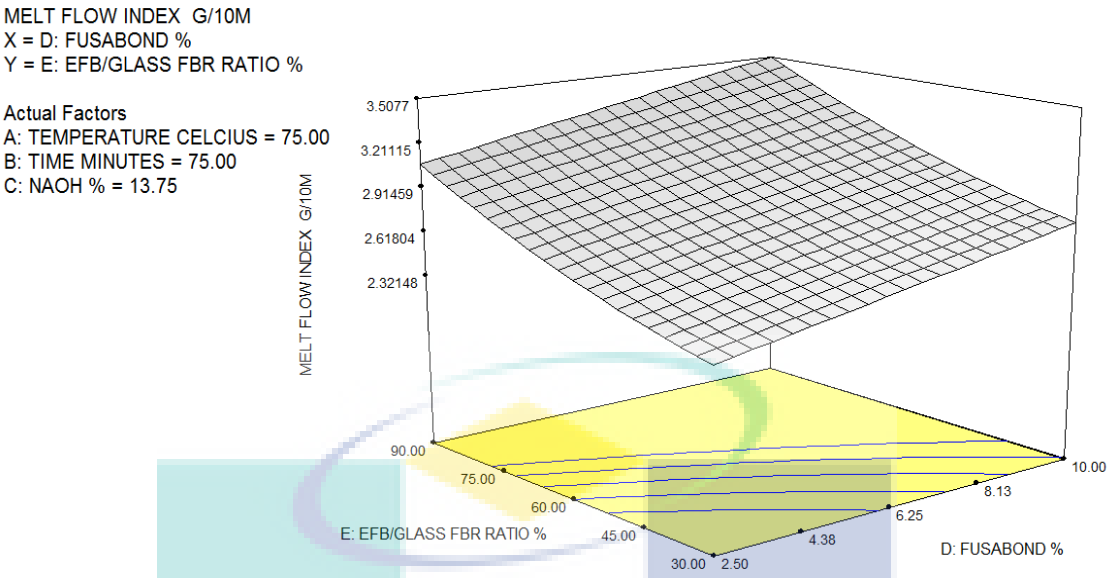

Figure 5.5: Melt Flow Index of EFB-Glass Fibre Composites

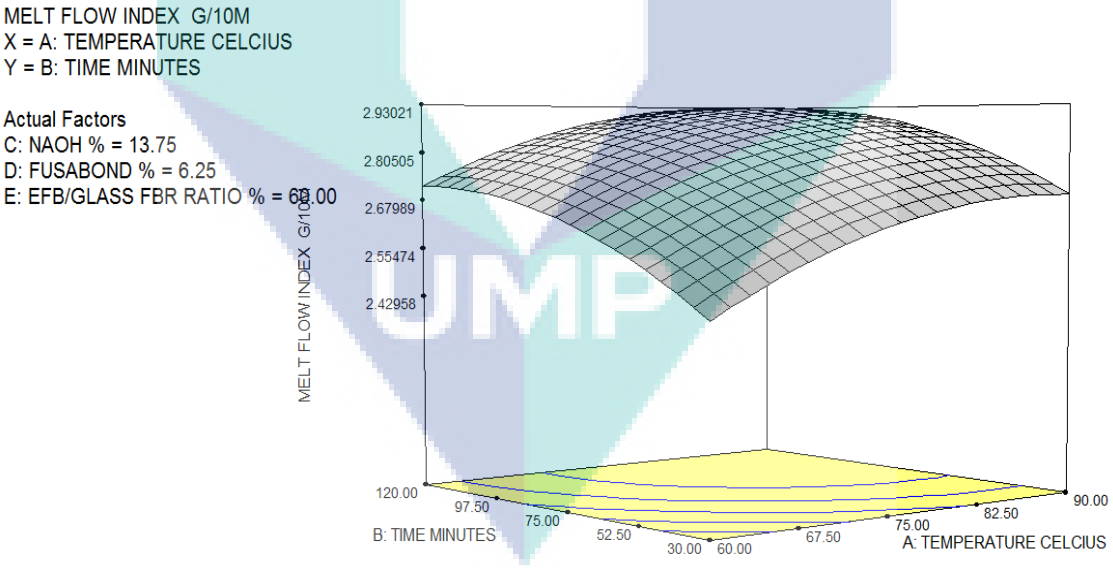

Figure 5.6: Melt Flow Index of EFB-Glass Fibre Composites

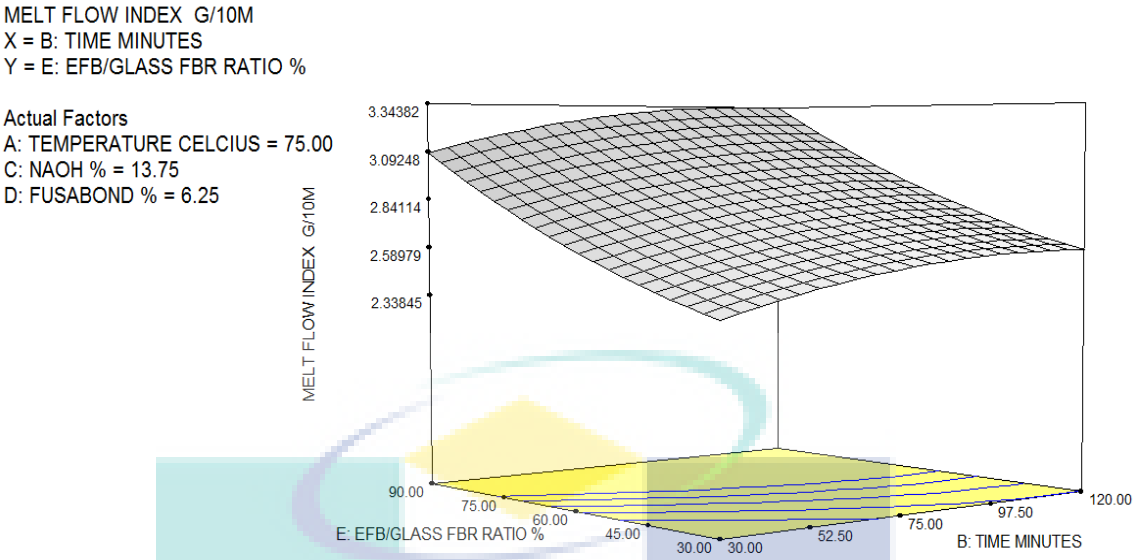

Figure 5.7: Melt Flow Index of EFB-Glass Fibre Composites

.

5.2 RESPONSE SURFACE AND VARIABLE INTERACTIONS

5.2.1 Response Surface and variable interactions of Tensile Strength

Figure 5.8 to Figure 5.11 show the response surface plots as functions of treatment time and NaOH % on the Tensile 0 H AW at 60% of the fibre ratio the typical plot like this is dome shaped. From the Figures, it is obvious that tensile strength increase from 30 to 120 minutes treatment time and 15 to 17.5 NaOH %. The tensile decrease when the treatment time increase from 30 to 120 minutes and NaOH % increase from 10 to 17.5. The appropriate maximum tensile strength was determined at a 120 minutes treatment time and 13.75 NaOH %, led to the maximum tensile strength at 34.5 MPa.

Table 5.2: Microwave factors levels

Factors	Unit	Levels 1	Levels 2	Levels 3	Levels 4
A:Temperature	Celsius	60	70	80	90
B:Treatent time	Minute	30	60	90	120
C:NaOH	%	10	13	15	18
D:Fusabond	%	2.5	5.0	7.5	10.0
E:Fibre ratio	%	50	60	70	80

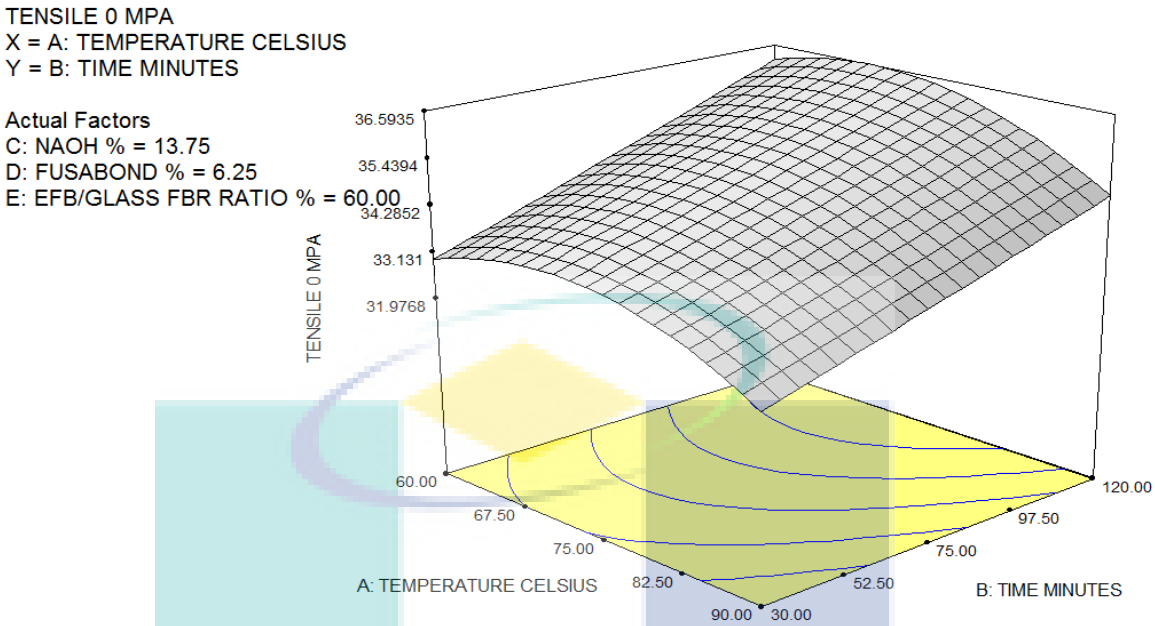

Figure 5.8: 3D graph of the treatment time – temperature tensile strength

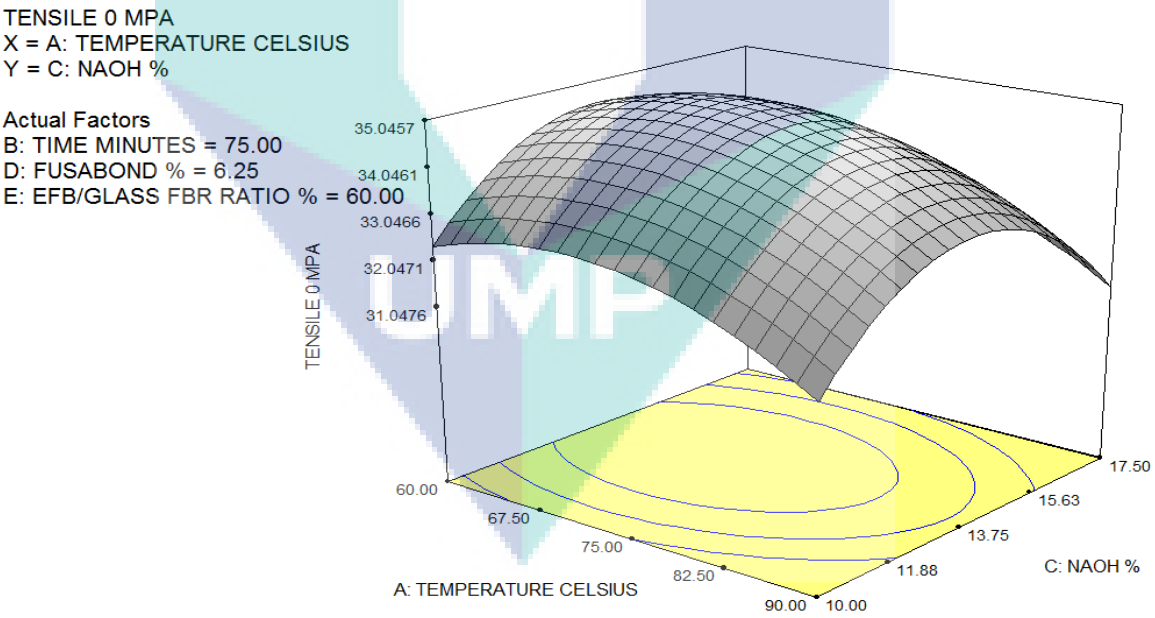

Figure 5.9: 3D graph of the temperature - NaOH % tensile strength

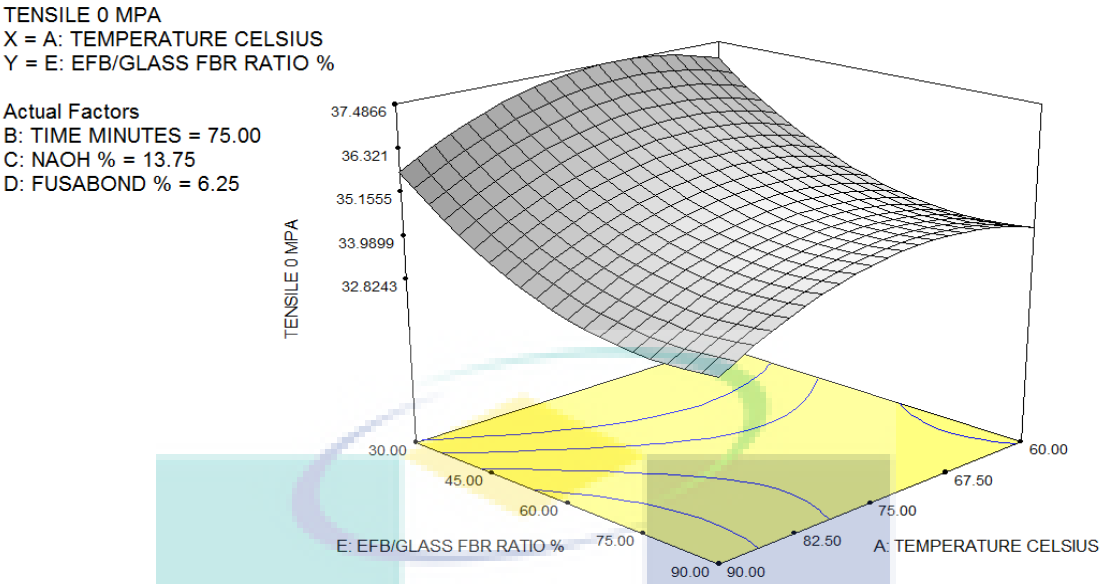

Figure 5.10: 3D graph of the fibre ratio - Temperature tensile strength

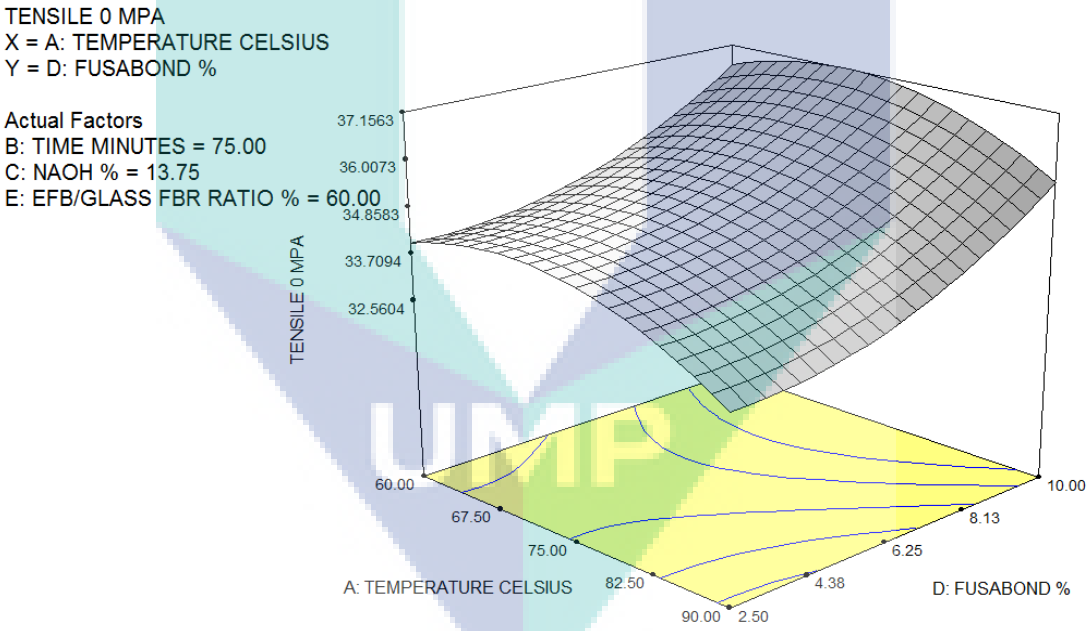

Figure 5.11: 3D graph of the Fusabond % – treatment temperature tensile strength

5.2.2 Response Surface and variable interactions of modulus

It could be seen that the maximum modulus corresponded in a positive correlation which indicated that interaction in synergistic effect. In particular, the modulus increased when the fibre ratio (C) was increased from 30 to 75 % and as NaOH % (B) was increased

from 15 to 17.5 %. When the NaOH % (B) setting was increased from 17.5 to 20 % and the fibre ratio (C) was increased from 75 to 90%, the modulus had decreased. While with the increase of treatment time from 4 to 5 hour and NaOH % around 17.5%, there was a gradual decline in the response. It could be explained that, as the treatment time and NaOH % prolonged, the better lignin decomposition of the fibre might occur, resulting in an increase in the tensile strength. Figure 5.12 to Figure 5.15 shows the 3D surface graph of modulus with respect to the treatment time (A) NaOH % (B) and the fibre ratio (C).

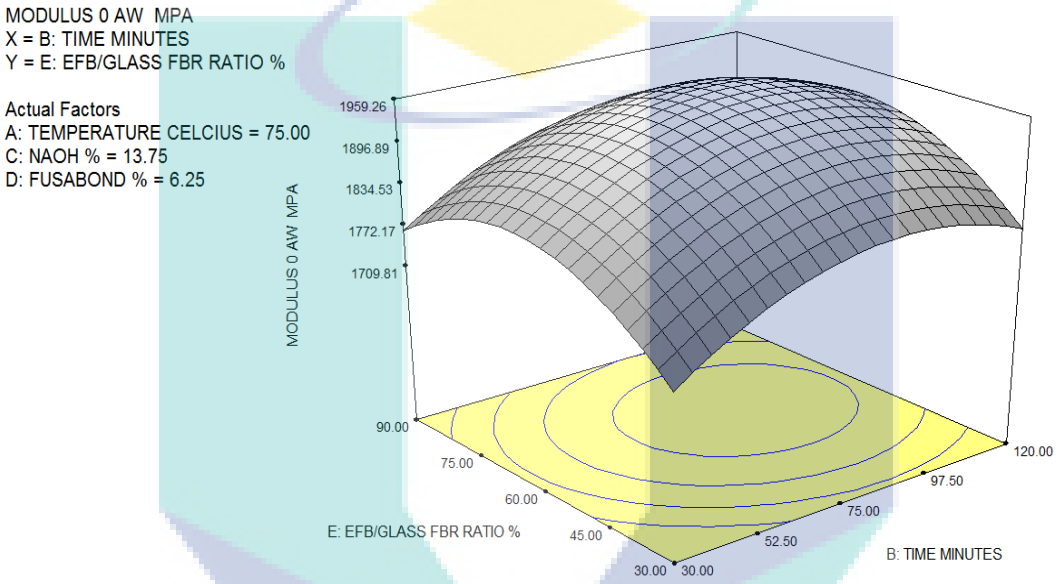

Figure 5.12: 3D graph of the fibre ratio % – treatment time modulus

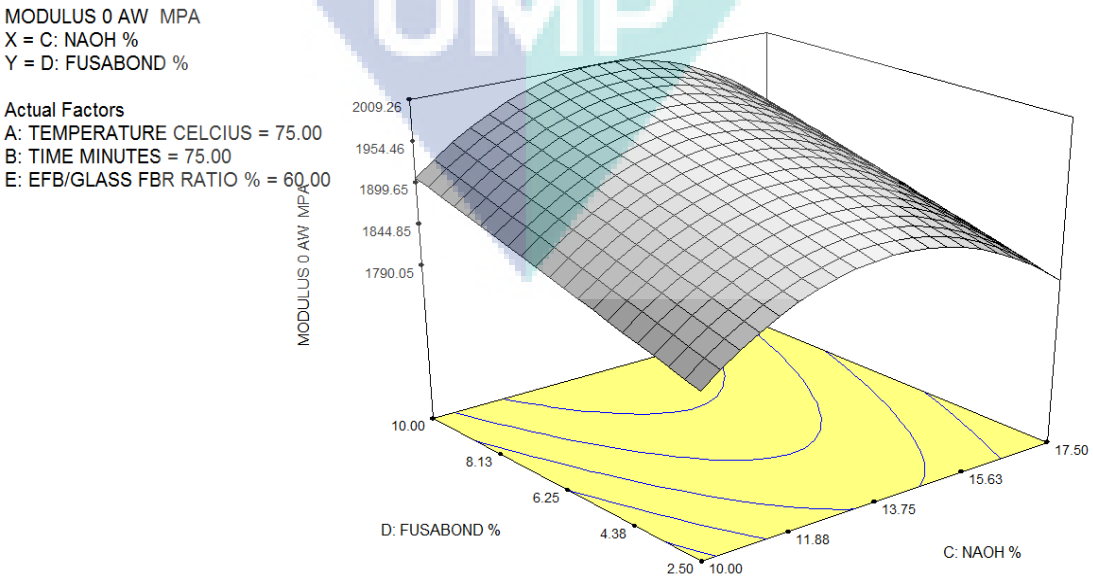

Figure 5.13: 3D graph of the NaOH % – MAPP % modulus

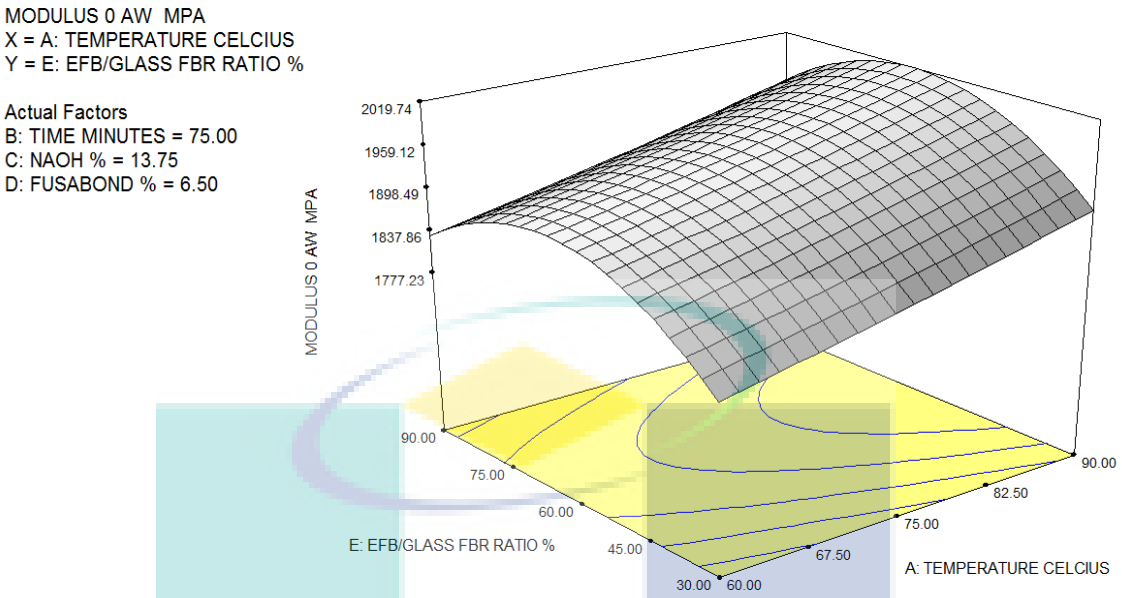

Figure 5.14: 3D graph of the fibre ratio % – treatment temperature modulus

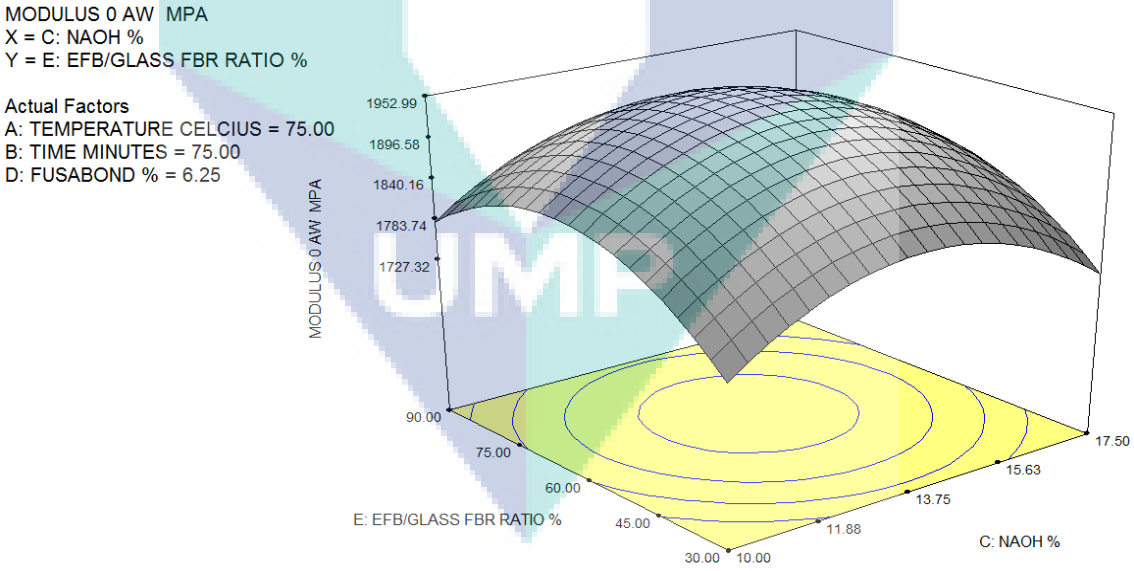

Figure 5.15: 3D graph of the NaOH % – fibre ratio % modulus

5.3 OPTIMISATION MICROWAVE HYBRID COMPOSITES

Unite Optimization procedure had been conducted for Hybrid Composites and the prediction results of the empirical model were tabulated in Table 5.3. Treatment temperature (A) treatment time (B) NaOH % (C) Fusabond (D) MAPP (E) and the fibre ratio (F), were set to range within the levels defined in Table 5.2 including tensile strength, modulus, elongation at break water absorption and melt flow index were explained to each goal and importance value. Results showed optimum treatment temperature (A) treatment time (B) NaOH % (C) Fusabond (D) MAPP (E) and the fibre ratio (F), for optimal tensile strength, modulus water absorption and melt flow index were determined in the table 6-12with total desirability value of 0.69 to 0.95 was obtained on a scale of 0 to 1, where 0 represented a completely undesirable response, and 1 represented the most desirable response. Under these proposed optimized conditions, the maximum value of the treatment temperature (A) treatment time (B) NaOH % (C) Fusabond (D) MAPP (E) and the fibre ratio (F), from the model were explained in the Table 5.4.

5.3.1 Combine Optimization of Run 1

Table 5.3: Conditions of the Combine Optimization Run 1

Name	Goal	Lower Limit	Upper Limit	Lower Weight	Upper Weight	Importance
Temperature Celsius	is in range	65	85	1	1	3
Time Minutes	is in range	35	110	1	1	3
Naoh %	is in range	10	17.5	1	1	3
Fusabond %	is in range	2.5	8	1	1	3
Fiber Fbr Ratio %	maximize	30	90	1	1	3
Tensile 0 Aw MPa	maximize	30.685	38.355	1	1	5
Modulus 0 Aw	maximize	1529.94	1988.93	1	1	4
Tensile Wtr 80^{o}C Ha	is in range	28	33.523	1	1	3
Modulus Sea Wtr 80^{o}C Ha	is in range	1097.88	1427.25	1	1	3
Wtr Absb 80^{o}C Ha %	is in range	2.386	4	1	1	3
Sea Wtr Absb 80^{o}C Ha %	is in range	2.186	4	1	1	3
Melt Flow Index G/10m	is in range	2	3.424	1	1	3

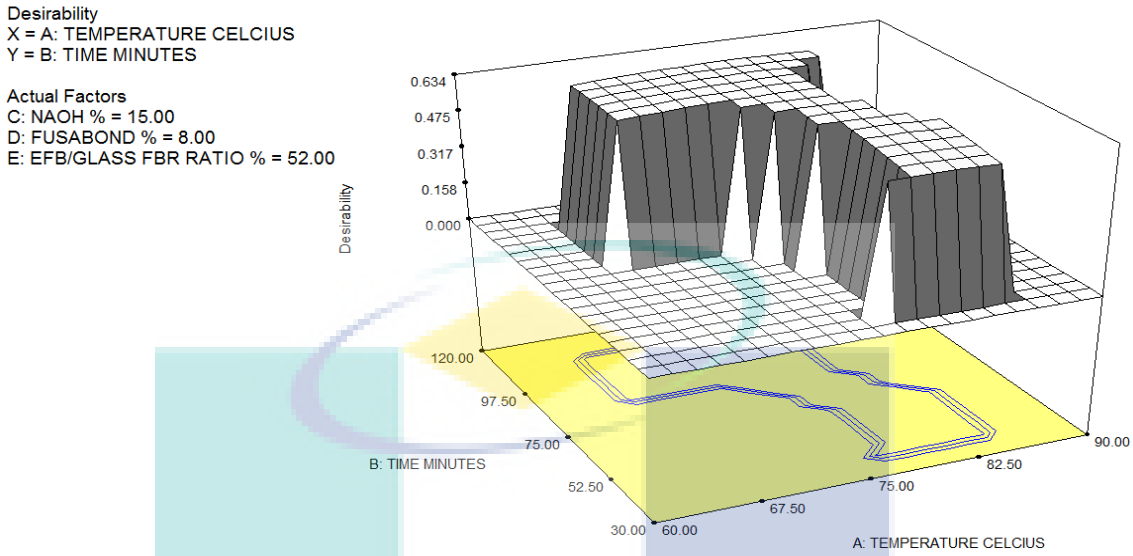

Figure 5.16: Result of the Combine Optimization Conditions Run 1 Graph

Table 5.4: Result of the Combine Optimization Conditions Run 1

Number	Temp Celsius	Time Minutes	Naoh %	Fusabond %	Fbr Ratio %	Tensile 0 Aw MPa	Modulus 0 Aw MPa	Tensile Wtr 80c Ha MPa	Modulus Sea Wtr 80c Ha MPa	Wtr Absb 80c Ha %	Sea Wtr Absb 80c Ha %	Melt Flow Index G/10m	Desirability
1	70.96	109.97	12.81	8	56.34	37.47	1938	32.75	1391	4.0	3.7	2.89	0.74
2	73.07	106.87	13.66	8	56.47	37.09	1958	32.42	1405	4.0	3.7	2.94	0.74
3	74.89	104.74	13.63	8	56.4	36.96	1969	32.31	1413	4.0	3.7	2.95	0.74
4	78.24	110	13.43	7.06	54.27	36.65	1955	32.03	1403	4.0	3.7	2.88	0.70
5	81.16	109.99	12.73	4.31	47.13	36.13	1879	31.58	1349	4.0	3.6	2.65	0.58
6	65.58	66.78	14.08	8	45.12	36.41	1880	31.82	1349	4.0	3.7	2.67	0.57
7	81.26	110	12.7	2.74	48.13	35.91	1848	31.39	1326	4.0	3.7	2.57	0.56
8	78.02	105.6	13.35	2.67	43.66	36.29	1844	31.72	1323	4.0	3.7	2.51	0.53
9	72.31	48.76	16.24	2.5	43.13	34.42	1755	30.09	1259	4.0	3.7	2.47	0.40
10	71.64	40.76	16.37	2.5	44.69	34.22	1731	29.91	1242	4.0	3.7	2.46	0.39

Table 5.5: Result of the Combine Optimization Conditions Run 2

Number	Temperature celsius	Time minutes	NaOH %	Fusabond %	EFB/Glass Fbr Ratio %	Tensile 0 AW MPa	Modulus 0 AW MPa	Tensile WTR 80C HA MPa	Modulus Sea WTR 80C HA MPa	WTR ABSB 80C HA %	Sea WTR ABSB 80C HA %	Melt flow index G/10M	Desirability
1	82.08	110	11.61	2.5	50.59	35.55	1826	31.07	1310	4.0	3.7	2.56	0.64
2	82.33	109.27	11.73	2.5	50.28	35.53	1830	31.05	1313	4.0	3.7	2.56	0.64
3	80.03	110	12.21	2.63	47.47	36.09	1835	31.55	1317	4.0	3.7	2.54	0.63
4	81.13	110	12.08	4.26	48.26	36.04	1870	31.50	1342	4.0	3.7	2.64	0.62
5	69.44	110	11.92	2.5	40.45	37.21	1803	32.52	1294	4.0	3.7	2.34	0.61
6	85	110	13.19	6.23	56.36	35.50	1962	31.03	1408	4.0	3.7	2.88	0.57
7	85	110	10.78	7	60.79	35.28	1929	30.83	1384	3.9	3.6	2.91	0.56
8	65	109.99	11.65	6.67	46.09	37.36	1852	32.65	1329	4.0	3.7	2.57	0.54
9	84.89	59.15	12.96	6.63	43.6	34.58	1930	30.23	1385	4.0	3.7	2.63	0.46
10	73.68	41.69	15.29	2.5	38.42	35.03	1735	30.62	1245	4.0	3.7	2.36	0.42

5.3.2 Combine Optimization of Run 2

Second Unite Optimization procedure had been conducted for Hybrid Composites and the prediction results of the empirical model were tabulated in Table 5.6. Treatment temperature (A) treatment time (B) NaOH % (C) Fusabond (D) MAPP (E) and the fibre ratio (F), were set to range within the levels defined in the Table 5.6 including tensile strength, modulus, elongation at break water absorption and melt flow index were explained to each goal and importance value. Results showed optimum treatment temperature (A) treatment time (B) NaOH % (C) Fusabond (D) MAPP (E) and the fibre ratio (F), for optimal tensile strength, modulus water absorption and melt flow index were determined in the table 6-12 with total desirability value of 0.942 to 0.998 was obtained on a scale of 0 to 1, where 0 represented a completely undesirable response, and 1 represented the most desirable response. Under these proposed optimized conditions, the maximum value of the treatment temperature (A) treatment time (B) NaOH % (C) Fusabond (D) MAPP (E) and the fibre ratio (F), from the model were explained in the Table 5.5.

Table 5.6: Conditions of the Combine Optimization Run 2

Name	Goal	Lower Limit	Upper Limit	Lower Weight	Upper Weight	Importance
Temperature	is in range	65	85	1	1	3
Time Minutes	is in range	35	110	1	1	3
Naoh %	minimize	10	17.5	1	1	3
Fusabond %	minimize	2.5	8	1	1	3
Fibre Ratio %	maximize	30	90	1	1	3
Tensile 0 Aw MPa	maximize	30.685	38.355	1	1	5
Modulus 0 Aw MPa	maximize	1529.94	1988.93	1	1	4
Tensile Wtr 80^{o}C Ha	is in range	28	33.523	1	1	3

Modulus Sea Wtr 80°C Ha	is in range	1097.88	1427.25	1	1	3
Wtr Absb 80°C Ha %	is in range	2.386	4	1	1	3
Sea Wtr Absb 80°C Ha %	is in range	2.186	4	1	1	3
Melt Flow Index G/10m	is in range	2	3.424	1	1	3

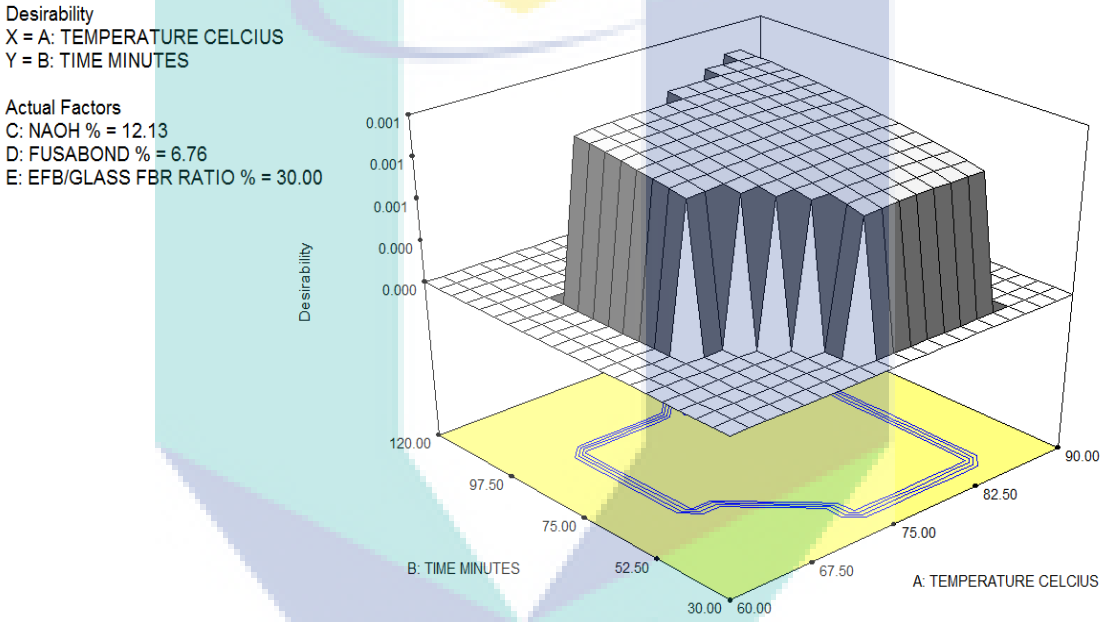

Figure 5.17: Result of the Combine Optimization Conditions Run 2 Graph

Microwave treatment optimum condition as explain in Table 5.4 and setting condition in Table 5.3 were at 70,96°C 109,97 minutes 12,81 % NaOH, 8 % Fusabond 56,34 % Fibre Ratio and composites properties predicted is 37,47 MPa Tensile Strength 1938 MPa Modulus and 4 % water absorbtion. Second optimum condition as show in the Table 5.5 setting condition at Table 5.6 were were at 82,08°C, 110 minutes 11,61 NaOH, 2,5 % Fusabond 50,59 % Fibre Ratio and composites properties predicted is 35,55 MPa Tensile Strength, 1826 Modulus and 4,0 % water absorbtion.

5.4 CHARACTERIZATION OF ULTRASONIC HYBRID COMPOSITES

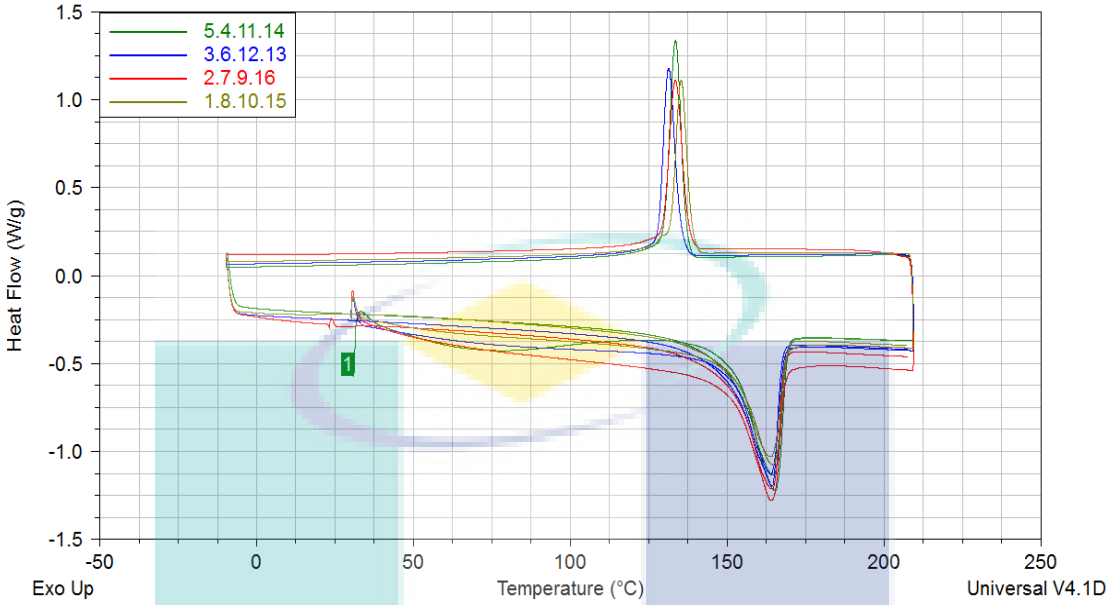

Figure 5.18: DSC graph of ultrasonic hybrid composites

Temperatures of crystallization, melting point and heat flow of crystallization of the EFB-Glass fibre hybrid composites have different value, as explained in Table 5.7, there was no significant change in the crystallization temperature with respect to the alkali treatment time and temperature of the composites. However, all composites presented higher crystallization temperatures compared to recycled polypropylene. A small difference between sample containing of the fibre ratio was also observed in all composites sample tested.

Figure 5.18 shows DSC scanning curves of samples containing ultrasonic of EFB fibre, prepared in 10 to 17.5% NaOH and 30 to 120 minutes fibre treatment. No significant changes in the melting temperature of composites containing the difference of fibre treatment and coupling agent were observed. Moreover, with changes in the fibre ratio. The melting and crystallization curves were not significantly different.

TGA curve of recycled polypropylene matrix, and ultrasonic hybrid composites are shown in Figure 5.19. All the composites TGA curves show the initial transition around 250 to 300^{o}C due to the start of EFB fibre degradations. The decomposition temperature of the samples slightly different in the range of 300 to 450 as shown in the Figure 5.19 where the TGA traces shifted to lower temperatures with increasing EFB

content. TGA transitions for composites remaining from500 up to 650ºC also found shifted to slightly lower doe the fibre ratio or glass fibre residual content of the composites.

Table 5.7: Crystallization and melting heat flow-temperature

Ultra sonic STD	Crystallization Heat flow W/G	Crystallization Temp C	Melting Heat flow W/G	Melting Temp C
1	0.985	131.32	-0.86	163.84
2	1.702	133.51	-1.41	163.99
3	1.324	133.54	-1.64	164.42
4	0.892	133.24	-0.72	165.21
5	0.962	133.45	-0.77	165.81
6	1.324	133.75	-1.44	164.32
7	1.202	133.91	-1.21	162.39
8	0.985	131.16	-0.83	163.19
9	1.102	133.87	-1.31	164.39
10	0.785	131.35	-0.84	163.59
11	0.972	133.86	-0.72	165.83
12	1.274	133.75	-1.47	164.42
13	1.224	133.35	-1.44	164.62
14	0.942	133.75	-0.72	165.29
15	0.895	131.71	-0.86	163.83
16	1.302	133.53	-1.21	164.85

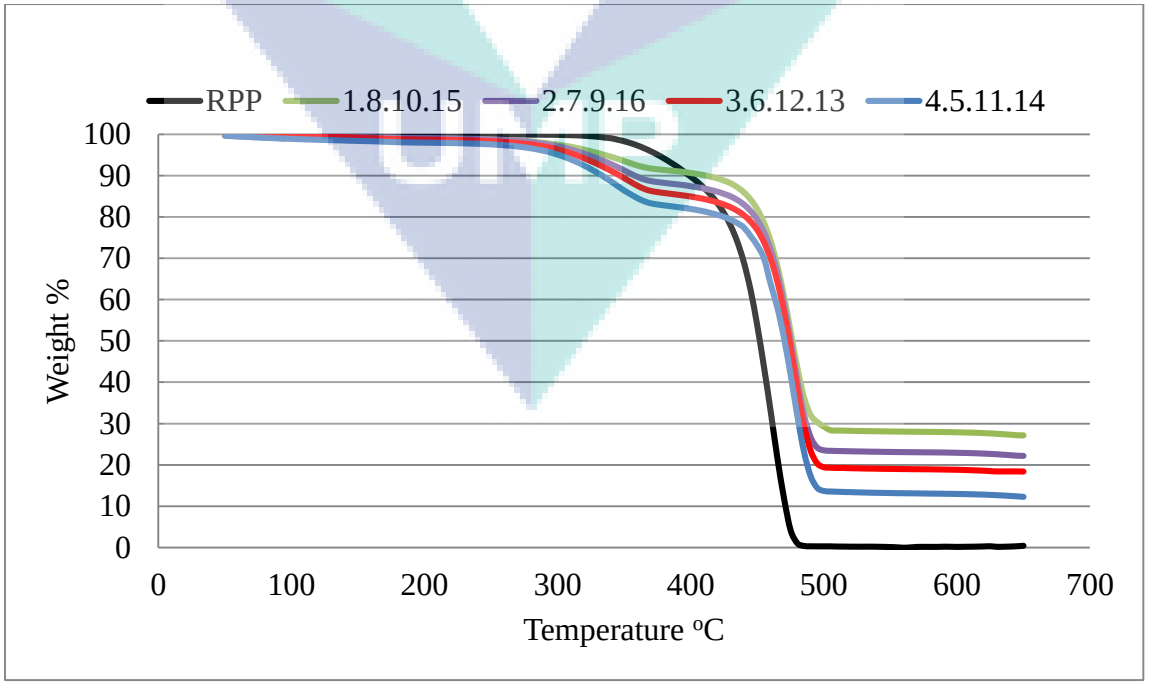

Figure 5.19: TGA graph of ultrasonic hybrid composites

5.4.1 Melt Flow Index

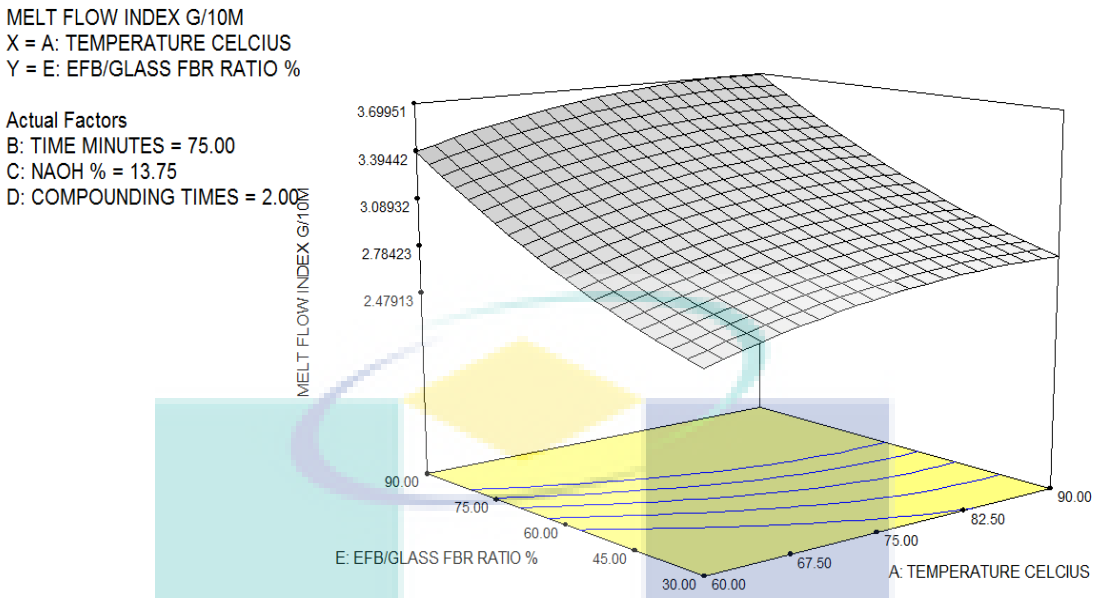

Figure 5.20: Melt Flow Index of EFB-Glass Fibre Composites

Figure 5.20 to Figure 5.22 shows the Melt Flow Index of ultrasonic alkaline treatment composite. From the Figure, it can be seen that Melt Flow Index of 30 to 120 minutes of treated ultrasonic composite is similar. Treated composite with higher treatment time, NaOH, and Compounding times was not noticeable changed to melt flow index response. Ratio of EFB/Glass fibre from 30 to 90 had been significant changed melt flow response. The response was decreased by increased of Ratio EFB/Glass fibre from 3.69 to only 2.33 G/10 M. This might be due on low fluidity of EFB fibre in the composites' melting condition.

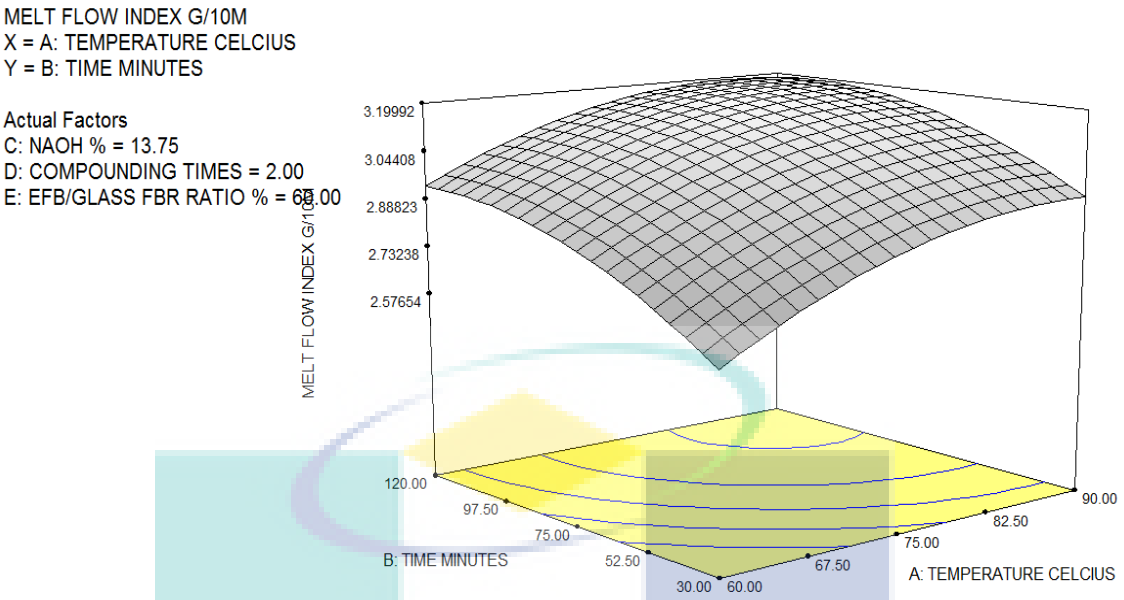

Figure 5.21: Melt Flow Index of EFB-Glass Fibre Composites

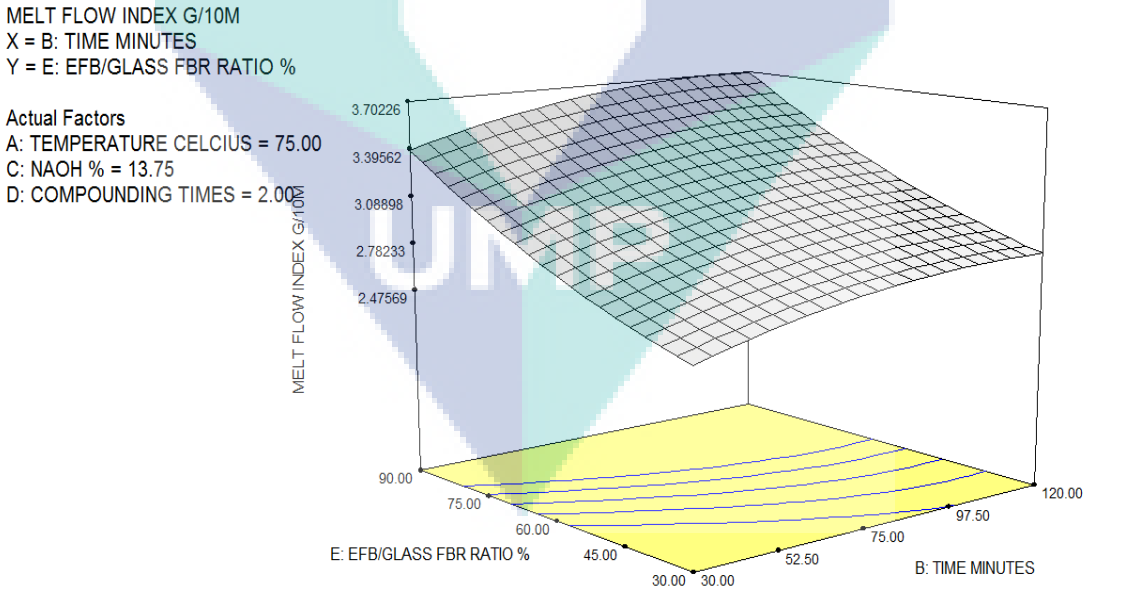

Figure 5.22: Melt Flow Index of EFB-Glass Fibre Composites

5.4.2 Response Surface and variable interactions of Tensile Strength

Figure 5.23 to Figure 5.26 show the response surface plots as functions of treatment time and NaOH % on the Tensile 0 H AW at 60% of the fibre ratio the typical plot like this is dome shaped. From the Figures, it is obvious that tensile strength increase from 30 to 120 minutes treatment time and 15 to 17.5 NaOH %. The tensile increase when the treatment time increase from 30 to 120 minutes and NaOH % increase from 10 to 17.5. The appropriate maximum tensile strength was determined at a 120 minutes treatment time and 13.75 NaOH %, led to the maximum tensile strength at 37.6 MPa.

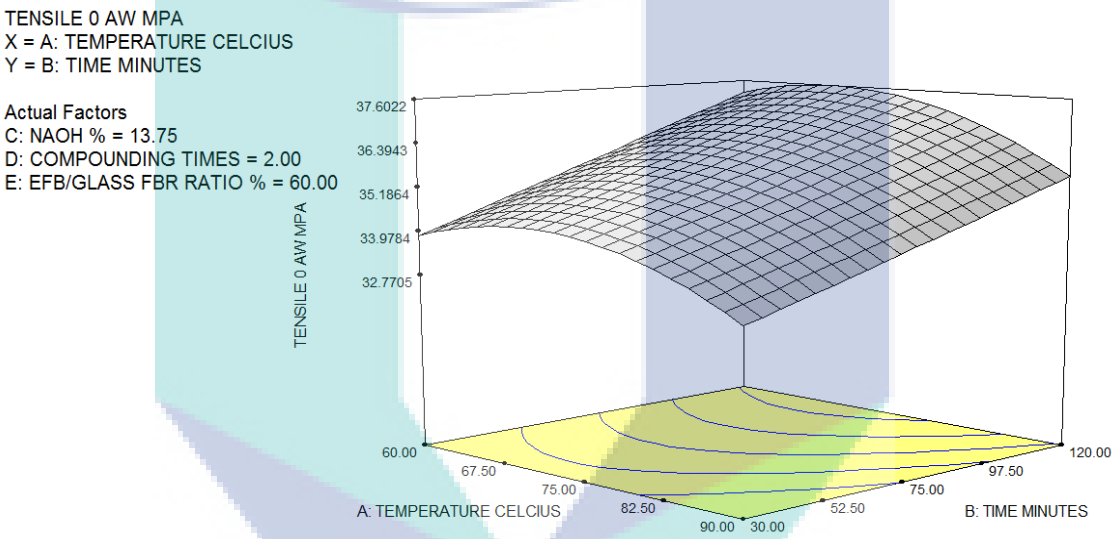

Figure 5.23: 3D graph of the treatment time – temperature tensile strength

Table 5.8: Ultrasonic factors levels

Factors	Unit	Levels 1	Levels 2	Levels 3	Levels 4
A: Temperature	Celsius	60	70	80	90
B:Treatment time	Minute	30	60	90	120
C:NaOH	%	10	13	15	18
D:Extrusion time	Times	1	2	3	4
E:Fibre ratio	%	50	60	70	80

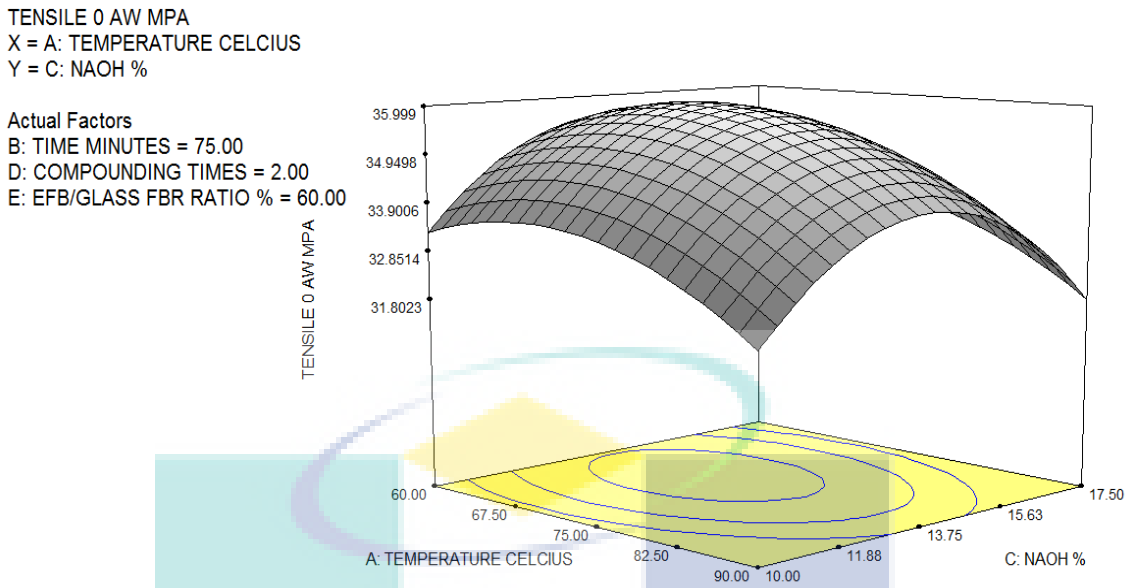

Figure 5.24: 3D graph of the temperature - NaOH % tensile strength

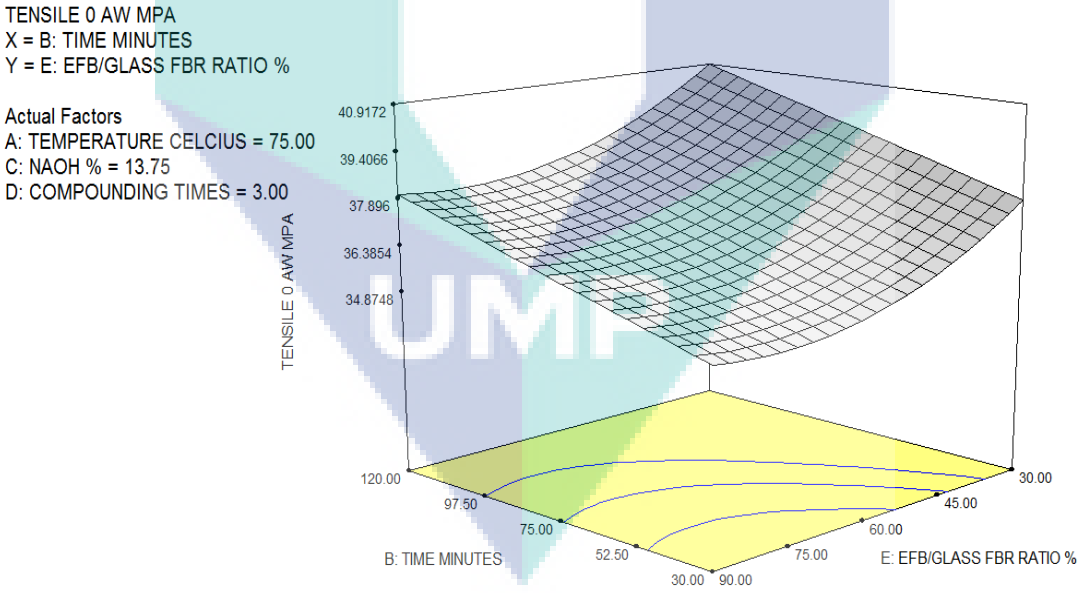

Figure 5.25: 3D graph of the Fibre % – treatment time tensile strength

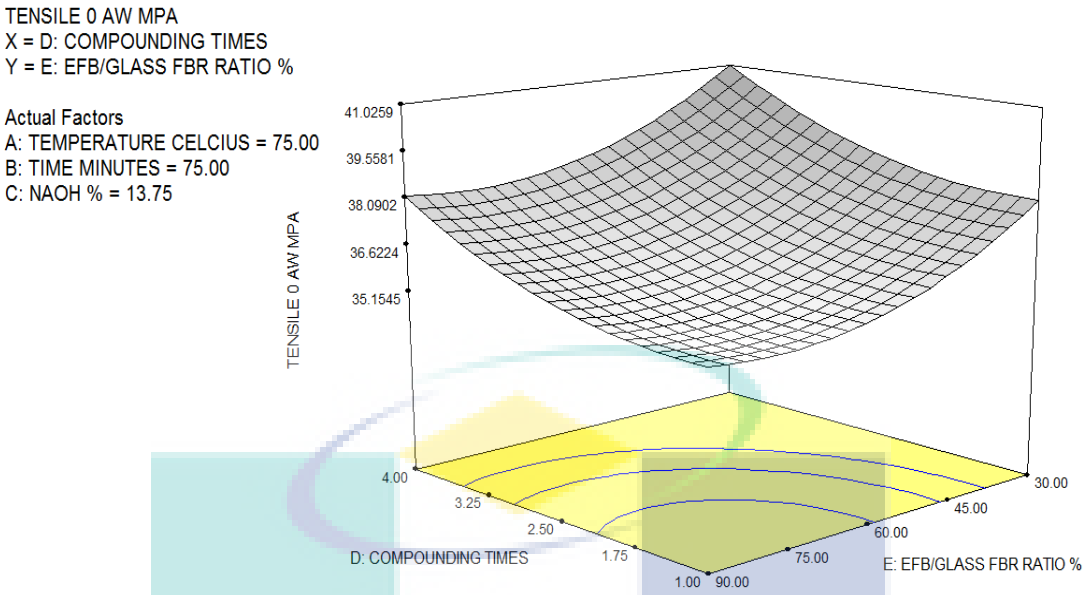

Figure 5.26: 3D graph of the compounding time - fibre ratio % tensile strength

5.4.3 Response Surface and variable interactions of modulus

It could be seen that the maximum modulus corresponded in a positive correlation which indicated that interaction in synergistic effect. In particular, the modulus increased when the fibre ratio (C) was increased from 30 to 60% and as NaOH % (B) was increased from 10 to 13.75%. When the NaOH % (C) setting was increased from 13.75 to 17.50% and the fibre ratio (E) was increased from 60 to 90%, the modulus had decreased. While with the increase of treatment time from 75 to 120 minutes and NaOH % around 13.5 to 17.5%, there was a gradual decline in the response. It could be explained that, as the treatment time and NaOH % continued, the cellulose decomposition of the fibre might occur, resulting in a decrease in the tensile strength. Figure 5.27 to Figure 5.30 shows the 3D surface graph of modulus with respect to the temperature (A),treatment time (B), NaOH % (C) compounding time (D) and the fibre ratio (E).

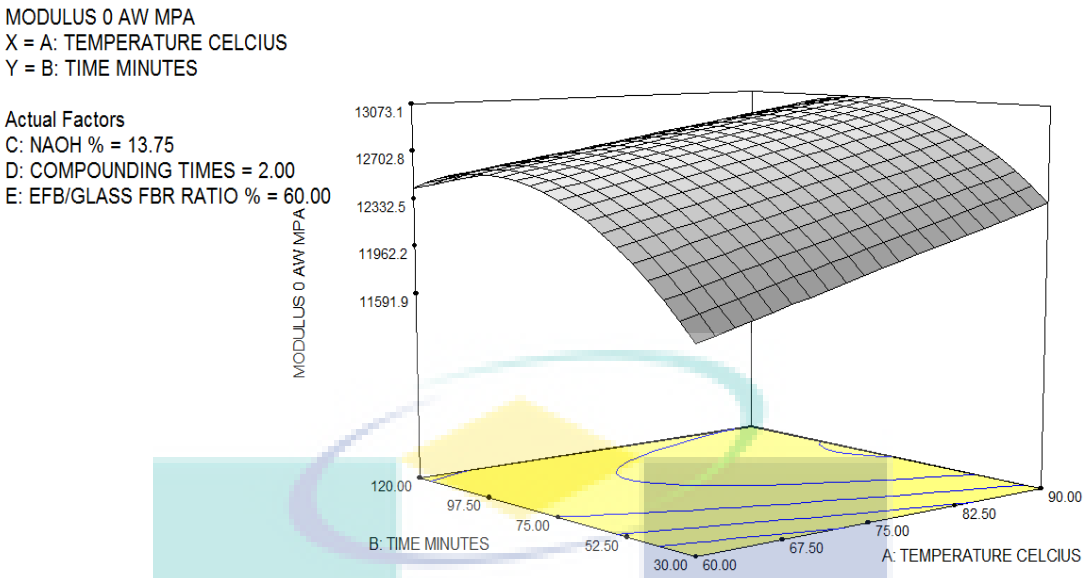

Figure 5.27: 3D graph of the Temperature – treatment time modulus

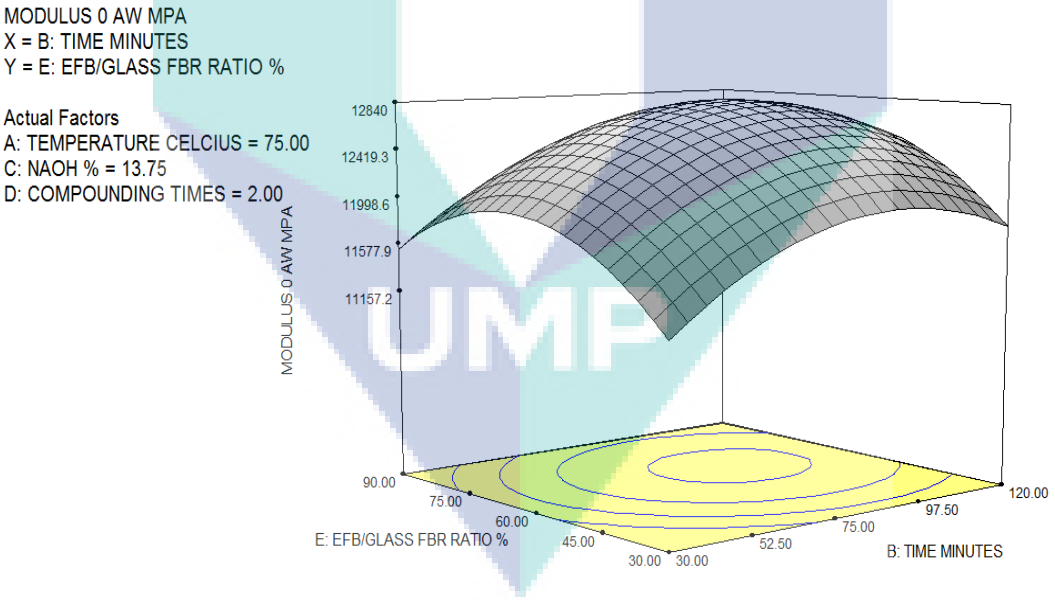

Figure 5.28: 3D graph of the fibre ratio % – treatment time modulus

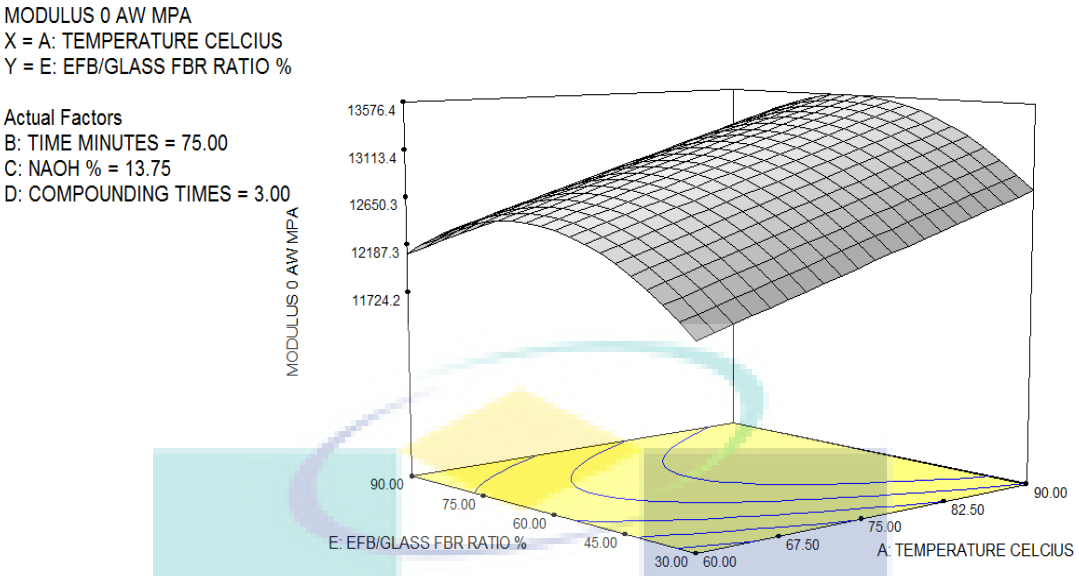

Figure 5.29: 3D graph of the fibre ratio % – treatment temperature modulus

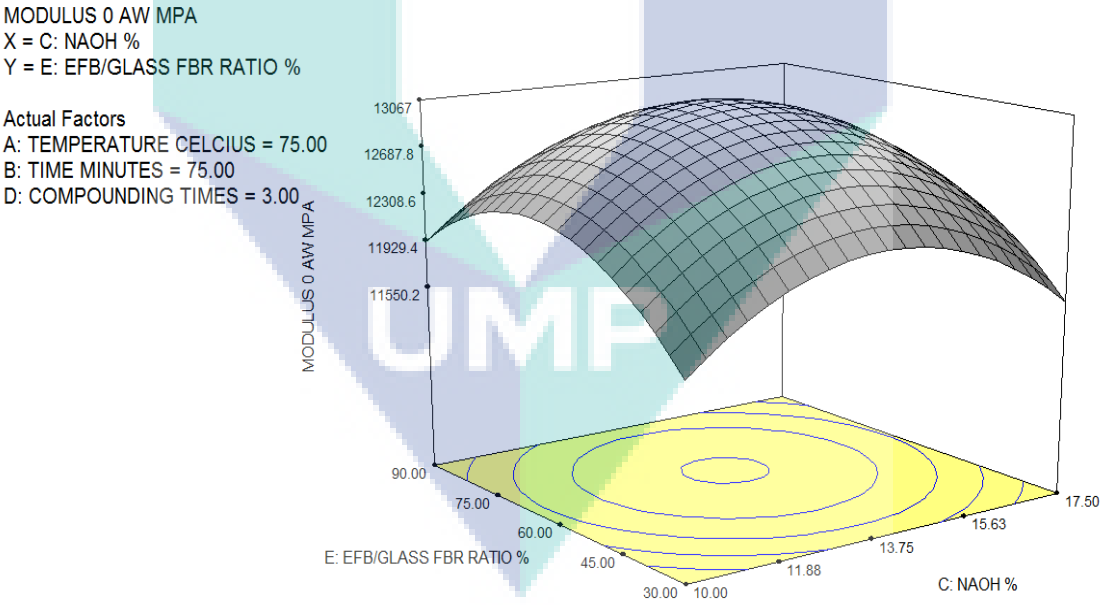

Figure 5.30: 3D graph of the NaOH % – fibre ratio % modulus

5.5 OPTIMISATION ULTRASONIC HYBRID COMPOSITES

Unite Optimization procedure had been conducted for Hybrid Composites and the prediction results of the empirical model were tabulated in Table 5.9. Treatment temperature (A) treatment time (B) NaOH % (C) compounding times(D) and the fibre ratio (E) were set to range within the levels defined in the Table 5.8 including tensile strength, modulus, elongation at break water absorption and melt flow index were explained to each goal and importance value. Results showed optimum treatment temperature (A) treatment time (B) NaOH % (C) compounding times (D) and the fibre ratio (E) for optimal tensile strength, modulus water absorption and melt flow index were determined in the Table 5.9 with total desirability value of 0.551 to 0.633 was obtained on a scale of 0 to 1, where 0 represented a completely undesirable response, and 1 represented the most desirable response. Under these proposed optimized conditions, the maximum value of the treatment temperature (A) treatment time (B) NaOH % (C) compounding times (D) the fibre ratio (E), from the model were explained in the Table 5.10.

5.5.1 Combine Optimization of Run 1

Table 5.9: Conditions of the Combine Optimization Run 1

Name	Goal	Lower Limit	Upper Limit	Lower Weight	Upper Weight	Importance
Temperature Celsius	is in range	6.50	85	1	1	3
Time Minutes	is in range	3.50	110	1	1	3
NaOH %	is in range	10	1.75	1	1	3
Compounding Times	is in range	2	3	1	1	3
Efb/Glass Fbr Ratio %	maximize	30	90	1	1	3
Tensile 0 Aw MPa	maximize	31.876	39.817	1	1	5
Modulus 0 Aw MPa	maximize	1006.9	1322.2	1	1	4
Tensile 1200 Aw MPa	is in range	34	38.427	1	1	3
Tensile Wtr 80^{o}C Ha	is in range	30	34.801	1	1	3
Wtr Absb 60^{o}C Ha %	is in range	1.995	4	1	1	3

Wtr Absb 80°C Ha %	is in range	1.995	3.5	1	1	3
Sea Wtr Absb 60°C Ha	is in range	1.834	3.5	1	1	3
Sea Wtr Absb 80°C Ha	is in range	1.995	3.5	1	1	3
Melt Flow Index G/10m	is in range	2	3.891	1	1	3

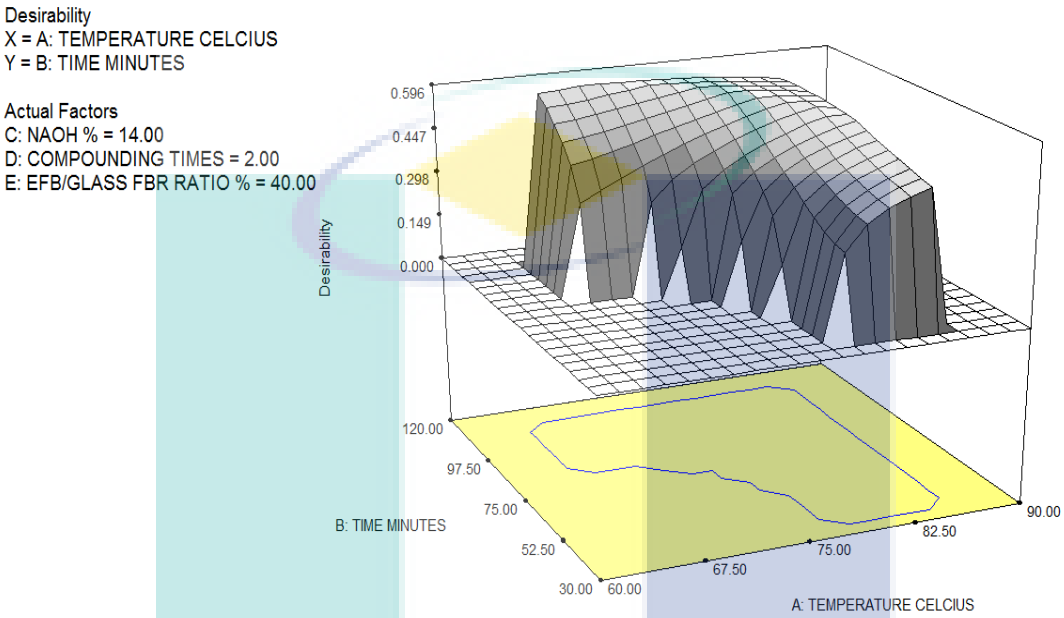

Figure 5.31: Result of the Combine Optimization Conditions Run 1 Graph

Table 5.10: Result of the Combine Optimization Conditions Run 1

Number	Temperature Celsius	Time Minutes	NaOH %	Compounding Times	Efb/Glass Fbr Ratio %	Tensile 0 AW MPa	Modulus 0 AW MPa	Tensile 1200 AW MPa	Tensile Wtr 80C HA MPa	Wtr Absb 60C HA %	Wtr Absb 80C HA %	Sea Wtr Absb 60C HA %	Sea Wtr Absb 80C HA %	Desirability
1	84	110	13	3	60	37.54	1318	36.23	32.81	3.30	3.30	3.03	3.30	0.6033
2	85	110	13	3	61	37.23	1326	35.93	32.54	3.30	3.30	3.03	3.30	0.6033
3	76	110	13	3	51	38.67	1291	37.32	33.80	3.23	3.23	2.97	3.23	0.6033
4	70	110	14	3	50	38.71	1271	37.35	33.83	3.30	3.30	3.03	3.30	0.6013
5	65	110	13	3	50	38.99	1252	37.63	34.08	3.30	3.30	3.03	3.30	0.5993
6	65	107	13	3	48	38.92	1252	37.56	34.01	3.30	3.30	3.03	3.30	0.5953
7	72	110	16	3	55	37.11	1271	35.81	32.43	3.30	3.30	3.03	3.30	0.5943
8	85	110	12	2	49	37.01	1261	35.72	32.35	3.24	3.24	2.98	3.24	0.5793
9	65	110	14	2	43	38.62	1233	37.27	33.76	3.30	3.30	3.03	3.30	0.5733
10	65	44	17	2	48	35.55	1163	34.31	31.07	3.30	3.30	3.03	3.30	0.5513

Table 5.11: Result of the Combine Optimization Conditions Run 2

Number	Temperature Celsius	Time Minutes	Naoh %	Compounding Times	Efb/Glass Fbr Ratio %	Tensile 0 Aw MPa	Modulus 0 Aw MPa	Tensile 1200 Aw MPa	Modulus 1200 Aw MPa	Tensile Wtr 80c Ha MPa	Wtr Absb 60c Ha %	Wtr Absb 80c Ha %	Sea Wtr Absb 60c Ha %	Desirability
1	74.8	80	13.7	3	51.6	37	1297	36	1172	32.77	3.50	3.50	3.22	0.615
2	75.4	78	13.8	3	51.7	37	1299	36	1173	32.70	3.50	3.50	3.22	0.615
3	77.1	86	13.1	3	53.3	37	1307	36	1181	32.77	3.50	3.50	3.22	0.615
4	76.6	75	13.8	3	45.4	38	1287	36	1163	32.97	3.34	3.34	3.07	0.613
5	78.9	83	14.1	3	48.5	38	1305	36	1180	32.80	3.31	3.31	3.05	0.611
6	69.0	85	13.6	3	47.0	38	1270	37	1147	33.31	3.42	3.42	3.14	0.607
7	76.9	85	14.3	3	46.7	38	1294	36	1170	33.05	3.28	3.28	3.02	0.606
8	73.3	83	13.4	3	47.9	38	1280	36	1157	32.94	3.50	3.50	3.22	0.591
9	65.1	90	13.3	2	41.4	38	1232	37	1113	33.16	3.50	3.50	3.22	0.585
10	82.6	35	16.2	3	50.3	36	1232	35	1113	31.25	3.06	3.06	2.81	0.563

5.5.2 Combine Optimization of Run 2

Second Unite Optimization procedure had been conducted for Hybrid Composites and the prediction results of the empirical model were tabulated in Table 5.12. Treatment temperature (A) treatment time (B) NaOH % (C) compounding times (D) and the fibre ratio (E) were set to range within the levels defined in the table 7-13 including tensile strength, modulus, elongation at break water absorption and melt flow index were explained to each goal and importance value. Results showed optimum treatment temperature (A) treatment time (B) NaOH % (C) compounding times (D) and the fibre ratio (E) for optimal tensile strength, modulus water absorption and melt flow index were determined in the Table 5.11 with total desirability value of 0.563 to 0.615 was obtained on a scale of 0 to 1, where 0 represented a completely undesirable response, and 1 represented the most desirable response. Under these proposed optimized conditions, the maximum value of the treatment temperature (A) treatment time (B) NaOH % (C) compounding times (D) and the fibre ratio (E) from the model were explained in the Table 5.12.

Table 5.12: Conditions of the Combine Optimization Run 2

Name	Goal	Lower Limit	Upper Limit	Lower Weight	Upper Weight	Importance
Temperature Celsius	is in range	65.0	85.0	1	1	3
Time Minutes	minimize	35.0	110.0	1	1	3
Naoh %	is in range	10.0	17.5	1	1	3
Compounding Times	is in range	2.0	3.0	1	1	3
Efb/Glass Fbr Ratio %	maximize	30.0	90.0	1	1	3
Tensile 0 Aw MPa	maximize	31.9	39.8	1	1	5
Modulus 0 Aw MPa	maximize	1006.9	1322.2	1	1	4
Tensile 1200 Aw MPa	maximize	34.0	38.4	1	1	3
Modulus 1200 Aw	maximize	909.0	1195.5	1	1	3
Tensile Wtr 80^{o}C Ha	is in range	30.0	34.8	1	1	3
Wtr Absb 60^{o}C Ha %	is in range	2.0	4.0	1	1	3
Wtr Absb 80^{o}C Ha %	is in range	2.0	3.5	1	1	3

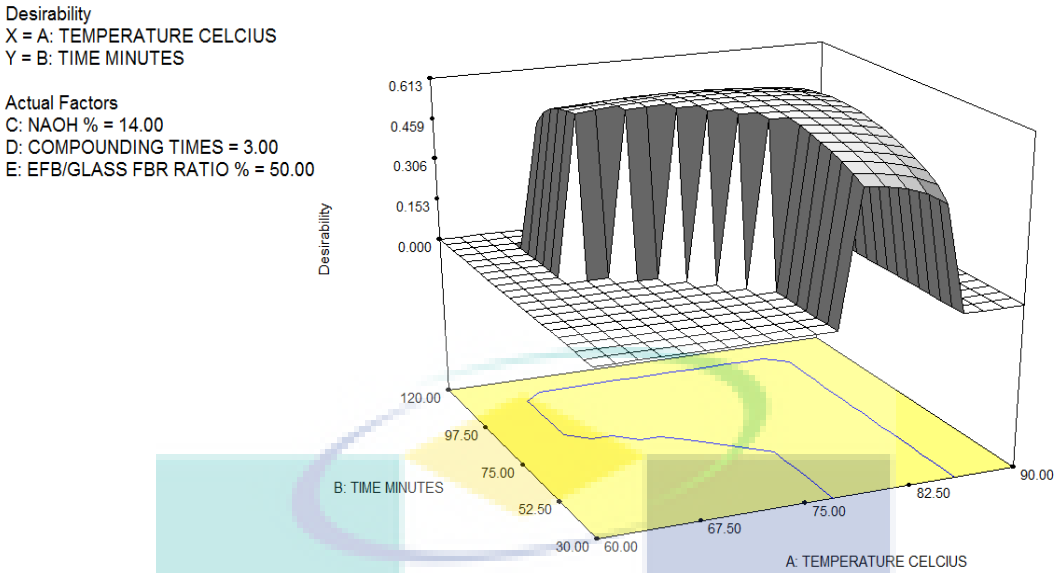

Figure 5.32: Result of the Combine Optimization Conditions Run 2 Graph

Ultrasonic treatment optimum condition as explain in Table 5.10 and setting condition in Table 5.9 were at 84^{o}C 110 minutes 13 % NaOH, 3 times compounding 60 % Fibre Ratio and composites properties predicted is 37,54 MPa Tensile Strength 1318 MPa Modulus and 3,3 % water absorbtion. Second optimum condition as show in the Table 5.11 setting condition at Table 5.12 were were at 74,8^{o}C, 80 minutes 13,7 NaOH, 3 times compounding 51,6 % Fibre Ratio and composites properties predicted is 37 MPa Tensile Strength 1297 Modulus and 3,5 % water absorbtion.

CHAPTER 6.

COMPARISON OF ALKALI TREATMENTS

In this chapter comparison of each treatment were explained and compared. Result of standard, homemade, microwave and ultrasonic alkali treatment were compared. This chapter was divided into four parts of results and discussion, namely: accelerated weathering comparison, hygrothermal ageing comparison, water absorption comparison and Melt flow index composites. In this chapter, bar chart from table property's average was used to calculate the average and standard deviation value of the response treatment. The Figures in this chapter show overall properties of the each treatment and comparison of each treatment.

6.1 COMPARISON OF ACCELERATED WEATHERING PROPERTIES

Composites with four different alkali treatment, compounding times, formulation coupling agent and fibre content for RPHC was successfully produced. Average of TS, YM and elongation each treatments were compared. Figure 6.1 to Figure 6.3 clearly explains that ultrasonic treatment was superior and produce better mechanical properties following by microwave modified homemade and finally is the conventional treatment. It could be doe the ability of ultrasonic wave to improve lignin removal effectively. Microwave treatments also have good properties result, the vibration of solvent cause by microwave's magnetron pulse improve lignin removal effectively. Furthermore homemade and conventional standard deviation results are higher, it explain that the treatments still has low quality's precision and also range of the treatment and formulation are too width.

Alkali process is needed in the Composite fabrication because It has goal to decrease the lignin content and to obtain a greater degree of surface area and bounding between natural fibre and matrix (Beckermann andPickering, 2008).There are many types of Alkali treatment equipment, such as Standart, Homemade Microwave and Ultrasonic alkali treatment. The differences in the types of Alkali treatment equipment create the energy density and the relative energy efficiency of their respective lignin removal to be different. Figure 6.1 to Figure 6.3 were shown the effect of alkali treatment technique. Figure 6.1 shown that the ultrasonic-assisted extraction could produce higher tensile strength than either the microvawe homemade or standard alkali treatment

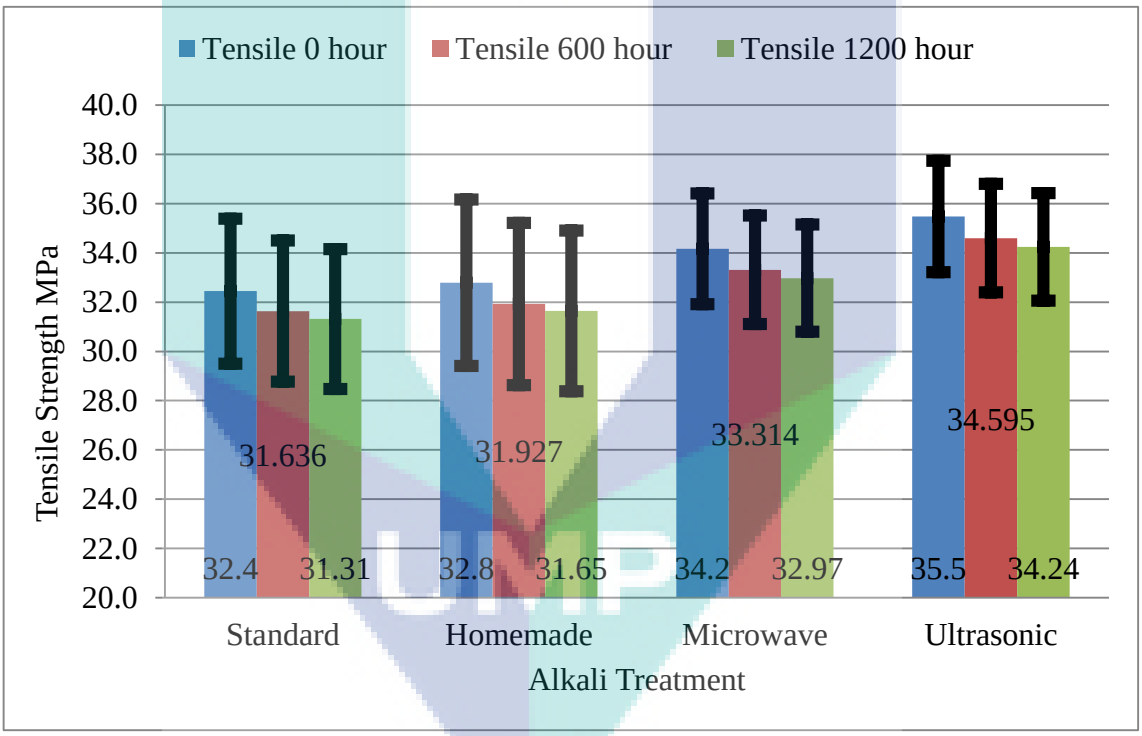

Figure 6.1: Tensile strength of accelerated weathering hybrid composites

The change in mechanical properties due to accelerated weathering from 0 to 1200 hour are presented in Figure 6.1 to Figure 6.3. Very little change in tensile was found for standart treatment, homemade, microwave and ultrasonic alkali treatment with increasing accelerated weathering time to 600 and 1200 hour. During 600 and 1200 hour accelerated weathering, ultrasonic hybrid composite showed higher mechanical properties following by microwave and homemade alkali treatment, Best EFB lignin

removal was provide by ultrasonic and microwave treatment and the composite also have better properties stability. Figure 6.1 to Figure 6.3 showed all of the composites have acceptable properties during 600 and 1200 accelerated weathering test (approximate 4 to 5 years in natural weathering) that means the material are suitable for outdoor application.

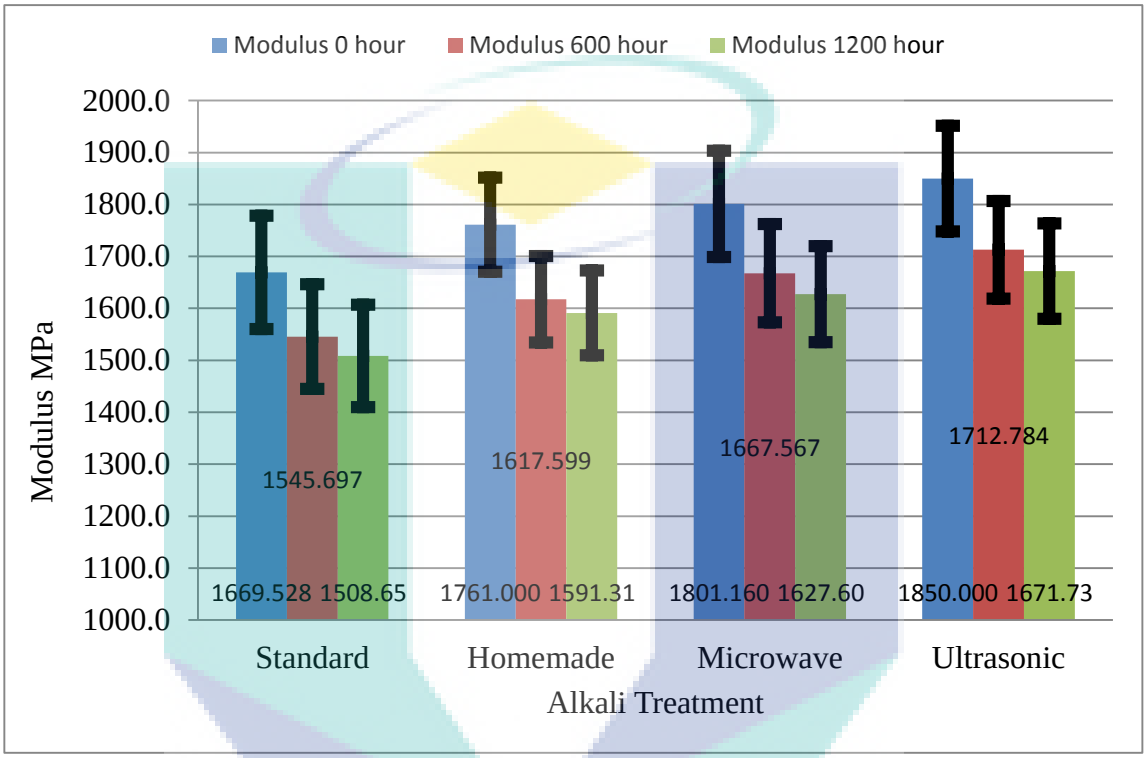

Figure 6.2: Modulus of accelerated weathering hybrid composites

A noticeable reduction of elongation at break was found as explain in the Figure 6.3. Accelerated weathering 600 and 1200 hour reduce elongation of ultrasonic treatment composites from 8% to 6.27 and 5.54 respectively, .dramatic reduction of elongation at break could be due fibre-matrix bonding degradation and cracking cause by water infiltration. The rate of moisture absorption increased with increase in hygrothermal temperature setting, high temperature operation lead to agresive water penetration in the fiber and fibre- matrix interface.

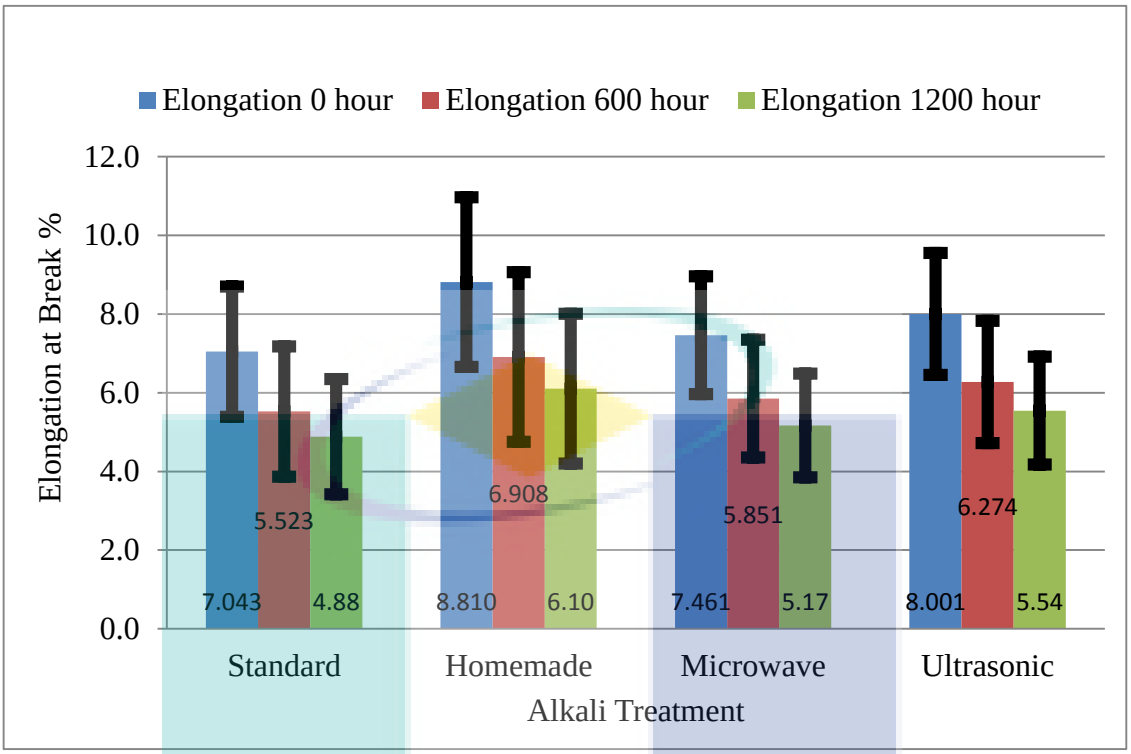

Figure 6.3: Elongation of accelerated weathering hybrid composites

6.2 COMPARISON HYGROTHERMAL AGEING PROPERTIES

During 2 months hygrothermal ageing, each specimen was soaking in the 27, 60 and 80°C. Tensile testing was carryout to examine the properties degradation under submerged application.

Figure 6.4 to Figure 6.9 explain the Tensile, modulus and elongation properties that plotted as a function of alkali treatment and hygrothermal temperature. Ultrasonic hybrid composite showed higher mechanical properties following by microwave and homemade alkali treatment, it could be due ultrasonic alkali treatment provide better lignin removal, high fibre-matrix bonding, additional Fusabond coupling agent and better fibre-matrix compounding. However homemade, ultrasonic and microwave treatment provide lower mechanical-hygrothermal properties, it could be due fibre-matrix bonding degradation and cracking cause by water infiltration. The rate of moisture absorption increased with increase in hygrothermal temperature setting, high temperature operation lead to agresive

water penetration in the fiber and fibre- matrix interface and hygrothermal properties decrease EFB fibre and damage fibre-matrix interface bonding.

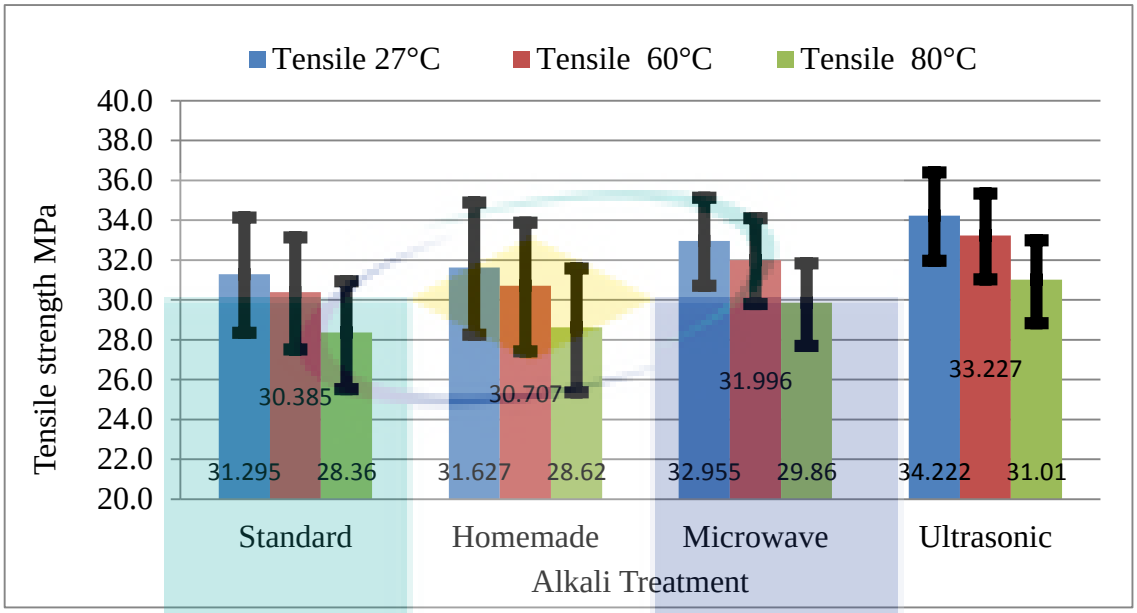

Figure 6.4: Tensile strength of plain water hygrothermal ageing hybrid composites

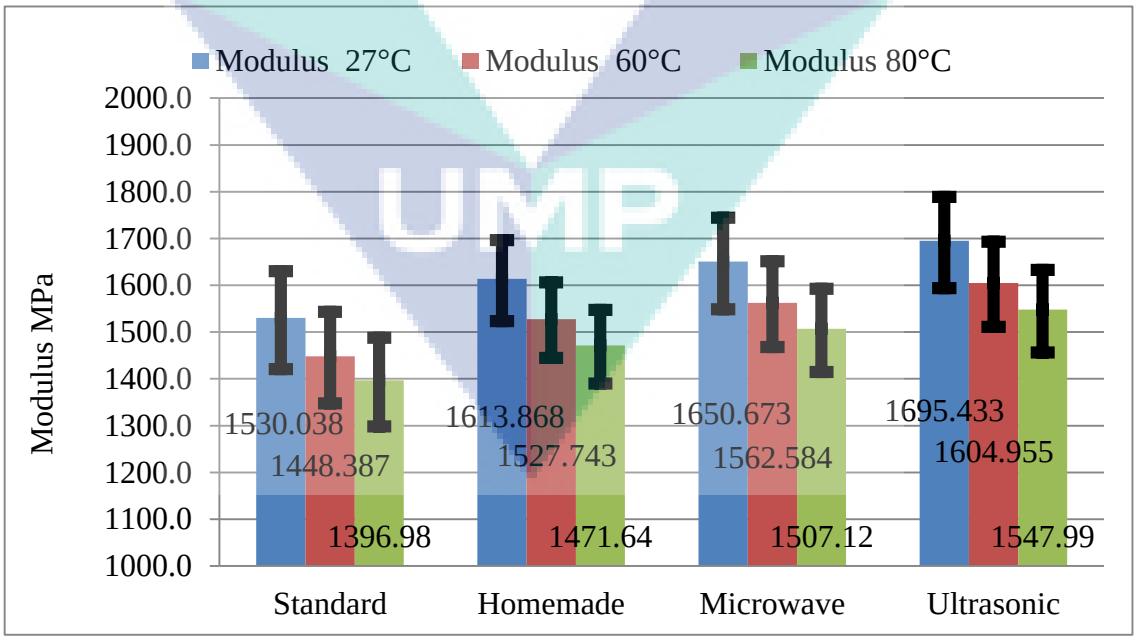

Figure 6.5: Modulus of plain water hygrothermal ageing hybrid composites

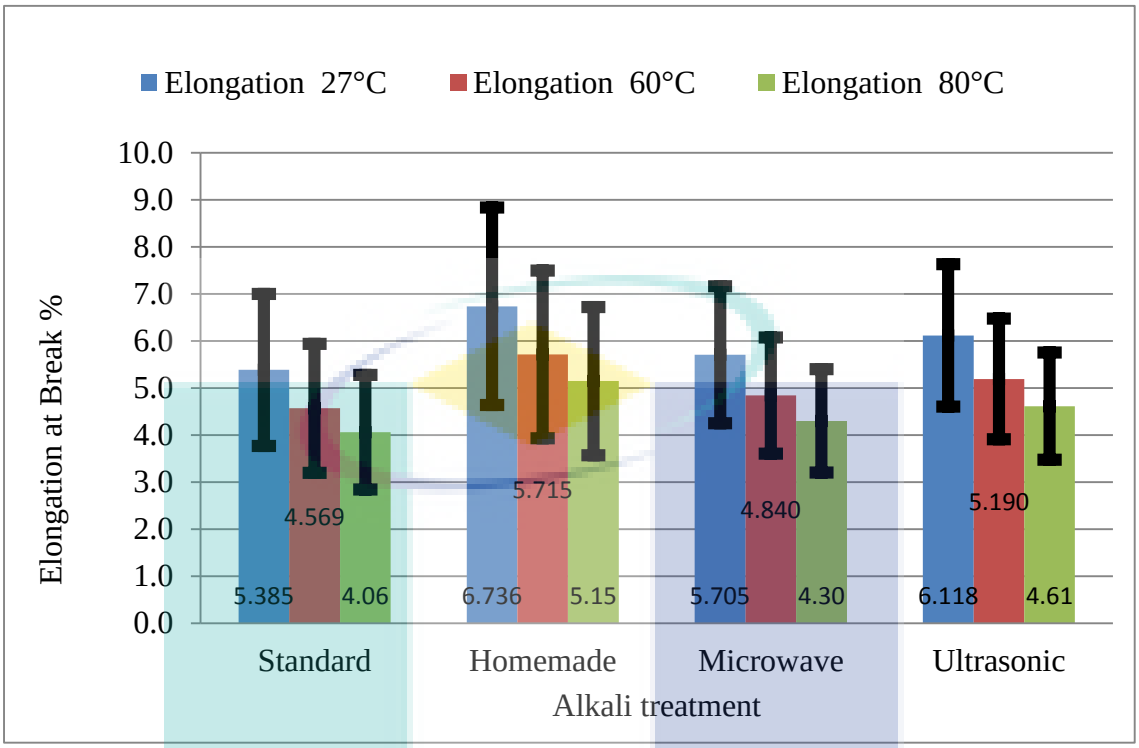

Figure 6.6: Elongation of plain water hygrothermal ageing hybrid composites

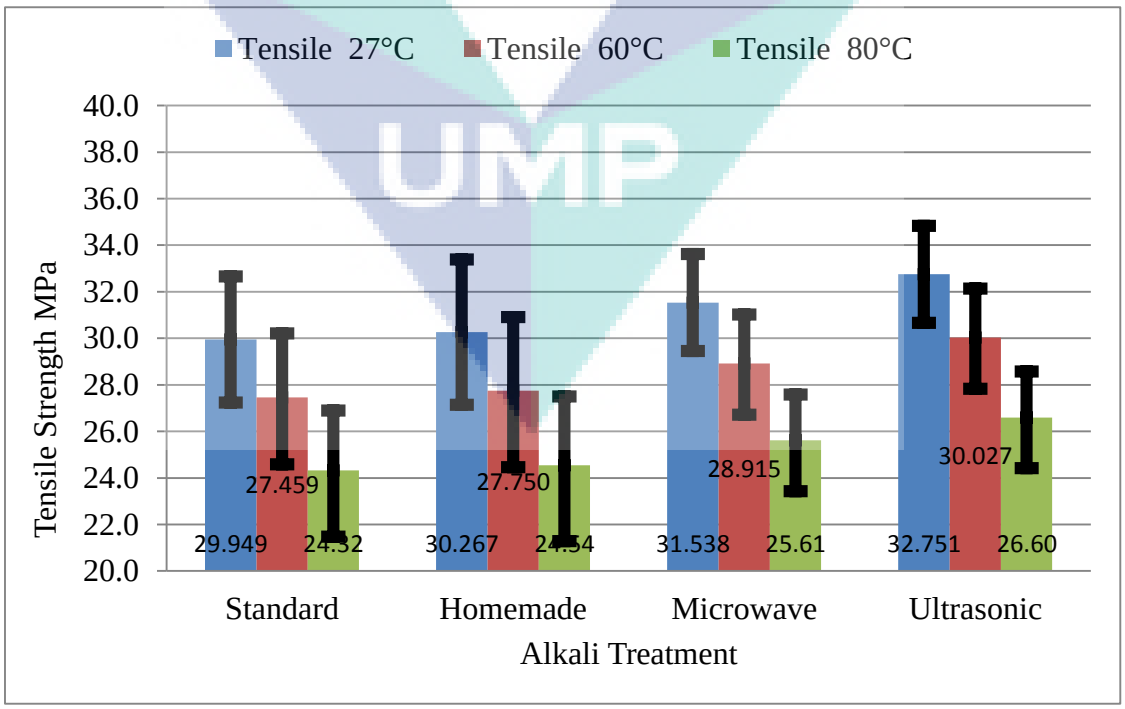

Figure 6.7: Tensile strength of sea water hygrothermal ageing hybrid composites

Examination of the properties degradation of the composites under submerged sea water was carryout, during 2 months of hygrothermal ageing; each specimen was soaking in the 27, 60 and 80ºC of the sea water and following by mechanical and water absorption testing. Figure 6.7 to Figure 6.9 explain the Tensile, modulus and elongation of the hybrid composites response. Ultrasonic hybrid composite showed higher mechanical properties following by microwave and homemade alkali treatment, TS and YM were found to decrease for sea water hygrothermal ageing due to fibre damage and damage of fibre-matrix interface bonding.

High EFB lignin removal was provided by ultrasonic and microwave treatments lead to better properties stability under sea water submerged condition. Figure 6.7 to Figure 6.9 also showed overall of the RPHC have acceptable properties during 80ºC seawater application tests that means the material are suitable for worm submerged marine application.

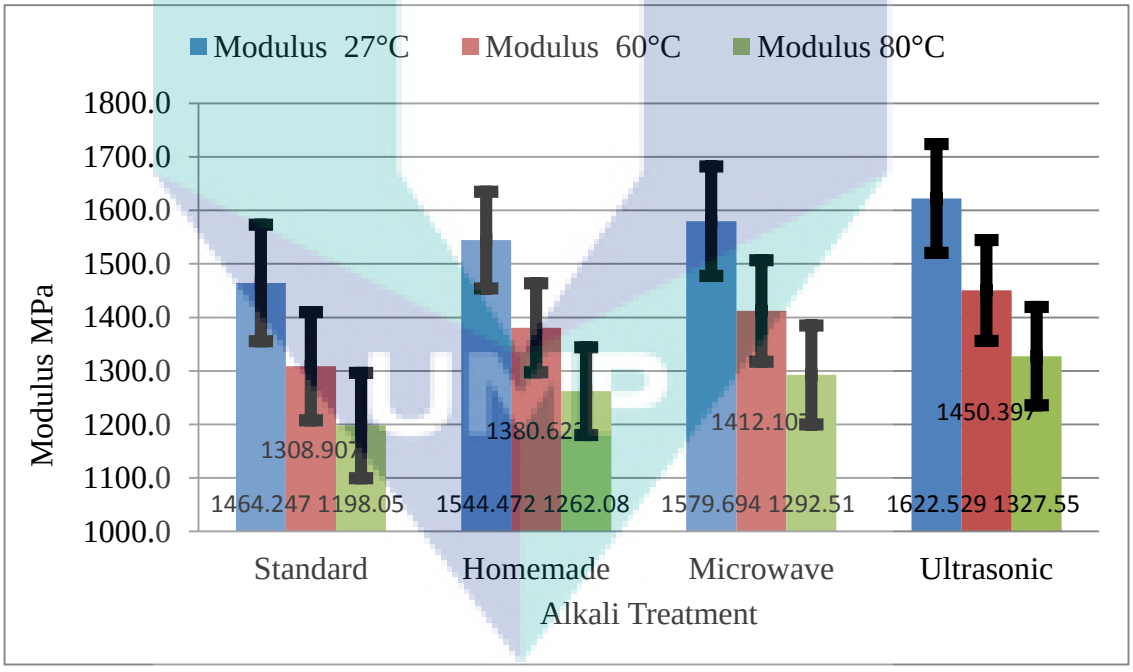

Figure 6.8: Modulus of sea water hygrothermal ageing hybrid composites

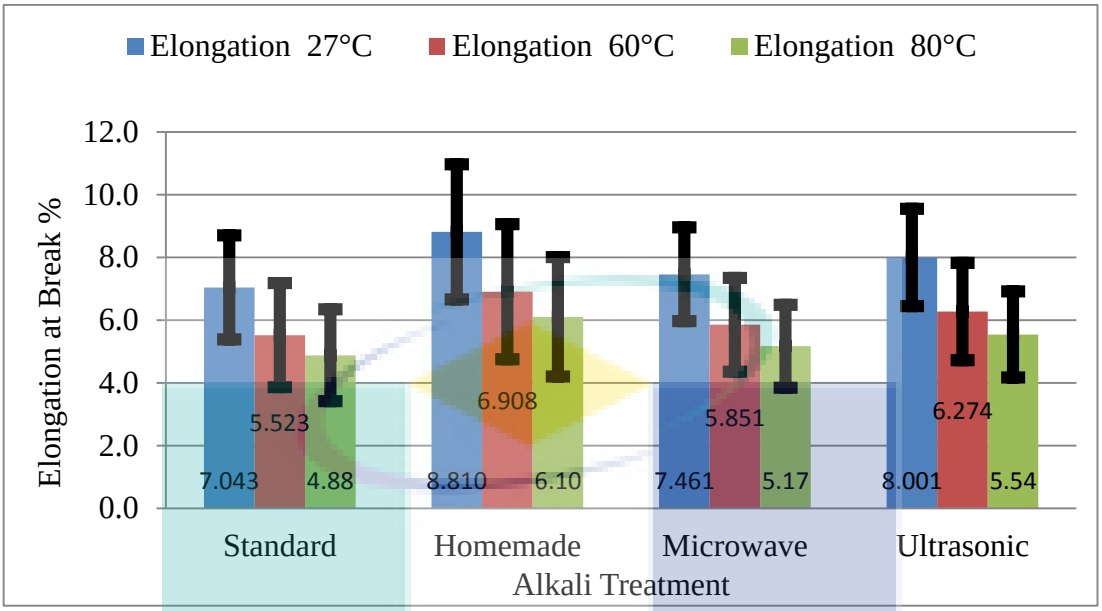

Figure 6.9: Elongation of sea water hygrothermal ageing hybrid composites

6.3 COMPARISON OF WATER ABSORPTION COMPOSITES

Water absorptions testing were carryout to examine the hybrid composites properties under elevated fresh water conditions. Hygrothermal testing devices were fixed at the temperature 27, 60 and 80°C for 2 month period. Each water absorption responses were explained in the Figure 6.10, Conventional alkali treatment provide high water absorption however homemade, ultrasonic and microwave treatment provide lower water absorption, it could be due to better lignin removal by ultrasonic alkali treatment, better fibre-matrix bonding and additional Fusabond coupling agent.The rate of moisture absorption increased with increase in hygrothermal temperature setting, high temperature operation lead to water penetration in the fiber and fibre- matrix interface.

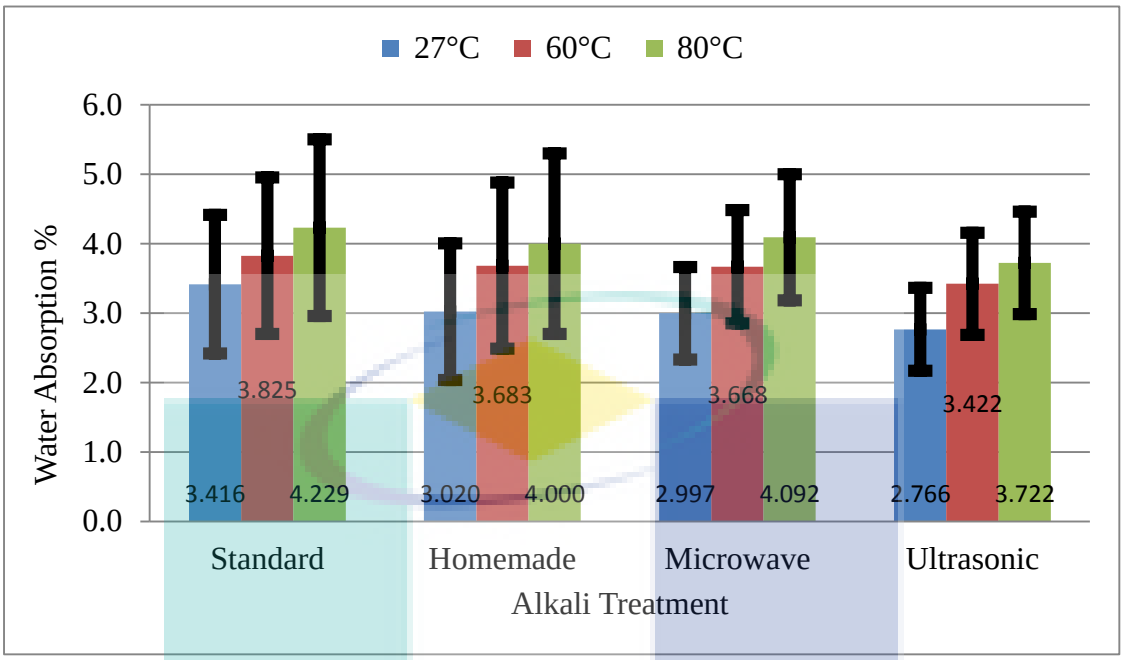

Figure 6.10: Plain water absorbtion of hybrid composites

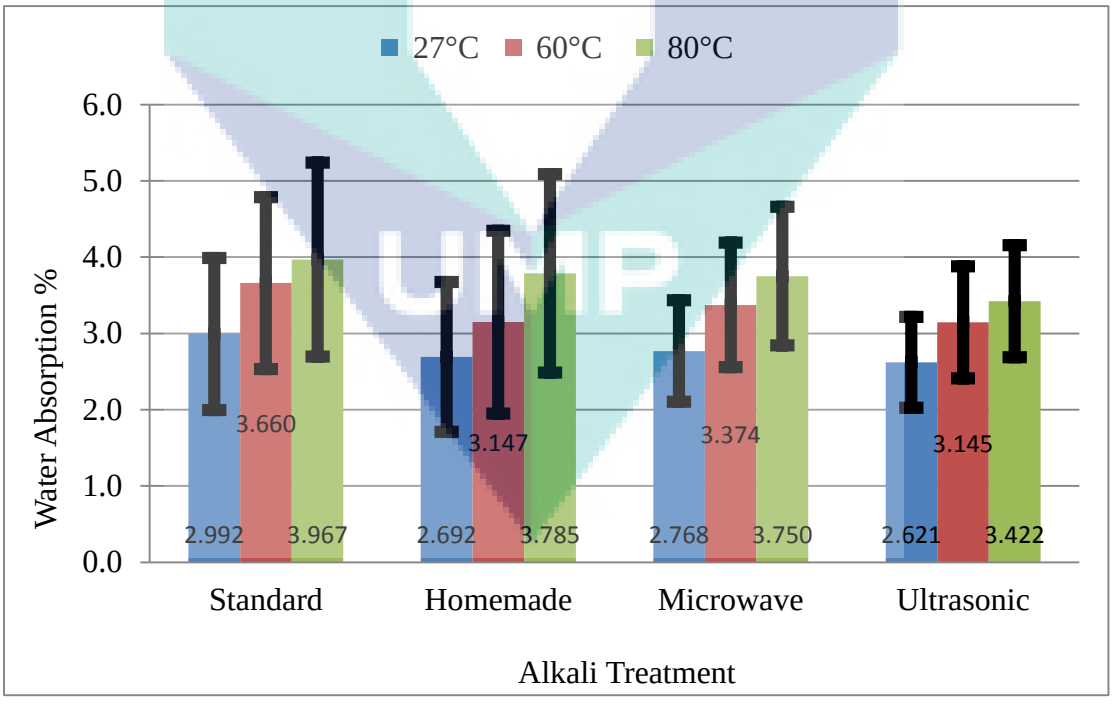

Figure 6.11: Sea water absorbtion of hybrid composites

Sea water absorptions testing were carryout to examine the hybrid composites properties under marine conditions. Hygrothermal testing devices were fixed in the temperature 27, 60 and 80^{o}C for 2 month period. Each sea water absorption responses were explained in the Figure 6.11. Conventional alkali treatment provide high water absorption however homemade, ultrasonic and microwave treatment provide low water absorption, it could be due to better fibre-matrix bonding and the actual contact area between EFB fibers and matrix become smaller. Better lignin removal, additional Fusabond coupling agent and compounding times also decrease of composites water absorption significantly. Increase in sea water hygrothermal temperature lead to degradation of fibe and fibre-matric interface, fibre swelling and composite cracking.

6.4 MELT FLOW INDEX COMPOSITES

Melt flow index testing were provide information of the ability of hybrid composites flowing in the moulding especially for small and complex shape, overall conventional, homemade and microwave alkali treatment have similar result at around 2.8 gram/10 minutes. However ultrasonic alkali treatments provide better MFI at around 3 gram/10 minutes, it could be due to flexibility of the ultrasonic EFB treatment and compounding times that lead to high composite homogeneity and fibre-matrix bounding. Compounding time and rotation speed cause fibre uniformly dispersed in the composites and fibre become more oriented (Teng et al., 2008), the Slender and flexibility of palm oil fibre in the hybrid composites increase (Feng et al., 2013) another reason are the actual contact area between EFB fibers and matrix become smaller and the viscosity of the composite slightly decrease.

Figure 6.12 explain that ultrasonic and home made alkali treatment profide better melt flow indexs it can be due Longger alkali treatment time can cause melt flow indexs increase. Longger alkali treatment and ultrasonic alkali treatment caused EFB fibre Shear rate and flexibility increase and deformed easily (S. K. Nayak, Mohanty, and Samal,

2009)(Feng et al., 2013) explain that the larger contact area between fibers and matrix

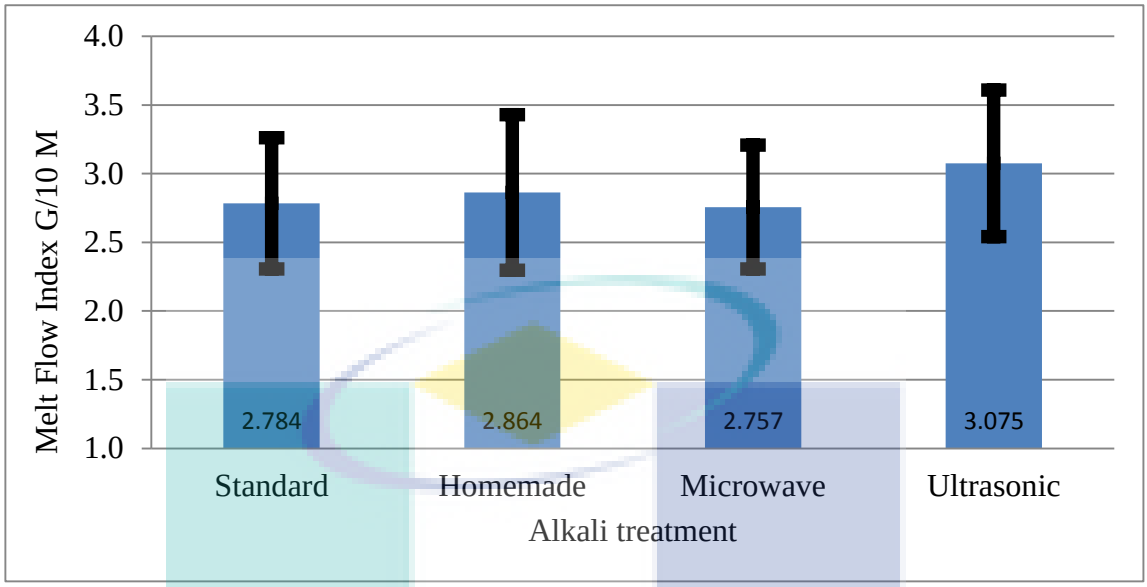

and increased in consistency index, the more difficult for the matrix to flow.

Figure 6.12: Melt Flow Index G/10 MIN

CHAPTER 7.

CONCLUSION AND RECOMENDATIONS

CONCLUSION

EFB Alkali treatment's techniques were identified as one of the important factors that influence the hybrid composites' properties. The ultrasonic-assisted alkali treatment method exhibited a higher tensile, and modulus compared to the other methods. It was followed by microwave, homemade and conventional-assisted alkali treatment. It could be due better lignin removal provide by ultrasonic treatment.

EFB and glass fibre applied to recycled PP had a significant effect on the composite mechanical properties. Moreover, adding MAPP and Fusabond coupling agent treated fibres increased composite tensile elongation and flexural strengths. Tensile testing and SEM study confirmed that glass fibre-recycled PP with the MAPP coupling agent has low interfacial adhesion; improvement was done by adding the Fusabond coupling agents to increase fibre-matrix bounding and composite's properties. Mechanical properties increased on addition Fusabond-MAPP mix -coupling agent in hybrid composites, which was related to improved interface bonding between the EFB-Glass fibre and the recycled matrix. Furthermore water absorption, and composite's degradation doe hygrothermal ageing and accelerated weathering treatment was also decreased.

The effect of water ageing on mechanical properties has been investigated for recycled PP hybrid composites and EFB-Glass fibre with addition MAPP and Fusabond coupling agent, the result showed that the composites have tensile, modulus and elongation stability in 27, 60 and 80^{o}C water and seawater. Furthermore, high EFB ratio led to increase composites properties degradation and the higher temperature during hygrothermal ageing not only increases the moisture uptake rate, but it may also modify the mechanical properties.

One year composite's natural accelerated weathering and 1200 accelerated weathering test result showed that the composites are suitable not only for outdoor environment but also marine application. Comparative study of water and sea water absorption on the mechanical properties of hybrid composites has been studied at the different temperatures. It slightly drops in strength and modulus due to the weakening of the interface between fibre, and matrix occurred. The water absorption pattern is found to follow EFB content fibre treatment and coupling agent.

In this investigation, the requirement complex optimum conditions were determined and the optimum performance under these conditions was predicted based on the analysis carried out by the RSM. Optimal conditions and result response's predictions were identified in each alkali treatment.it was also found that compounding times of fibre reinforced polypropylene composite had increased the mechanical properties and composites stability in accelerated weathering and hygrothermal ageing of all the composites tested, due to the better composite mixing and fibre-matrix surface adhesion. The thermal stabilities of hybrid composites were also analysed by TGA and DSC, and it was found that high EFB fibre ratio was less thermally stable than the low fibre ratio.

RECOMMENDATIONS

Recommendations are made to suggest for future work, which could be performed to give better understanding and improvement on the EFB alkali treatment process and hybrid composites' formulations.

Below are some of the recommendations for future work in the EFB-Glass fibre recycled polypropylene productions.

The influence of ultrasonic frequency and intensity on ultrasonic fibre treatment performance is suggested to be studied. Higher ultrasound frequencies produce smaller cavitation bubbles. The change in the cavitation activities is expected to influence the overall performance of the lignin removal process. In another aspect, ultrasonic intensity is expected to influence the degree of alkali treatment quality during treatment, which will directly affect the composites' properties.

Developing of controllable microwave alkali treatment for natural fibre treatments was done (See Appendix F) however; design and improvement for longer alkali treatment, low chemical needed and robust magnetron capacity should be developed to produce better lignin treatment's efficiency.

Homemade-assisted mercerifications were conducted to provide low chemical, low cost fibre treatment and to prepare and examine of a pilot scale commercial production. Alkali Chemical needed was already reduced. Low cost equipment were developed but the design of the automatic advance alkali treatment system that provide all the treatment processes, including washing and drying fibre not yet done.

Black liquor as a bad side or waste product from fibre alkali treatment also the main concern in this research even though ultrasonic, microwave and homemade treatment already decrease chemical waste produced than conventional method, Totally chemical-free fibre treatments were also studied.

REFERENCES

Abdelmouleh, M., Boufi, S., Belgacem, M. N., and Dufresne, A. (2007). Short natural-fibre reinforced polyethylene and natural rubber composites: Effect of silane coupling agents and fibres loading. *Composites Science and Technology, 67*(7â8), 1627-1639.

Abdul Khalil, H. P. S., Hanida, S., Kang, C. W., and Nik Fuaad, N. A. (2007). Agro-hybrid composite: The effects on mechanical and physical properties of oil palm fiber (EFB)/glass hybrid reinforced polyester composites. *Journal of Reinforced Plastics and Composites, 26*(2), 203-218.

Agrawal, Richa, Saxena, N. S., Sharma, K. B., Thomas, S., and Sreekala, M. S. (2000). Activation energy and crystallization kinetics of untreated and treated oil palm fibre reinforced phenol formaldehyde composites. *Materials Science and Engineering: A, 277*(1â2), 77-82.

Ahmad, E. E. M., and Luyt, A. S. (2012). Effects of organic peroxide and polymer chain structure on morphology and thermal properties of sisal fibre reinforced polyethylene composites. *Composites Part A: Applied Science and Manufacturing, 43*(4), 703-710. doi: 10.1016/j.compositesa.2011.12.011

Akers, S. A. S., and Studinka, J. B. (1989). Ageing behaviour of cellulose fibre cement composites in natural weathering and accelerated tests. *International Journal of Cement Composites and Lightweight Concrete, 11*(2), 93-97.

Akil, Hazizan Md, Cheng, Leong Wei, Mohd Ishak, Z. A., Abu Bakar, A., and Abd Rahman, M. A. (2009). Water absorption study on pultruded jute fibre reinforced unsaturated polyester composites. *Composites Science and Technology, 69*(11â12), 1942-1948.

Al-Madfa, H., Mohamed, Z., and Kassem, M. E. (1998). Weather ageing characterization of the mechanical properties of the low density polyethylene. *Polymer Degradation and Stability, 62*(1), 105-109. doi: 10.1016/S0141-3910(97)00266-8

Alix, S., Lebrun, L., Morvan, C., and Marais, S. (2010). Study of water behaviour of chemically treated flax fibres-based composites: A way to approach the hydric interface. *Composites Science and Technology, 71*(6), 893-899.

Alsaeed, T., Yousif, B. F., and Ku, H. (2013). The potential of using date palm fibres as reinforcement for polymeric composites. *Materials & Design, 43*(0), 177-184. doi: 10.1016/j.matdes.2012.06.061

Arbelaiz, A., Fernandez, B., Cantero, G., Llano-Ponte, R., Valea, A., and Mondragon, I. (2005). Mechanical properties of flax fibre/polypropylene composites. Influence of fibre/matrix modification and glass fibre hybridization. *Composites Part A: Applied Science and Manufacturing, 36*(12), 1637-1644.

Arbelaiz, A., Fernández, B., Ramos, J. A., Retegi, A., Llano-Ponte, R., and Mondragon, I. (2005). Mechanical properties of short flax fibre bundle/polypropylene composites: Influence of matrix/fibre modification, fibre content, water uptake and recycling. *Composites Science and Technology, 65*(10), 1582-1592.

ASM-International, ASM. (2003). Characterization and failure analysis of plastics. *USA: ASM*

International: The Materials Information Society.

Assarar, M., Scida, D., El Mahi, A., PoilÃ¢ne, C., and Ayad, R. (2010). Influence of water ageing on mechanical properties and damage events of two reinforced composite materials: Flaxâ€“fibres and glassâ€“fibres. *Materials & Design, 32*(2), 788-795.

Asumani, O. M. L., Reid, R. G., and Paskaramoorthy, R. (2012). The effects of alkali–silane treatment on the tensile and flexural properties of short fibre non-woven kenaf reinforced polypropylene composites. *Composites Part A: Applied Science and Manufacturing, 43*(9), 1431-1440. doi: 10.1016/j.compositesa.2012.04.007

Ayrilmis, Nadir, Jarusombuti, Songklod, Fueangvivat, Vallayuth, Bauchongkol, Piyawade, and White, Robert. (2011). Coir fiber reinforced polypropylene composite panel for automotive interior applications. *Fibers and Polymers, 12*(7), 919-926. doi: 10.1007/s12221-011-0919-1

B.C, Ray. (2006). Temperature effect during humid ageing on interfaces of glass and carbon fibers reinforced epoxy composites. *Journal of Colloid and Interface Science, 298*(1), 111-117.

Barone, Justin R., Schmidt, Walter F., and Liebner, Christina F. E. (2005). Compounding and molding of polyethylene composites reinforced with keratin feather fiber. *Composites Science and Technology, 65*(3â€“4), 683-692.

Beckermann, G. W., and Pickering, K. L. (2008). Engineering and evaluation of hemp fibre reinforced polypropylene composites: Fibre treatment and matrix modification. *Composites Part A: Applied Science and Manufacturing, 39*(6), 979-988.

Beckermann, G. W., and Pickering, K. L. (2009). Engineering and evaluation of hemp fibre reinforced polypropylene composites: Micro-mechanics and strength prediction modelling. *Composites Part A: Applied Science and Manufacturing, 40*(2), 210-217.

Beg, M. D. H., and Pickering, K. L. (2008a). Accelerated weathering of unbleached and bleached Kraft wood fibre reinforced polypropylene composites. *Polymer Degradation and Stability, 93*(10), 1939-1946.

Beg, M. D. H., and Pickering, K. L. (2008b). Mechanical performance of Kraft fibre reinforced polypropylene composites: Influence of fibre length, fibre beating and hygrothermal ageing. *Composites Part A: Applied Science and Manufacturing, 39*(11), 1748-1755.

Beg, M. D. H., and Pickering, K. L. (2008c). Reprocessing of wood fibre reinforced polypropylene composites. Part II: Hygrothermal ageing and its effects. *Composites Part A: Applied Science and Manufacturing, 39*(9), 1565-1571.

Beier, Uwe, Wolff-Fabris, Felipe, Fischer, Frank, Sandler, Jan K. W., Altstädt, Volker, Hülder, Gerrit, . . . Buchs, Wolfgang. (2008). Mechanical performance of carbon fibre-reinforced composites based on preforms stitched with innovative low-melting temperature and matrix soluble thermoplastic yarns. *Composites Part A: Applied Science and Manufacturing, 39*(9), 1572-1581. doi: http://dx.doi.org/10.1016/j.compositesa.2008.06.003

Bergeret, A., Ferry, L., and Ienny, P. (2009). Influence of the fibre/matrix interface on ageing mechanisms of glass fibre reinforced thermoplastic composites (PA-6,6, PET, PBT) in a hygrothermal environment. *Polymer Degradation and Stability, 94*(9), 1315-1324.

Bicerano, J. (1996). Prediction of polymer properties. *2 nd ed. New York: Marcel Dekker,Inc.*

Bledzki, Andrzej K., Mamun, Abdullah A., Jaszkiewicz, Adam, and Erdmann, Karsten. (2009). Polypropylene composites with enzyme modified abaca fibre. *Composites Science and Technology, 70*(5), 854-860.

Bourry, D., and Favis, B. D. (1998). Morphology development in a polyethylene/polystyrene binary blend during twin-screw extrusion. *Polymer, 39*(10), 1851-1856. doi: http://dx.doi.org/10.1016/S0032-3861(97)00397-2

Busico, Vincenzo, and Cipullo, Roberta. (2001). Microstructure of polypropylene. *Progress in Polymer Science, 26*(3), 443-533. doi: http://dx.doi.org/10.1016/S0079-6700(00)00046-0

Cervenka, A. J., Young, R. J., and Kueseng, K. (2005). Micromechanical phenomena during hygrothermal ageing of model composites investigated by Raman spectroscopy. Part II: comparison of the behaviour of PBO and M5 fibres compared with Twaron. *Composites Part A: Applied Science and Manufacturing, 36*(7), 1020-1026.

Colom, X., Carrasco, F., Pagès, P., and Cañavate, J. (2003). Effects of different treatments on the interface of HDPE/lignocellulosic fiber composites. *Composites Science and Technology, 63*(2), 161-169.

Demir, H., Atikler, U., Balköse, D., and TihmInlIoglu, F. (2006). The effect of fiber surface treatments on the tensile and water sorption properties of polypropylene-luffa fiber composites. *Composites Part A: Applied Science and Manufacturing, 37*(3), 447-456.

Dhakal, H. N., Zhang, Z. Y., and Richardson, M. O. W. (2007). Effect of water absorption on the mechanical properties of hemp fibre reinforced unsaturated polyester composites. *Composites Science and Technology, 67*(7â€“8), 1674-1683.

Errajhi, O. A. Z., Osborne, J. R. F., Richardson, M. O. W., and Dhakal, H. N. (2005). Water absorption characteristics of aluminised E-glass fibre reinforced unsaturated polyester composites. *Composite Structures, 71*(3–4), 333-336. doi: http://dx.doi.org/10.1016/j.compstruct.2005.09.008

Espert, Ana, Vilaplana, Francisco, and Karlsson, Sigbritt. (2004). Comparison of water absorption in natural cellulosic fibres from wood and one-year crops in polypropylene composites and its influence on their mechanical properties. *Composites Part A: Applied Science and Manufacturing, 35*(11), 1267-1276.

Feng, Yan-Hong, Li, Yi-Jie, Xu, Bai-Ping, Zhang, Da-Wei, Qu, Jin-Ping, and He, He-Zhi. (2013). Effect of fiber morphology on rheological properties of plant fiber reinforced poly(butylene succinate) composites. *Composites Part B: Engineering, 44*(1), 193-199. doi: 10.1016/j.compositesb.2012.05.051

Foulc, M. P., Bergeret, A., Ferry, L., Ienny, P., and Crespy, A. (2005). Study of hygrothermal ageing of glass fibre reinforced PET composites. *Polymer Degradation and Stability, 89*(3), 461-470.

Fu, Shanju, Wu, Pingping, and Han, Zhewen. (2002). Tensile strength and rupture energy of hybrid poly(methylvinylsiloxane) composites reinforced with short PET fibers and wollastonite whiskers. *Composites Science and Technology, 62*(1), 3-8.

Gellert, E. P., and Turley, D. M. (1999). Seawater immersion ageing of glass-fibre reinforced polymer laminates for marine applications. *Composites Part A: Applied Science and Manufacturing, 30*(11), 1259-1265.

George, Jayamol, Bhagawan, S. S., and Thomas, Sabu. (1997). Effects of environment on the properties of low-density polyethylene composites reinforced with pineapple-leaf fibre. *Composites Science and Technology, 58*(9), 1471-1485.

Harnnecker, Fernanda, dos Santos Rosa, Derval, and Lenz, Denise. (2011). Biodegradable Polyester-Based Blend Reinforced with Curauá Fiber: Thermal, Mechanical and Biodegradation Behaviour. *Journal of Polymers and the Environment, 20*(1), 237-244. doi: 10.1007/s10924-011-0382-5

Huang, Yanling, and Young, Robert J. (1996). Interfacial micromechanics in thermoplastic and thermosetting matrix carbon fibre composites. *Composites Part A: Applied Science and Manufacturing, 27*(10), 973-980. doi: http://dx.doi.org/10.1016/1359-835X(96)00060-7

Hung, Ke-Chang, Chen, Yong-Long, and Wu, Jyh-Horng. (2012). Natural weathering properties of acetylated bamboo plastic composites. *Polymer Degradation and Stability, 97*(9), 1680-1685. doi: http://dx.doi.org/10.1016/j.polymdegradstab.2012.06.016

Islam, M. S., Pickering, K. L., and Foreman, N. J. (2009). Influence of accelerated ageing on the physico-mechanical properties of alkali-treated industrial hemp fibre reinforced poly(lactic acid) (PLA) composites. *Polymer Degradation and Stability, 95*(1), 59-65.

Jacob, Maya, Varughese, K., and Thomas, Sabu. (2006). Dielectric characteristics of sisal–oil palm hybrid biofibre reinforced natural rubber biocomposites. *Journal of Materials Science, 41*(17), 5538-5547. doi: 10.1007/s10853-006-0298-y

Jawaid, M., Abdul Khalil, H. P. S., and Abu Bakar, A. (2010). Mechanical performance of oil palm empty fruit bunches/jute fibres reinforced epoxy hybrid composites. *Materials Science and Engineering: A, 527*(29â€“30), 7944-7949.

Joseph, Kuruvilla, Thomas, Sabu, and Pavithran, C. (1995). Effect of ageing on the physical and mechanical properties of sisal-fiber-reinforced polyethylene composites. *Composites Science and Technology, 53*(1), 99-110.

Joseph, Seena, Sreekala, M. S., Oommen, Z., Koshy, P., and Thomas, Sabu. (2002). A comparison of the mechanical properties of phenol formaldehyde composites reinforced with banana fibres and glass fibres. *Composites Science and Technology, 62*(14), 1857-1868.

Kalam, Anizah, Sahari, B. B., Khalid, Y. A., and Wong, S. V. (2005). Fatigue behaviour of oil palm fruit bunch fibre/epoxy and carbon fibre/epoxy composites. *Composite Structures, 71*(1), 34-44. doi: http://dx.doi.org/10.1016/j.compstruct.2004.09.034

Karlsson, J. O., Andersson, M., Berntsson, P., Chihani, T., and Gatenholm, P. (1998). Swelling behavior of stimuli-responsive cellulose fibers. *Polymer, 39*(16), 3589-3595. doi: http://dx.doi.org/10.1016/S0032-3861(97)10353-6

Khalil, H. P. S. A., Bhat, I. U. H., and Sartika, M. Y. (2010). Degradation, mechano-physical, and morphological properties of empty fruit bunch reinforced polyester composites. *BioResources, 5*(4), 2278-2296.

Kim, Seonghun, Park, Jang Min, Seo, Jeong-Woo, and Kim, Chul Ho. (2012). Sequential acid-/alkali-pretreatment of empty palm fruit bunch fiber. *Bioresource Technology, 109*(0), 229-233. doi: 10.1016/j.biortech.2012.01.036

Lee, Je Kyum, and Han, Chang Dae. (2000). Evolution of polymer blend morphology during compounding in a twin-screw extruder. *Polymer, 41*(5), 1799-1815. doi: http://dx.doi.org/10.1016/S0032-3861(99)00325-0

Lee, W. C., Yusof, S., Hamid, N. S. A., and Baharin, B. S. (2006). Optimizing conditions for hot water extraction of banana juice using response surface methodology (RSM). *Journal of Food Engineering, 75*(4), 473-479. doi: 10.1016/j.jfoodeng.2005.04.062

Leng, Y. (2008). Materials Characterization: Introduction to Microscopic and Spectroscopic Methods. Singapore:. *: John Wiley & Sons (Asia).*

Li, Yan, Mai, Yiu-Wing, and Ye, Lin. (2000). Sisal fibre and its composites: a review of recent developments. *Composites Science and Technology, 60*(11), 2037-2055.

Li, Yan, and Pickering, K. L. (2008). Hemp fibre reinforced composites using chelator and enzyme treatments. *Composites Science and Technology, 68*(15-16), 3293-3298.

Liu, Dagang, Song, Jianwei, Anderson, DebbieP, Chang, PeterR, and Hua, Yan. (2012). Bamboo fiber and its reinforced composites: structure and properties. *Cellulose, 19*(5), 1449-1480. doi: 10.1007/s10570-012-9741-1

López-Manchado, M. A., and Arroyo, M. (2000). Thermal and dynamic mechanical properties of polypropylene and short organic fiber composites. *Polymer, 41*(21), 7761-7767. doi: 10.1016/S0032-3861(00)00152-X

Lu, Jue, Askeland, Per, and Drzal, Lawrence T. (2008). Surface modification of microfibrillated cellulose for epoxy composite applications. *Polymer, 49*(5), 1285-1296. doi: http://dx.doi.org/10.1016/j.polymer.2008.01.028

Madsen, Bo, Thygesen, Anders, and Lilholt, Hans. (2009). Plant fibre composites - porosity and stiffness. *Composites Science and Technology, 69*(7-8), 1057-1069.

Mascia, L., and Zhang, J. (1995). Mechanical properties and thermal ageing of a perfluoroether-modified epoxy resin in castings and glass fibre composites. *Composites, 26*(5), 379-385.

Mohd Ishak, Z. A., Ariffin, A., and Senawi, R. (2001). Effects of hygrothermal aging and a silane coupling agent on the tensile properties of injection molded short glass fiber reinforced poly(butylene terephthalate) composites. *European Polymer Journal, 37*(8), 1635-1647.

Mohd Ishak, Z. A., Ishiaku, U. S., and Karger-Kocsis, J. (2000). Hygrothermal aging and fracture behavior of short-glass-fiber-reinforced rubber-toughened poly(butylene terephthalate) composites. *Composites Science and Technology, 60*(6), 803-815.

Mukhopadhyay, S., and Srikanta, R. (2008). Effect of ageing of sisal fibres on properties of sisal â€“ Polypropylene composites. *Polymer Degradation and Stability, 93*(11), 2048-2051.

Nayak, Sanjay. (2009). Degradation and flammability behavior of PP/ banana and glass fiber-based hybrid composites. *International Journal of Plastics Technology, 13*(1), 47-67. doi: 10.1007/s12588-009-0006-2

Nayak, Sanjay K., Mohanty, Smita, and Samal, Sushanta K. (2009). Influence of short bamboo/glass fiber on the thermal, dynamic mechanical and rheological properties of polypropylene hybrid composites. *Materials Science and Engineering: A, 523*(1–2), 32-38. doi: 10.1016/j.msea.2009.06.020

Ojeda, Telmo, Freitas, Ana, Birck, Kátia, Dalmolin, Emilene, Jacques, Rodrigo, Bento, Fátima, and Camargo, Flávio. (2011). Degradability of linear polyolefins under natural weathering. *Polymer Degradation and Stability, 96*(4), 703-707. doi: 10.1016/j.polymdegradstab.2010.12.004

Ota, W. N., Amico, S. C., and Satyanarayana, K. G. (2005). Studies on the combined effect of injection temperature and fiber content on the properties of polypropylene-glass fiber composites. *Composites Science and Technology, 65*(6), 873-881.

Padmanabhan, Babu. (2008). Understanding the Extruder Processing Zone: the heart of a twin screw extruder. *Plastics, Additives and Compounding, 10*(2), 30-35. doi: http://dx.doi.org/10.1016/S1464-391X(08)70058-8

Pantani, R., Coccorullo, I., Speranza, V., and Titomanlio, G. (2007). Morphology evolution during injection molding: Effect of packing pressure. *Polymer, 48*(9), 2778-2790. doi: http://dx.doi.org/10.1016/j.polymer.2007.03.007

Peacock, A.J. . (2000). Handbook of Polyethylene:Structures, Properties, and Applications. *New York: Marcel Dekker, Inc.*

Pegoretti, Alessandro, and Penati, Amabile. (2004). Effects of hygrothermal aging on the molar mass and thermal properties of recycled poly(ethylene terephthalate) and its short glass fibre composites. *Polymer Degradation and Stability, 86*(2), 233-243.

Pejic, Biljana M., Kostic, Mirjana M., Skundric, Petar D., and Praskalo, Jovana Z. (2008). The effects of hemicelluloses and lignin removal on water uptake behavior of hemp fibers. *Bioresource Technology, 99*(15), 7152-7159. doi: http://dx.doi.org/10.1016/j.biortech.2007.12.073

Peng, Xinwen, Zhong, Linxin, Ren, Junli, and Sun, Runcang. (2010). Laccase and alkali treatments of cellulose fibre: Surface lignin and its influences on fibre surface

properties and interfacial behaviour of sisal fibre/phenolic resin composites. *Composites Part A: Applied Science and Manufacturing, 41*(12), 1848-1856. doi: http://dx.doi.org/10.1016/j.compositesa.2010.09.004

Plonka, R., MÃ¤der, E., Gao, S. L., Bellmann, C., Dutschk, V., and Zhandarov, S. (2004). Adhesion of epoxy/glass fibre composites influenced by aging effects on sizings. *Composites Part A: Applied Science and Manufacturing, 35*(10), 1207-1216.

Rauwendaal, Chris. (2002). New directions for extrusion: compounding with single screw extruders. *Plastics, Additives and Compounding, 4*(6), 24-27. doi: http://dx.doi.org/10.1016/S1464-391X(02)80090-3

Reid, R. G., I'Ons, T. A., and Paskaramoorthy, R. (2004). The mechanical properties of oxyfluorinated hybrids of glass fibre and polypropylene fibre. *Composite Structures,66*(1–4),611-616.doi: http://dx.doi.org/10.1016/j.compstruct.2004.05.009

Roy, Aparna, Chakraborty, Sumit, Kundu, Sarada Prasad, Basak, Ratan Kumar, Basu Majumder, Subhasish, and Adhikari, Basudam. (2012). Improvement in mechanical properties of jute fibres through mild alkali treatment as demonstrated by utilisation of the Weibull distribution model. *Bioresource Technology,107*(0),222-228.doi: http://dx.doi.org/10.1016/j.biortech.2011.11.073

Saujanya, C., and Radhakrishnan, S. (2001). Structure development and properties of PET fibre filled PP composites. *Polymer, 42*(10), 4537-4548. doi: 10.1016/S0032-3861(00)00860-0

Seki, Yoldaş. (2009). Innovative multifunctional siloxane treatment of jute fiber surface and its effect on the mechanical properties of jute/thermoset composites. *Materials Science and Engineering: A, 508*(1–2), 247-252. doi: 10.1016/j.msea.2009.01.043

Selmy, A. I., Elsesi, A. R., Azab, N. A., and Abd El-baky, M. A. (2012). Interlaminar shear behavior of unidirectional glass fiber (U)/random glass fiber (R)/epoxy hybrid and non-hybrid composite laminates. *Composites Part B: Engineering, 43*(4), 1714-1719. doi: 10.1016/j.compositesb.2012.01.031

Selzer, R., and Friedrich, K. (1997). Mechanical properties and failure behaviour of carbon fibre-reinforced polymer composites under the influence of moisture. *Composites Part A: Applied Science and Manufacturing, 28*(6), 595-604.

Shanmugam, D., and Thiruchitrambalam, M. (2013). Static and dynamic mechanical properties of alkali treated unidirectional continuous Palmyra Palm Leaf Stalk Fiber/jute fiber reinforced hybrid polyester composites. *Materials & Design, 50*(0), 533-542. doi: http://dx.doi.org/10.1016/j.matdes.2013.03.048

Shinoj, S., Visvanathan, R., Panigrahi, S., and Kochubabu, M. Oil palm fiber (OPF) and its composites: A review. *Industrial Crops and Products, 33*(1), 7-22.

Shinoj, S., Visvanathan, R., Panigrahi, S., and Kochubabu, M. (2009). Oil palm fiber (OPF) and its composites: A review. *Industrial Crops and Products, 33*(1), 7-22.

Singh, B., Gupta, M., and Verma, Anchal. (2000). The durability of jute fibre-reinforced phenolic composites. *Composites Science and Technology, 60*(4), 581-589.

Singh, Baljit, and Sharma, Nisha. (2008). Mechanistic implications of plastic degradation. *Polymer Degradation and Stability, 93*(3), 561-584. doi: 10.1016/j.polymdegradstab.2007.11.008

Sobczak, Lukas, Lang, Reinhold W., and Haider, Andreas. (2012). Polypropylene composites with natural fibers and wood – General mechanical property profiles. *Composites Science and Technology, 72*(5), 550-557. doi: 10.1016/j.compscitech.2011.12.013

Sreekala, M. S., George, J., Kumaran, M. G., and Thomas, S. (2002). The mechanical performance of hybrid phenol-formaldehyde-based composites reinforced with glass and oil palm fibres. *Composites Science and Technology, 62*(3), 339-353.

Sreekala, M. S., Kumaran, M. G., Joseph, Reethamma, and Thomas, Sabu. (2001). Stress-relaxation behaviour in composites based on short oil-palm fibres and phenol formaldehyde resin. *Composites Science and Technology, 61*(9), 1175-1188. doi: http://dx.doi.org/10.1016/S0266-3538(00)00214-1

Sreekala, M. S., and Thomas, S. (2003). Effect of fibre surface modification on water-sorption characteristics of oil palm fibres. *Composites Science and Technology, 63*(6), 861-869.

Sreekumar, P. A., Thomas, Selvin P., Saiter, Jean marc, Joseph, Kuruvilla, Unnikrishnan, G., and Thomas, Sabu. (2009). Effect of fiber surface modification on the mechanical and water absorption characteristics of sisal/polyester composites

fabricated by resin transfer molding. *Composites Part A: Applied Science and Manufacturing, 40*(11), 1777-1784.

Stark, Nicole M., and Matuana, Laurent M. (2006). Influence of photostabilizers on wood flourâ€“HDPE composites exposed to xenon-arc radiation with and without water spray. *Polymer Degradation and Stability, 91*(12), 3048-3056.

Sun, Yongxu, Liu, Jicheng, and Kennedy, John F. (2010). Application of response surface methodology for optimization of polysaccharides production parameters from the roots of Codonopsis pilosula by a central composite design. *Carbohydrate Polymers, 80*(3), 949-953. doi: 10.1016/j.carbpol.2010.01.011

Tabtiang, A., and Venables, R. A. (2002). Compatibiliser activity and morphology stability during twin-screw extrusion and injection moulding of compatibilised blends. *Polymer, 43*(17), 4791-4801. doi: http://dx.doi.org/10.1016/S0032-3861(02)00289-6

Teng, Chih-Chun, Ma, Chen-Chi M., Huang, Yen-Wei, Yuen, Siu-Ming, Weng, Cheng-Chih, Chen, Cheng-Ho, and Su, Shun-Fua. (2008). Effect of MWCNT content on rheological and dynamic mechanical properties of multiwalled carbon nanotube/polypropylene composites. *Composites Part A: Applied Science and Manufacturing, 39*(12), 1869-1875. doi: 10.1016/j.compositesa.2008.09.004

Tjong, Sie Chin, Xu, Shi-Ai, Li, Robert Kwok-Yiu, and Mai, Yiu-Wing. (2002). Mechanical behavior and fracture toughness evaluation of maleic anhydride compatibilized short glass fiber/SEBS/polypropylene hybrid composites. *Composites Science and Technology, 62*(6), 831-840.

Torres, F. G., and Cubillas, M. L. (2005). Study of the interfacial properties of natural fibre reinforced polyethylene. *Polymer Testing, 24*(6), 694-698. doi: 10.1016/j.polymertesting.2005.05.004

Van de Weyenberg, I., Ivens, J., De Coster, A., Kino, B., Baetens, E., and Verpoest, I. (2003). Influence of processing and chemical treatment of flax fibres on their composites. *Composites Science and Technology, 63*(9), 1241-1246.

Vasile, Cornelia, and Pascu, Mihaela. (2005). Practical Guide to Polyethylene. *Rapra Technology Limited, Shawbury, Shrewsbury, Shropshire, SY4 4NR, UK.*

Vilay, V., Mariatti, M., Mat Taib, R., and Todo, Mitsugu. (2008). Effect of fiber surface treatment and fiber loading on the properties of bagasse fiber-reinforced

unsaturated polyester composites. *Composites Science and Technology, 68*(3-4), 631-638.

Wang, W., Sain, M., and Cooper, P. A. (2006). Study of moisture absorption in natural fiber plastic composites. *Composites Science and Technology, 66*(3-4), 379-386.

Xie, Yanjun, Hill, Callum A. S., Xiao, Zefang, Militz, Holger, and Mai, Carsten. (2010). Silane coupling agents used for natural fiber/polymer composites: A review. *Composites Part A: Applied Science and Manufacturing, 41*(7), 806-819. doi: 10.1016/j.compositesa.2010.03.005

Yao, Lan, Li, Wenbin, Wang, Nan, Li, Wang, Guo, Xu, and Qiu, Yiping. (2007). Tensile, impact and dielectric properties of three dimensional orthogonal aramid/glass fiber hybrid composites. *Journal of Materials Science, 42*(16), 6494-6500. doi: 10.1007/s10853-007-1534-9

Yin, Xiulian, You, Qinghong, and Jiang, Zhonghai. (2011). Optimization of enzyme assisted extraction of polysaccharides from Tricholoma matsutake by response surface methodology. *Carbohydrate Polymers, 86*(3), 1358-1364. doi: 10.1016/j.carbpol.2011.06.053

Yusoff, Nooryusmiza, Ramasamy, M., and Yusup, Suzana. (2011). Taguchi's parametric design approach for the selection of optimization variables in a refrigerated gas plant. *Chemical Engineering Research and Design, 89*(6), 665-675. doi: 10.1016/j.cherd.2010.09.021

Zheng, Yu-Tao, Cao, De-Rong, Wang, Dong-Shan, and Chen, Jiu-Ji. (2007). Study on the interface modification of bagasse fibre and the mechanical properties of its composite with PVC. *Composites Part A: Applied Science and Manufacturing, 38*(1), 20-25.

APPENDIX

APPENDIX A

LIST OF PUBLICATIONS

1. Oil Palm Empty Fruit Bunch and Glass Fibre Reinforced Recycled Polypropylene Composites.**International Conference On Chemical Innovation ICCI 2011.**23-24 May 2011,Terengganu, MALAYSIA. Makson Rivai, Arun Gupta and M.D.H.Beg.Faculty of Chemical and Natural Resources Engineering, University Malaysia Pahang,Gambang 26300, Kuantan, Malaysia

2. Oil Palm Bio-Fiber Reinforced Thermoplastic Composites-Effects of Matrix Modification on Mechanical and Thermal Properties.
   S.S. Suradi ; R.M. Yunus ; M.D.H. Beg ; M. Rivai ; Z.A.M. Yusof.
   Journal of applied science ISSN 18125654 (Online)

3. Optimisation of Manufacturing Process of Recycled Polypropylene Hybrid Composites Using Design Expert.
   ICCEIB -SOMChE 2011.UNIVERSITI MALAYSIA PAHANG, KUANTAN.28th November to 1st December 2011.Makson Rivai, Arun Gupta And M.D.H.Beg

APPENDIX B

CONVENTIONAL HYBRID COMPOSITES ANOVA

Table B. 1: Conventional tensile strength 0 AW ANOVA

Factor	Estimate	Coefficient DF	Standard Error	95% CI Low	95% CI High	VIF
Intercept	35.36	1.00	0.14	35.05	35.66	
A- Treatment Time	-0.01	1.00	0.07	-0.16	0.15	1.26
B-NaOH %	0.11	1.00	0.07	-0.04	0.27	1.24
C-Fibre Ratio %	2.90	1.00	0.08	2.73	3.06	1.21
A2	-1.95	1.00	0.11	-2.19	-1.71	1.03
B2	-2.81	1.00	0.12	-3.06	-2.56	1.08
C2	-0.13	1.00	0.12	-0.38	0.13	1.00
AB	-0.01	1.00	0.09	-0.20	0.19	1.26
AC	0.07	1.00	0.09	-0.14	0.27	1.21
BC	-0.12	1.00	0.09	-0.32	0.09	1.21

Table B. 2: Conventional modulus 0 AW ANOVA

Factor	Estimate	Coefficient DF	Standard Error	95% CI Low	95% CI High	VIF
Intercept	1840.16	1.00	17.62	1802.36	1877.95	
A- Treatment Time	71.32	1.00	8.91	52.21	90.43	1.26
B-NaOH %	9.01	1.00	8.86	-9.98	28.01	1.24
C-Fibre Ratio %	66.89	1.00	9.56	46.38	87.40	1.21
A2	-26.42	1.00	13.98	-56.41	3.57	1.03
B2	-139.48	1.00	14.30	-170.16	-108.80	1.08
C2	-108.05	1.00	14.60	-139.37	-76.73	1.00
AB	-6.75	1.00	11.31	-31.00	17.50	1.26
AC	18.36	1.00	11.74	-6.82	43.54	1.21
BC	11.57	1.00	11.72	-13.58	36.71	1.21

Table B. 3: Conventional elongation 0 AW ANOVA

Factor	Estimate	Coefficient DF	Standard Error	95% CI Low	95% CI High	VIF
Intercept	8.04	1.00	0.13	7.77	8.31	
A- Treatment Time	0.78	1.00	0.06	0.65	0.92	1.26
B-NaOH %	0.03	1.00	0.06	-0.11	0.17	1.24
C-Fibre Ratio %	-2.55	1.00	0.07	-2.70	-2.40	1.21
A2	0.04	1.00	0.10	-0.18	0.26	1.03
B2	-1.55	1.00	0.10	-1.77	-1.33	1.08
C2	0.01	1.00	0.11	-0.21	0.24	1.00
AB	-0.10	1.00	0.08	-0.27	0.08	1.26
AC	-0.08	1.00	0.09	-0.26	0.10	1.21
BC	0.09	1.00	0.09	-0.09	0.27	1.21

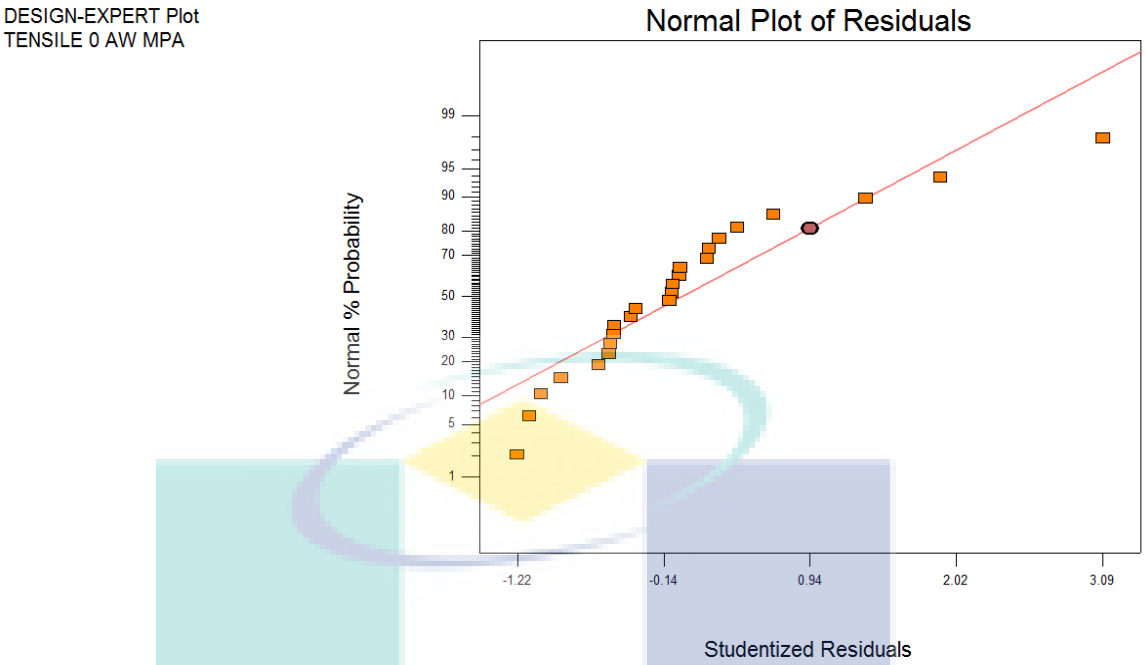

Figure B. 1: Normal probability plot of the residuals for tensile strength 0 AW

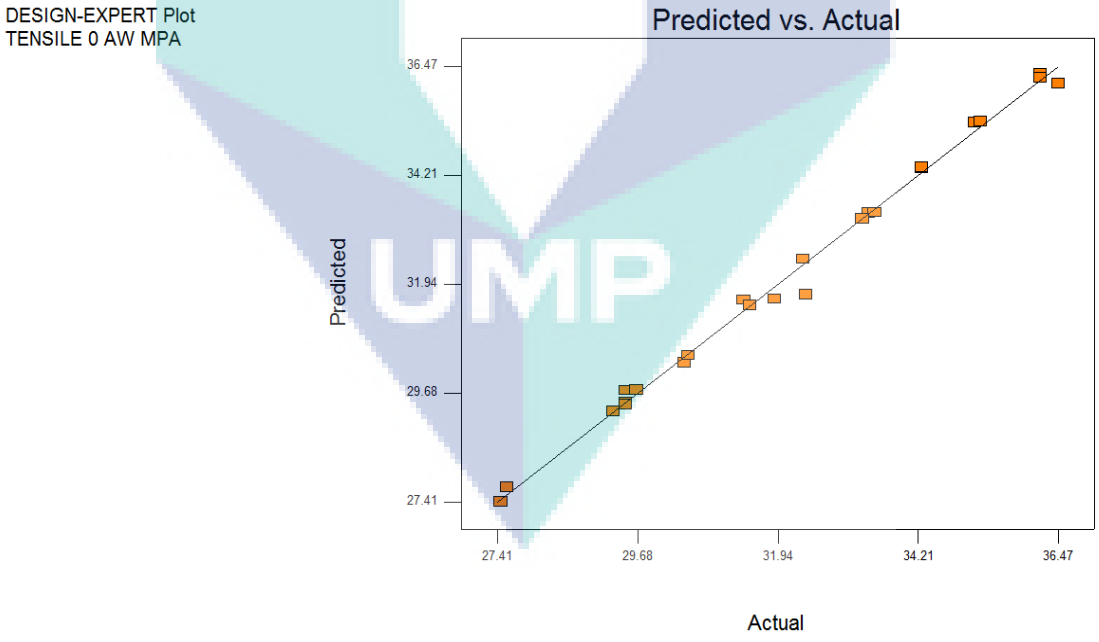

Figure B. 2: Predicted versus actual values for tensile strength 0 AW

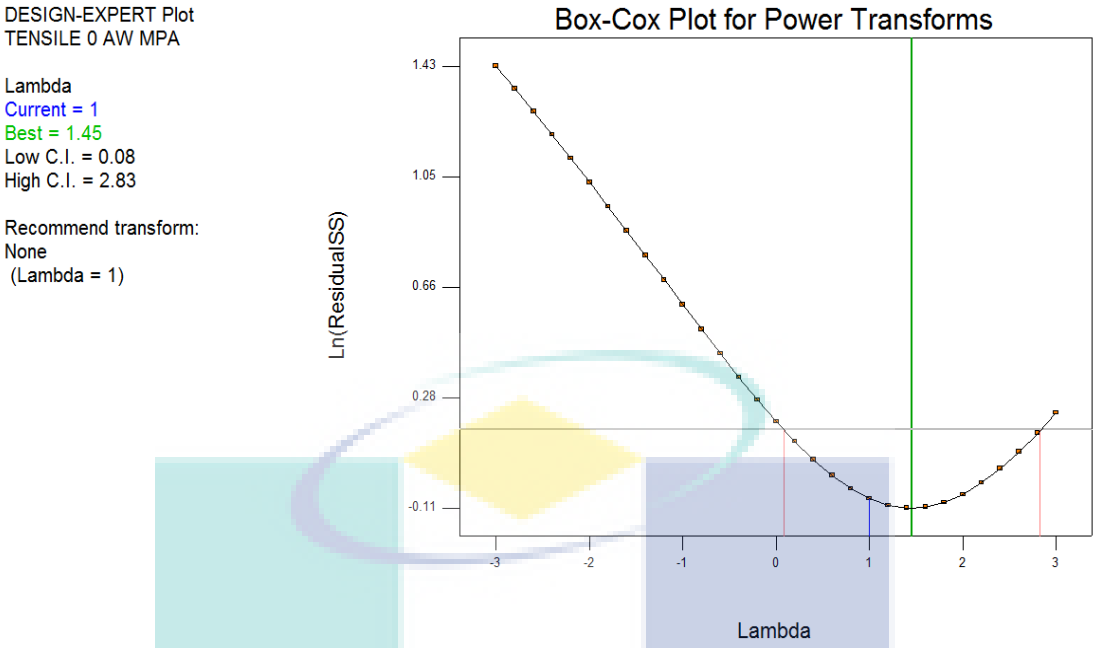

Figure B. 3: Box-Cox plot for tensile strength 0 AW

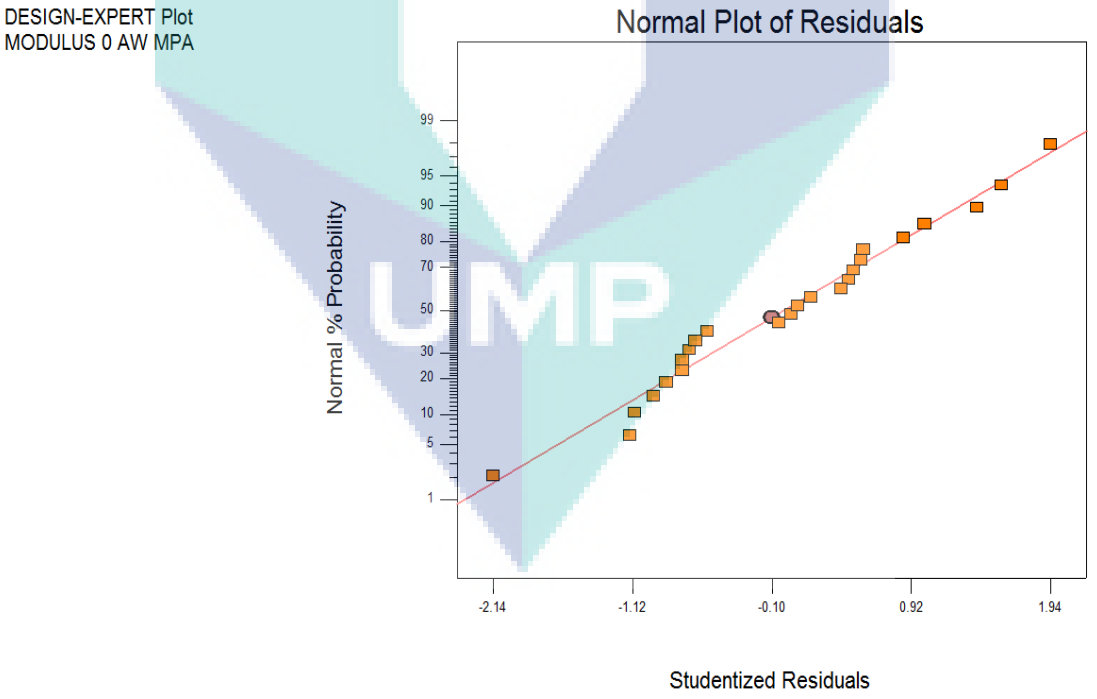

Figure B. 4: Normal probability plot of the residuals for modulus 0 AW

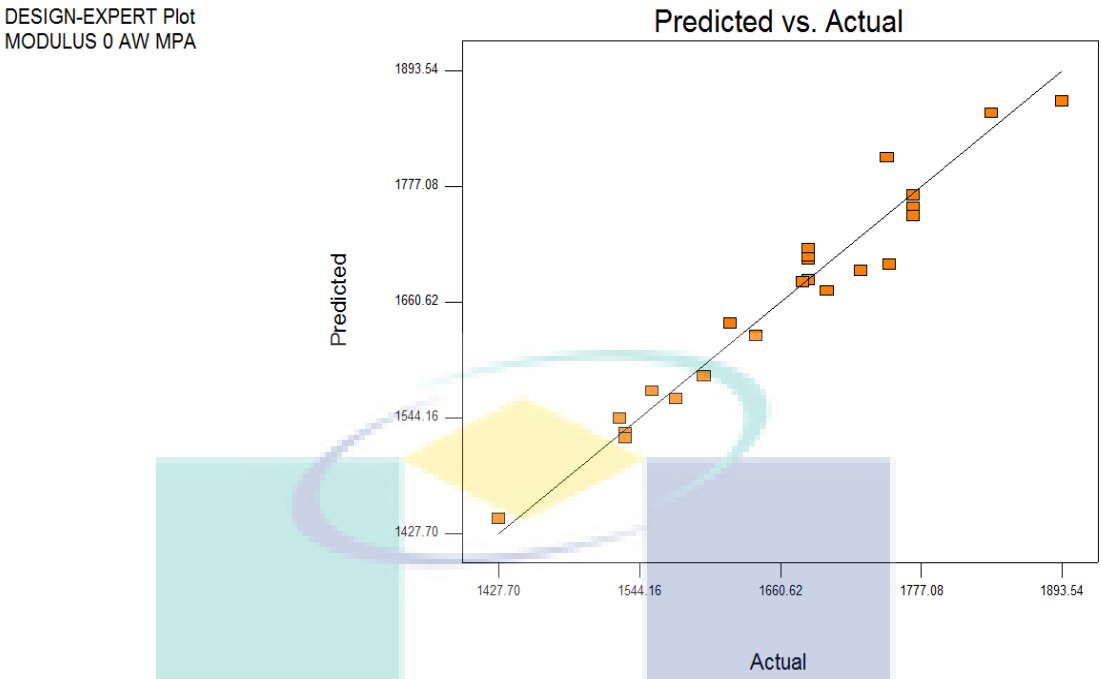

Figure B. 5: Predicted versus actual values for modulus 0 AW

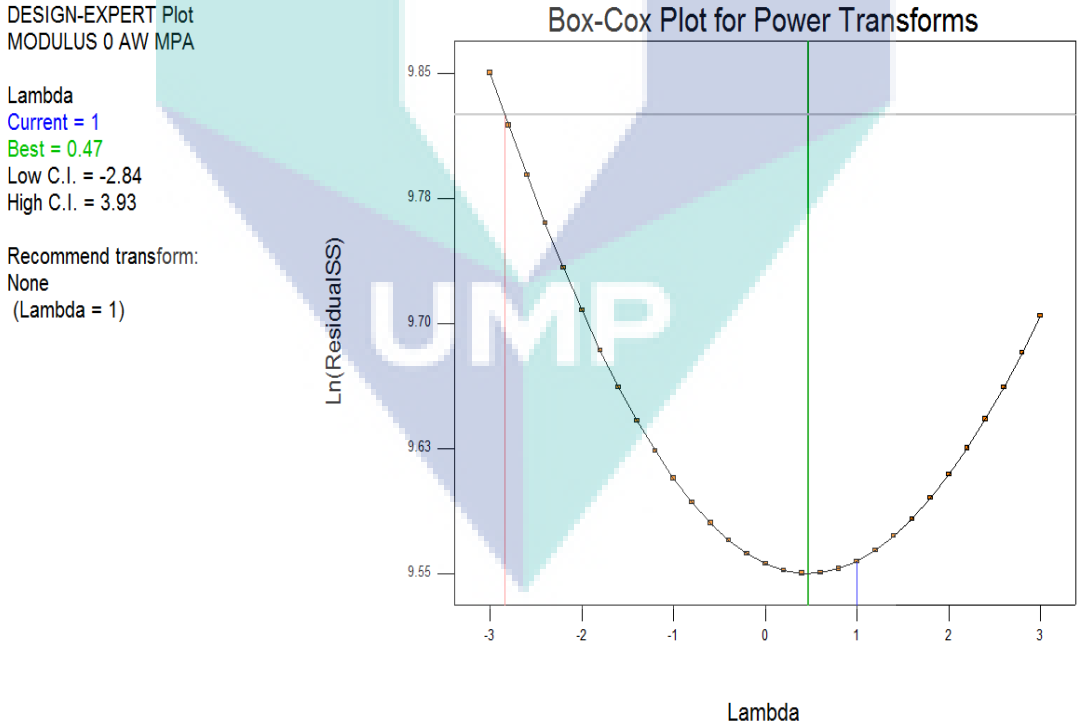

Figure B. 6: Box-Cox plot for modulus 0 AW

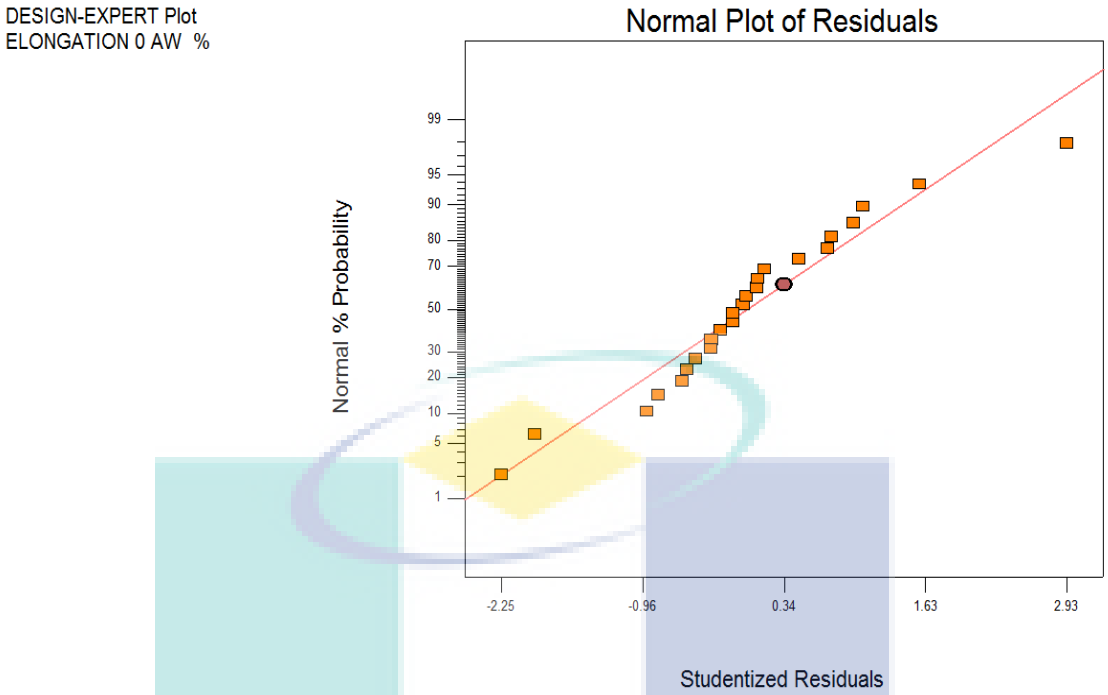

Figure B. 7: Normal probability plot of the residuals for elongation 0 AW

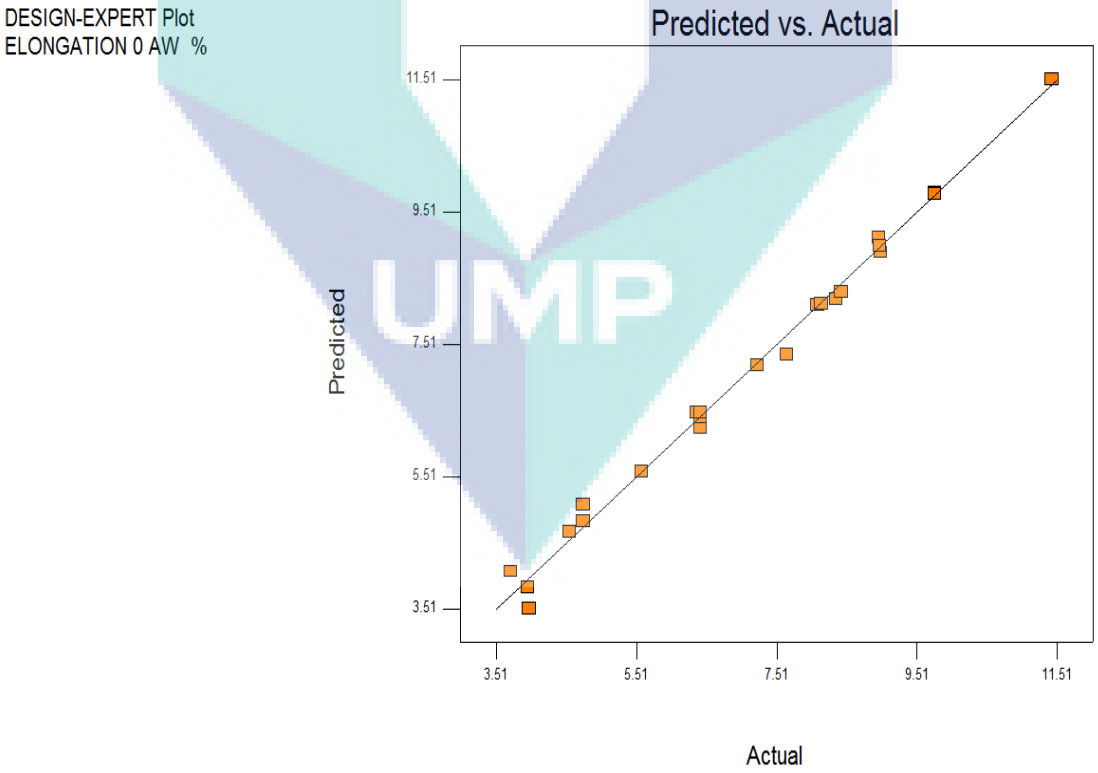

Figure B. 8: Predicted versus actual values for elongation 0 AW

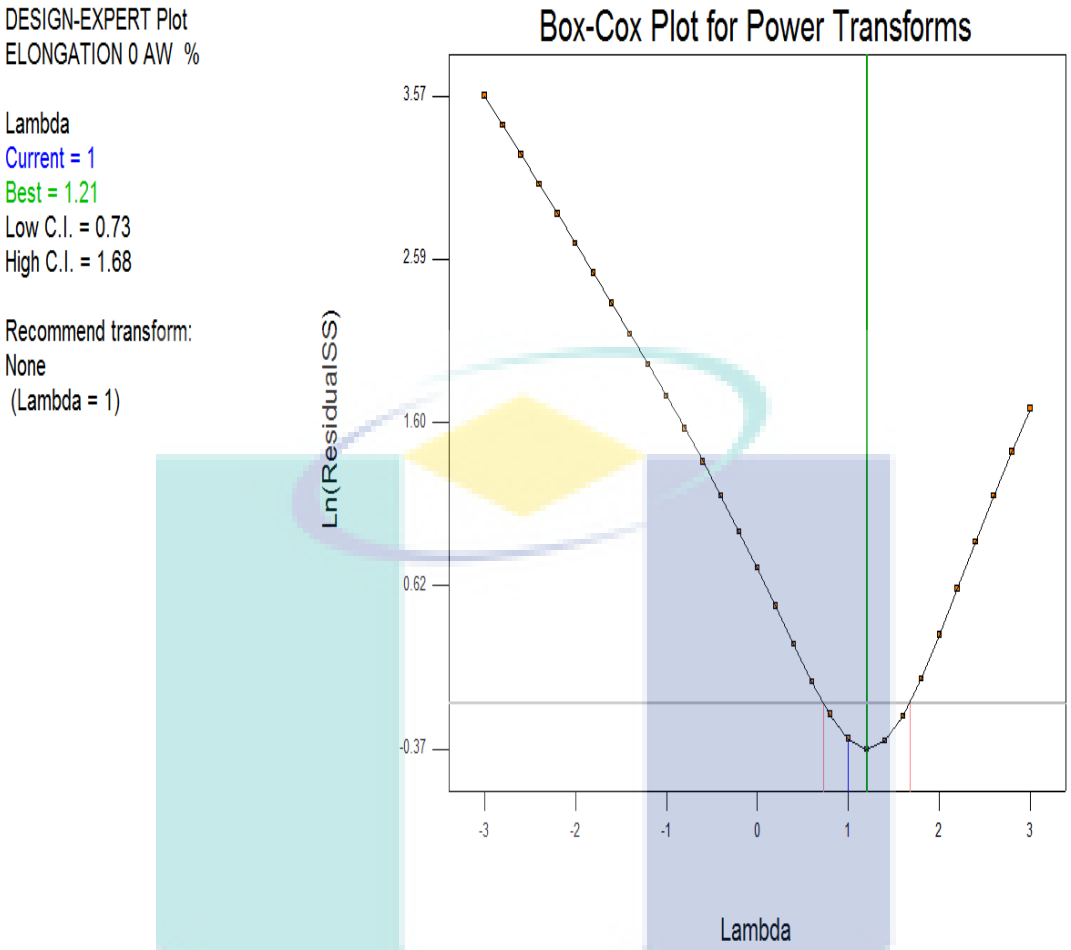

Figure B. 9: Box-Cox plot for elongation 0 AW

APPENDIX C

HOMEMADE HYBRID COMPOSITES ANOVA

Table C. 1: Homemade tensile strength 0 AW ANOVA

Factor	Estimate	Coefficient DF	Standard Error	95% CI Low	95% CI High	VIF
Intercept	36.51	1.00	0.60	35.10	37.92	
A- TEMP. CELCIUS	1.12	1.00	0.26	0.50	1.73	1.87
B-TREATMN TIME	-0.93	1.00	1.12	-3.57	1.71	34.77
C-NaOH %	-1.15	1.00	0.93	-3.34	1.05	24.10
D-FUSABOND %	1.40	1.00	0.80	-0.49	3.30	17.97
E-MAPP %	0.95	1.00	0.86	-1.09	2.99	20.77
F-EFB/G FIBER RATIO	0.60	1.00	1.20	-2.24	3.44	40.37
A2	-1.25	1.00	0.35	-2.09	-0.41	1.22
B2	-0.66	1.00	0.75	-2.43	1.11	5.49
C2	-0.39	1.00	0.97	-2.68	1.89	9.16
D2	-0.61	1.00	0.75	-2.39	1.16	5.48
E2	-2.67	1.00	1.25	-5.63	0.28	15.29
F2	-1.84	1.00	1.25	-4.80	1.12	15.29
AB	-0.16	1.00	0.90	-2.28	1.96	11.20
AC	-1.64	1.00	1.31	-4.72	1.45	23.80
AD	-2.73	1.00	1.79	-6.96	1.51	44.80
AE	-2.88	1.00	1.68	-6.84	1.08	39.20
BD	0.93	1.00	0.71	-0.74	2.61	7.00

Table C. 2: Homemade modulus 0 AW ANOVA

Factor	Estimate	Coefficient DF	Standard Error	95% CI Low	95% CI High	VIF
Intercept	1959.27	1.00	30.48	1887.21	2031.34	
A- TEMP. CELCIUS	34.09	1.00	13.23	2.80	65.38	1.87
B-TREATMN TIME	-28.24	1.00	56.98	-162.99	106.50	34.77
C-NaOH %	-28.90	1.00	47.44	-141.07	83.28	24.10
D-FUSABOND %	0.47	1.00	40.97	-96.41	97.34	17.97
E-MAPP %	4.56	1.00	44.04	-99.59	108.71	20.77
F-EFB/G FIBER RATIO	-41.39	1.00	61.40	-186.58	103.80	40.37
A2	-38.21	1.00	18.08	-80.96	4.54	1.22
B2	-3.30	1.00	38.25	-93.76	87.15	5.49
C2	-30.86	1.00	49.43	-147.76	86.03	9.16
D2	-81.06	1.00	38.25	-171.52	9.39	5.48
E2	-95.91	1.00	63.86	-246.91	55.09	15.29
F2	-147.10	1.00	63.86	-298.10	3.90	15.29
AB	-16.63	1.00	45.73	-124.77	91.51	11.20
AC	-85.87	1.00	66.67	-243.51	71.78	23.80
AD	-59.19	1.00	91.47	-275.47	157.10	44.80
AE	-75.94	1.00	85.56	-278.26	126.38	39.20
BD	28.42	1.00	36.16	-57.07	113.92	7.00

Table C. 3: Homemade elongation 0 AW ANOVA

Factor	Estimate	Coefficient DF	Standard Error	95% CI Low	95% CI High	VIF
Intercept	8.98	1.00	0.14	8.65	9.31	
A- TEMP. CELCIUS	0.18	1.00	0.06	0.04	0.33	1.87
B-TREATMN TIME	0.35	1.00	0.26	-0.27	0.97	34.77
C-NaOH %	0.60	1.00	0.22	0.08	1.11	24.10
D-FUSABOND %	0.86	1.00	0.19	0.42	1.31	17.97
E-MAPP %	1.04	1.00	0.20	0.56	1.52	20.77
F-EFB/G FIBER RATIO	-3.40	1.00	0.28	-4.07	-2.73	40.37
A2	-0.06	1.00	0.08	-0.26	0.13	1.22
B2	-0.20	1.00	0.18	-0.61	0.22	5.49
C2	-0.12	1.00	0.23	-0.66	0.42	9.16
D2	0.00	1.00	0.18	-0.41	0.42	5.48
E2	0.04	1.00	0.29	-0.66	0.74	15.29
F2	0.00	1.00	0.29	-0.70	0.70	15.29
AB	0.14	1.00	0.21	-0.36	0.63	11.20
AC	0.16	1.00	0.31	-0.57	0.89	23.80
AD	0.18	1.00	0.42	-0.81	1.18	44.80
AE	0.16	1.00	0.39	-0.77	1.09	39.20
BD	-0.13	1.00	0.17	-0.52	0.27	7.00

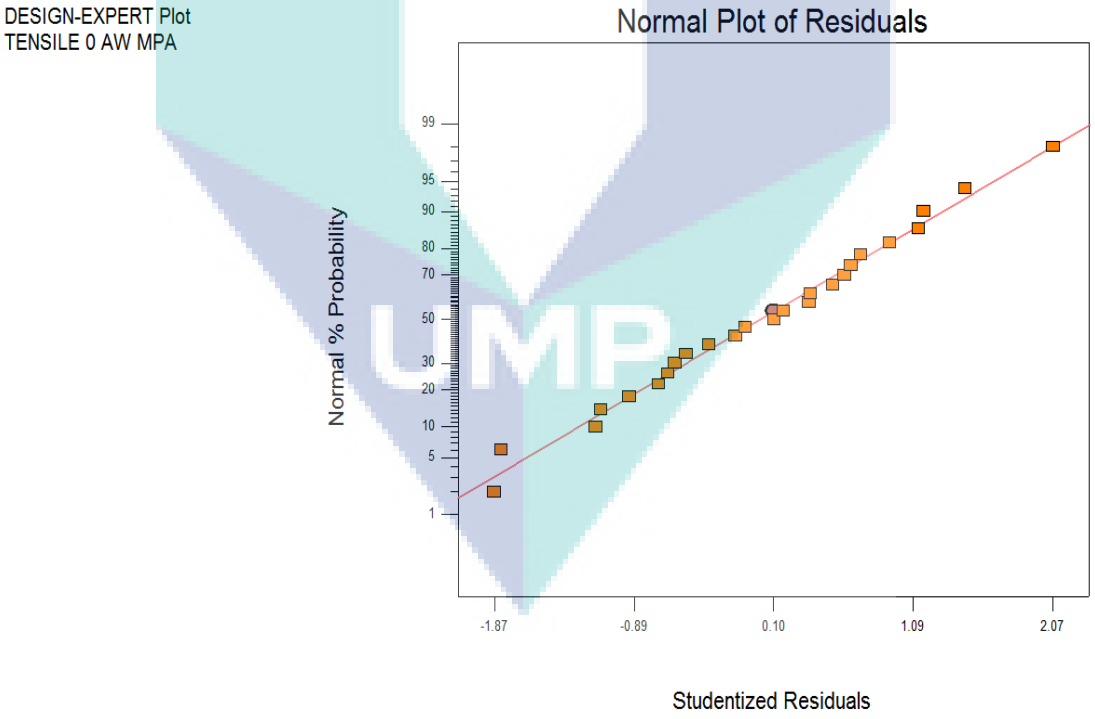

Figure C. 1: Normal probability plot of the residuals for tensile strength 0 AW

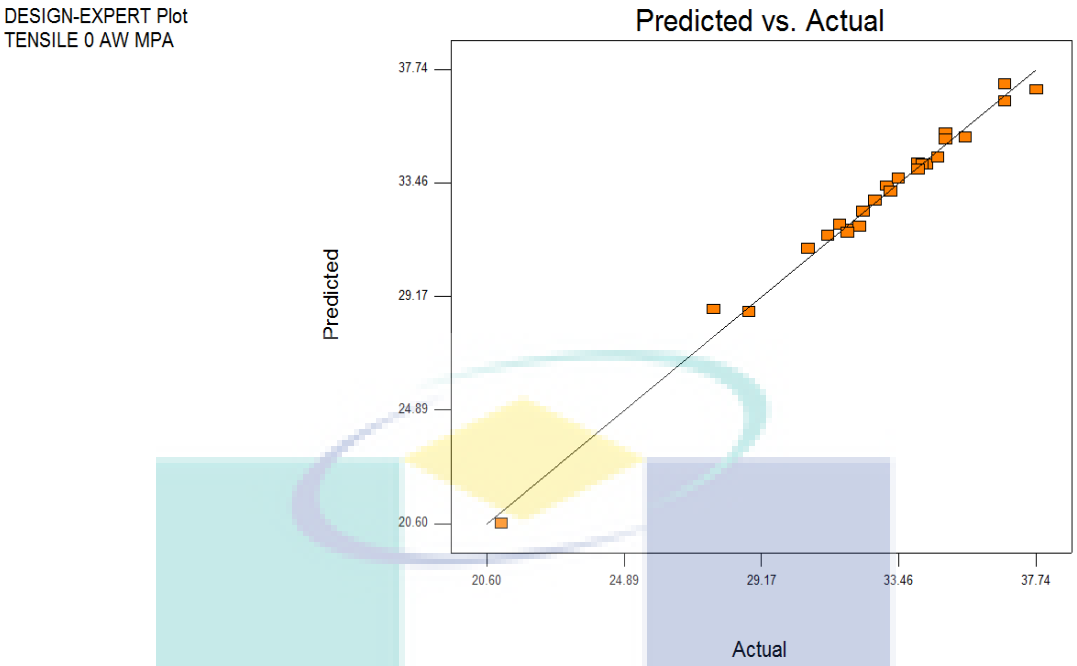

Figure C. 2: Predicted versus actual values for tensile strength 0 AW

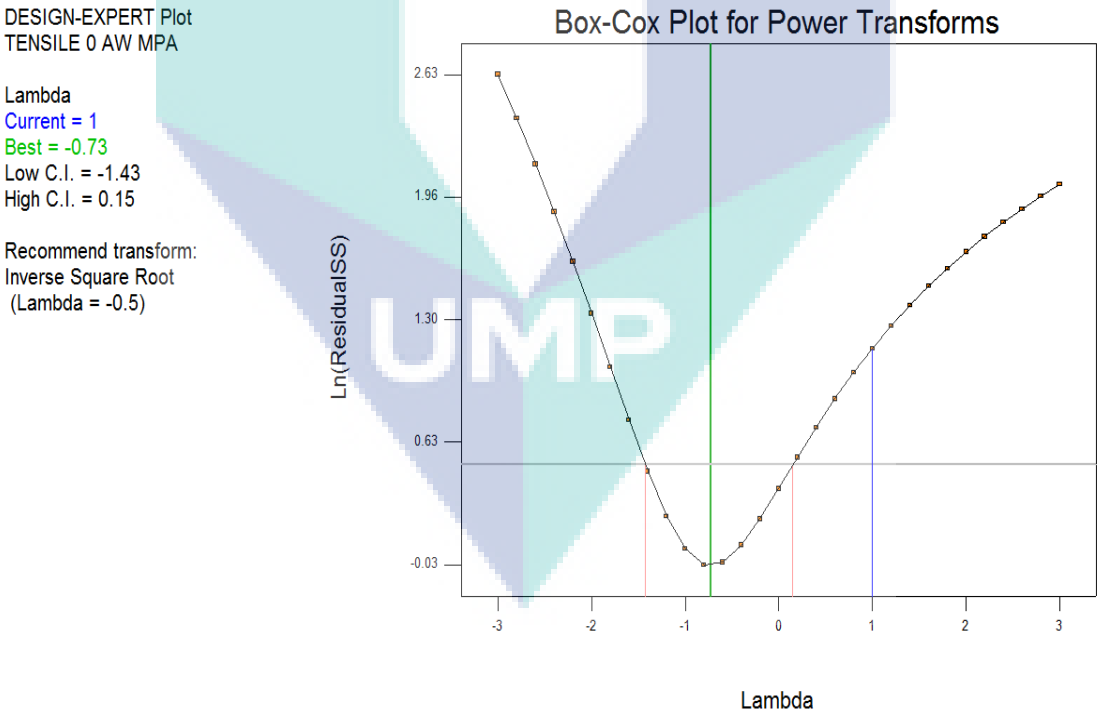

Figure C. 3: Box-Cox plot for tensile strength 0 AW

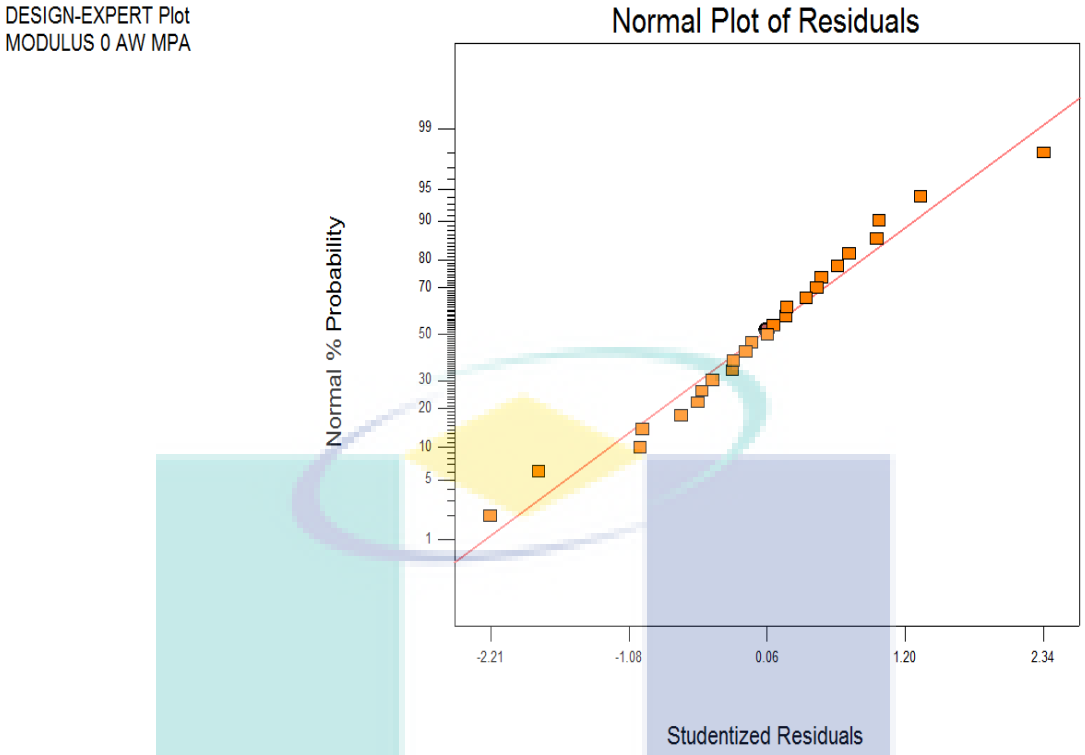

Figure C. 4: Normal probability plot of the residuals for modulus 0 AW

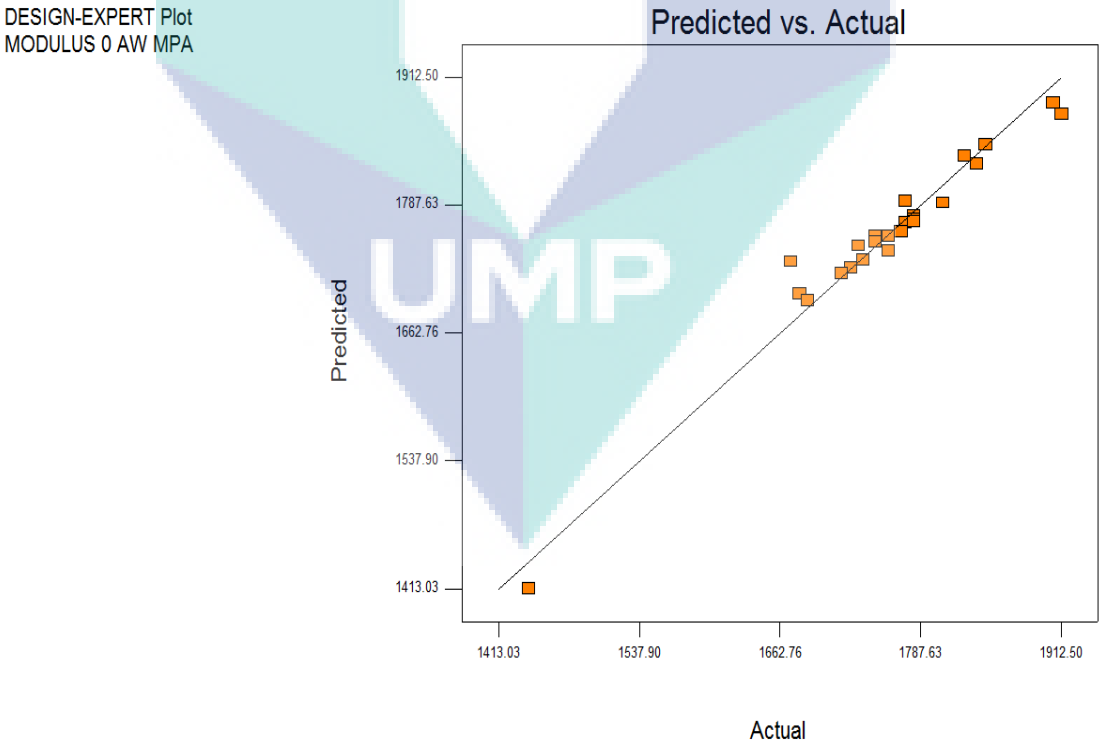

Figure C. 5: Predicted versus actual values for modulus 0 AW

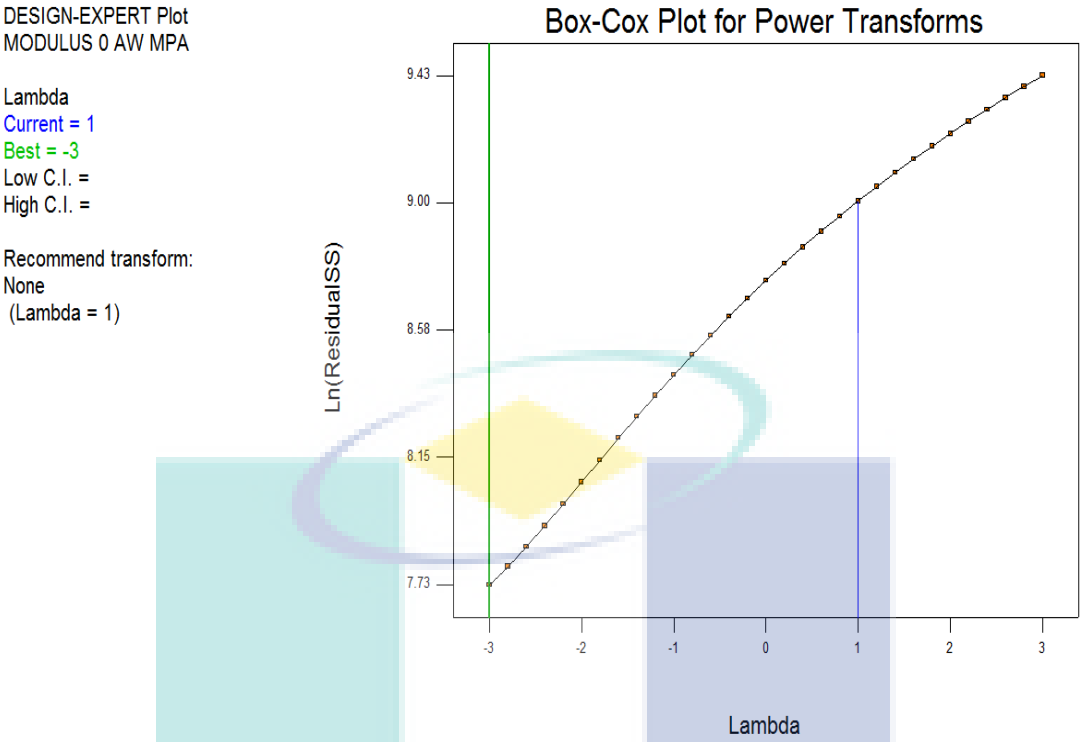

Figure C. 6: Box-Cox plot for modulus 0 AW

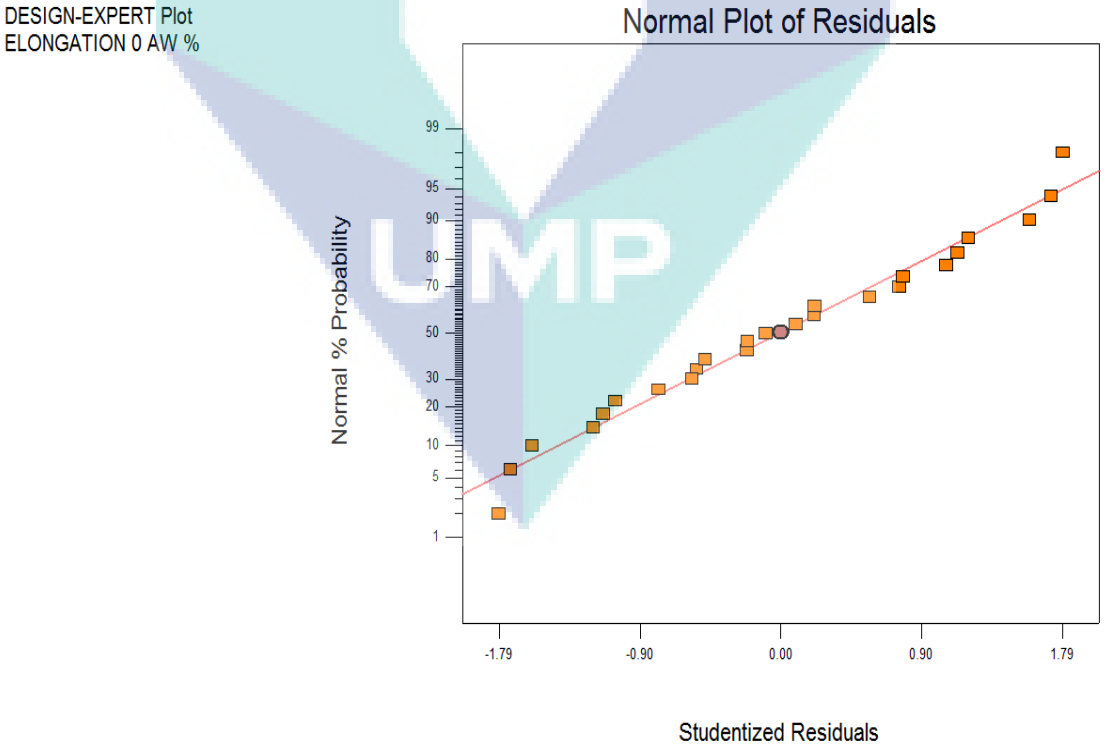

Figure C. 7: Normal probability plot of the residuals for elongation 0 AW

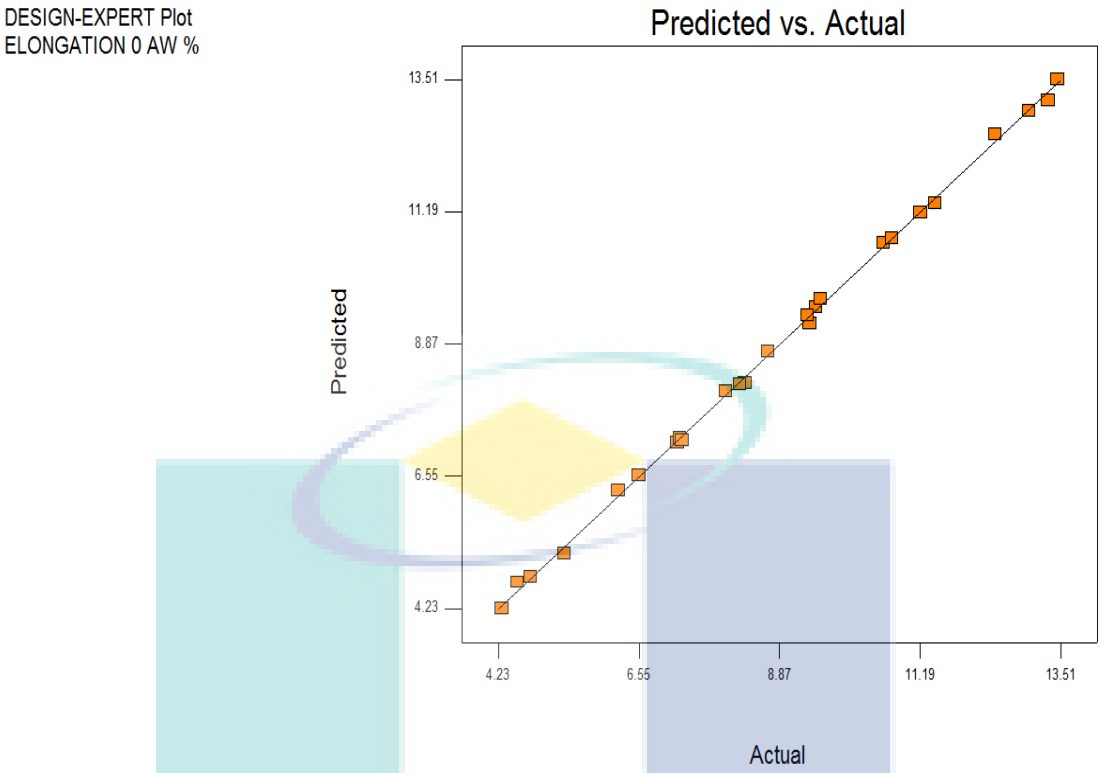

Figure C. 8: Predicted versus actual values for elongation 0 AW

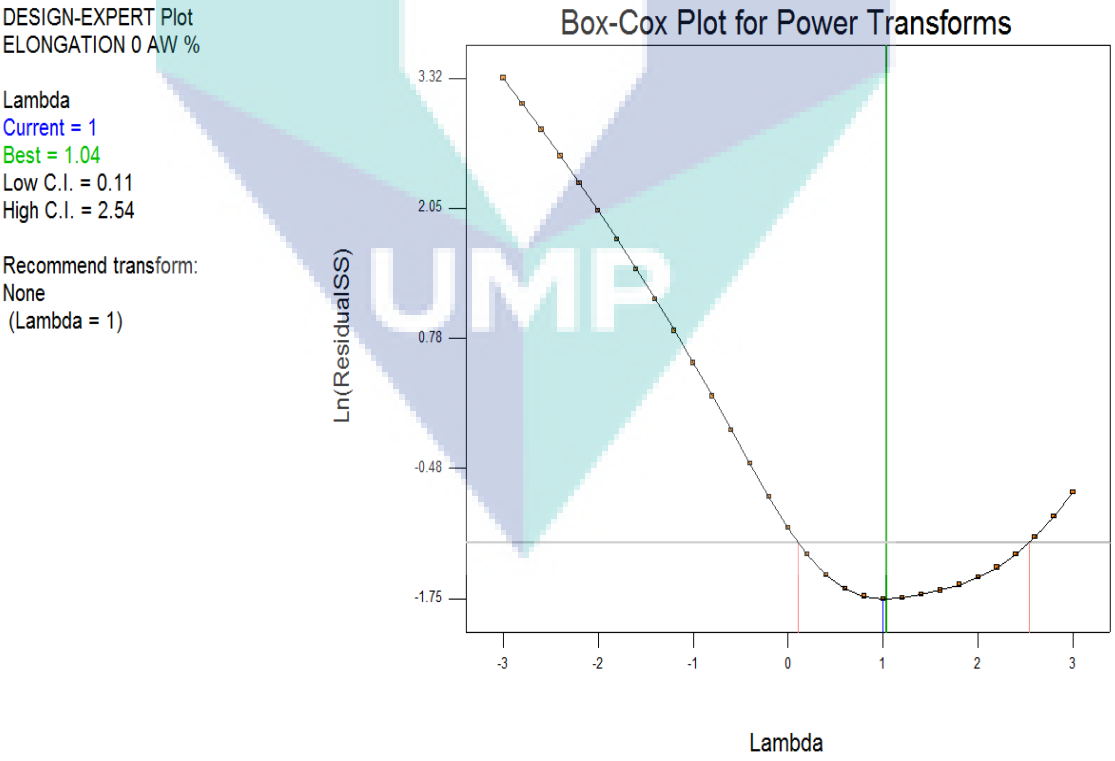

Figure C. 9: Box-Cox plot for elongation 0 AW

APPENDIX D

MICROWAVE HYBRID COMPOSITES ANOVA

Table D. 1: Microwave tensile strength 0 AW ANOVA

Factor	Estimate	Coefficient DF	Standard Error	95% CI Low	95% CI High	VIF
Intercept	34.94	1.00	0.08	33.94	35.95	
A-TEMPERATURE	-0.64	1.00	0.08	-1.63	0.34	21.25
B-TIME MINUTES	1.47	1.00	0.06	0.68	2.26	13.69
C-NAOH %	-0.02	1.00	0.05	-0.68	0.65	9.70
D-FUSABOND %	1.39	1.00	0.04	0.95	1.83	4.31
E-EFB/GLASS FBR	-1.39	1.00	0.06	-2.17	-0.60	13.45
A2	-1.02	1.00	0.03	-1.38	-0.67	1.00
B2	0.02	1.00	0.03	-0.34	0.38	1.00
C2	-2.20	1.00	0.03	-2.56	-1.84	1.00
D2	0.74	1.00	0.07	-0.13	1.62	6.00
E2	1.05	1.00	0.07	0.18	1.93	6.00
AB	-0.15	1.00	0.07	-1.04	0.75	9.77
AC	-0.01	1.00	0.09	-1.15	1.12	15.62
AD	0.07	1.00	0.07	-0.82	0.97	9.77
BC	-1.97	1.00	0.13	-3.57	-0.37	31.25

Table D. 2: Microwave modulus 0 AW ANOVA

Factor	Estimate	Coefficient DF	Standard Error	95% CI Low	95% CI High	VIF
Intercept	1951.29	1.00	29.21	1580.12	2322.47	
A-TEMPERATURE	55.55	1.00	28.54	-307.13	418.23	21.25
B-TIME MINUTES	43.50	1.00	22.91	-247.58	334.58	13.69
C-NAOH %	3.64	1.00	19.29	-241.43	248.72	9.70
D-FUSABOND %	58.90	1.00	12.86	-104.49	222.28	4.31
E-EFB/GLASS FBR	26.61	1.00	22.71	-261.96	315.19	13.45
A2	3.70	1.00	10.38	-128.25	135.64	1.00
B2	-75.43	1.00	10.38	-207.38	56.51	1.00
C2	-97.78	1.00	10.38	-229.72	34.17	1.00
D2	-0.93	1.00	25.44	-324.13	322.27	6.00
E2	-95.94	1.00	25.44	-419.14	227.26	6.00
AB	-17.50	1.00	25.96	-347.36	312.36	9.77
AC	-1.51	1.00	32.84	-418.75	415.74	15.62
AD	53.65	1.00	25.96	-276.21	383.51	9.77
BC	-5.53	1.00	46.44	-595.61	584.54	31.25

Table D. 3: Microwave elongation 0 AW ANOVA

Factor	Estimate	Coefficient DF	Standard Error	95% CI Low	95% CI High	VIF
Intercept	8.88	1.00	0.85	-1.91	19.66	
A-TEMPERATURE	1.20	1.00	0.83	-9.34	11.74	21.25
B-TIME MINUTES	2.05	1.00	0.67	-6.40	10.51	13.69
C-NAOH %	0.29	1.00	0.56	-6.83	7.41	9.70
D-FUSABOND %	1.60	1.00	0.37	-3.14	6.35	4.31
E-EFB/GLASS FBR	1.19	1.00	0.66	-7.19	9.58	13.45
A2	0.00	1.00	0.30	-3.83	3.83	1.00
B2	0.00	1.00	0.30	-3.83	3.83	1.00
C2	-1.20	1.00	0.30	-5.03	2.63	1.00
D2	0.00	1.00	0.74	-9.39	9.39	6.00
E2	-1.35	1.00	0.74	-10.74	8.04	6.00
AB	0.34	1.00	0.75	-9.25	9.92	9.77
AC	1.35	1.00	0.95	-10.78	13.47	15.62
AD	0.34	1.00	0.75	-9.25	9.92	9.77
BC	0.00	1.00	1.35	-17.15	17.15	31.25

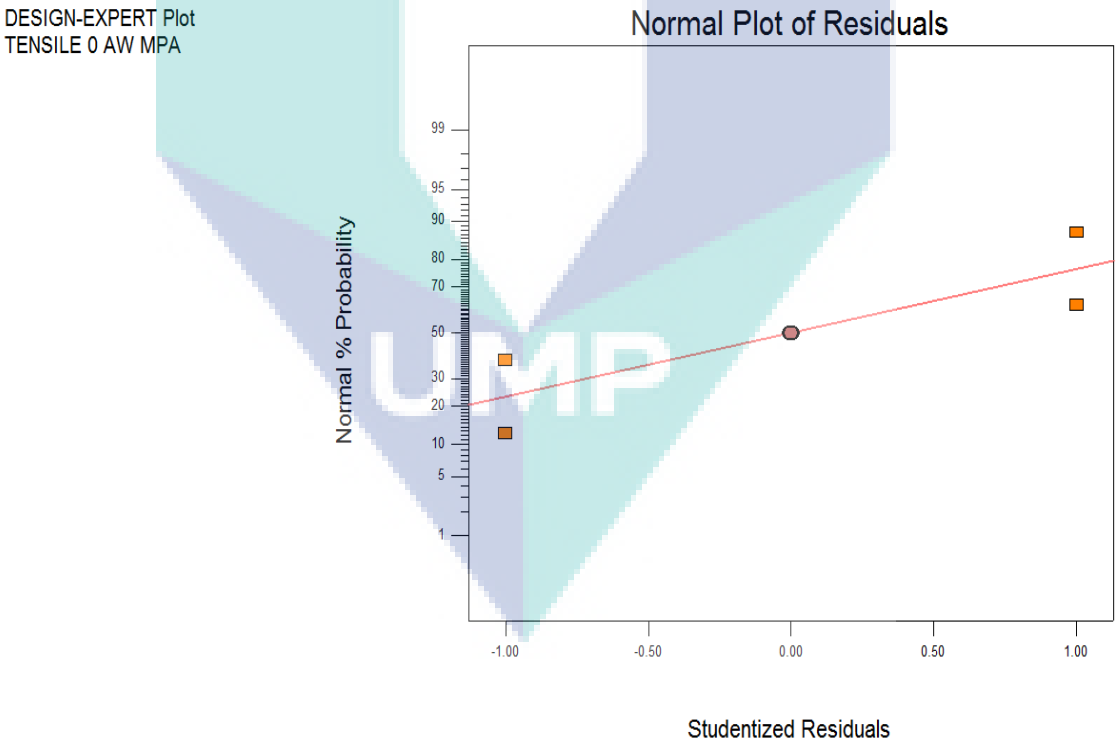

Figure D. 1: Normal probability plot of the residuals for tensile strength 0 AW

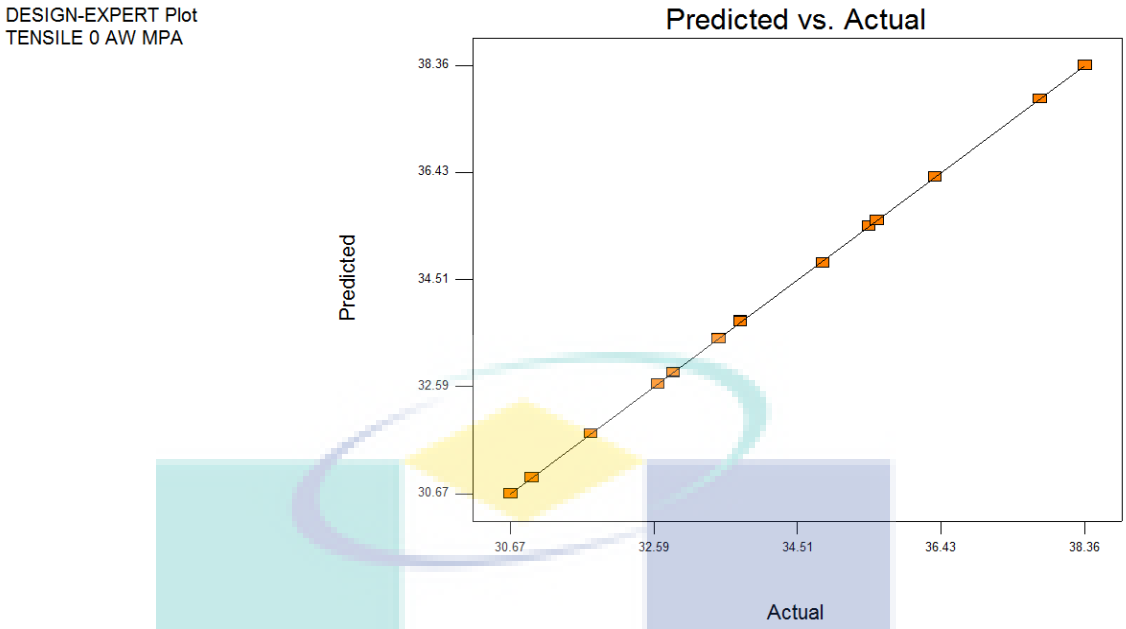

Figure D. 2: Predicted versus actual values for tensile strength 0 AW

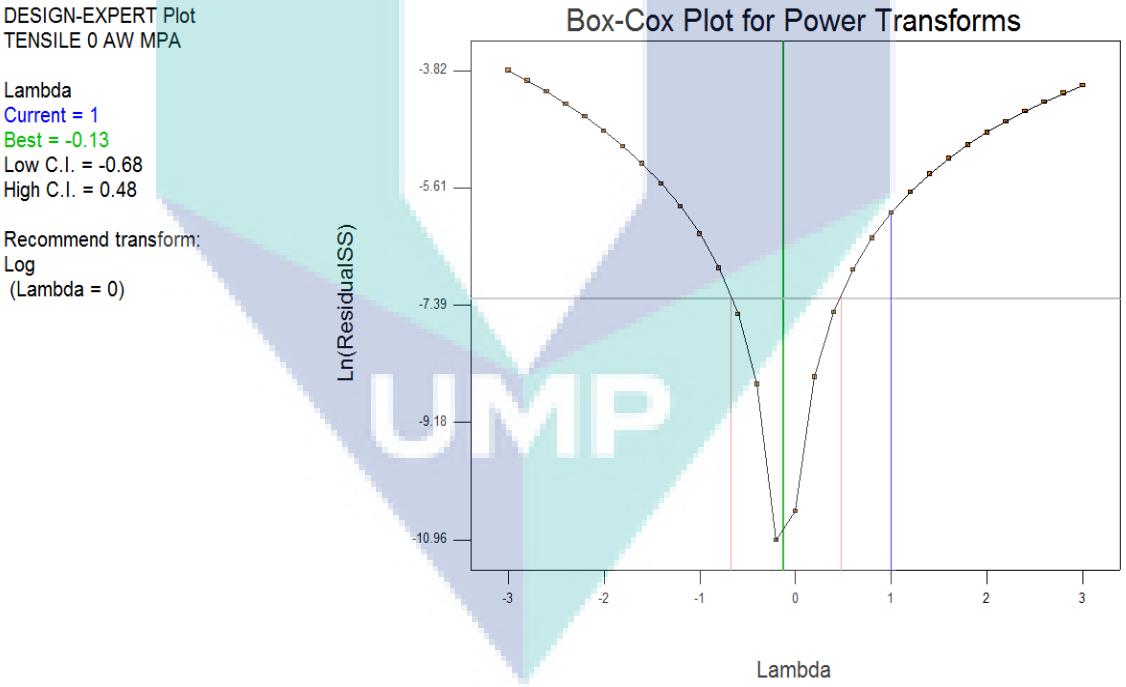

Figure D. 3: Box-Cox plot for tensile strength 0 AW

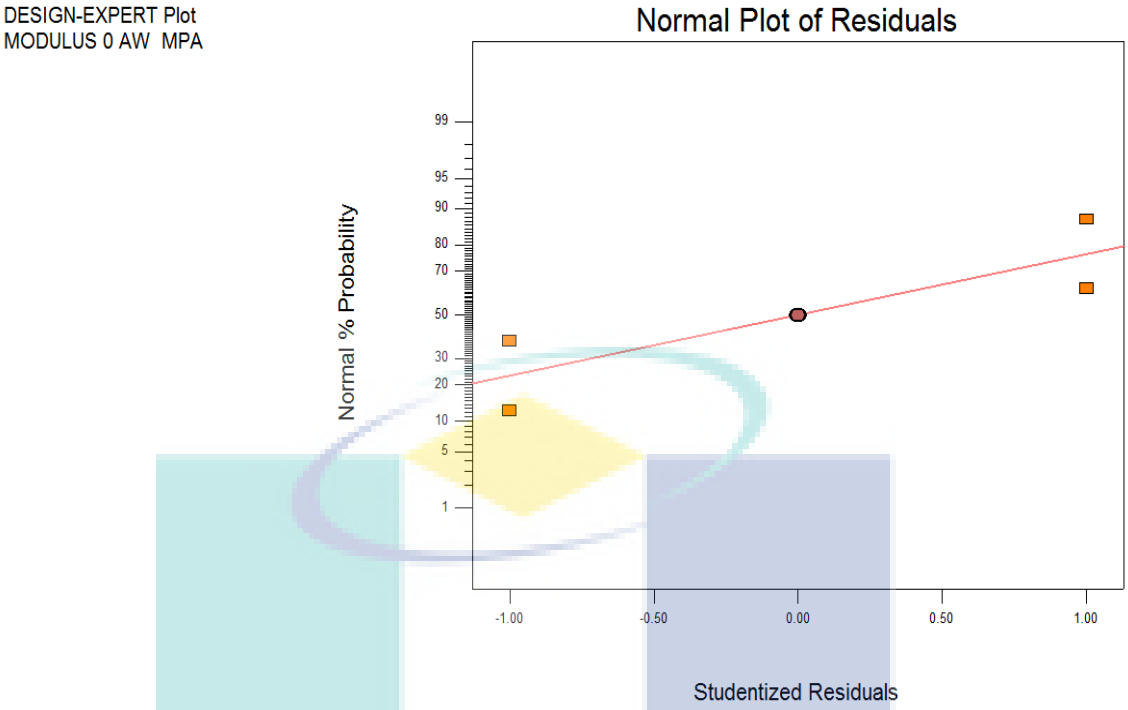

Figure D. 4: Normal probability plot of the residuals for modulus 0 AW

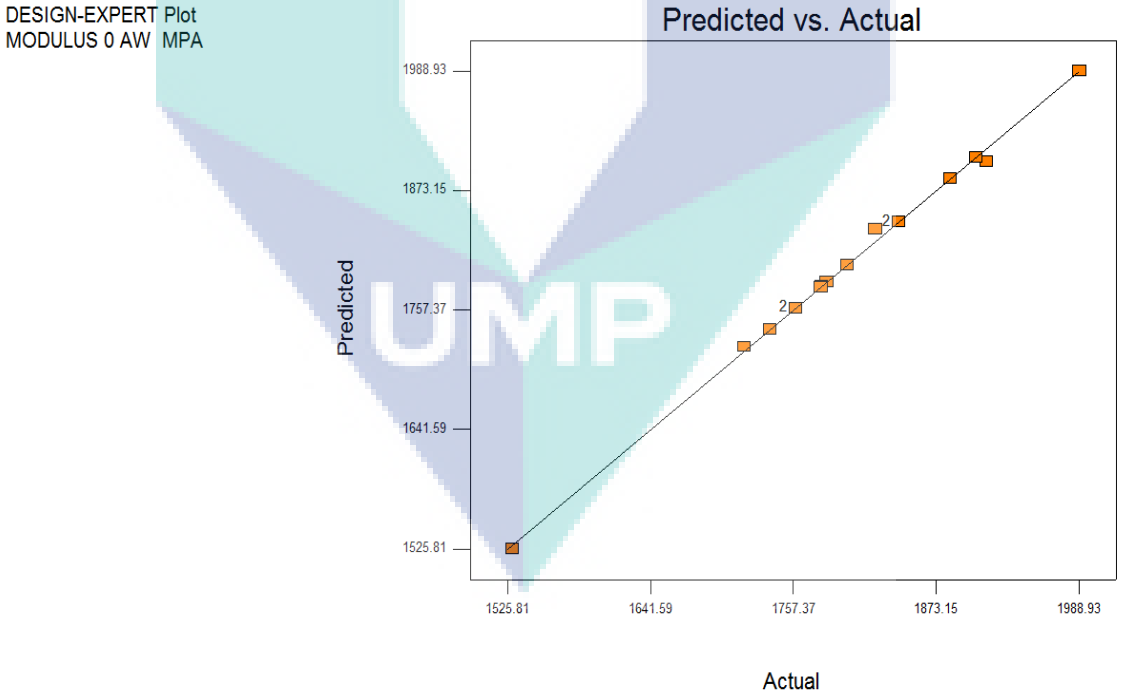

Figure D. 5: Predicted versus actual values for modulus 0 AW

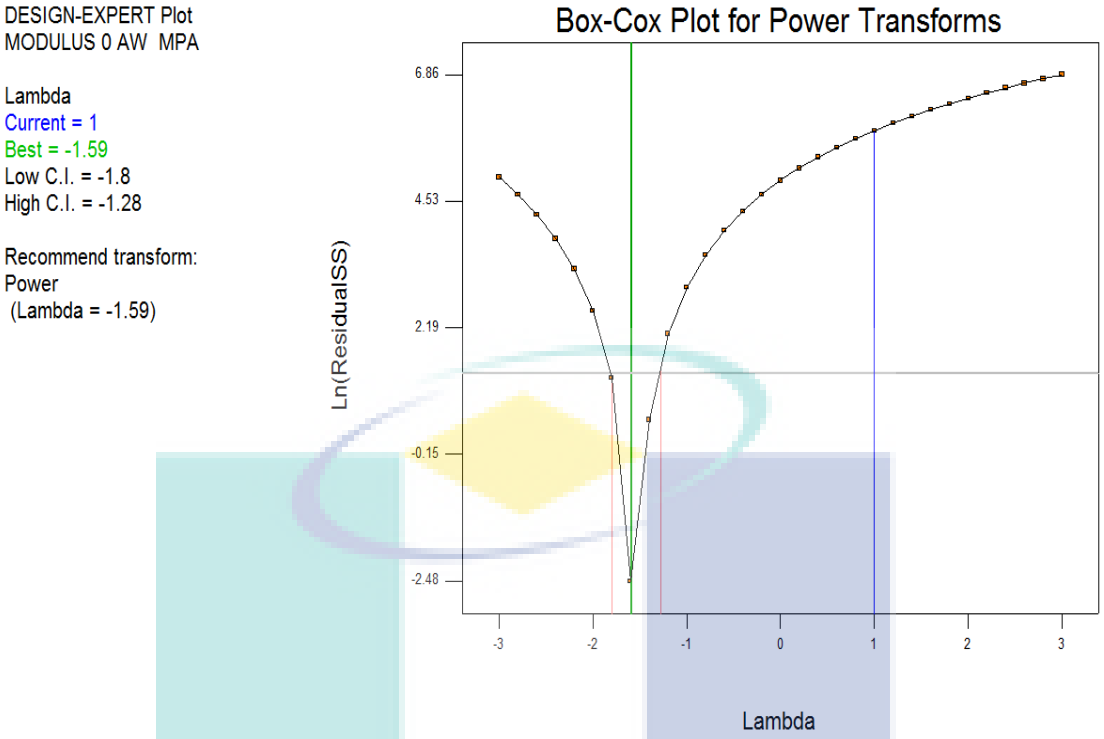

Figure D. 6: Box-Cox plot for modulus 0 AW

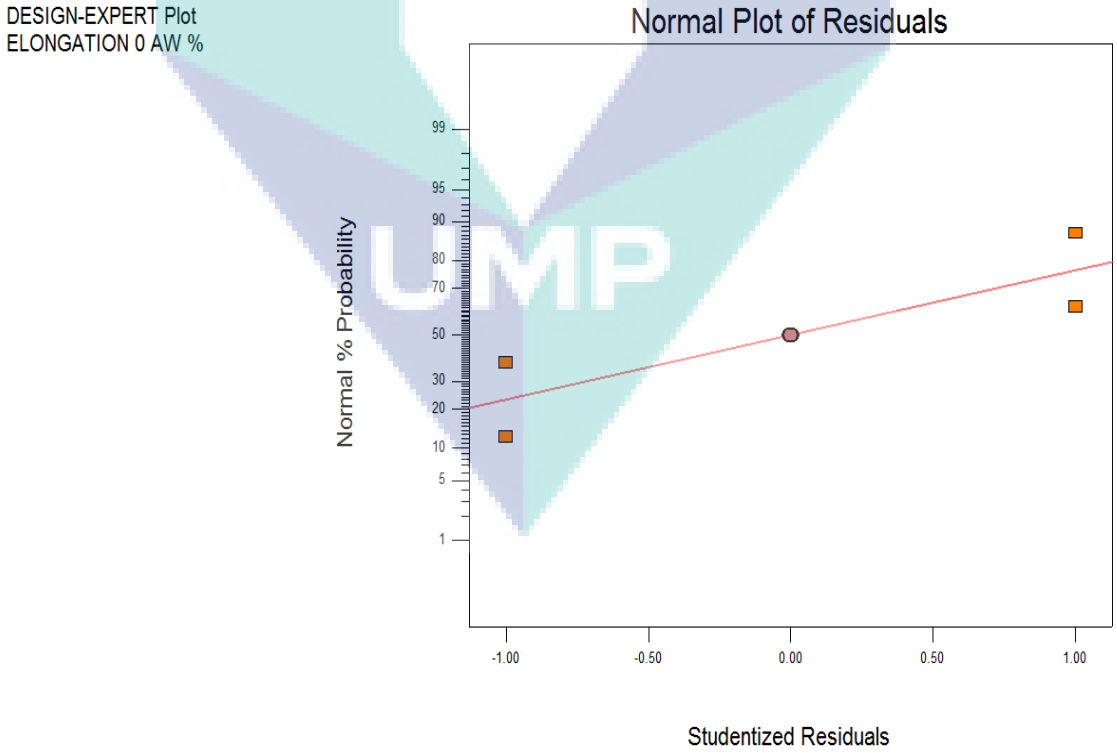

Figure D. 7: Normal probability plot of the residuals for elongation 0 AW

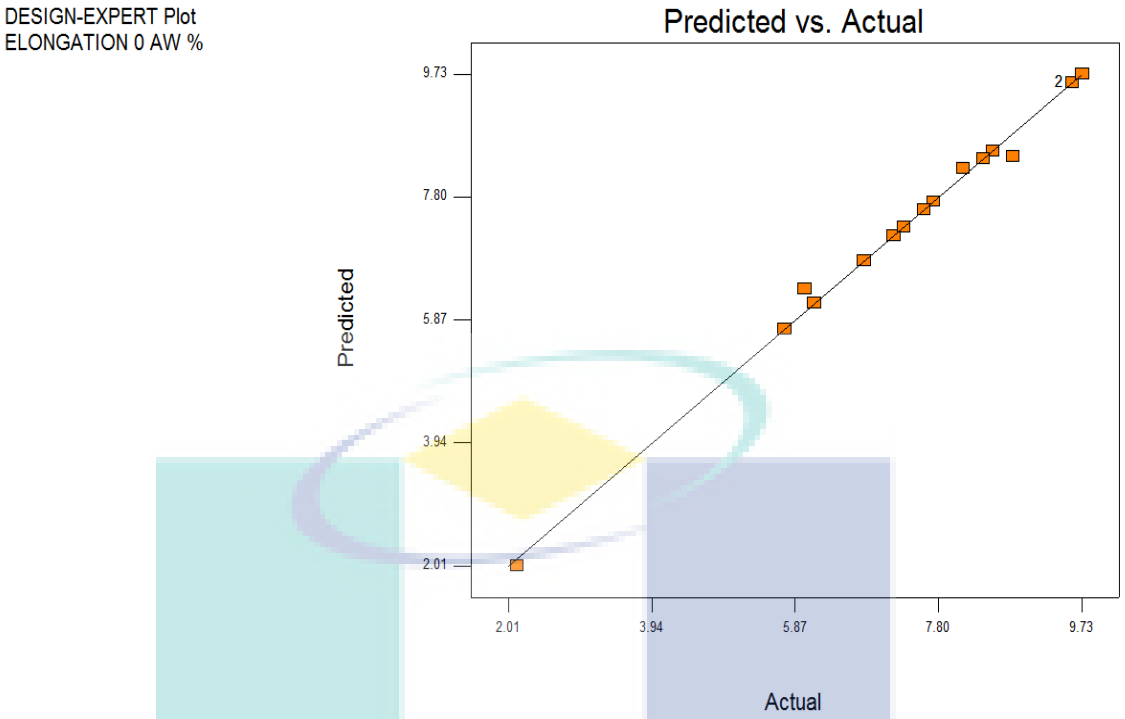

Figure D. 8: Predicted versus actual values for elongation 0 AW

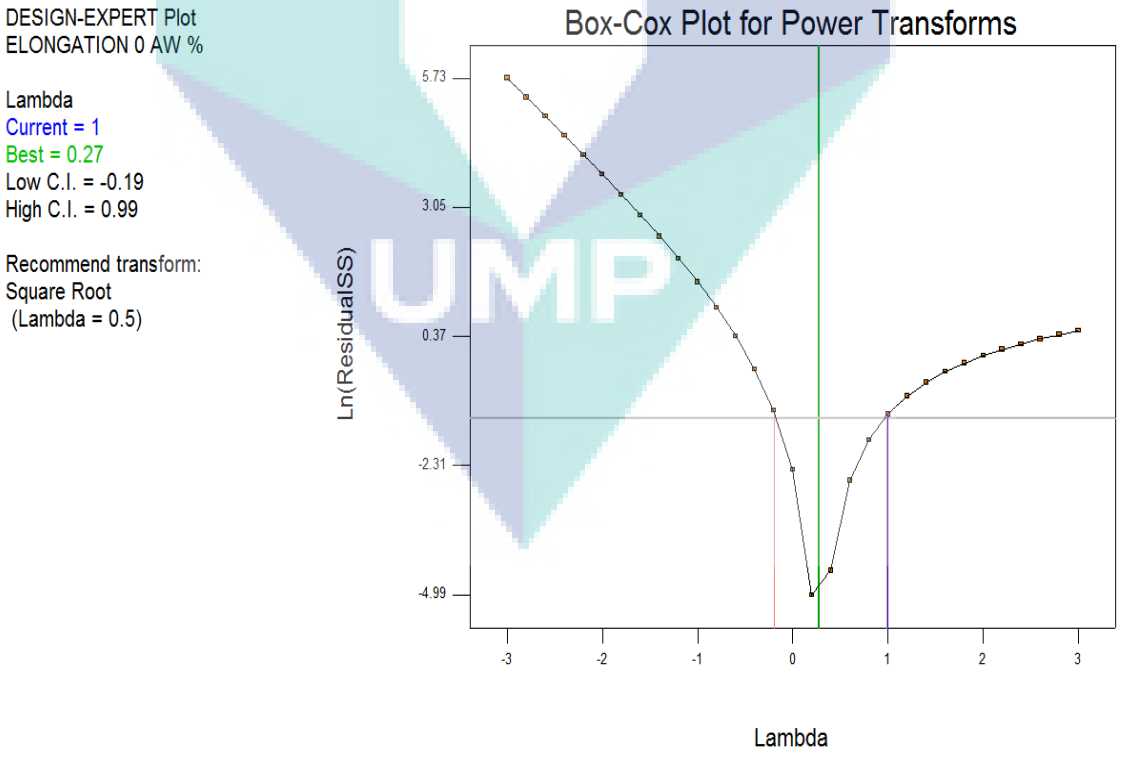

Figure D. 9: Box-Cox plot for elongation 0 AW

APPENDIX E

ULTRASONIC HYBRID COMPOSITES ANOVA

Table E. 1: Ultrasonic tensile strength 0 AW ANOVA

Factor	Estimate	Coefficient DF	Standard Error	95% CI Low	95% CI High	VIF
Intercept	36.27	1.00	0.08	35.22	37.33	
A-TEMPERATURE	-0.68	1.00	0.08	-1.71	0.35	21.25
B-TIME MINUTES	1.52	1.00	0.07	0.70	2.35	13.69
C-NAOH %	-0.02	1.00	0.06	-0.72	0.67	9.70
D-COMPOUNDING TIMES	1.44	1.00	0.04	0.97	1.90	4.31
E-EFB/GLASS FBR	-1.43	1.00	0.07	-2.25	-0.61	13.45
A2	-1.06	1.00	0.03	-1.44	-0.68	1.00
B2	0.02	1.00	0.03	-0.36	0.39	1.00
C2	-2.27	1.00	0.03	-2.65	-1.90	1.00
D2	0.78	1.00	0.07	-0.14	1.70	6.00
E2	1.10	1.00	0.07	0.18	2.02	6.00
AB	-0.16	1.00	0.07	-1.10	0.78	9.77
AC	-0.02	1.00	0.09	-1.21	1.17	15.62
AD	0.08	1.00	0.07	-0.86	1.02	9.77
BC	-2.06	1.00	0.13	-3.74	-0.38	31.25

Table E. 2: Ultrasonic modulus 0 AW ANOVA

Factor	Estimate	Coeff DF	Standard Error	95% CI Low	95% CI High	VIF
Intercept	12913.03	1.00	262.21	9581.35	16244.71	
A-TEMPERATURE	394.60	1.00	256.21	-2860.84	3650.04	21.25
B-TIME MINUTES	314.62	1.00	205.63	-2298.10	2927.33	13.69
C-NAOH %	28.54	1.00	173.13	-2171.28	2228.35	9.70
D-COMPOUNDING TIMES	415.67	1.00	115.42	-1050.87	1882.21	4.31
E-EFB/GLASS FBR	185.82	1.00	203.86	-2404.43	2776.07	13.45
A2	-3.84	1.00	93.21	-1188.18	1180.50	1.00
B2	-492.37	1.00	93.21	-1676.71	691.97	1.00
C2	-662.56	1.00	93.21	-1846.90	521.78	1.00
D2	27.93	1.00	228.32	-2873.10	2928.96	6.00
E2	-627.58	1.00	228.32	-3528.61	2273.45	6.00
AB	-98.94	1.00	233.02	-3059.80	2861.91	9.77
AC	3.46	1.00	294.75	-3741.76	3748.67	15.62
AD	355.98	1.00	233.02	-2604.87	3316.83	9.77
BC	-48.02	1.00	416.85	-5344.55	5248.52	31.25

Table E. 3: Ultrasonic elongation 0 AW ANOVA

Factor	Estimate	Coefficient DF	Standard Error	95% CI Low	95% CI High	VIF
Intercept	9.52	1.00	0.91	-2.03	21.07	
A-TEMPERATURE	1.29	1.00	0.89	-10.00	12.57	21.25
B-TIME MINUTES	2.20	1.00	0.71	-6.86	11.26	13.69
C-NAOH %	0.31	1.00	0.60	-7.31	7.94	9.70
D-COMPOUNDING TIMES	1.72	1.00	0.40	-3.36	6.80	4.31
E-EFB/GLASS FBR	1.28	1.00	0.71	-7.70	10.26	13.45
A2	0.00	1.00	0.32	-4.11	4.11	1.00
B2	0.00	1.00	0.32	-4.11	4.11	1.00
C2	-1.29	1.00	0.32	-5.39	2.82	1.00
D2	0.00	1.00	0.79	-10.06	10.06	6.00
E2	-1.45	1.00	0.79	-11.50	8.61	6.00
AB	0.36	1.00	0.81	-9.90	10.63	9.77
AC	1.45	1.00	1.02	-11.54	14.43	15.62
AD	0.36	1.00	0.81	-9.90	10.63	9.77
BC	0.00	1.00	1.45	-18.36	18.36	31.25

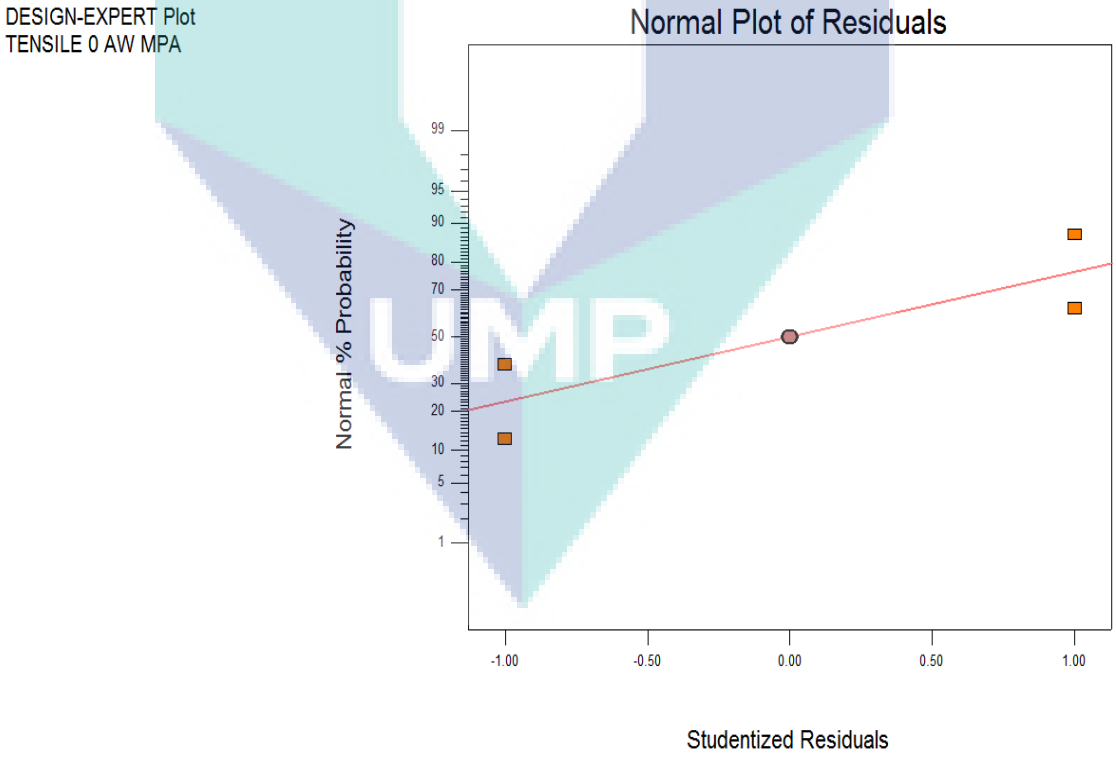

Figure E. 1: Normal probability plot of the residuals for tensile strength 0 AW

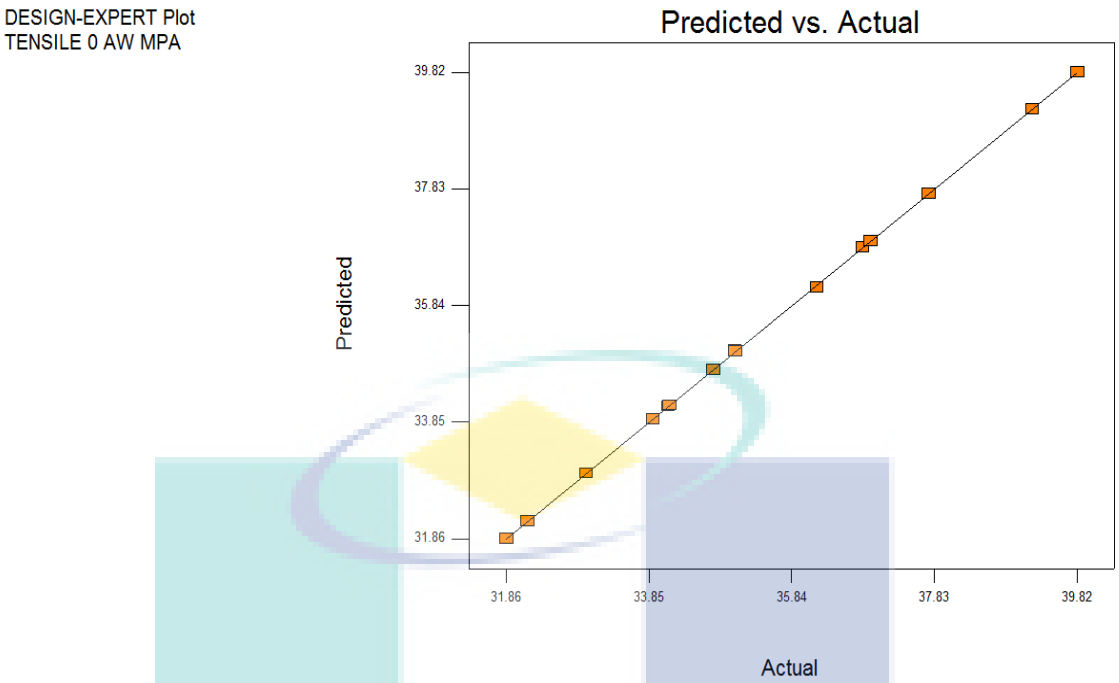

Figure E. 2: Predicted versus actual values for tensile strength 0 AW

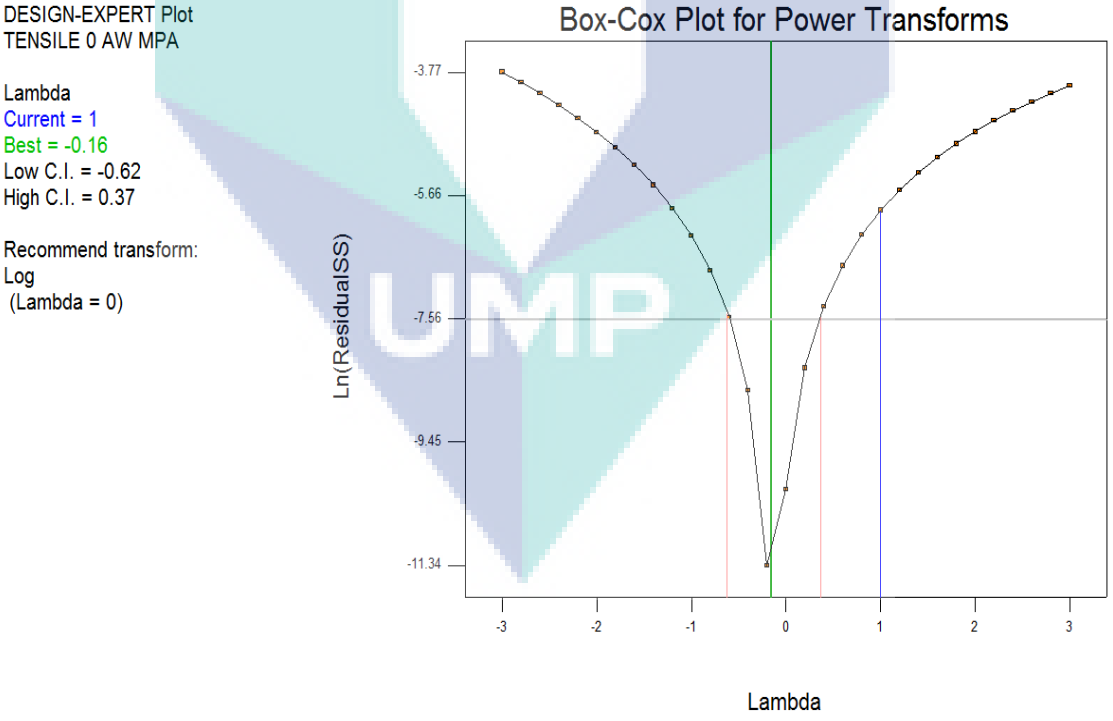

Figure E. 3: Box-Cox plot for tensile strength 0 AW

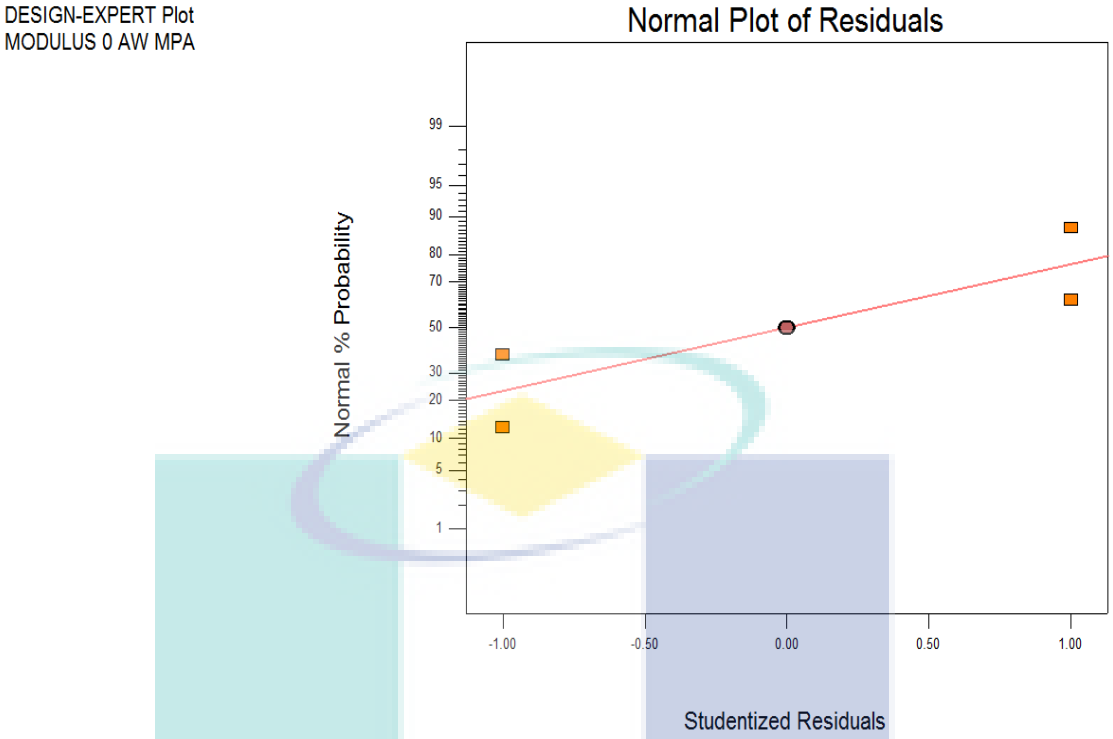

Figure E. 4: Normal probability plot of the residuals for modulus 0 AW

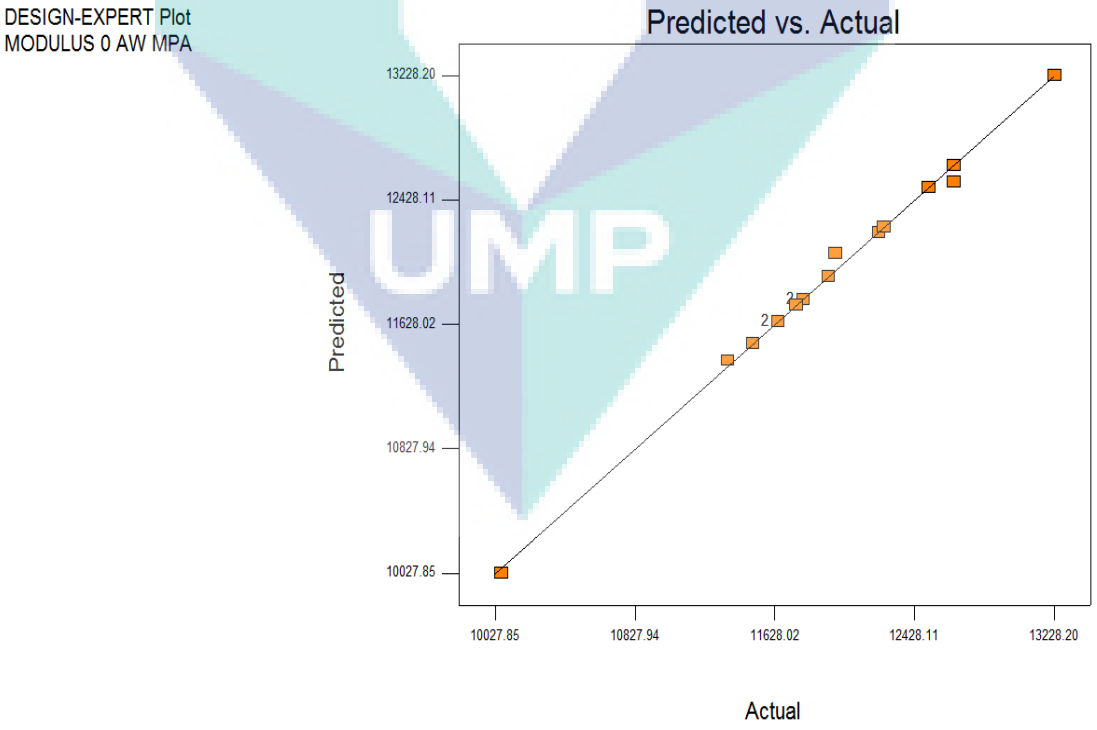

Figure E. 5: Predicted versus actual values for modulus 0 AW

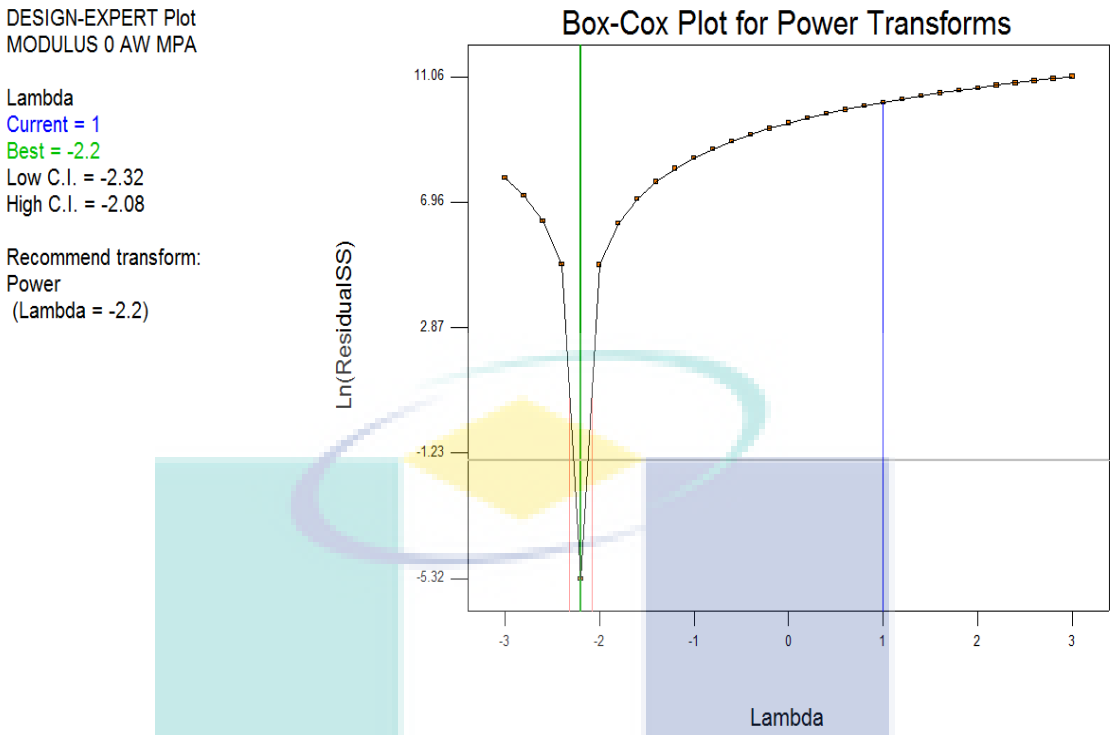

Figure E. 6: Box-Cox plot for modulus 0 AW

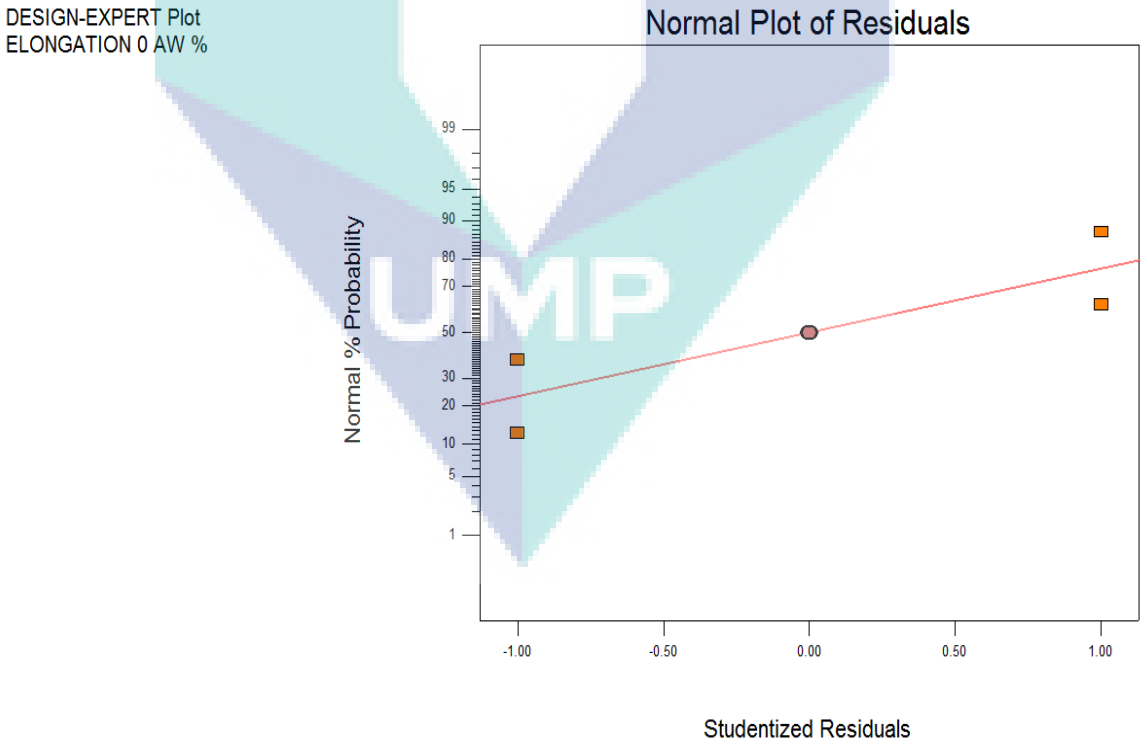

Figure E. 7: Normal probability plot of the residuals for elongation 0 AW

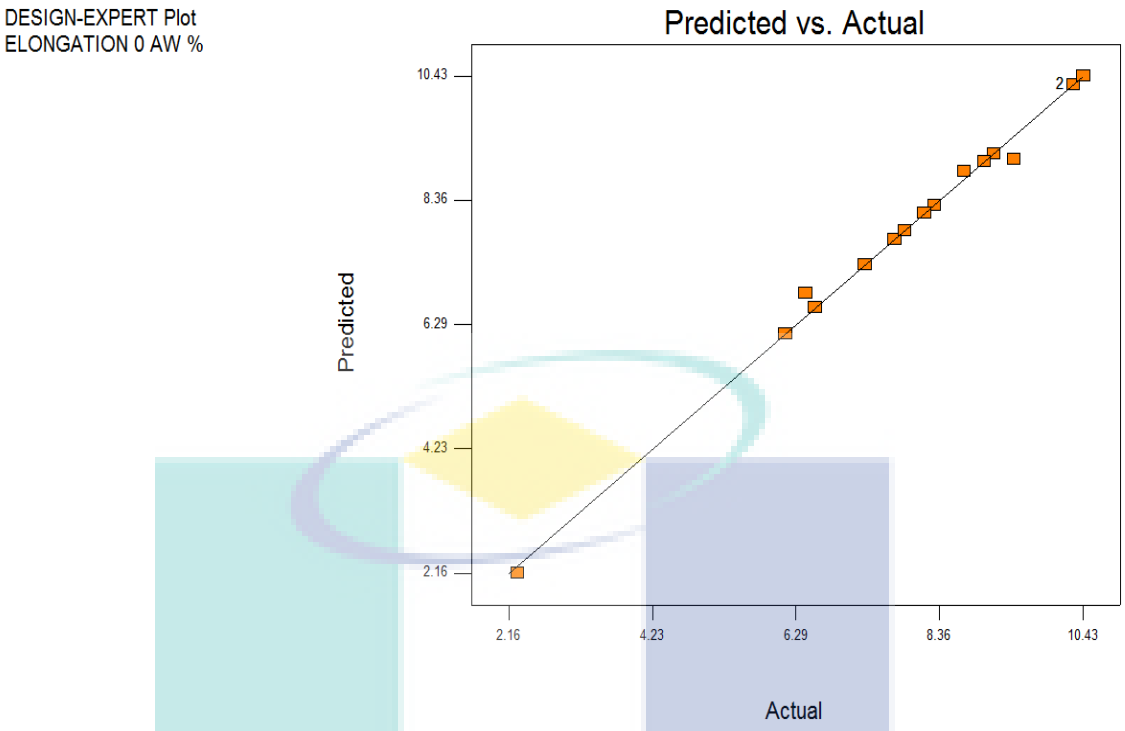

Figure E. 8: Predicted versus actual values for elongation 0 AW

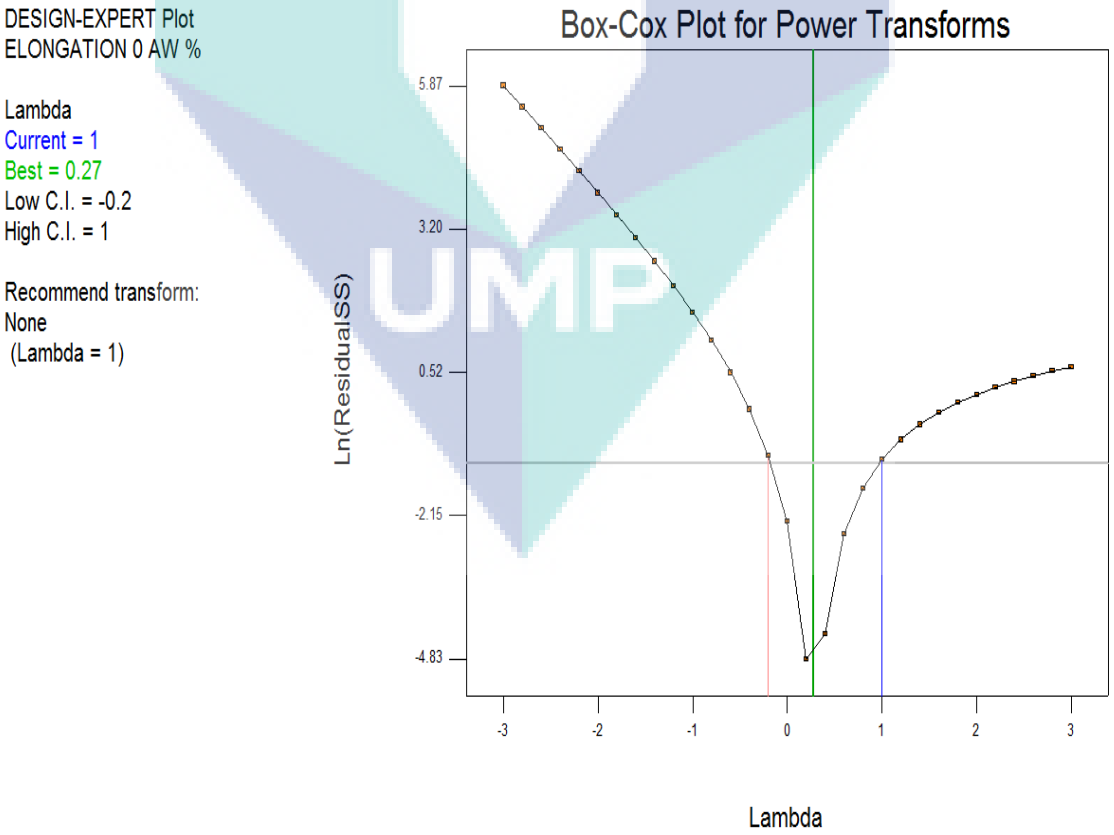

Figure E. 9: Box-Cox plot for elongation 0 AW

APPENDIX F

MAGNETRON CONTROLLER FOR EFB TREATMENT

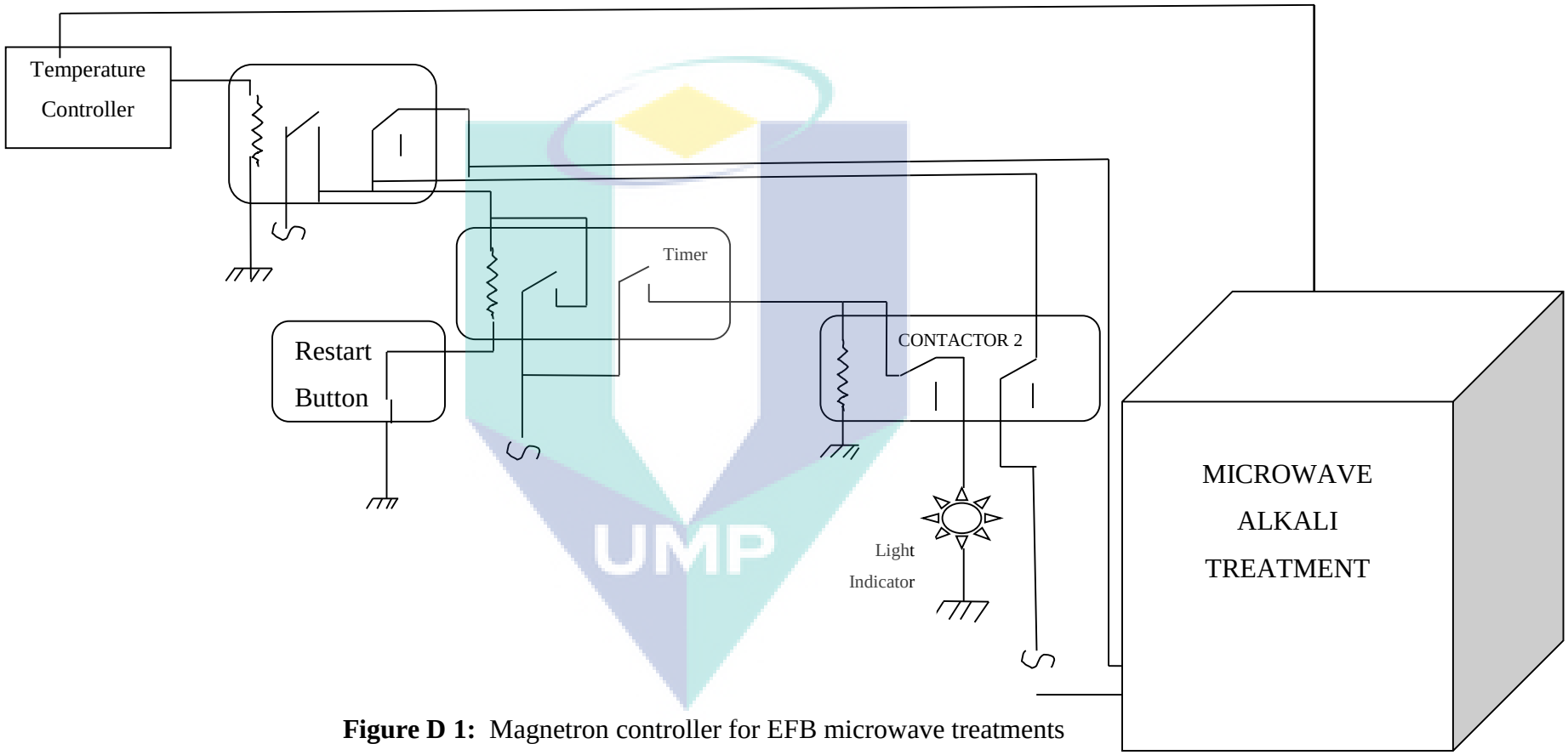

Figure D 1: Magnetron controller for EFB microwave treatments

APPENDIX G

COMPOSITES HYGROTHERMAL AGEING CONTROLLER

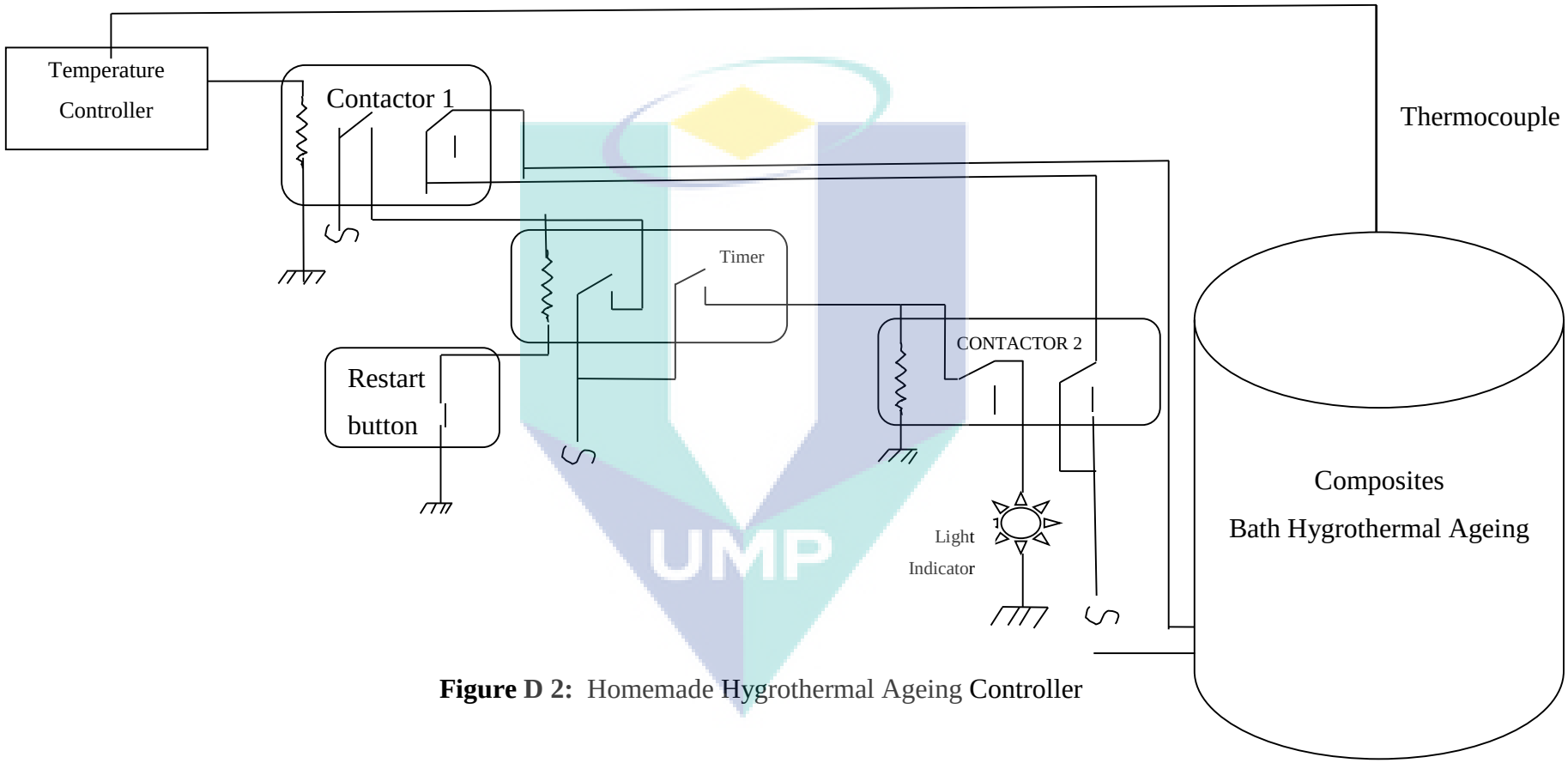

Figure D 2: Homemade Hygrothermal Ageing Controller

APPENDIX H

HOMEMADE ALKALI TREATMENT CONTROLLER

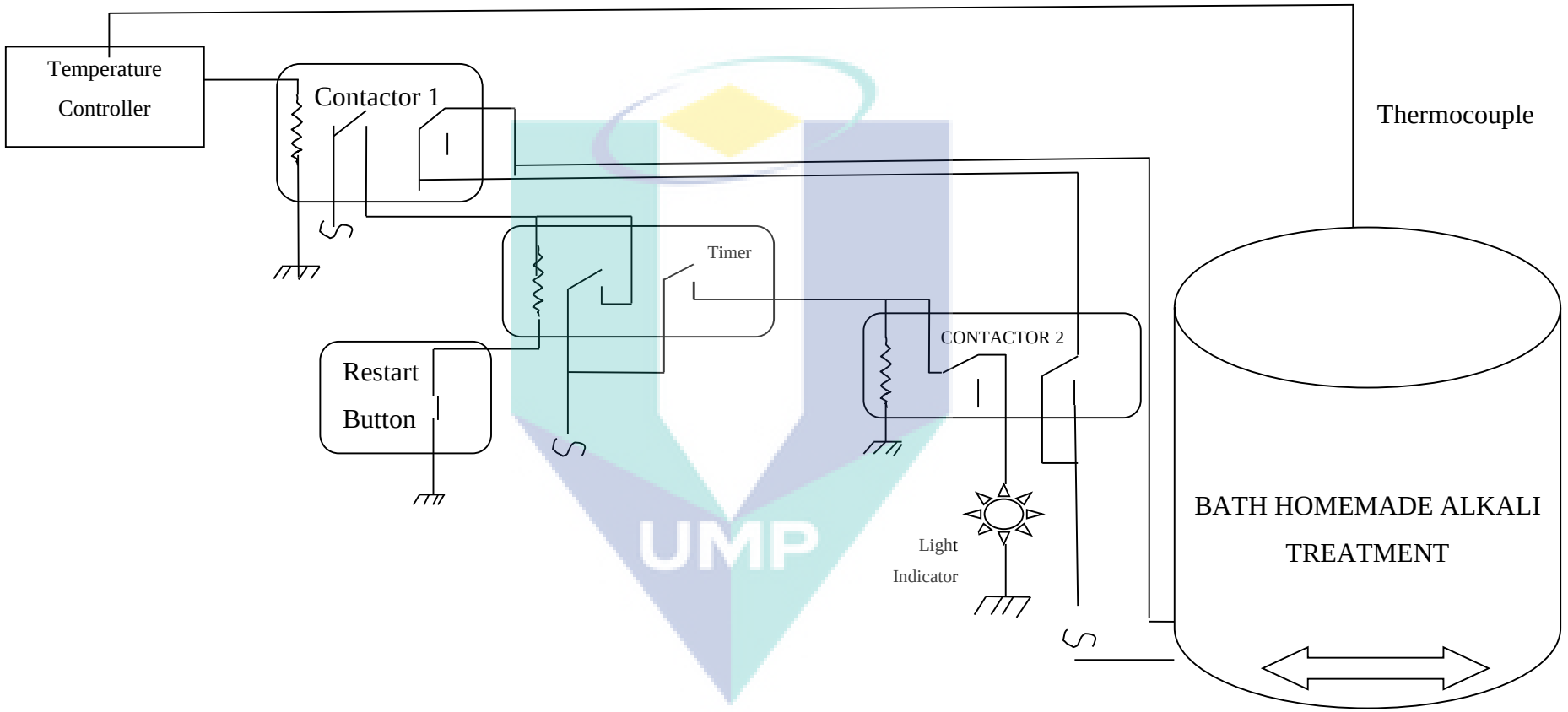

Figure D 3: Homemade EFB Alkali Treatment controller